AL.2.1986-820
#2

# PROCEEDINGS AIR POLLUTION SESSIONS

## Canadian Meteorological
## and
## Oceanographic Society

15th Annual Congress, Saskatoon, Saskatchewan

May 27-29, 1981

DDN
4083581

Alberta
ENVIRONMENT

CANADIA
C2
FEB 8 - 1

# PROCEEDINGS

# AIR POLLUTION SESSIONS

# CANADIAN METEOROLOGICAL AND OCEANOGRAPHIC SOCIETY

# FIFTEENTH ANNUAL CONGRESS

27 - 29 May 1981

SASKATOON, SASKATCHEWAN

A Report

by

The Special Interest Group in Air Pollution Meteorology

Digitized by the Internet Archive
in 2015

https://archive.org/details/proceedingsairpo00cana

About the Cover

The map of Canada is shaded according to the precipitation - weighted mean sulphate ion concentration as reported by CANSAP for the period May 1977 - April 1978 with coastal areas corrected for sea salt contributions. The lightest zone corresponds to concentrations of less than 2 mg/l; the intermediate zone, to concentrations of 2 - 4 mg/l and the darkest zone, to concentrations in excess of 4 mg/l.

# PREFACE

It is a truism that a country as vast as Canada offers commensurate opportunities and problems. Climatic and regional variations together with a resource based industry mean no lack of opportunities for environmental science in a country where large undeveloped regions give us a special sensitivity for our environment. However, sparse population means only limited manpower resources can be addressed to any one problem. Large distances hinder communication, even in these days of the information revolution.

The Special Interest Group on Air Pollution Meteorology has been formed within the Canadian Meteorological and Oceanographic Society to aid communication between specialists in the field and stimulate ideas through organization of meetings. The first major meeting was at the Society's 15th Annual Congress at the University of Saskatchewan, Saskatoon, held from 27 to 29 May 1981. The present volume of unrefereed papers from these air pollution sessions is designed to further aid communication. It is noteworthy that publication of a conference proceedings is a new departure for the Society and, we hope, one in which we will be joined by others for future Congresses.

We were particularly pleased to be able to welcome a distinguished visitor, Dr. F.B. Smith from the British Meteorological Office, as our theme speaker. Dr. Smith is well known in the air pollution community for a wide variety of studies primarily related to turbulent dispersion. His theme paper "A Review of the European EMEP Programme on the Long-Range Transport of Pollution, and some ideas on how to treat Wet Deposition" results from an intensive study recently completed under the sponsorship of the World Meteorological Organization. This review nicely complements the understanding presently being developed in Eastern North America and the papers in this volume on the potential for acidification resulting from Western Canadian development.

Production of this volume was subsidized by Alberta Environment and supervised by Mr. R.P. Angle. The Special Interest Group would also like to acknowledge the assistance of the Congress Program Committee (Chairman, Dr. B. Goodison), and the Local Arrangement Committee (Chairman, Dr. J. Whiting).

J.D. Reid

CMOS Air Pollution Meteorology Steering Committee

J.D. Reid (Chairman)
R.P. Angle (Secretary)
R.E. Munn
D.G. Steyn
B. Weisman

# TABLE OF CONTENTS

PAGE

Preface iii

SPECIAL SESSION 4A AIR POLLUTION

Chairman: J. D. Reid

A REVIEW OF THE EUROPEAN EMEP PROGRAMME ON THE LONG-RANGE TRANSPORT OF POLLUTION, AND IDEAS ON HOW TO TREAT WET DEPOSITION 1
F. B. Smith, British Meteorological Office, Bracknell, Berkshire, U. K. RG12 2SZ

SESSION 5A AIR POLLUTION FIELD STUDIES - PLANNED AND INADVERTENT

Chairman: D. G. Steyn

TETROON FLIGHTS ACROSS A RIDGE 25
R. D. Rowe, S. F. Benjamin and K. P. Chung, Dept. of Chemical and Petroleum Engineering, The University of Calgary, Calgary, Alberta T2N 1N4

ESTIMATION OF THE RATE OF GASEOUS MASS TRANSFER FROM A SURFACE SOURCE PLOT TO THE ATMOSPHERE 39
J. D. Wilson, Boundary-Layer Research Division, Atmospheric Environment Service, Downsview, Ont. M3H 5T4
G. W. Thurtell, G. E. Kidd, E. G. Beauchamp, Dept. of Land Resource Science, University of Guelph, Guelph, Ont. N1G 2W1

SHORT-RANGE ATMOSPHERIC TRANSPORT AND DIFFUSION OVER THE PRECAMBRIAN SHIELD 47
P. A. Davis and A. Reimer, Whiteshell Nuclear Research Establishment, Pinawa, Man. R0E 1L0
S. K. Sakiyama and P. R. Slawson, University of Waterloo, Ont. N2L 3G1

THE MACGREGOR VINYL CHLORIDE SPILL: A PRACTICAL EXERCISE IN DISPERSION 61
H. M. Fraser, Atmospheric Environment Service, Winnipeg, Man. R3C 3V4

SESSION 6A ACIDIFICATION IN WESTERN CANADA

Chairman: A. S. Mann

THE EXTENT OF ACIDIC DEPOSITION IN A REGIONAL CONTEXT OF WESTERN CANADA 75
S. R. Shewchuk, Physics Division, Saskatchewan Research Council, Saskatoon, Sask. S7N 0X1

PAGE

METEOROLOGICAL CONTROLS ON AIR POLLUTANTS IN A SELECTED REGION OF WESTERN CANADA 87
R. F. Hopkinson and J. Dublin, Atmospheric Environment Service, Airport Terminal Bldg., Regina, Sask. S4P 3N5

SENSITIVITY OF SOILS TO ACIDIC DEPOSITION IN A SELECTED REGION OF WESTERN CANADA 99
N. Holowaychuk, G. Padbury and B. Schreiner, Agriculture Canada, Soil Survey Unit, Saskatoon, Sask. S7N 0W0

POTENTIAL EFFECTS OF ACIDIC DEPOSITION ON PLANTS WITH SPECIAL REFERENCE TO NORTHERN SAKATCHEWAN AND NORTHEASTERN ALBERTA 119
Z. M. Abouguendia and R. C. Godwin, Chemistry and Biology Division, Saskatchewan Research Council, Saskatoon, Sask. S7N 0X1

SESSION 7A ALBERTA OIL SANDS ENVIRONMENTAL STUDIES 135

Chairman: R. P. Angle

A USER-ORIENTED CLIMATOLOGICAL DISPERSION MODEL FOR THE ALBERTA OIL SANDS
D. S. Davison, E. D. Leavitt, R. McKenna and R. Rudolph, Intera Environmental Consultants Ltd., P.O. Box 5487, Station A, Calgary, Alta T2H 1X9

AN ANALYSIS OF PRECIPITATION CHEMISTRY IN THE OIL SANDS AREA OF NORTHERN ALBERTA 147
R. R. Peters, W. D. Hume and H. S. Sandhu, Alberta Environment, Oxbridge Place, Edmonton, Alta T5K 2J6

ION AND METAL CONTENT OF THE SNOW COVER OF THE AOSERP STUDY AREA 159
W. Murray, Promet Environmental Group Ltd., 2021-41 Ave. N.E., Calgary, Alta T2E 6P2

SESSION 8A AIR POLLUTION MODELLING AND ASSESSMENT

Chairman: R. V. Portelli

USER CONSIDERATIONS IN AIR QUALITY MODELLING 171
R. P. Angle, Alberta Environment, Oxbridge Place, Edmonton, Alta T5K 2J6

A MIXED LAYER STATISTICS DISPERSION MODEL 183
C.S. Matthias, Atmospheric Environment Service, Downsview, Ont. M3H 5T4

CROSSWIND DISPERSION FUNCTIONS FROM TURBULENT ENERGY SPECTRA VIA THE STATISTICAL THEORY OF DIFFUSION 201
D. G. Steyn, Dept. of Geography, The University of British Columbia, Vancouver, B.C. V6T 1W5

PAGE

THE APPROPRIATE CHOICE OF $\sigma_z$ AND $\bar{u}$ FOR PREDICTING SURFACE CONCENTRATION USING THE GAUSSIAN MODEL 207
J. D. Reid, Boundary-Layer Research Division, Atmospheric Environment Service, Downsview, Ont. M3H 5T4

A MODEL FOR URBAN AREA SOURCE CO CONCENTRATIONS 217
K. D. Hage and P. Hopps, Dept. of Geography, The University of Alberta, Edmonton, Alta T6G 2H4

SESSION 9A AIR POLLUTION MODELLING AND ASSESSMENT

Chairman: R. V. Portelli

INCOMPATIBILITY BETWEEN AIR QUALITY MODEL PREDICTIONS AND REGULATORY REQUIREMENTS: ATTEMPT AT SOLUTION 231
S. G. Djurfors, Syncrude Canada Ltd., 10030-107 St. Edmonton Alta T5J 3E5

TRAITEMENT AMELIORE DE LA PRECIPITATION DANS UN MODELE DE POLLUTION DE L'AIR PAR L'UTILISATION D'UNE DOUBLE CHAINE DE MARKOV 239
C. Lelievre, Service de la Meteorologie, 194 ave St-Sacrement, Que. G1N 4J5

A MODEL FOR ESTIMATING STATIC STABILITY IN THE SURFACE AND PLANETARY BOUNDARY LAYERS FROM STANDARD HOURLY TEMPERATURE DATA 249
R. Verreault, L. Perelman and D. Begin, Universite du Quebec a Chicoutimi, Chicoutimi (Quebec) G7H 2B1

POSTER SESSION

Poster 13

A LONG-RANGE CLIMATOLOGICAL DISPERSION MODEL 261
C. S. Matthias and A. K. Lo, Air Quality and Inter-Environmental Research Branch, Atmospheric Environment Service, Downsview, Ontario M3H 5T4

Poster 15

RESULTS OF THE NANTICOKE SHORELINE DIFFUSION EXPERIMENT: JUNE 1978 275
R. V. Portelli, Atmospheric Environment Service, Downsview, Ontario M3H 5T4

Poster 16

MOVEMENT OF MOUNT ST HELENS ASH CLOUD OVER WESTERN CANADA 291
G. B. Atkinson, Atmospheric Environment Service, Winnipeg Manitoba R3C 3V4

# A REVIEW OF THE EUROPEAN EMEP PROGRAMME ON THE LONG-RANGE TRANSPORT OF POLLUTION, AND SOME IDEAS ON HOW TO TREAT WET DEPOSITION

by

F. B. Smith
**Meteorological Office**
Bracknell, Berkshire, U.K. RG12 2SZ

Abstract: The EMEP Programme, started in January 1978, has just completed its First Phase. A network of monitoring stations has been established across Europe. Two Meteorological Synthesising Centres, one in Oslo and the other in Moscow, have developed trajectory models which are run operationally to give daily fluxes, concentrations and depositions of sulphur pollutants. Wet deposition is deduced from rainfall fields which are spatially and temporally smoothed. The smoothing results in underestimation of transport to distant receptors. Introduction of stochastic concepts offers hope of improvement.

## INTRODUCTION

Using the atmosphere as a dumping ground for industrial waste gases has for centuries been criticised as a practice dangerous to the health of people living nearby. In the last few decades Clean Air Acts and the increasing use of tall chimneys have brought enormous benefits to people living in industrialised areas by greatly reducing local ground-level concentrations of these pollutants. Just as we were congratulating ourselves for this success, the bad news broke. Pollution has to come down somewhere, sometime. And when it does it can cause damage if the local ecosystem is critically sensitive, even at remote places where the average air concentrations are relatively low. This hard fact first became evident in southern Scandinavia where local emissions are very modest compared with those in a central band of Europe some 1000km to the south, stretching from the U.K. in the west to Poland in the east. Salmon and trout populations in many of the lakes and rivers were decreasing rapidly and this seemed to be linked to increasing water acidity. And the cause of the increasing acidity was believed to be the increasing European consumption of fossil-fuels and the resulting gaseous emissions into the atmosphere. As a result, considerable concern was generated, and this was aided by the U.N. Conference on the Environment in Stockholm in 1972. Research and monitoring programmes were initiated, and over the last 10 years considerable progress has been made in understanding, if not solving, the problem. Even so, many questions, some of them vital questions, remain either unanswered or only partially answered. Of necessity only a few of these issues and only a small part of the total work can be reviewed in this paper. In particular our present understanding of the effects side of the problem can only be touched on briefly: how does acid rain effect the ecosystem? The Proceedings of the International Conference on the Ecological Impact of Acid Precipitation (Norway, 1980) gives a detailed account which should be referred to for fuller details. The Proceeding is prefaced with an excellent summary by F. T. Last et al. To paraphrase just some points from this summary: "Serious changes in the aquatic ecosystem are evident and there is no doubt these are linked to acid precipitation. The exact nature of this relationship and the role of soil processes are under discussion. The release of aluminium from the soil as a result of acid rain is postulated to cause significant toxicity effects to sensitive aquatic plants and invertibrates. Although acid rain can affect the rates of ground-litter decomposition, microbiological activity and nitrogen fixation, it is as yet unproven whether or not forest and crop growth rates are affected as a result".

Overrein et al. in their Final Report of the SNSF-Project (1980) reproduce a map by Munic and Leivestal (1980) showing quite extensive areas in Southern Norway with strongly affected fish populations. Comparison of these areas with those in Figures 4.2 and 4.3 of the same Report giving the annual deposition of excess sulphate in precipitation and the mean pH of precipitation, respectively, show only very rough agreement and point to the importance of other factors. These three figures are compounded in our Figure 1.

## OECD PROGRAMME

In addition considerable research started into the emission, airborne transport and deposition aspects of sulphur pollution. Much of this effort in Europe was centred on an OECD programme set up in 1971 with its operational centre at the Norwegian Institute for Air Research (NILU). The programme involved 15 western European nations who operated some 76 ground-level sampling stations between August 1972 and March 1975. In addition various countries operated sporadic aircraft sampling flights either with specific research questions in mind or as part of a general objective to supplement ground-level measurements with flux profiles aloft. Detailed surveys of sulphur emissions were made within participating countries by the countries themselves and estimates of emissions were made by NILU for other countries on the basis of their distributions of population and estimated industrial activity. Finally trajectory models were developed to simulate the whole emission-transport-deposition process in order to supplement the actual measured values of concentration and deposition, and to provide a reasonable basis for estimating sulphur budgets or transboundary fluxes between nations in Europe, (i.e. how much country X contributes to the sulphur deposition in country Y).

The models were essentially quite simple in nature and were unable to simulate in detail, for example, the complex air-chemistry processes that result in the oxidation of sulphur dioxide gas to sulphate aerosol. To have attempted to have done so would have required a much better understanding of the processes involved, a much better knowledge than was available of the emissions of other involved species, e.g. ammonia, nitrogen oxides, ozone etc, as well as that of sulphur itself, and much more computer time and capability than was available at the time. In any case there was no evidence or reasonable expectation that more complex models would provide more reliable results. Nevertheless the long-term averaged results of the models agreed quite well with the fields of concentration and deposition inferred from the station-network measurements (see for example Eliassen (1978)). In fact the model's parameters were tuned to optimise the agreement. Nevertheless there were some significant differences which will be

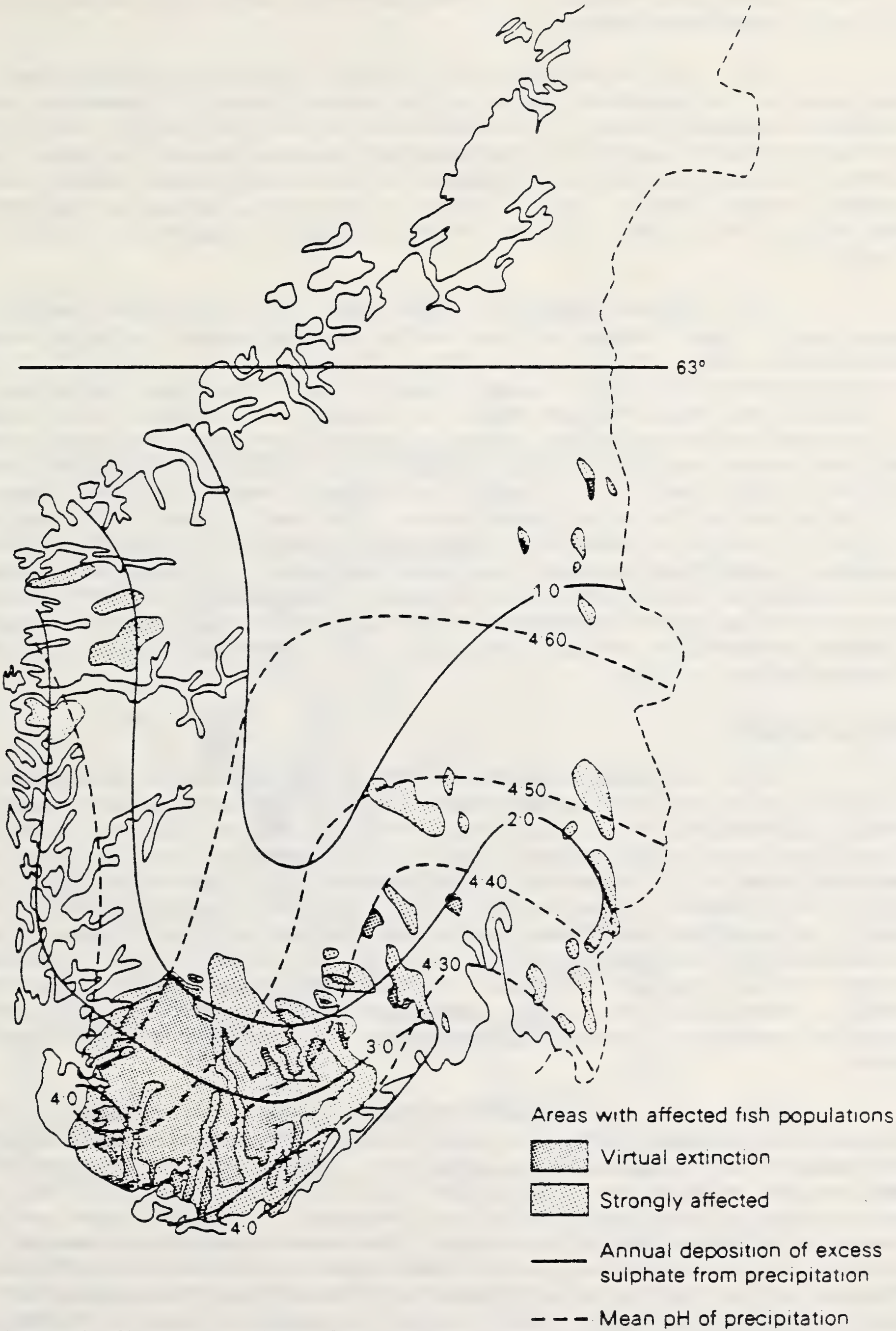

Figure 1. Areas in Norway in which lakes have badly affected fish populations compared with annual wet deposition of sulphate and the mean pH of precipitation.

discussed later and much of the broad agreement inevitably arose from the following considerations:-

(i) air concentrations of sulphur dioxide at ground-level are dominated by the emission levels within several tens of kilometres, except where these are extremely small. The concentration contour pattern should therefore correspond very closely with the smoothed emission contour pattern. As we have noted the emissions tend to be highest within a rough band running east-west through central Europe, and fall away to very small levels in the extreme north and south. The sulphur dioxide concentrations are observed to follow this same trend.

(ii) The wet deposition maps also to a large degree reflect the local emissions in that, except in those rather extreme areas (including most of Scandinavia) where emissions are relatively small, if it rains r% of the time (where for much of Europe r lies between 5 and 10) the same percentage fraction r of the local emissions are deposited locally (i.e. within a few hundred kilometres) and constitute a rather sizeable fraction of the whole deposition in these areas, as can be shown by simple calculations using known emission fields. Again then the wet deposition contours peak in central Europe and fall to low values in the more distant areas. The real success or otherwise of the trajectory models in simulating long-range transport is therefore rather hard to assess. Indications are that they show some skill in long-term assessments, but very little in short-term (daily or weekly) assessments, and are able to provide reasonable "ball-park" estimates of the long-term inter-country pollution budget figures, referred to earlier, especially for those countries like Norway, whose ecosystems are at risk.

## EMEP PROGRAMME

After the OECD experiment came to its conclusion, successful efforts were made to initiate a new programme involving as many European countries as could be persuaded to join in. One reason for the new programme was that a significant part of the errors in the OECD budgets had their origins in the uncertainties in the emission fields, especially in the non-cooperating countries. Another reason was that if it should be thought sensible to adopt a policy of modifying emissions to minimise the amount of acid rain in sensitive areas then all contributing countries should be involved, both to maximise the effect and to equalise the consequent financial penalties that would inevitably result. Most important of all, many aspects of the work required further detailed research if the modelling were to be improved to a really satisfactory level.

The result was the EMEP Programme, whose letters stand for "The Cooperative European Monitoring and Evaluation Programme of the long-range transmission of air pollutants in Europe". EMEP started in January 1978 and has now been running for three years. The end is approaching of what has come to be known as the First Phase of the programme. A second phase and perhaps even a third phase are now envisaged. Two meteorological centres and one chemical centre were established. The former carry the imposing titles "Meteorological Synthesising Centre-West" (MSC-W) and "Meteorological Synthesising Centre-East" (MSC-E) and are situated in Oslo and Moscow respectively. The "Chemical Coordinating Centre" (CCC) is in Lillestrøm in Norway. Two MSC's were established as a vital cross-check of results and to utilise emission data for the USSR available only to MSC-E.

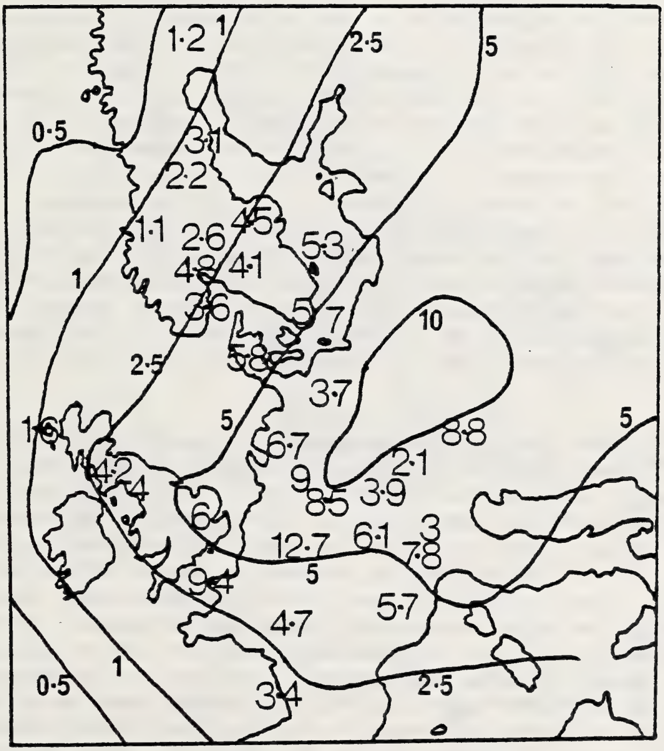

Figure 2. Estimated and observed mean concentrations of particulate sulphate for 1974. The estimated values were obtained using the OECD/EMEP MSC-W trajectory model. Units are $\mu g\ SO_4 m^{-3}$. (Eliassen,1978).

The comparison suggests the model overestimates the concentrations near to industrial areas and underestimates them at long range.

Essentially, as in the OECD study, the main objective of the MSC's in the EMEP Programme has been to develop and routinely apply mathematical models of the atmospheric life-cycle of major pollutants involved in the "acid-rain" problem. They are to provide usable data on transboundary fluxes in Europe and to complement those limited daily measurements to provide an understanding of the spatial distribution of surface depositions throughout the continent. In the first phase in their modelling the MSC's have concentrated entirely on sulphur compounds as the primary pollutants in the problem.

## EMEP Models

MSC-W started their work in this Programme with the well-tried OECD model. Some modifications were essential, notably a major revision of the analysis area and a reorganisation of input data. Results were available from January 1st 1978. MSC-E having started from scratch took longer to become operational but data on transboundary fluxes across the western USSR - boundary became available after August 1st 1979. Improvements to the model have followed and are still being applied. The two models are basically similar. They represent the transport of pollution by a one-layer model in which a series of discrete trajectories are advected by the appropriate 850mb geostrophic wind. Conversion of sulphur dioxide to sulphate takes place linearly at a rate determined empirically to give good long-term fit with observed concentrations. Dry deposition of both sulphur dioxide and sulphate is assumed to be proportional to the respective air concentration and a velocity of deposition (different for the two species) which at present is independent of the nature of the underlying surface. Wet deposition is treated differently in the two models: in the MSC-W model, rainfall is inferred by interpolation from neighbouring meteorological observing stations reporting in the international data exchanges. If some rain is inferred, then sulphur is washed out at a prescribed rate independent of the inferred rainfall, otherwise no wash-out occurs. In the MSC-E model rain is considered to be occurring everywhere at all times and a corresponding wash-out included. We will comment much more fully on these simple assumptions later.

Vertical and horizontal lateral spread are dealt with quite differently by the two models. The original MSC-W model had a fixed mixing depth of 1km and all pollution is supposedly contained below this height. The stage immediately following release when vertical dispersion is incomplete and ground-level concentrations are relatively high, at least for low-level sources, is recognised in a very simple way: 15% of the sulphur is assumed to be dry deposited within the emission grid square (150km x 150km in area) over and above that which would be deposited if the pollution were immediately dispersed throughout the whole depth of the layer. The MSC-E model on the otherhand does not have a mixing depth but allows pollution to spread upwards continuously according to an eddy-diffusivity formulation. Although at first sight the MSC-W model may seem more realistic in this respect, provided the eddy-diffusivity profile in the MSC-E model is well chosen the unlimited upward diffusion may in fact help to allow for some of the loss processes which undoubtedly exist, and which carry material out of the boundary layer. The loss may occur at source where large industrial plumes can rise under their own buoyancy well above the mixing layer. Several other processes may also be effective in pulling pollution upwards e.g. non-precipitating convective cloud, overturning in mountainous areas, fronts etc. Once out of the boundary layer the pollution will probably be advected with markedly different winds and may be deposited ultimately in a totally different place from that which remained within the boundary layer. The only way of dealing with this, if it is important, would be to develop a multi-layered model.

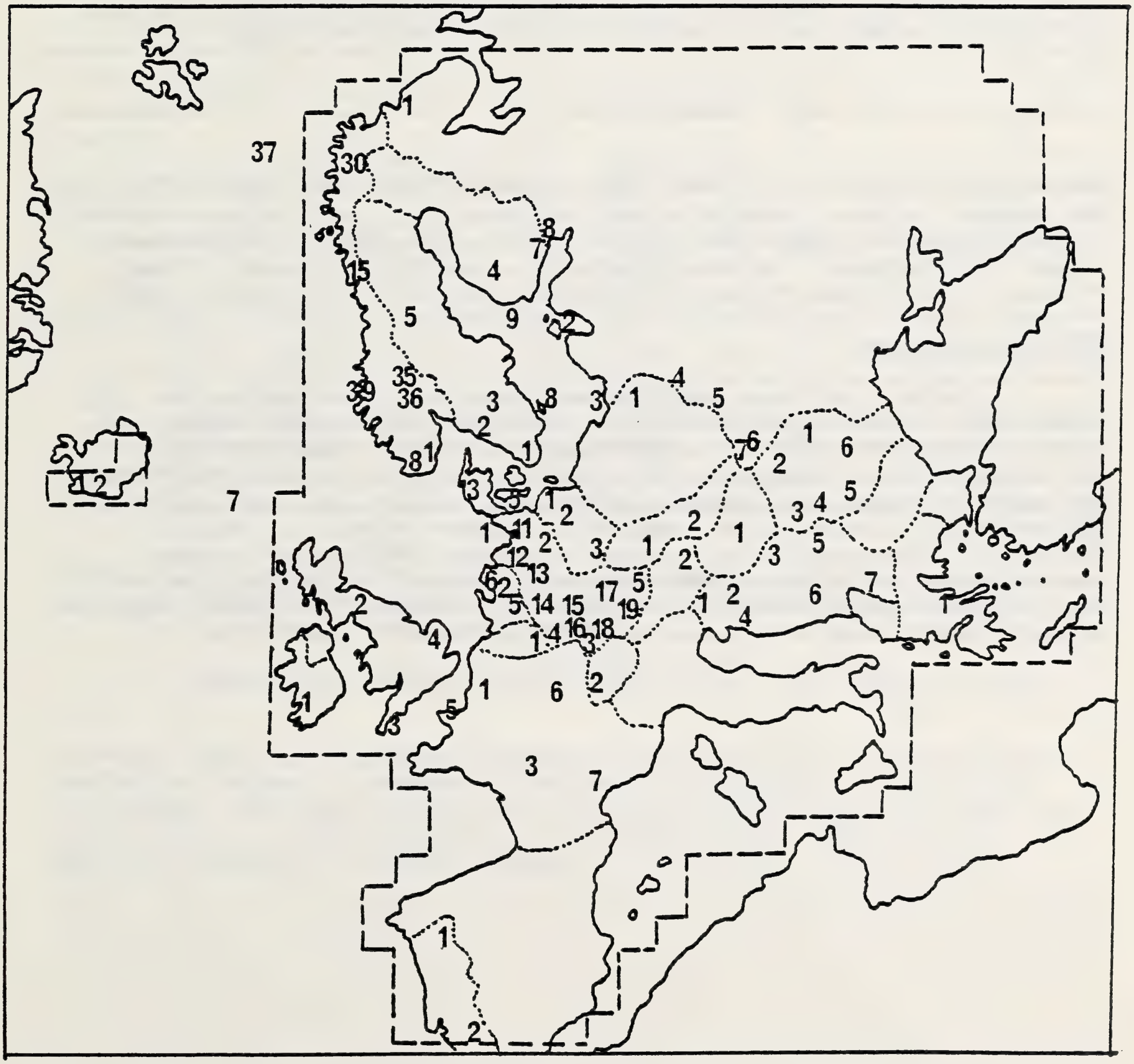

Figure 3 : The area in which trajectories are followed. Concentrations and depositions are calculated within the smaller pecked-line areas. EMEP monitoring stations are shown by their national numbers.

The MSC-W model ignores lateral dispersion on the principle that, if enough trajectories are followed over a sufficiently long period of time, it contributes nothing to the fluxes and depositions except in areas where there are very marked gradients in the directional distribution of trajectories. However there is no evidence that such areas exist, certainly in Europe.

The MSC-E model nevertheless does incorporate an empirical lateral spread about each of its trajectories, which is believed by the Centre to provide a refinement to the calculation of fluxes across national boundaries, especially on a shorter time-scale. Essentially at the end of each time step a new position of the trajectory end-point from each source location is determined. The pollution being carried is then sub-divided into 15 points surrounding the position in a section of a cone whose width is given by

$$\sigma(x) = 0.1\,x \tag{1}$$

(where $x$ is the distance of travel from the source) and whose length is given by the downwind distance travelled in one time step. Each point is then advected by the appropriate interpolated wind through one time step and the necessary fluxes are determined. The mass of pollution, modified by losses, is then returned to the trajectory position, advected forward and the process repeated.

## EMEP Model Results

In the First Phase the MSC-W model gave air concentrations and depositions at monitoring stations, for comparison with measured values, and at all grid points within the area of analysis. Table 1 summarises some of the implied national depositions for a six-monthly winter period (1978/79) and how these are broken down according to the country of origin. Only 9 of the main emitting countries and one "sensitive" country (Norway) is included in the Table. Fuller details can be found in the main EMEP Summary Reports. Czechoslovakia has an implied sulphur deposition rate, per unit surface area, over ten times greater than that of Norway, but because of the latters sensitive ecosystem the adverse effects are apparently much more evident there.

Emitting country

| | Country | Czech | GDR | Belg | FDR | Pol | U.K. | Holl | Fra | USSR | Norw | Undecided | Other | Total |
|---|---|---|---|---|---|---|---|---|---|---|---|---|---|---|
| | Czech | 4.7 | 1.7 | 0.1 | 0.9 | 0.7 | 0.2 | 0.1 | 0.4 | 0.1 | 0 | 0.7 | 0.4 | 10.9 |
| | GDR | 0.6 | 5.5 | 0.1 | 0.9 | 0.2 | 0.2 | 0.1 | 0.2 | 0 | 0 | 0.3 | 0.2 | 8.3 |
| | Belgium | 0 | 0.1 | 2.6 | 1.1 | 0 | 0.7 | 0.2 | 1.1 | 0 | 0 | 0.4 | 0 | 6.2 |
| | FDR | 0.2 | 0.6 | 0.2 | 2.8 | 0.1 | 0.4 | 0.1 | 0.5 | 0 | 0 | 0.4 | 0 | 5.2 |
| Receiving Country | Poland | 0.5 | 0.8 | 0 | 0.3 | 1.9 | 0.1 | 0 | 0.1 | 0.1 | 0 | 0.3 | 0.7 | 4.8 |
| | U.K. | 0 | 0.1 | 0 | 0.1 | 0 | 3.3 | 0 | 0.1 | 0 | 0 | 0.3 | 0.2 | 4.1 |
| | Holland | 0 | 0.2 | 0.4 | 1.5 | 0 | 0.7 | 1.2 | 0.4 | 0 | 0 | 0.3 | 0 | 4.4 |
| | France | 0 | 0.1 | 0.1 | 0.2 | 0 | 0.2 | 0 | 1.3 | 0 | 0 | 0.3 | 0.4 | 2.6 |
| | USSR | 0.1 | 0.1 | 0 | 0.1 | 0.1 | 0 | 0 | 0 | 1.0 | 0 | 0.4 | 0.3 | 2.1 |
| | Norway | 0 | 0 | 0 | 0 | 0 | 0.1 | 0 | 0 | 0 | 0.1 | 0.3 | 0.3 | 0.8 |

Table 1 National average total sulphur depositions in gS $m^{-2}$ for the six-month winter period 1978/79 according to the MSC-W model, listed in order of overall total deposition.

(numbers are rounded to one decimal place. Thus 0 means < 0.05).

The MSC-E model has to date only produced fluxes across the western boundary of the USSR but is shortly expected to produced data comparable to that of the MSC-W model. The fluxes compare very satisfactorily with those from MSC-W on a daily basis, and such differences as do occur probably result from the differeing treatment of lateral spread.

## Research Findings

Both models advect pollution in a vertical column with a single horizontal wind vector. At present this wind is the 850mb geostrophic wind, roughly appropriate to a height of about 1500m which is rather too high for a typical boundary layer wind. The hope that 925mb wind data might become available by making 925mb a special point on radiosonde ascents has so far not materialised.

Research at both Centres has indicated that a better correlation between model and measured concentrations occurs when some modification of the 850mb wind is made. MSC-E found better agreement when the wind was reduced 10% and backed by 15°. MSC-W has shown what appears to be an annual cycle: in February when the boundary layer depth is relatively low over land a reduction of 10% in speed and a backing of between 15° and 20° gave best results, in agreement with MSC-E. In June however with supposedly deeper boundary layers the unmodified 850 mb wind seems to give the optimum results.

MSC-W have tried varying some of the other parameters in their model to see if the results can be improved. Their experiments to date do not cover all possible combinations of the possible changes and so the conclusions must be therefore somewhat tentative. The following seem to be beneficial however:

(i) Assume the effective mixing depth h for a 24-hour period is determined by its midday value which is deduced by interpolation from actual values inferred from neighbouring radiosonde ascents. When h decreases from one day to the next, no resulting change in concentration is assumed, but if h increases this is assumed to have been caused by the entrainment of "clean" air from above the layer and the concentrations within the mixing layer are diluted accordingly.

(ii) Optimise the wash-out coefficients $\lambda$ for sulphur dioxide and sulphate in the model equations. The best values for $\lambda(SO_2)$ and $\lambda(SO_4)$ seem to be about 2.5 and 6 respectively.

Other ideas seemed to produce rather inconclusive results. For example one suggestion was to vary the dry deposition velocity $V_d$ so that $V_d/h$ remained constant, on the assumption that in winter increased stability in the lower layers should reduce $V_d$ in rough proportion to the decrease in $h$. Results did not really confirm this and if anything supported the original supposition of keeping $V_d$ constant independent of $h$.

Further research is required in the following areas:

(a) seasonal variations in emissions

(b) variations in local depositions (referred to earlier) with source height and local topography. Emissions in deep valleys, for example, could give significantly higher local depositions than identical emissions from elevated terrain.

(c) the magnitudes and origins of background concentrations. Near the western seaboard, air coming in from the open Atlantic usually has a very low sulphur concentration. However since much of the rain comes with these winds, the total wet deposition depends to quite a large extent on these small concentrations which may originate across the Atlantic. In seven European countries the contribution from these background concentrations are more than 25% of the total deposition and in Iceland and Portugal are more than 60%. This of course assumes small local sources are not confusing the picture.

(d) variations in the velocity of deposition with the nature of the underlying surface. If these variations are significant, different seasonal values could be ascribed to each grid square.

(e) the magnitude of losses of pollution from the mixing layer to the air above and the synoptic situations in which they occur.

(f) a better understanding of the relationship between the sulphur content of precipitation and that of the air being drawn into the precipitating cloud.

(g) differences in the above relationship between rain and snow precipitation.

(h) how to model episodes. A sizeable fraction of the total annual wet deposition at a receptor can occur on just a few days, called episode-days. We do not know whether the models work as well on episode-days as on others. Apparently the frequency distributions of wet deposition, calculated and observed, have similar areas in winter but the 'calculated' area is too small compared to the 'observed' area in summer. In both cases the observed distribution shows more high depositions than is predicted by the MSC-W model.

(i) investigate whether there are geographical, topographical and synoptic areas where the model results are not good, or are significantly worse than average, to see if explanations can be found. Such studies might point the way to worthwhile model improvements.

(j) one of the initial objectives of the EMEP Programme was to consider ways of estimating transboundary fluxes and depositions from meteorological data and actual measurements of concentration and deposition at the network of monitoring stations. In principle it is possible to derive objectively analysed fields of concentration and to interpret these, given the wind field, in terms of fluxes and net source-sinks, and achieve the objective. In practise this may be possible only over part of Europe when the station network is sufficiently dense (separations less than 300km).

(k) better ways of modelling wet deposition (see later).

## The Second Phase

The Second Phase of the EMEP Programme envisages broadening the list of pollutants to include other components of acid rain, in particular nitrates. This would present considerable problems: estimating the emissions would be difficult for all species, almost impossible for some; monitoring concentrations of some of these components is also difficult; an assessment of the ecological effects of nitrates, for example, is not easily made; modelling would involve simulating highly complex air chemistry which would entail the employment of men, time and money that perhaps could be employed more profitably elsewhere in the Programme. In fact neither Centre is in a position (to undertake this work in the immediate future).

## FURTHER CONSIDERATION OF WET DEPOSITION

For simplicity we will use the terms "rain" and "rainfall" in this section to represent more general forms of precipitation. As already noted the MSC-W model assesses wet deposition along a trajectory by interpolating observations of 6-hour rainfall made at those rather widely separated meteorological stations which regularly appear in the 6-hourly international transmissions. The situation is particularly acute over the sea where observations are few in number and quantitatively rather uncertain. Even over land the locations of the stations are not always without bias, the majority are in open level terrain, in valleys or at coastal sites. Elevated mountainous sites, where the rainfall is probably greater than elsewhere, are usually unrepresentatively few and far between. Thus the wet depositions are deduced from interpolated rainfalls that are the result of spatial and temporal smoothing and may contain 'topographical' bias. The MSC-E model assumes it is raining all the time, everywhere: an assumption implying even more radical spatial and temporal smoothing.

Effort has been applied over the last couple of years to try to understand the consequences of this smoothing and to explore ways of improving the situation. Essentially the problem is this: any form of smoothing tends to result in lower intensities of rain occurring over wider areas and more continuously in time than actually occurs in practice. For pollutants, like sulphur dioxide and sulphate, which are removed by precipitation rather quickly (continuous moderate rain will effectively remove all the airborne sulphur within 200km), this implies a greater probability of interception of rain in the models which as a result statistically underestimates the amount reaching areas one or more thousands of kilometres from the source. As far as Europe and North America are concerned these areas contain the most sensitive ecological regions.

This supposition has been largely verified by the results of the OECD study (Eliassen, 1978) and by the modelling work of Smith (1981). Rodhe and Grandell (1972) in a study of the lifetime of atmospheric aerosols were the first to consider the effect of moving wet regions (like frontal zones and unstable polar outbreaks) and dry regions (like summer anticyclones) on the average transport and deposition of airborne material. Fisher (1978), Smith (1980 & 1981 ) and Venkatram (1980) have developed these original ideas and applied them to the study of sulphur in the atmosphere. Their results give significantly different deposition rates to models which fail to differentiate between wet and dry regions. Smith's formulation for example differentiates between the relative fractions of $SO_2$ and sulphate that exist in a statistical sense after a given time of travel t in dry regions and in wet regions. If q refers to $SO_2$ , Q to sulphate, suffix D to dry regions and W to wet regions, then four Lagrangian rate of change equations are required to describe the statistical fate of the original emission:

$$
\begin{aligned}
\frac{d}{dt} q_D &= S_W q_W - S_D q_D - \frac{V_d}{h} q_D - \alpha_D q_D \\
\frac{d}{dt} q_W &= S_D q_D - S_W q_W - \frac{V_d}{h} q_W - \alpha_W q_W - A q_W \qquad (2) \\
\frac{d}{dt} Q_D &= S_W Q_W - S_D Q_D + \alpha_D q_D \\
\frac{d}{dt} Q_W &= S_D Q_D - S_W Q_W + \alpha_W q_W - A Q_W
\end{aligned}
$$

$S_D$ is proportional to the probability that the individual element of polluted air that is being followed will, at any instant of time, flow from a dry region into a wet region (recognising that boundary layer air moves with a different velocity to that moving the main synoptic features). $S_W$ is likewise proportional to the probability of flowing from a wet region into a dry region. These probabilities are linked to the average duration of dry and wet periods experienced at a fixed station, as the regions flow past; the durations being of the order of 40 hours and 8 hours respectively. $v_d$ is the deposition velocity of $SO_2$ to the ground ( $\sim 1$ $cms^{-1}$) and h is the depth of the polluted layer usually assumed constant at 1km. The terms including $v_d$ and h therefore represent, albeit somewhat crudely, the loss by dry deposition. Similar terms can also appear in the last two equations for the sulphate, as Venkatram has done, but $v_d$ for sulphate is normally very small and Smith chose to ignore these terms. $\alpha$ represents the rate of oxidation of $SO_2$ to sulphate and since $\alpha$ depends to some extent on relative humidity, Smith allowed $\alpha_W$ $(= .05h^{-1})$ to be larger than $\alpha_D$ $(= .005h^{-1})$ on the assumption that the humidity is likely to be greater in wet regions than in dry. A represents the removal rate by precipitation and is assumed significant only in wet regions. A can be made a function of wind direction, altitude of the underlying surface, geographical position and any other relevant parameters.

These linear first-order simultaneous differential equations are readily solved by conventional means. Smith did this for various trajectories across central Europe. For one such typical trajectory, 900km long, he compared results with results from a simplified model where no differentiation between wet and dry regions was made. In every other respect the models were identical. The results are given in Table 2.

Table 2. A comparison of results from Model A where wet and dry regions are recognised and from Model B where they are not and the probability of rain is constant. Quoted values are those at the end of a typical 900km trajectory across central Europe.

| | $q_D$ + | $q_W$ = | $q$ | $Q_D$ + | $Q_W$ = | $Q$ | Total fraction of S $q+Q$ | Average Wet deposition |
|---|---|---|---|---|---|---|---|---|
| Model A | 0.152 | 0.013 | 0.165 | 0.046 | 0.006 | 0.052 | 0.217 | 0.0051 |
| Model B | - | - | 0.081 | - | - | 0.038 | 0.120 | 0.0065 |

Although the actual numbers are particular to the trajectory chosen, the relative magnitudes are very typical of all possible trajectories. They show that the full model retains far more sulphur in the air at this range than the oversimplified model and this difference must increase as the range increases. Although the wet deposition rates are very similar at 900km they must eventually become significantly greater for model A at great range since little sulphur will still be airborne in model B to be wet deposited.

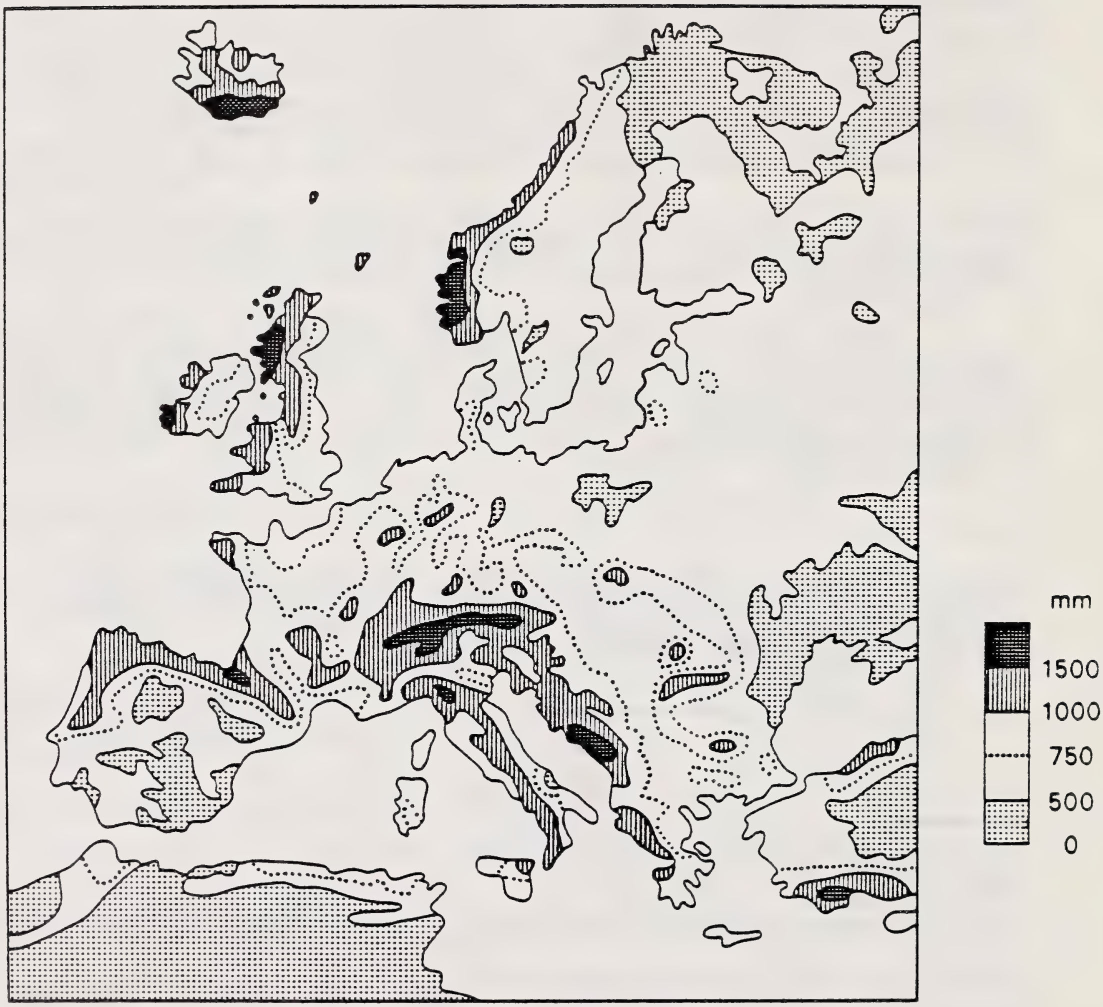

Figure 4a. Annual rainfall map for Europe

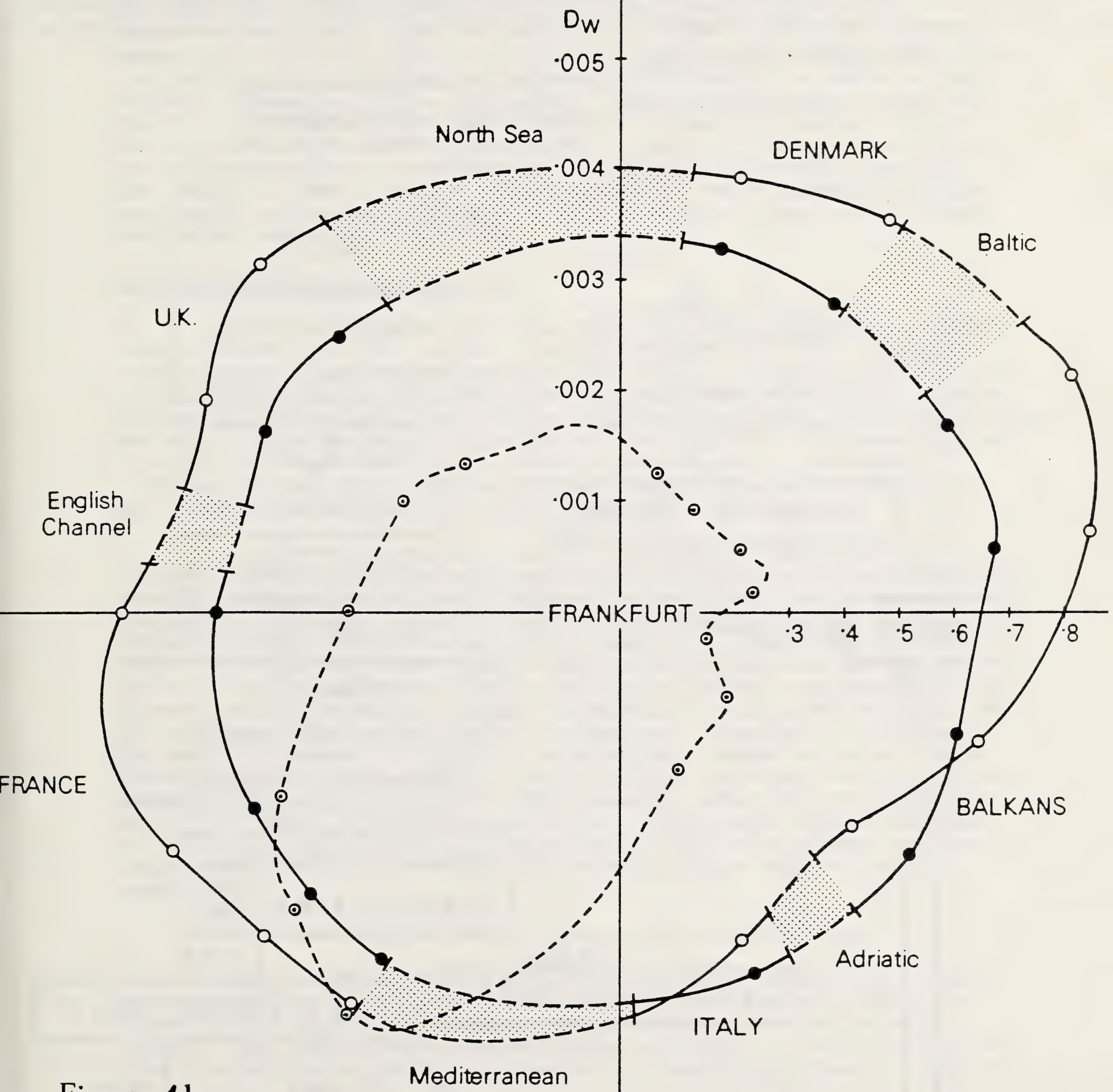

Figure 4b.

- - -⊙- - - - -⊙- - -Average rainfall en route

——○————○——Average wet deposition (900km range)

——●————●——Fraction lost by deposition

Figure 5

Stochastic Technique to simulate Wet Deposition along Trajectory

At each time step:

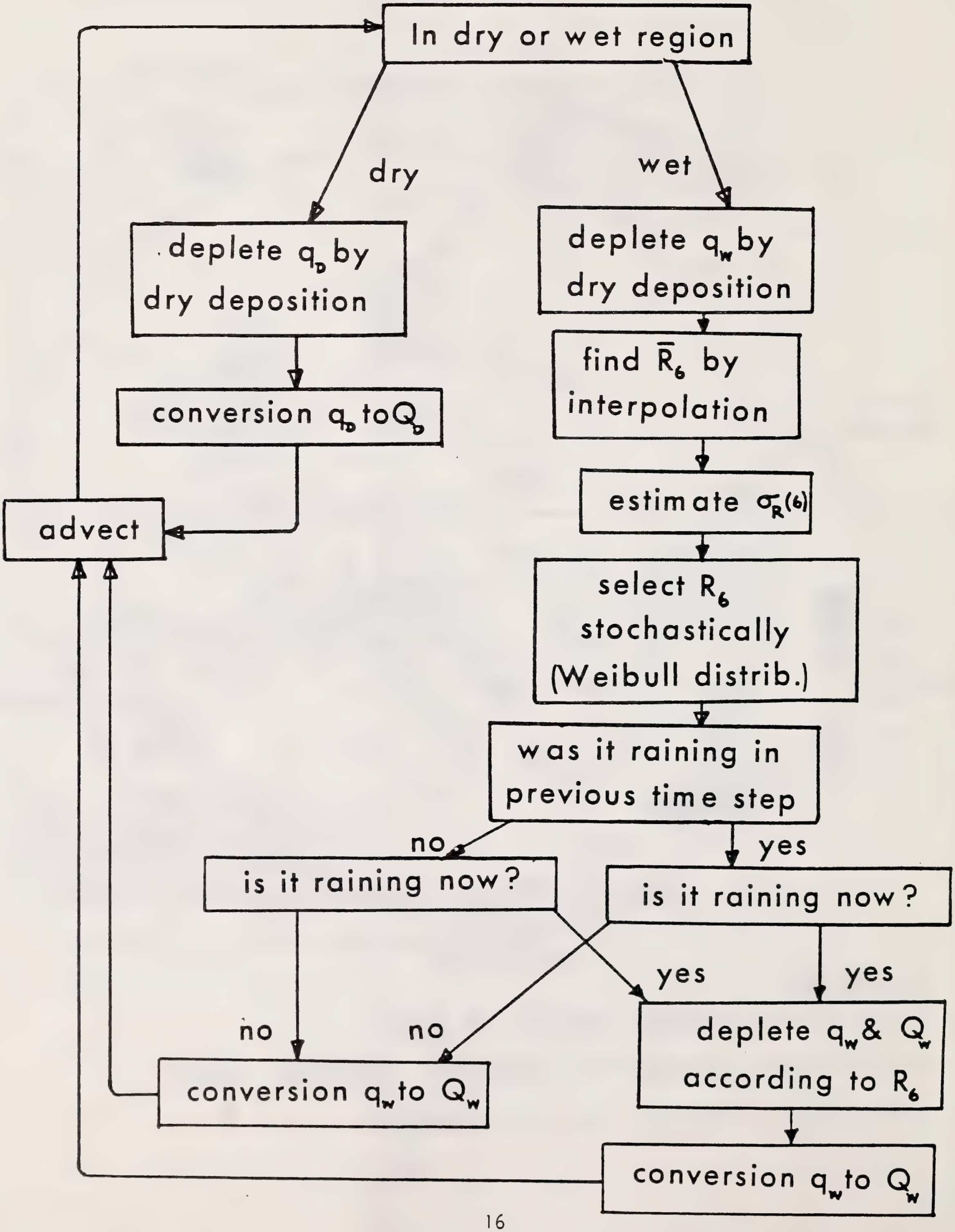

In dry or wet region
dry
wet
deplete $q_D$ by dry deposition
conversion $q_D$ to $Q_D$
advect
deplete $q_w$ by dry deposition
find $\bar{R}_6$ by interpolation
estimate $\sigma_{R(6)}$
select $R_6$ stochastically (Weibull distrib.)
was it raining in previous time step
no
yes
is it raining now?
is it raining now?
yes
yes
no
no
deplete $q_w$ & $Q_w$ according to $R_6$
conversion $q_w$ to $Q_w$
conversion $q_w$ to $Q_w$

Figures 9 and 10 of Eliassen's (1978) paper describing model-estimated wet depositions and interpolated measured wet depositions during the OECD experiment seem to support the above conclusions, even though the model parameters were tuned to give the best fit over Europe as a whole. Model wet depositions exceed the measured values over a wide area in central Europe which includes the main source areas and underestimates them in the remote northern regions. Agreement with the conclusions of Table 2 is even more obvious when the implied and measured air concentrations are compared (Eliassen's Figures 3 and 4). Another conclusion of this study was that provided the values given to the various parameters in the equations are of the right general magnitude, the results in terms of wet and dry deposition are really insensitive to the exact magnitudes chosen. The model is therefore rather robust and the overall conclusions reasonably reliable.

## Introduction of stochastic concepts

Current operational modelling by the two MSC's involves fairly substantial smoothing of the rainfall fields, as we have seen, with the danger of underestimating long-range transport and deposition. One way round this problem would be to incorporate the probability approach described above. But agreement with measured values could certainly not be expected on a daily basis and averaging over a very large ensemble of occasions would be required. For certain purposes this might not be serious, but for research purposes and for monitoring programmes lasting only one or two years meaningful comparison between model and measured results would be virtually impossible.

An alternative approach would be to attempt to unscramble, in a statistical sense, the reported 6-hour rainfalls at the surrounding meteorological observing stations in a way that simulates the most likely spatial and temporal variations in rainfall intensity. Thin line-trajectories would be replaced by broader strip-trajectories one model grid-length wide. Each time the strip-trajectory encountered a wet region, some fraction of its total sulphur would be removed. The fraction would depend on the 6-hour rainfall measurements at the neighbouring meteorological stations, the duration of the encounter and the overall topography. The fraction would be determined in principle by considering the fate of an ensemble of thin line trajectories. Whether or not any simple parameterisation is possible which could effectively eliminate the need for this elaborate process is a matter for future research. After the strip-trajectory has left any given wet region and has entered a dry region, lateral dispersion will mix the differing amount of sulphur left in each of the ensemble of line trajectories forming a quasi-uniform distribution before the next wet region is encountered.

The problem can be seen to consist of the following steps:

(i) consider a single thin-line trajectory. Determine the nearest three meteorological stations surrounding the trajectory point. Reduce the observed rainfalls at these stations to equivalent sea-level values using Figure 6. Use these at all subsequent stages below until (v) when the inferred rainfall should be re-enhanced to allow for the underlying surface altitude at the trajectory point.

(ii) at any time step, estimate the most likely 6-hour rainfall by plane-interpolation between the altitude-reduced rainfalls at two of the three surrounding stations and that at the previous time-step upwind along the trajectory.

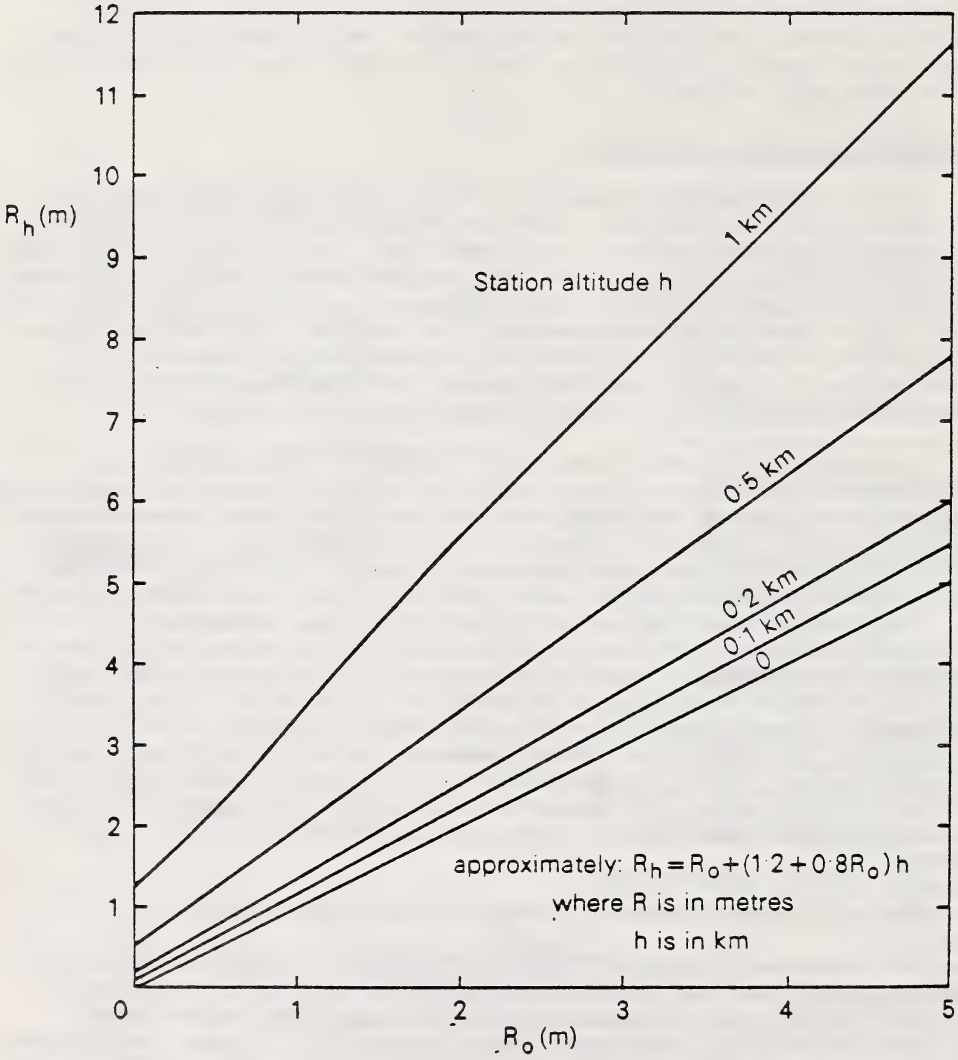

Figure 6 . The average annual rainfall $R_h$ in an area can have the effect of average surface altitude h removed, to give an effective sea-level annual rainfall $R_o$ .

(iii) add a stochastic element, to this inferred rainfall, made up of two parts: the first being correlated to the stochastic element at the previous time step, and the second uncorrelated part belonging to a Weibull distribution (Figure 7 ) whose parameters are determined by the most likely 6-hour rainfall and the supposed 'parent' rainfall population standard devation as reflected in the differences in rainfall observed at the three stations. (This procedure parallels in some respects the Monte Carlo techniques currently being used to simulate dispersion in a turbulent boundary layer).

(iv) decide whether or not it is raining during the current time-step. This decision is made in the light of whether or not it was raining in the previous time-step and the inferred 6-hour rainfall at the trajectory point. An example of this is shown in Figure 8 where the conditional probabilities are expressed in terms of the 6-hour rainfalls when the time-steps are of 15 minutes duration and the trajectory element is 5km x 5km in area. These curves have been deduced from a study of radar-inferred rainfall intensities over the U.K.

(v) deduce the loss of pollution during the time-step. If it rained, assume a constant rainfall rate consistent with the 6-hour rainfall. March forward and repeat steps (ii) to (v) until the trajectory emerges from the wet region.

(vi) Repeat the whole process N times with starting points randomly chosen across the strip. Deduce the average loss of pollution. The question remains as to how large N should be. If, when this scheme is developed and tried, it is found that little significant variation in deposition occurs between one run and the next then N could be very small. If the variations are however large, then N should be chosen as small as possible consistent with the need, if any, to make each occasion as meaningful as possible on its own. Clearly the larger N is the slower and more uneconomic the process becomes, and could only be redeemed if some fairly simple parameterisation scheme emerged.

All these matters await detailed research in the coming year.

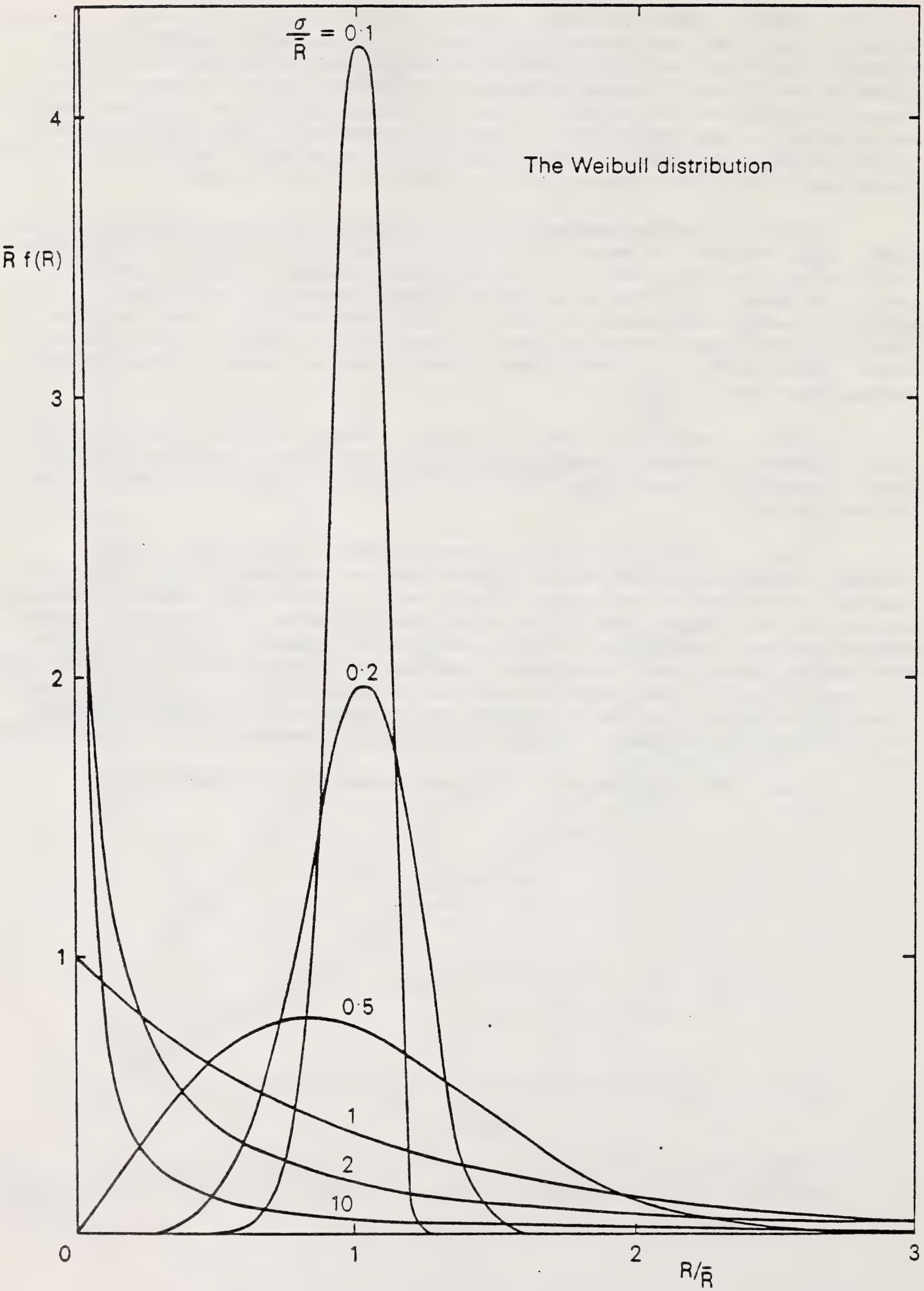

Figure 7. The Weibull distribution f(R) gives the probability of a rainfall R in terms of the population mean rainfall $\bar{R}$ and its standard deviation $\sigma$. The mathematical form of the distribution is as follows:

$$f(R) = \frac{C}{A}\left(\frac{R}{A}\right)^{C-1}\exp\left(-\left(\frac{R}{A}\right)^{C}\right) \quad \text{where} \quad \bar{R} = A\left(\frac{1}{C}\right)! \;, \; \sigma = A\left[\left(\frac{2}{C}\right)! - \left(\frac{1}{C}\right)!^{2}\right]^{1/2}$$

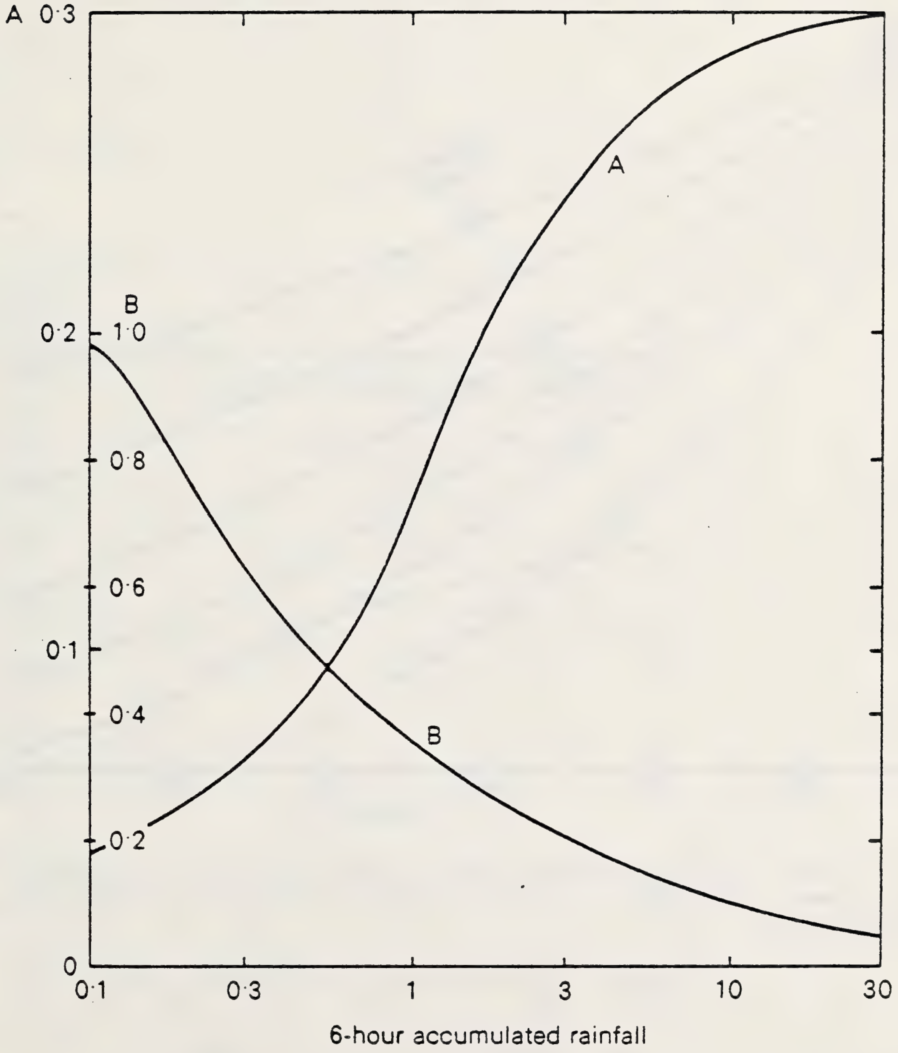

Figure 8. Two probability curves: Curve A is the probability that rain will occur in the next 15-minute time interval given NO rain in the current interval. Curve B is the probability that NO rain will occur in the next 15-minute time interval given some rain fell in the current interval. Both probabilities are expressed in terms of the 6-hour accumulated rainfall (in mm.) within which the intervals lie.

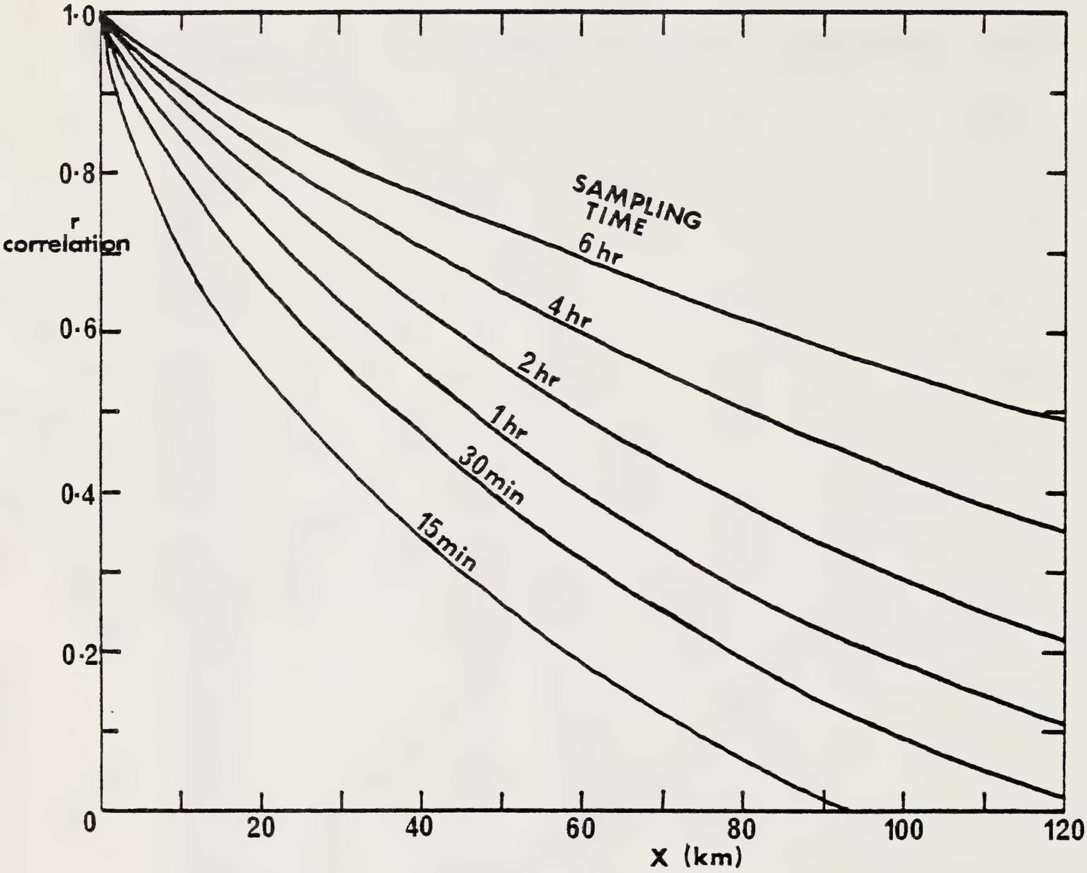

Figure 9. Variation of rainfall-correlation with distance x for various sampling times. The rainfalls are radar measured rainfalls averaged over 5 x 5 km squares.

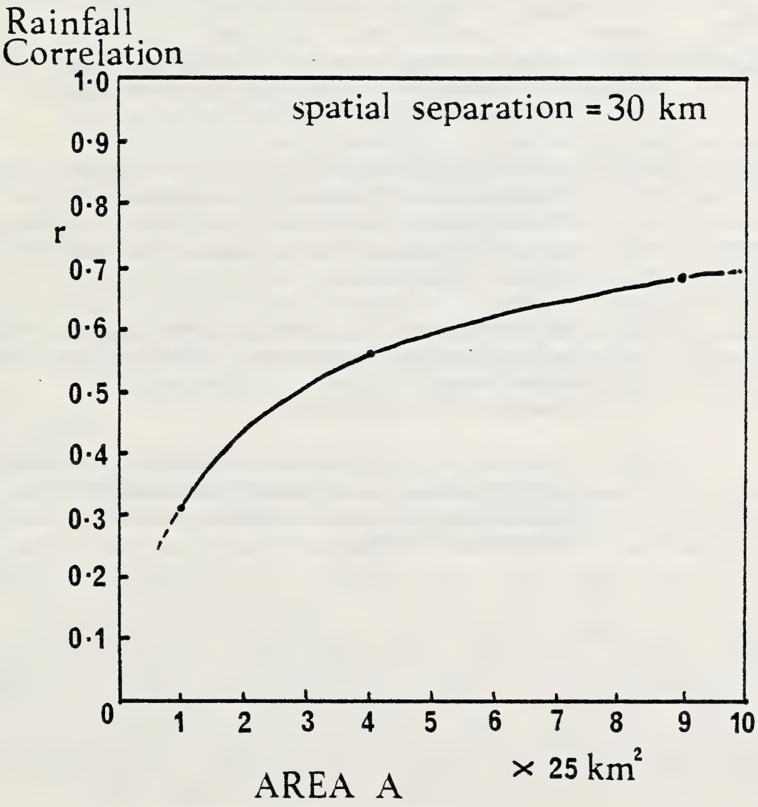

Figure 10. 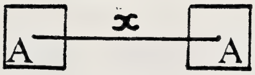

A tentative estimate of how the correlation between areally-averaged rainfall varies as the area A changes for a specified value of x (based on limited data).

## References

| | | |
|---|---|---|
| Drabløs, D. and Tollan, A. | 1980 | Proceeding of an international conference on the 'Ecological Impact of Acid Precipitation". SNSF Project, Oslo. |
| Eliassen, A. | 1978 | The OECD Study of long range transport of air pollutants: long range transport modelling. Atmospheric Environment, Vol.12,pp.479-487. |
| Fisher, B.E.A. | 1978 | The calculation of long term sulphur deposition in Europe. Atmospheric Environment, Vol.12,pp.489-501. |
| Muniz, I.P. and Leivestad, H. | 1980 | Acidification-effects on freshwater fish. pp.84-92 in Drabløs and Tollan (see above). |
| Overrein, L.N.,Seip, H.M. and Tollan, A. | 1980 | Acid precipitation - effects on forest and fish. Final Report of the SNSF-project 1972-1980. Research Report FR 19/80. Oslo. |
| Rodhe, H. and Grandell, J. | 1972 | On the removal time of aerosol particles from the atmosphere by precipitation scavenging. Tellus XXIV,5,pp.442-454. |
| Smith, F.B. | 1980 | Probability prediction of the wet deposition of airborne pollution. Proceedings of the 11th NATO-CCMS International Technical Meeting on Air Pollution Modelling and its Application. pp.1-28. Amsterdam. |
| Smith, F.B. | 1981 | The significance of wet and dry synoptic regions on long range transport of pollution and its deposition. Atmospheric Environment, Vol.15. |
| Venkatram, A. | 1980 | A scheme to incorporate scavenging processes in statistical long-range transport models. Unpublished note, Atmospheric Canada, Downsview, Canada. |

# TETROON FLIGHTS ACROSS A RIDGE

by

R.D. Rowe, S.F. Benjamin, and K.P. Chung
Department of Chemical and Petroleum Engineering
The University of Calgary
Calgary, Alberta, T2N 1N4

Abstract: Two series of tetroon flights across a long reasonably two-dimensional ridge with a crest elevation of $\sim$100 m were performed during the summers of 1977 and 1978. All of the tetroons were ballasted to float at an equilibrium level of 100 m above the ground. The first series of tetroons were released in the daytime. Large instabilities were observed during windy neutral atmospheric conditions as well as on days with strong thermal convection. Under more stable conditions the air flow was observed to reflect the structure of the terrain more closely. The second series of tetroons were released on clear nights when stable atmospheric conditions prevail. The natural air wavelengths for these flights were approximately the same as the total base width of the ridge ($\sim$1.5 km). Some implications for pollutant dispersion calculations in areas of complex terrain are discussed.

## INTRODUCTION

A field program is being conducted around a sour gas processing plant to determine the extent to which a ridge, situated near the stack, affects the air quality and air flow that would otherwise be observed over a flat terrain. A variety of experimental techniques have been used and an overview of all of the results obtained to date has recently been given by Rowe et al. (1981). The objective of these studies is to provide actual field data for air flow and plume diffusion around this ridge that can be used to test the predictions of theoretical and laboratory investigations (e.g. Hunt and Snyder, 1980). This paper describes in detail two series of tetroon flights which were conducted during the summers of 1977 and 1978. The first field study of this type was performed many years ago by Gifford (1953), who used zero-lift pilot balloons rather than tetroons to examine air flow patterns over hilly terrain.

Tetroons have been used as air tracers for a number of years to study both large and small scale transport and diffusion processes. Tetroons are designed such that they can be made to float along a preselected constant density (isopycnic) surface, hence they are primarily suitable for studies of horizontal air trajectories and lateral diffusion problems (Angell, Allen, and Jessup, 1971). However, they respond reasonably well to vertical air motions and in this context vertical air movements over a complex terrain (Hoecker and Angell, 1969) in lee waves (Vergeiner and Lilly, 1970) and over a city (Angell and Bernstein, 1975), for example, have been derived from their use. Indeed, Angell, Hoecker, and Dickson (1977) showed from observations of the vertical motions of paired tetroons that there is good evidence that paired tetroon vertical motions are basically consistent. The implication is that it is meaningful to use tetroons to determine vertical air motions.

Hoecker (1975) has provided a simple scheme for recovering air parcel motions from tetroon derived vertical motions. He assumes that external accelerations are of low order and that the buoyancy restoring force balances the static drag force. Hoecker shows that the tetroon derived vertical velocities are good approximations to air parcel motion for typical convective waves. The range of vertical velocities and periods encountered during our experiment suggests that it is appropriate to use tetroon velocities as indicators of air parcel velocities to first order (Chung, 1979). Therefore, no corrections have been made to the tetroon trajectories to attempt to account for the tetroon dynamics.

## EXPERIMENTAL SITE

The location of these studies was considered suitable for several reasons. The stack is close to a ridge of comparable size; that is, closer than the point of maximum ground level concentration expected for a flat terrain, and the ridge is significant enough to modify the airflow at stack height. The ridge is reasonably well defined so that qualified generalizations to flows in similar cases can be made (Rowe et al., 1981). Figure 1 shows a map of the region, which is located in the foothills to the east of the Rocky Mountains, Alberta. The ridge, called Copithorne Ridge, runs along a line NNW-SSE about 1 km east of the plant. The major source of $SO_2$ is a sulphur recovery plant incinerator stack; the highest point of the ridge is ∿100 m above the base of this stack. Two trailers, routinely recording wind and $SO_2$ data, are situated on the ridge: the NE trailer is placed at the highest point, and the SE trailer is located on a hillock (known as Rhodes Hill) about 23 m below the NE trailer. A second ridge, called Towers Ridge, is situated ∿4 km east of the Copithorne Ridge. It has a comparable altitude to Copithorne Ridge, but it is much larger in width.

## TETROON DEPLOYMENT

The tetroons used in this study are constructed of 2 mil Mylar and when fully inflated occupy approximately 1 $m^3$ of volume. They were inflated with helium and ballasted with sand so that they would float at typical stack heights, i.e. about 100 m above the ground. For a given flight level, it can be shown that the required surface free lift of a tetroon is a function of only one parameter: the temperature difference between the inflation shelter (a large furniture van) $T_s$ and the preselected flight level temperature $T_f$ (Hoecker, 1975). The sensitivity of flight level to lift and $T_s - T_f$ should be noted: one gram of lift is equivalent to about a 10 m change in flight level, and one degree change in the value of $T_s - T_f$ corresponds to 3 g of lift or a 30 m change in flight level. In practise, it was not possible to balance the tetroons much better than ± 1 g.

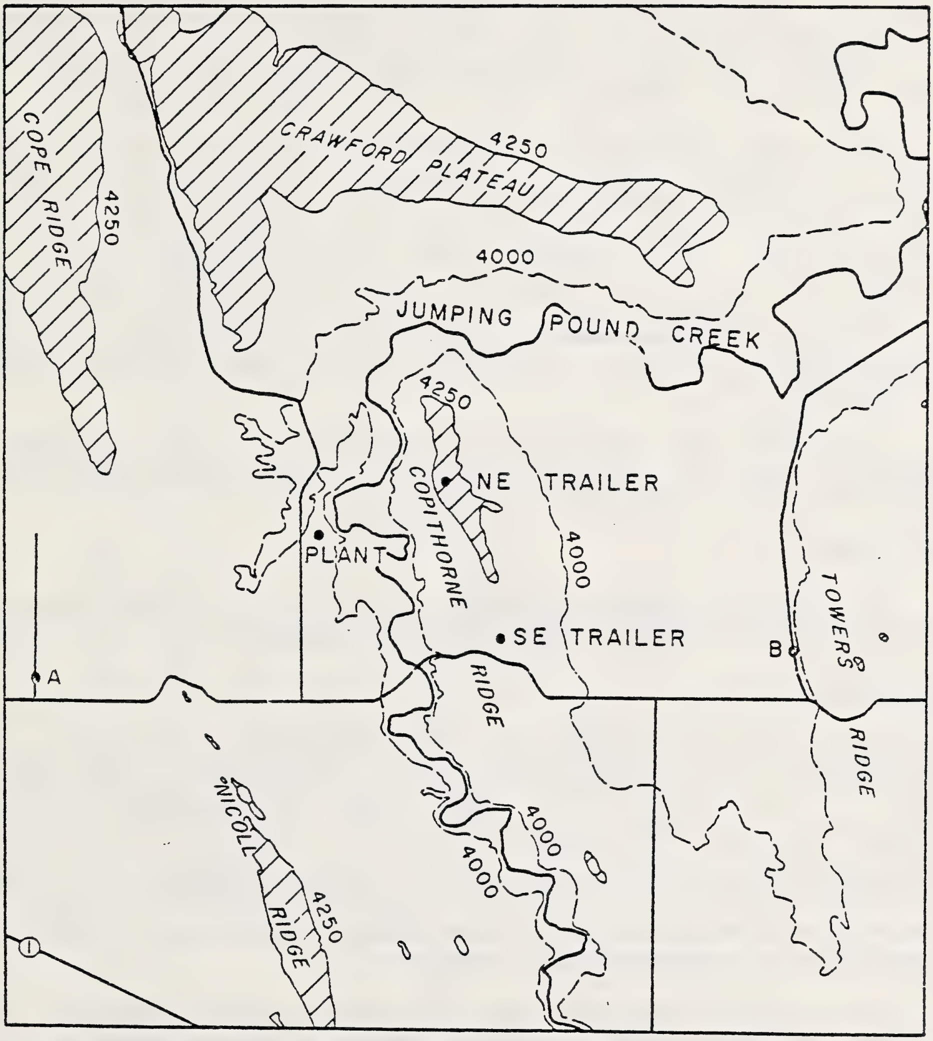

Fig. 1. Map of plant site. Elevation above 4250 feet ASL has been shaded to indicate the topography.

The tetroon release position was determined by the wind direction and location accessibility. A position was chosen such that the nearest high ground downwind was at least 2 km from the release point so that the tetroon could level off over flat terrain. On all days but one reported here there was a west wind. With a west wind the tetroons were released from the road running north-south located about four kilometers west of the plant (position A). For a south or east wind the launching point (position B) was on the north-south running road immediately west of Towers Ridge, see Figure 1.

On the day of an experiment, theodolites were placed near the NE and SE trailers on Copithorne Ridge, which are separated by about 1.3 km. These two theodolites provided maximum coverage for most tetroon trajectories as they were situated on high ground. A third theodolite was positioned at the tetroon release point. Three theodolites were necessary because when the tetroon passed over the crest of Copithorne Ridge it was usually close to one of the trailers and several critical readings were lost from the theodolite near that trailer. Theodolite readings were taken every 30 seconds, and these data were subsequently reduced by the method of Thyer (1962) to determine the tetroon path.

A minisonde pibal was released at the beginning of each experiment to determine the lapse rate $\Lambda$ and the temperature at the tetroon flight level $T_f$. A minisonde was also attached to each tetroon.

## UNSTABLE FLIGHTS

This section provides an analysis of the results of tetroon experiments conducted on three separate days during the summer of 1977.

### Experimental Day 9-6-77

On this day five tetroons were released at approximately hourly intervals between 11 40 and 16 20. Winds below 400 m were moderately strong of strength 12 m/s and from the west. They became lighter and more southerly at greater heights. The lapse rate was approximately adiabatic up to 600 m above ground. Tetroons were released from position A (Figure 1) and the wind carried them over Copithorne Ridge and beyond. Four of the trajectories passed between the two theodolite positions on the ridge with the first trajectory travelling more southerly. The shortest and longest trajectories recorded were 11 and 21 km for tetroons 4 and 2 respectively.

Figure 2a shows the height-time relationships for all tetroons. As seen in Figure 2a, there exists a consistent pattern of tetroon behavior throughout the day. The main feature common to all flights is a wave period of about 20 minutes and amplitude about 800 m. These waves are associated with tetroon vertical velocities of about $\pm$ 2 $m.s^{-1}$. The lapse rates in both the ascent and descent stages of the flights are approximately the same (near adiabatic).

### Experimental Day 22-7-77

On this day seven tetroons were released between 11 40 and 17 40. The temperature difference between the inside and outside of the furniture

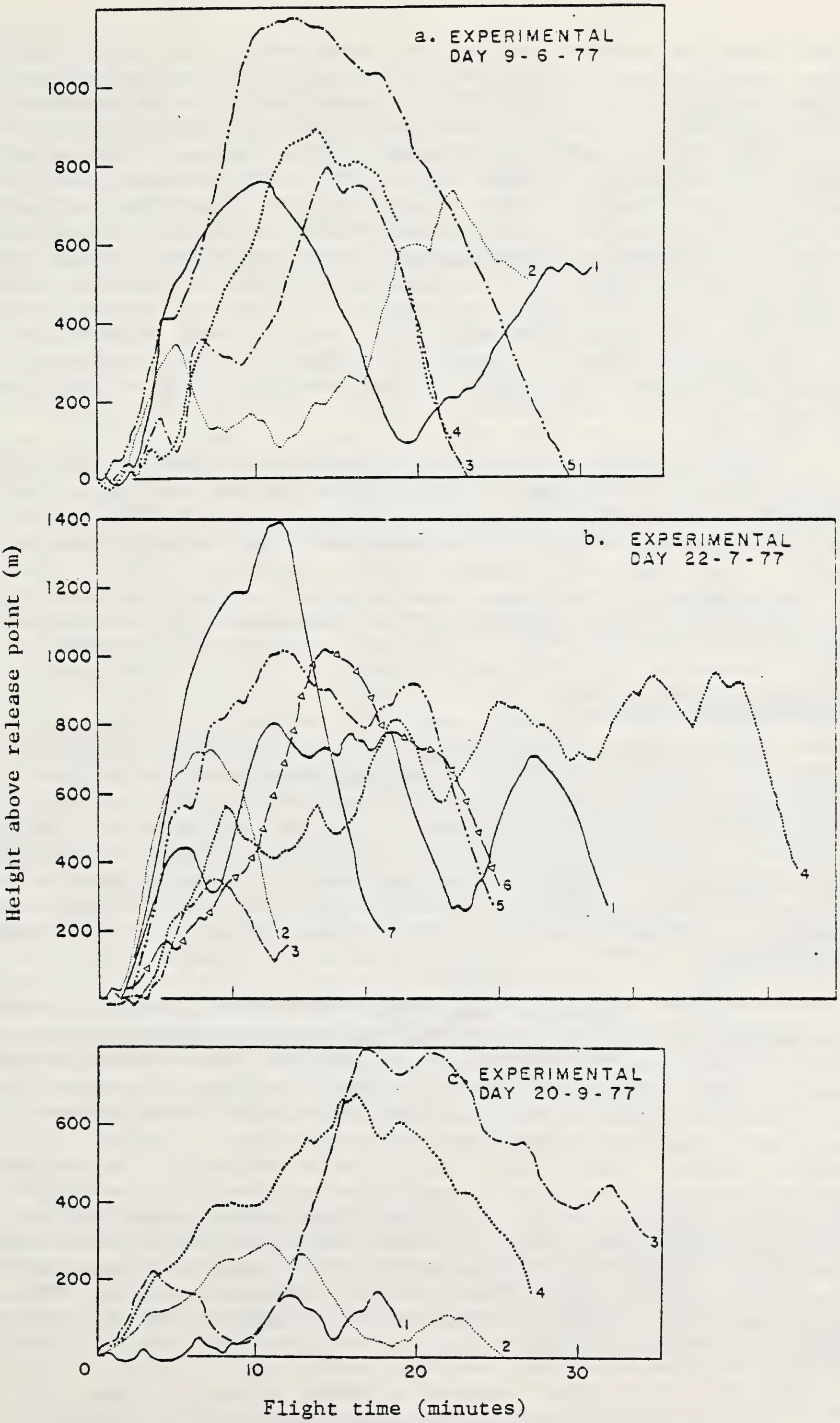

Fig. 2. Unstable tetroon height-time relationships.

van was about the same as that for the experimental day 9-6-77 ($\sim 3^{o}C$). However, this day was characterised by strong solar heating and surface temperatures averaged $\sim 27^{o}C$. A minisonde ascent at 11 00 indicated a slightly stable lapse rate. However in a dynamic convective field a single sounding does not constitute a meaningful average. The atmosphere was probably near adiabatic on the average. Hence the weighing off procedure should have been identical to that used on 9-6-77. Larger weights were added to the tetroons because on previous similar experimental days (not reported here) the tetroons were observed to execute excursions well above their equilibrium level. The surface lifts used during this day should theoretically provide equilibrium levels about 100 m below the release point! Winds were of strength $\sim 7$ m.s$^{-1}$ up to 700 m above ground and from the SE. The tetroons were released from position B at intervals of 30-90 minutes throughout the afternoon. The shortest and longest trajectories recorded were 6 and 22 km for flights 3 and 4 respectively.

These tetroons departed considerably from their equilibrium level and executed waves of various amplitudes and periods; see Figure 2b. Generally, the shorter period waves are of smaller amplitude. The larger waves occurred in the latter part of the experiment when surface temperatures were greatest. The lapse rates recorded on the ascending portions of the waves were superadiabatic. The lapse rates recorded on the descending portions of the flights were roughly one half of the lapse rates recorded in the ascent stages.

### Experimental Day 20-9-77

Four tetroons were released on this day between 09 30 and 12 50 at approximately one hour intervals. The flights were begun early in the morning to examine the effect of stability on tetroon behavior. A pibal wind speed profile showed a maximum of 14 m.s$^{-1}$ at 400 m above ground with winds dropping to 8 m.s$^{-1}$ at higher levels and nearer the surface. Surface winds were from the NW becoming more westerly at higher levels. A chinook arch was observed in the west. The tetroons were released from position A in Figure 1. The longest and shortest trajectories recorded were 19 and 9 km for flights 3 and 1 respectively.

Figure 2c shows the height-time relationships for all tetroons; it can be seen that the tetroon behavior was quite different for each flight. Tetroon 1 flew close to the ground and reflected the variation of surface elevation. This tetroon, which is designated flight A in the next section, peaked downwind of Copithorne Ridge and peaked again over Towers Ridge (Figure 4a). Vertical velocities were about $\pm 1$ m.s$^{-1}$. Tetroon 2 also stayed relatively close to the ground. This tetroon reached its maximum amplitude midway between the two ridges. Vertical velocities of $\pm 1$ m.s$^{-1}$ were observed along its trajectory. Tetroon 3 stayed close to the ground for the first 10 minutes of travel time. The first lower amplitude peak occurred well upwind of Copithorne Ridge. The tetroon was then subjected to a sustained upward motion above Towers Ridge and was carried to heights exceeding 800 m above the release point. Tetroon 4 executed a long wave of period $\sim 30$ minutes peaking above Towers Ridge.

## Discussion of Results

On all three experimental days the tetroons were observed to execute waves of considerable amplitude on a scale much greater than the height variations of the underlying terrain. However, the dynamics of these waves are different. The waves observed on 9-6-77 were relatively consistent in amplitude and period. Winds were moderately strong and insolation was not as high as that on 22-7-77. In contrast the waves observed on 22-7-77 were almost certainly thermally induced because of strong insolation and lighter winds. The variations in amplitude and frequency are characteristic of the differences expected between thermals. The increase in wave amplitude throughout this day reflects the growth of the convective boundary layer. The different temperature structure observed during the ascent and descent portions of the tetroon trajectory suggests that the tetroon is rising in a thermal and subsiding in the more stable environment that surrounds the thermals. The first two tetroons released on 20-9-77 show that under more stable conditions large disturbances are suppressed. The later tetroons on this day suffered instabilities on the scale observed on 9-6-77. These disturbances may have been promoted by thermal convection although, as mentioned earlier, chinook conditions prevailed and these conditions can promote significant instabilities near the surface.

It should be remembered that the purpose of these tetroon experiments was to provide information on the effect of the underlying terrain near the Jumping Pound gas plant on the transport and diffusion processes at typical stack heights ($\sim 100$ m). It is clear that these effects can be masked by large instabilities in the incident turbulent velocity field. These variations can evidently be an order of magnitude greater than any effects expected from the terrain. The possibility does exist, however, that there are terrain influences which are not immediately apparent from the analysis presented so far. Certainly for conditions of strong thermal convection, the structure of the underlying surface determines to a degree the pattern of the spatial and temperature variations observed in the thermal field. Also, under neutral atmospheric conditions and with strong winds the possibility exists of resonance effects promoted by a series of ridges. It is clear, however, that for an unambiguous interpretation of terrain induced disturbances it is desirable that the incident velocity field be substantially free of instabilities on a scale greater than that of the terrain variations. Stable atmospheres with light winds would evidently meet this criteria, and further tetroon flights to investigate the drainage flow from the Rocky Mountains towards the Copithorne Ridge in the early morning hours were therefore conducted the following summer; these flights are presented in the next section.

## STABLE FLIGHTS

This section provides a description of the second series of tetroon flights, which were conducted on clear nights when stable atmospheric conditions prevail. A flashing light device was attached to each nighttime tetroon so that it could be tracked with the theodolites (Chung, 1979). All but one of the 13 flights reported here were made during the summer of 1978; the additional case was obtained from the daytime flights during the previous summer (flight A above). All of these tetroons were released close to point A (Figure 1) in westerly winds. Their horizontal trajectories are shown in Figure 3; the dashed curves denote late evening and nighttime tetroons that

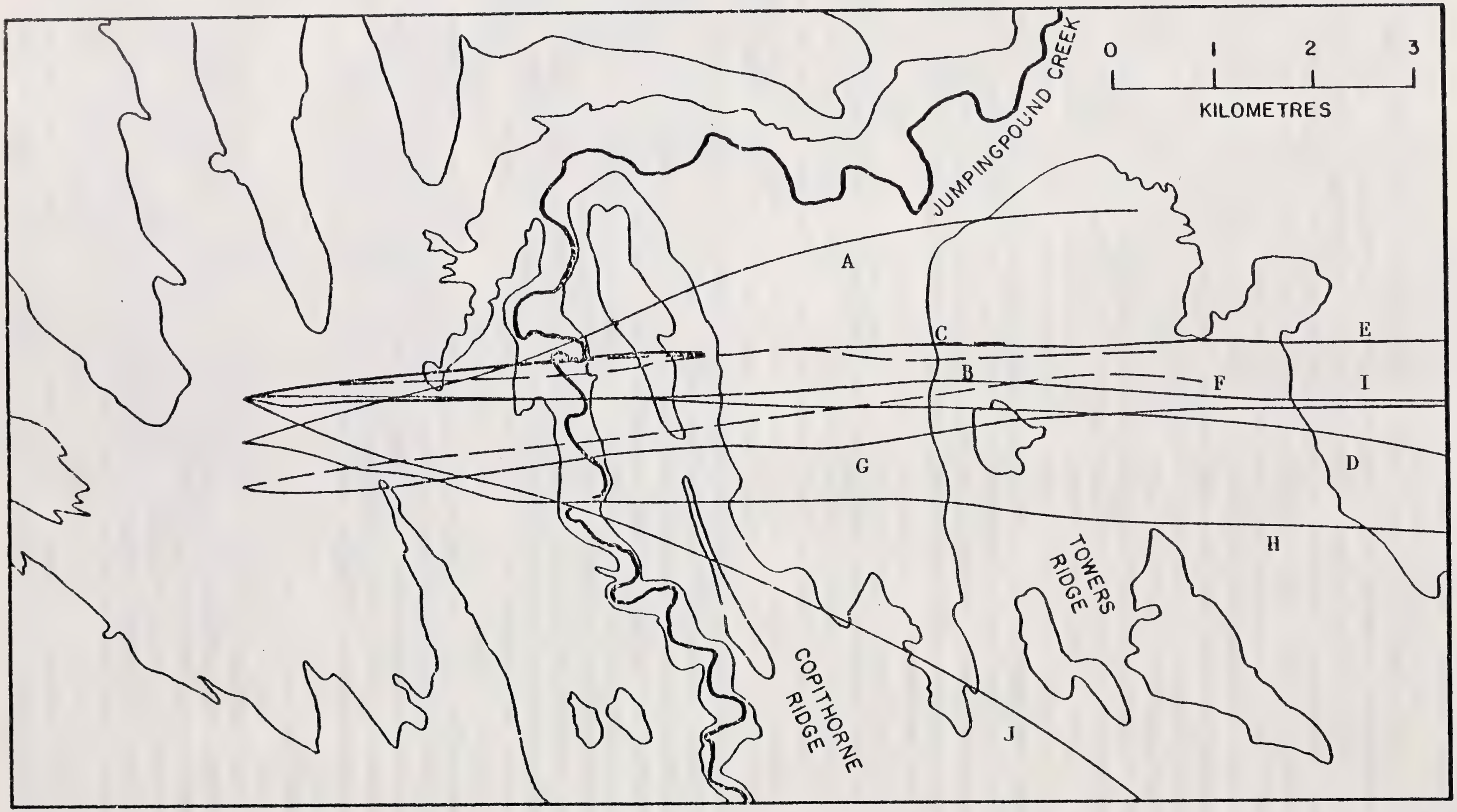

Fig. 3. Horizontal trajectories for stable atmosphere tetroon flights. The contour lines are for the elevations 4000 and 4200 feet ASL.

Table 1. Stable Tetroon Flight Parameters.

| Tetroon | Date | Release Time MDT | Lapse Rate, $\Lambda$ ($^{o}$C/100 m) | Wind Speed, U (m/s) | Natural Air Wavelength, $2\pi U/N$ (m) |
|---|---|---|---|---|---|
| A | 20-9-77 | 0930 | 0 | 10 | 3000 |
| B | 11-7-78 | 2140 | 0 | 8 | 2500 |
| C | 12-7-78 | 0220 | -1 | 12 | 3000 |
| D | 12-7-78 | 0540 | -2 | 14 | 3000 |
| E | 12-7-78 | 0640 | -1 | 12 | 3000 |
| F | 19-6-78 | 0100 | -2 | 8 | 1500 |
| G | 19-6-78 | 0630 | -3 | 8 | 1500 |
| H | 19-6-78 | 0800 | -2 | 5 | 1000 |
| I | 19-7-78 | 0630 | -2 | 8 | 1500 |
| J | 28-6-78 | 0700 | -2 | 6 | 1000 |
| K | 19-7-78 | 0020 | -1 | 7 | 1500 |
| L | 19-7-78 | 0210 | -2 | 5 | 1000 |
| M | 19-7-78 | 0410 | -2 | 7 | 1000 |

required flashing lights, whereas the solid curves denote early morning flights. Flights A-I flew across the ridge in directions that were approximately normal to its crest line. All of these 9 tetroons followed almost straight paths across the ridge. Flights K, L, and M have horizontal trajectories that are very similar to flight J. These flights traversed the ridge at an angle of about 45° to the crest line.

Unfortunately, it was not normally possible to determine the lapse rate $\Lambda$ from the minisonde data more accurately than to the nearest degree Celsius per 100 m. The mean wind speed U could be found from the tetroon flight data to the nearest metre per second. Thus, the natural air wavelength $2\pi U/N$, where N is the Brunt-Vaisala frequency, could only be estimated to the nearest half kilometre. These parameters for each of the 13 flights are given in Table 1. It can be seen that the flights can be grouped into three sets: the natural air wavelengths are about 3, 1.5, and 1 km for flights A-E, F-I, and J-M respectively. The vertical trajectories for each of the three sets are shown in Figures 4 a, b, and c.

The average ridge crest elevation h for these 13 flights is approximately 60 m. The Froude numbers $F = U/(Nh)$ are about 8 and 4 for flights A-E and F-I respectively. For flights J-M, the Froude number based on the component of the wind normal to the ridge crest line is about 2.

## Discussion of Results

The cross-sectional shape of Copithorne Ridge is reasonably symmetrical with a total base width of approximately 1.5 km. Possible flow

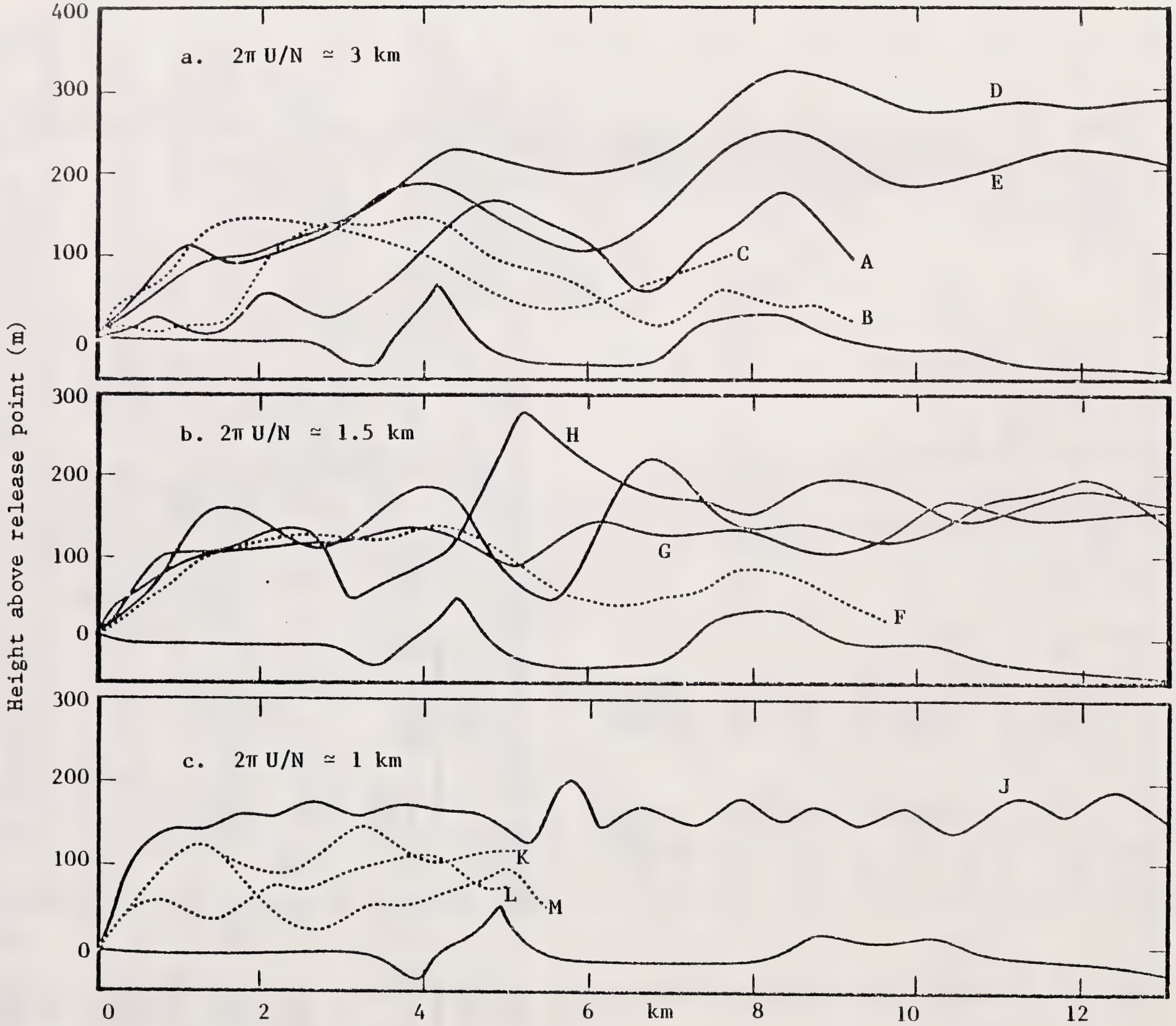

Fig. 4. Vertical elevation of stable atmosphere tetroons as functions of downwind distance.

patterns which may occur when the natural air wavelengths are a little larger and a little less than the total base width of a ridge have been given by Hunt and Snyder (1980) (figures 3(c) and (d) on page 677 of their paper). The natural air wavelengths of flights A-E and F-I are twice as large and the same as the total base width of Copithorne Ridge respectively; however, it is not possible to discern any systematic difference between the two sets of flights (Figures 4a and b). It should be noted that two of the flights, B and F, pass very close to Towers Ridge, which is about 4 km downwind from Copithorne Ridge. This behaviour is presumably due to Towers Ridge being located in phase with the lee wave; see, for example, Scorer (1978) (Fig. 5.16.i on page 202 of his book).

When the Froude number F is less than one ($F < 1$) it is found that the air flow upstream of a terrain obstacle splits into two layers: the lower layer either stagnates or alternatively this layer moves around the terrain feature, whereas the upper layer moves over the terrain feature (e.g. Hunt and Snyder, 1980). When $F > 1$ all of the air flows over the terrain obstacle. Rowe (1980) proposed, for simplicity, that the streamlines in the layer that passes over the ridge, whether it be the upper of two layers or a single layer, can be approximated by potential flow.

The first 9 tetroon trajectories (A-I) are shown together in Figure 5. In this figure, flights A-E ($F \simeq 8$) are denoted by solid curves, whereas flights F-I ($F \simeq 4$) are given by dashed curves. All of these trajectories are, on the average, in reasonably agreement with the potential flow streamline, whose upwind elevation is 100 m, for single layer flow over Copithorne Ridge.

Flights K to M (Figure 4c) could not be tracked further downwind because each tetroon became hidden behind the ridge out of view from the theodolites. These tetroons came very close to the ridge crest, and it therefore appears that the lower air layer was defleted along rather than over the ridge. For the lower air parcel speeds close to the ground, the Froude number could well have been less than one.

For tetroon J, the normal frequency of oscillation of the tetroon was about the same as the natural frequency for the air and it appears that a resonant oscillation of the tetroon was initiated by the displacement caused by the ridge. An investigation of all of the other 12 flights has shown that the observed frequency of oscillation is always a bit slower than the natural frequency for the air (Chung, 1979). The natural frequencies for the air are in turn slower than those for the tetroons themselves. Therefore, it appears that the tetroon trajectories are indeed imitating the vertical air motions.

## IMPLICATIONS FOR POLLUTANT DISPERSION

A detailed analysis of the wind and $SO_2$ data collected at the two trailers on Copithorne Ridge for two two-year periods has been reported by Benjamin and Rowe (1979). One of the two-year periods covers emissions when the incinerator stack height was 68.6 m and the other two-year period is for a new incinerator stack 102.1 m high. The results show that there are a variety of weather types producing peak concentrations at each trailer; a "peak" concentration is defined as any $SO_2$ concentration greater than 0.1 ppm. The weather types providing the highest sum total duration of peak concentrations are the light wind stable and the strong wind neutral atmospheres. Increasing the incinerator stack height reduced the frequency of occurrence of peaks at the NE trailer by about 50% irrespective of weather type with the exception of those during the middle of a summer's day; these frequencies are not significatly different from those for the old stack. This lack of sensitivity of the midday peaks to stack height is due to the large instabilities in the boundary layer structure as observed by the daytime tetroon flights in 1977.

For light wind stable atmospheres (F = 0(1)), if the plume height has about the same or greater elevation than that of the terrain feature then the plume follows the upper layer flow over the topography. Because the diffusion of the plume about its centreline is small for this type of atmosphere, the plume may well clear the crest of the terrain feature completely. This type of behaviour explains the reduced frequency of occurence of $SO_2$ peaks on the ridge crest with increased incinerator stack height. However, the plume could still be brought down to the ground in the lee side flow (Hunt and Snyder, 1980). In particular, the stable tetroon flights have shown that very high ground level pollutant concentrations could occur with multiple ridges suitably phased with the lee waves.

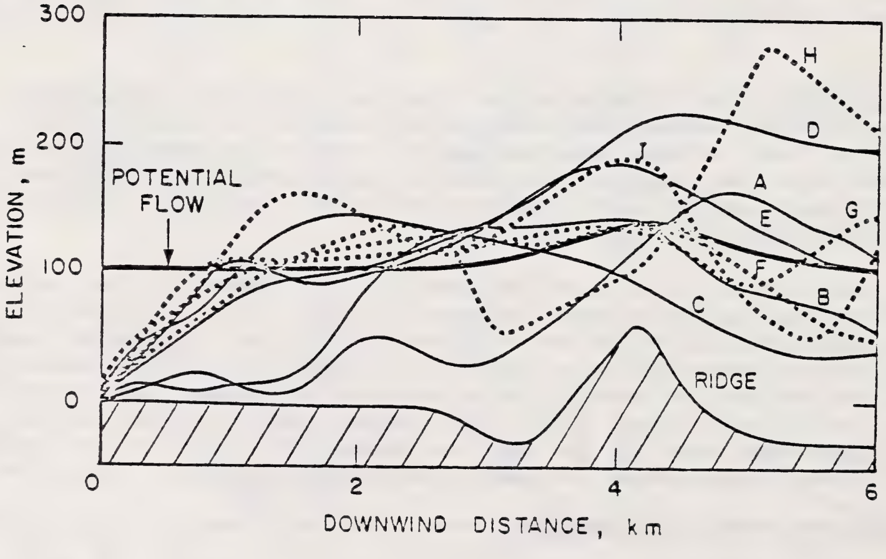

Fig. 5. Stable atmosphere tetroon trajectories compared with the potential flow streamline across Copithorne Ridge.

## ACKNOWLEDGEMENT

These experiments were supported by a cooperative grant from the Alberta Environmental Research Trust and Shell Canada Resources Limited.

## REFERENCES

Angell, J.K., Allen, D.W. and Jessup, E.A.: 1971, "Mesoscale Relative Diffusion Estimates from Tetroon Flights", J. App. Meteor., 10, 43-46.

Angell, J.K. and Bernstein, A.B.: 1975, "Flow Across an Urban Area Determined from Double-theodolite Pilot Balloon Observations", J. Appl. Meteor., 14, 1072-1079.

Angell, J.K., Hoecker, W.H. and Dickson, C.R.: 1977, "Comparison of the Vertical Motions of Paired Tetroon Flights", J. Appl. Meteor., 16, 774-779.

Benjamin, S.F. and Rowe, R.D.: 1979, "Analysis of $SO_2$ Data on a Ridge", 13th Congress of the Canadian Meteorological and Oceanographic Society, Victoria.

Chung, K.P.: 1979, Tetroon Flights Across a Two-dimensional Ridge Under Stable Atmospheric Conditions, M.Sc. Thesis, Univ. of Calgary, Alberta.

Gifford, Jr. F.: 1953, "A Study of Low Level Air Trajectories at Oak Ridge, Tenn.", Mon. Weather Review, 81, 179-192.

Hoecker, W.H. and Angell, J.K.: 1969, "Effect of a Sudden Change in Terrain Height on the Three-dimensional Low-level Air Flow, as Estimated from Tetroon Flights", Mon. Weather Review, 97, 845-849.

Hoecker, W.H.: 1975, "A Universal Procedure for Deploying Constant-volume Balloons and for Deriving Vertical Air Speeds from Them", J. Appl. Meteor., 14, 1118-1124.

Hunt, J.C.R. and Snyder, W.H.: 1980, "Experiments on Stably and Neutrally Stratified Flow over a Model Three-Dimensional Hill", J. Fluid Mech., 96, 671-704.

Rowe, R.D.: 1980, "A Simple Two-layer Model for Stable Air Flow across Terrain Features", Proceedings of the 2nd Joint Conference on Applications of Air Pollution Meteorology, New Orleans, 559-566.

Rowe, R.D. et al.: 1981, "Field Studies of Stable Air Flow Over and Around a Ridge", Atmospheric Environment (in press).

Scorer, R.S.: 1978, Environmental Aerodynamics, Ellis Horwood Ltd.

Thyer, N.: 1962, "Double Theodolite Pibal Evaluation by Computer", J. Appl. Meteor., 1, 66-68.

Vergeiner, I. and Lilly, D.K.: 1970, "The Dynamic Structure of Lee Wave Flow as Obtained from Balloon and Airplane Observations", Mon. Weather Review, 98, 220-232.

# ESTIMATION OF THE RATE OF GASEOUS MASS TRANSFER FROM A SURFACE SOURCE PLOT TO THE ATMOSPHERE

by

J. D. Wilson
Atmospheric Environment Service
4905 Dufferin Street,
Downsview, Ontario, Canada.

G. W. Thurtell, G. E. Kidd, E. G. Beauchamp
Department of Land Resource Science,
University of Guelph,
Guelph, Ontario, Canada.

Abstract: Using the predictions of a trajectory-simulation model of turbulent dispersion it is shown that the rate of gaseous mass transfer from a small (radius $R \lesssim 50$ m) disc-shaped source plot to the atmosphere may be calculated from measurements of mean cup windspeed $\bar{s}$ and mean concentration $\bar{c}$ at a single height ZINST, where ZINST is a function of roughness length $z_0$ and source radius R. This is an inexpensive and simple alternative to the use of a large (~ 300 m fetch) plot and eddy-correlation or profile measurements to determine the source strength.

## INTRODUCTION

A problem which frequently confronts the agricultural meteorologist, the agricultural engineer, and the agronomist is the estimation of the rate of loss of material from the ground to the atmosphere. Recently Denmead et al. (1974) and Beauchamp et al. (1978) have used micrometeorological methods to experimentally determine the rate of loss of nitrogen to the atmosphere (from grazed alfalfa pasture and from sludge applied to a bare field, respectively) and to relate the deduced source strength to other environmental variables. This paper proposes a very inexpensive and simple technique for the determination of surface source strength.

It is possible to estimate the loss from the surface $\overline{F}_z(0)$ from a knowledge of the vertical flux across a plane z in the atmospheric surface layer above the source $\overline{F}_z(z)$, obtained either directly, by the eddy correlation method, or indirectly, by profile methods. If there is no divergence in the horizontal of the horizontal flux and conditions are steady we may write $\overline{F}_z(0) = \overline{F}_z(z)$. The requirement of uniform horizontal flux implies that the experimental situation must be horizontally homogeneous - the measurement of $\overline{F}_z(z)$ must be made with a large upstream fetch of uniform conditions - uniform source strength, roughness length, wind field, and turbulence. As the height z is increased (to alleviate the problem of ensuring adequate frequency response of the sensors) the required length of uniform conditions increases. Therefore a very large experimental plot must be used (with correspondingly large expense). To add to these obstacles, if the profile or Bowen ratio method is used, additional assumptions arise, such as equivalence of the eddy conductivities for different additives, or equivalence of eddy conductivity and eddy viscosity. Given possible unequal source distributions, and the well documented limitations of the concept of an eddy conductivity (see Taylor, 1921; Corrsin, 1974; Tennekes and Lumley, 1972) these are assumptions which one would rather avoid.

These difficulties may be avoided by an alternative approach to the problem. Let the source be a disc of radius R over which $\overline{F}_z(0)$ is assumed to be constant, with a tower at the axis of the disc. The effect of the changing wind direction is to position the tower at the same distance downwind of a changing segment of the source. Therefore dispersion of the gas from the source is in effect a 2-dimensional process, horizontal movement at the cup windspeed (s) and vertical movement with a fluctuating turbulent velocity. Upwind of the tower there is a source strip of width 1 cm and length R from which the average rate of emission is $\overline{F}_z(0)$ . 1 cm . R, and this material must all pass the tower through a vertical strip of width 1 cm and unknown height. Therefore

$$\overline{F}_z(0) = {}^1/_R \int_{z_0}^{\infty} \overline{F}_x(z)\, dz$$

where $\overline{F}_z(z) = \overline{sc}$ , c = concentration. The surface flux to the atmosphere from a uniform disc source may be deduced by measuring the time average profiles of cup windspeed and concentration along the vertical at the axis of the disc and performing an integration on their product. If there is a non-zero background concentration CBACK(z), due to material (of the same species) other than that emitted by the source this must be subtracted from the measured profile before the integration is performed.

## THE TRAJECTORY-SIMULATION MODEL

Wilson, Thurtell, and Kidd (1981a, b, c) have described a method of numerical simulation of particle trajectories in inhomogeneous turbulence and have shown the predictions of the trajectory-simulation (TS) model to be in precise agreement with analytical solutions, where available, and with experimental data for the atmospheric surface layer over a wide range of values of the Monin-Obukhov length L. A particle is moved in the horizontal at a steady height dependent windspeed (in this application the mean cup windspeed) and along the vertical axis with a turbulent velocity $w_L$ having the correct root-mean-square value ($\sigma_w$, the velocity scale) and the correct Lagrangian time scale ($\tau_L$, a measure of the persistence of the vertical velocity. This TS model is similar to that described by Reid (1979). For further details of the TS model the reader is referred to the papers cited above. An important point is that the model predicts that for fixed roughness length and experimental geometry (ie for this application the radius R) the horizontal flux $\overline{sc}$ is independent of $u_*$.

The TS model has been used to investigate the expected profiles of $\overline{sc}/\overline{F}_z(0)$ at the axis of a source disc of radius R, with roughness length $z_0$. It has been found that for given ($z_0$, R) there is a height ZINST at which $\overline{sc}/\overline{F}_z(0)$ is quite insensitive to changes in stability (L) which implies that a measurement at ZINST of $\overline{s}$ and $\overline{c}$ alone is sufficient to determine $\overline{F}_z(0)$ for the plot.

## ESTIMATION OF SOURCE STRENGTH FROM MEASUREMENT AT A SINGLE HEIGHT OF WINDSPEED AND CONCENTRATION

Consider a source disc of radius 50 m at ground and let the roughness length be 1 cm. Specification of the friction velocity is unnecessary because it does not (on its own) affect the profile of horizontal flux. The trajectory-simulation method predicts that the vertical profile of horizontal flux normalized by source strength is a function only of L (for fixed $z_0$ and experimental geometry). Figure 1 presents the profile of normalized horizontal flux for neutral ($L = \infty$), very unstable (L = -5m), and very stable (L = +5m) stratification. In the top corner of the figure, on an expanded scale, are values of the profiles for other values of L at the level at which the profiles for L = +5m and L = -5m intersect. Let us call this level (where the intersection occurs) ZINST ($z_0$, R). Then ZINST (1, 5000) = 191 (all lengths in cm).

The expanded figure shows that at ZINST (1, 5000) all profiles with $|L| \gtrsim 5$m lie between the curves for neutral conditions and L = ± 5m. The spread between these limits, expressed as a % of the neutral value, is about 16%. Thus without knowledge of $u_*$ of L (which will on a large majority of occasions have a magnitude which exceeds 5 m), with a measurement of $\overline{s}$ and $\overline{c}$ (minus $\overline{\text{CBACK}}$ if present) at a single height, ZINST, we may deduce the source strength to within about 8%. The experienced observer, having the ability to roughly guess whether |L| lies near infinity or near 5 m, will do better. For many purposes, an accuracy of 8% is adequate, and the uncertainty will often be less than this (decreasing with decreasing fetch because particle are then confined closer to the surface where buoyancy has little effect on the motion, and with decreasing roughness length, because the windspeed is accordingly higher, decreasing travel times and again confining material closer to the surface).

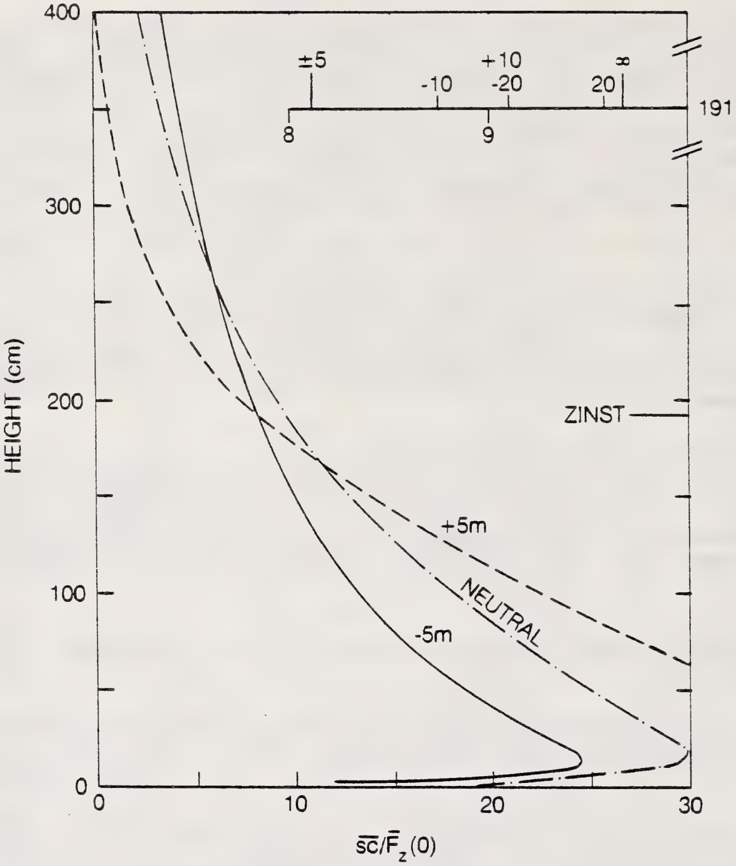

Figure 1. Predictions of the trajectory-simulation model for the vertical profile of dimensionless normalized horizontal flux $\overline{sc}/\bar{F}_z(0)$ at the center of a surface disc source of radius R = 50 m. Roughness length $z_0$ = 1 cm.

———— L = - 500 cm

- - - - - L = + 500 cm

—— - —— L = ∞

The height of intersection of the curves for L = + 500 cm and L = - 500 cm is labelled ZINST. At the top right of the diagram is an expanded scale showing the predicted values of the normalized horizontal flux at z = ZINST for other values of L (given in meters).

Figure 2 summarizes the predictions of the TS model for R = 50 m and $z_0$ = 0.05, 0.1, 0.2, 0.5, 0.75, 1, 2, 5 cm. It should be pointed out that there is a statistical uncertainty in each of the generated profiles of horizontal flux which decreases in proportion to the reciprocal of the square root of the number of particles released. In the profiles summarized here, the uncertainty has been reduced to a very low level, but some smoothing of the profiles was still necessary. This is probably the cause of the small irregularities seen in Figure 2.

As an example of the use of Figure 2, suppose that urea has been applied on a disc of radius 50 m. The surface roughness length 0.1 cm, determined prior to the experiment. A measurement height ZINST(0.1, 5000)=140 cm is chosen. On an overcast breezy afternoon, half hour averages at 140 cm were:

cup windspeed = 500 cm $s^{-1}$

$NH_3$ concentration = $2.5 \times 10^{-4}$ µg $cm^{-3}$

Therefore

$$\frac{500 \times 2.5 \times 10^{-4} \ \mu g \ cm^{-2} \ s^{-1}}{F_z(0)} \simeq 12.0$$

$$\overline{F}_z(0) \simeq 1.04 \times 10^{-2} \ \mu g \ cm^{-2} s^{-1}$$

$NH_3$ is being emitted at a time average rate of $1.0 \times 10^{-2}$ µg $cm^{-2}$ $s^{-1}$, and the uncertainty is much less than 10%. If the same values of windspeed and concentration were observed the next day under clear skies the estimated source strength should be increased by 10%.

## CONCLUSION

The use of a disc-shaped source plot to overcome many of the problems associated with estimation of loss from surface to atmosphere has been briefly discussed. The source strength may be obtained by performing an integration along the vertical of the horizontal flux at the axis of the disc.

A two-dimensional model of turbulent dispersion, described in full elsewhere, has been applied to this two-dimensional experimental geometry to generate and tabulate predictions which may be used to reduce the experimental input to a measurement of the horizontal flux at a single height (rather than the measurement of the complete profile). If the dispersion model is accurate, as is believed to be the case, these predictions allow a substantial reduction in the experimental complexity with little or no loss of accuracy. A more detailed report on this work is given by Wilson et al (1981d, 1982).

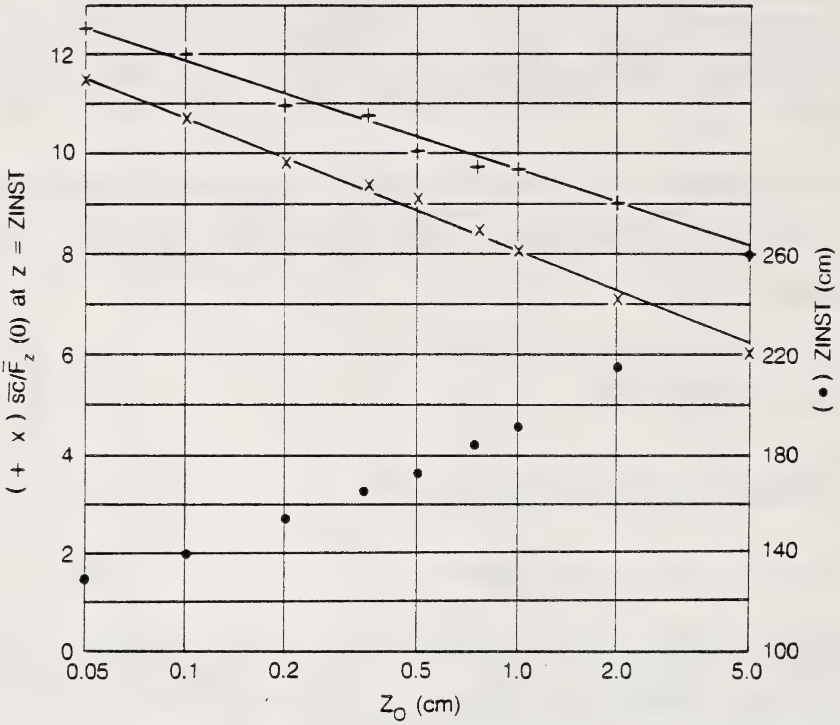

Figure 2. Predictions of the dimensionless normalized horizontal flux $\overline{sc}/\overline{F}_z(0)$ at height ZINST ($z_0$, 5000) for a disc source of radius R = 5000 cm.

| | |
|---|---|
| • | Values of ZINST versus $z_0$ |
| + | Values of normalized flux at ZINST for L = ∞ |
| X | Values of normalized flux at ZINST for L = +500, -500 cm. |

## REFERENCES

Beauchamp, E. G., Kidd, G. E., and Thurtell, G. W.: 1978, "Ammonia volatilization from sewage sludge applied in the field", *J. Environ. Qual. 7*, 141-146.

Corrsin, S.: 1974, "Limitation of gradient transport models in random walks and in turbulence", *Adv. Geophys*. 18A, 25-49.

Denmead, O. T., Simpson, J. R., and Freney, J. R.: 1974, "Ammonia flux into the atmosphere from a grazed pasture", *Science* *185*, *No. 4151*, 609-610.

Reid, J. D.: 1979, "Markov chain simulations of vertical dispersion in the neutral surface layer for surface and elevated releases", *Boundary-Layer Meteorol*. *16*, 3-22.

Taylor, G. I.: 1921, "Diffusion by continuous movements", *Proc. London Math*. *Soc. 20*, 196-211.

Tennekes, H., and Lumley, J. L.: 1972, *A First Course in Turbulence*, M.I.T. Press, Cambridge, Massachusetts.

Wilson, J. D., Thurtell, G. W., and Kidd, G. E.: 1981a, "Numerical Simulation of particle trajectories in inhomogeneous turbulence, I: Systems with constant turbulent velocity scale", to appear in *Boundary-Layer Meteorol*.

Wilson, J. D., Thurtell, G. W., and Kidd, G. E.: 1981b, "Numerical Simulation of particle trajectories in inhomogeneous turbulence, II: Systems with variable turbulent velocity scale", to appear in *Boundary-Layer Meteorol*.

Wilson, J. D., Thurtell, G. W., and Kidd, G. E.: 1981c, "Numerical Simulation of particle trajectories in inhomogeneous turbulence, III: Comparison of predictions with experimental data for the atmospheric surface layer", to appear in *Boundary-Layer Meteorology*.

Wilson, J. D., Thurtell, G. W., Kidd, G. E., and Beauchamp, E. G.: 1981d, "Estimation of the rate of gaseous mass transfer from a surface source plot to the atmosphere", Internal Report, Atmospheric Environment Service, Downsview, Ontario, Canada.

Wilson, J. D., Thurtell, G. W., Kidd, G. E., and Beauchamp, E. G.: 1982, "Estimation of the rate of gaseous mass transfer from a surface source plot to the atmosphere", submitted to *Atmospheric Environment*.

# SHORT-RANGE ATMOSPHERIC TRANSPORT AND DIFFUSION OVER THE PRE-CAMBRIAN SHIELD

by

P.A. Davis and A. Reimer
Whiteshell Nuclear Research Establishment
Pinawa, Manitoba, R0E 1L0

and

S.K. Sakiyama* and P.R. Slawson
University of Waterloo
Waterloo, Ontario, N2L 3G1

Abstract: A series of 50 atmospheric diffusion trials has been conducted over the past two years at the Whiteshell Nuclear Research Establishment under conditions of climate and topography representative of the Pre-Cambrian Shield. Each trial involved the release of a tracer gas, sulphur hexafluoride ($SF_6$), from a 45-m stack, downwind sampling of the tracer, and collection of supporting meteorological information. Lateral and vertical $SF_6$ concentration profiles were measured at distances ranging from 300 m to 12.5 km from the source. Trials were conducted in both summer and winter under a variety of stability conditions. Values of the lateral and vertical dispersion parameters calculated from the observed tracer concentration distributions correlate well with predictions that take into account the effects of surface roughness on the diffusion process.

## INTRODUCTION

The present concept of nuclear fuel waste management in Canada involves the emplacement of immobilized, high-level waste deep within geologically stable rock in the Pre-Cambrian Shield. Atomic Energy of Canada Limited (AECL) has the responsibility of assessing the impact of this means of disposal on the natural and human environment, including the impact of any radioactivity released to the atmosphere. The dispersive properties of the atmosphere are reasonably well known over relatively smooth, uniform terrain under moderate climatic conditions. However, our understanding of dispersion in more complex situations has developed from a series of site-specific experiments which may or may not have any relevance to dispersion over the Shield, with its characteristic surface of forests, lakes, rocks and snow, and its extreme climate.

---

* Present address: Alberta Environment, Edmonton, Alberta T5K 2J6

Accordingly, over the past two years, the meteorology group at the Whiteshell Nuclear Research Establishment (WNRE) at Pinawa, Manitoba, together with researchers at the University of Waterloo, have conducted a series of short-range atmospheric diffusion trials under conditions of climate and topography representative of the Pre-Cambrian Shield. Each diffusion trial involved the release of a tracer gas, sulphur hexafluoride ($SF_6$), from an elevated source, downwind sampling of the tracer, and collection of supporting meteorological information. The data assembled in the study are being used to develop a computer model to predict downwind concentrations of contaminants released routinely or accidentally to the atmosphere from a source on the Shield. This model has been given the acronym AERAD, for atmospheric environment, radioactivity and dose, and the diffusion trials described herein will be referred to collectively as the AERAD project. The purpose of this paper is to acquaint other workers in the air pollution field with the extensive data set collected during the AERAD program, and to report some preliminary results of its analysis.

## PHYSICAL SETTING

The WNRE site (Figure 1) is located in south-eastern Manitoba, about 100 km east-north-east of Winnipeg, in the broad, shallow basin containing the Winnipeg River. The walls of this basin rise gradually to 35 m above the valley floor 50 km to the east of WNRE, and to 15 m above the floor at the crest of Milner Ridge 10 km to the west. The elevation of the basin drops 50 m over a 50 km distance as it opens out onto the lowlands adjoining southern Lake Winnipeg to the north.

On the large scale, the terrain to the south and west of the site is fairly flat parkland, the vegetation consisting of agricultural crops interspersed with mixed stands of deciduous and coniferous trees. To the north and east, the land is more rolling and is covered by coniferous trees of the Boreal forest, averaging about 10 m in height, broken by an occasional patch of farmland. Wind profile measurements performed above the forest indicate approximate values for the surface roughness $z_0$ and zero-plane displacement d of 0.6 and 8 m respectively.

The WNRE site itself consists of a number of relatively low buildings scattered throughout a clearing one kilometre in diameter in the surrounding forest. The Winnipeg River flows from south to north through the western side of the site in a narrow cut about 12 m below the general level of the terrain. Seven kilometres south of the site, the river flows from the east and broadens to a width of 2.5 km behind a major hydroelectric dam. The vegetation adjacent to the site consists of Boreal forest interspersed with swamp and a few open fields. More extensive open areas are found a few kilometres to the north and south.

Southern Manitoba experiences a semi-arid, continental climate. The area is snow-covered during four to six months of the year.

## EXPERIMENTAL PROCEDURE

### Dispersion Measurements

The AERAD trials were conducted during three main periods:

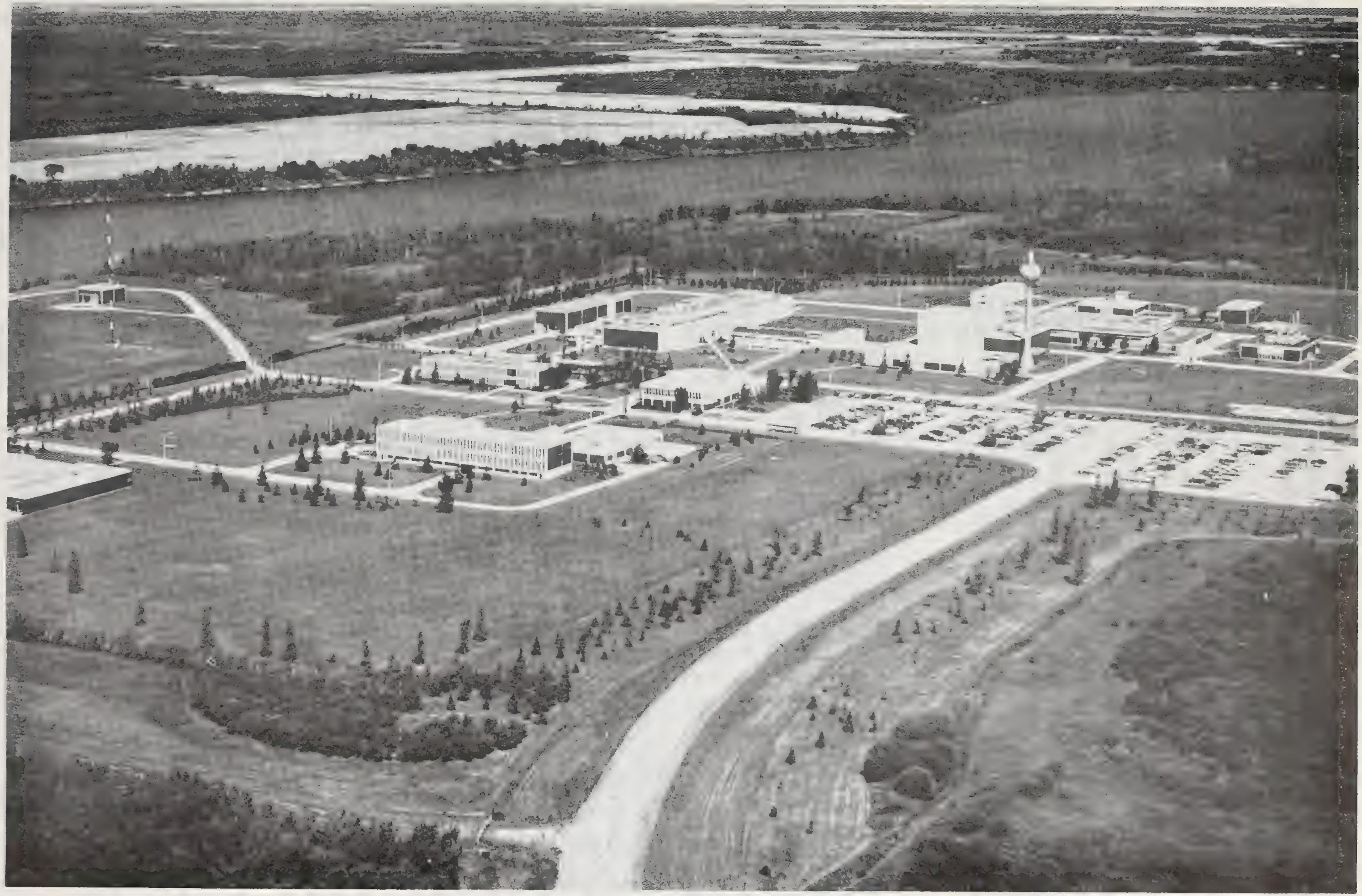

FIGURE 1

Whiteshell Nuclear Research Establishment Site

1979 July-September; 1980 June-August; and 1980 November-1981 March. Trials were run only when the meteorological conditions were expected to remain steady, and only on precipitation-free days.

A few trials involving ground-level releases were conducted, but will not be discussed here. The emphasis was placed on dispersion from an elevated source since the most likely source of radioactivity emitted to the atmosphere from a nuclear fuel waste repository will be the stack associated with the surface facility that will process the waste prior to actual underground storage. In the AERAD trials, the tracer gas was injected into the main stack of the plant (see middle right of Figure 1). This stack is 45 m high and 1.52 m inside diameter at the exit point. The stack gases have an exit velocity of approximately 26 $m \cdot s^{-1}$ and a temperature of 38°C. A numerical plume-rise model (Slawson et al., 1979) adequately describes the observed plume behaviour. Under typical conditions, plume rise increases the effective height of the stack to about 65 m.

In each diffusion trial, the $SF_6$ was injected into the ductwork at the base of the stack. The release rate was set approximately by a regulator valve to give concentrations about two orders of magnitude above background $SF_6$ levels ($<10^{-12}$ L/L in the WNRE area) at the downwind sampling location. The precise release rate in effect during the trial was determined by weighing the $SF_6$ cylinder before and after the trial. The length of release varied from one-half hour during neutral or stable conditions, when atmospheric turbulence is dominated by relatively small-scale eddies, to one hour during unstable conditions, when larger eddies predominate.

Prior to the start of the AERAD project, markers indicating the azimuthal bearing from the stack were set up at 2° intervals along all roads within 15 km of the WNRE site. Each diffusion trial began with the installation of samplers at (and occasionally between) these locations along roads that were expected to intersect the plume. In a limited number of trials, vertical profiles were also obtained by suspending samplers from the tetherline of a captive balloon of 26 $m^3$ volume. The samplers themselves consisted of inexpensive, battery-powered Kassner aerating pumps (similar to those described by Sawford and Manins (1979)) which pumped air into disposable polyethylene bags for later analysis. The pumps were triggered remotely by a radio-frequency signal to a servo-switch. Thus all the samplers in a vertical string could be activated simultaneously once the balloon was at its maximum altitude. Samplers in the ground string could not all be turned on simultaneously because of the limited range of the transmitter, but the delay was no more than one or two minutes between the extreme ends of the string.

In the first year of the trials, two cross-wind arcs of samplers were usually set up, with 11 samplers spaced at 2° intervals on each arc. In subsequent trials, a single arc of 21 samplers was used, spaced at 1° intervals near the expected centreline of the plume and at 2° intervals near the edges. The number of vertical samplers was limited to seven by the lift of the balloon; the samplers were usually equally spaced along the tether-line to a maximum height of 300 m.

The $SF_6$ concentration in the air samples was determined using electron-capture gas chromatography, which was carried out routinely by the Analytical Science Branch at WNRE (Arneson and Chambers, 1981). In the first year of the trials, standard gas-chromatographic procedures provided a sensitivity of $10^{-11}$ L/L; subsequently, a preconcentration technique extended the sensitivity to $5 \times 10^{-13}$ L/L. Results from a given sample were reproducible to ± 5%; the absolute magnitude of the concentration, which depends upon calibration with a standard of known concentration, is accurate to ± 15%.

### Meteorological Measurements

Measurements of the mean atmospheric flow are made routinely at WNRE at the 6.6-, 26-, and 60.4-m levels of a 61-m tower, located in a clearing 500 m to the west of the stack (Figure 1). At each level, Bendix-Friez aerovanes measure wind speed and direction, and platinum resistance thermometers, in Beckman-Whitley aspirated radiation shields, measure air temperature. Other measurements made routinely near the tower include net radiation, hours of bright sunshine, cloud type and amount, and soil temperature, moisture and heat flux.

Profiles of mean wind speed, wind direction and air temperature above the height of the tower were obtained during each diffusion trial by means of double theodolite minisonde flights. Temperature soundings were taken twice during each trial, once at the start of gas release and once at the end of sampling. These soundings provided a reliable estimate of the height of the mixed layer. Pibal flights at 20-minute intervals were run between the minisonde ascents.

Fast-response, turbulence measurements were also made during each diffusion trial. Gill U-V-W anemometers were installed at the 6.6- and 60.4-m levels on the main tower, and a Gill anemometer-bivane was located at 26 m. Custom-made, fast-response temperature sensors consisting of 25 thermocouples were installed in conjunction with the U-V-W anemometers. Signals from all of these sensors were sampled at 10 points per second over a time interval somewhat longer than the $SF_6$ sampling time and recorded directly onto magnetic tape. These measurements provide estimates of the variances of the meteorological parameters, together with heat and momentum fluxes, Monin-Obukhov lengths, and spectra for use in interpreting the diffusion data.

## RESULTS

### The Data Set

A total of 47 diffusion trials involving the elevated source have been run to date. Some of these trials resulted in data that were not suitable for further analysis because of low or non-detectable concentration levels, incomplete coverage of the plume, or meteorological conditions that were not steady in time. Elimination of the unsuitable data left 30 reliable cross-wind distributions of concentration obtained at distances ranging from 0.75 to 12.5 km from the source. Near-neutral conditions prevailed during the majority of these trials, but stable and unstable conditions are also represented. Seven of the trials were run in winter; five of these were run over snow-covered ground. In addition, nine reliable vertical distributions of concentration were obtained, at distances ranging from 310 m to 4.5 km from the stack, again mostly under near-neutral conditions. The 30 ground-level distributions can also be used to deduce information about the vertical profile. Values for all the meteorological parameters discussed in the above section are available for each trial, except in isolated cases of instrument failure. Examples of a horizontal and a vertical concentration distribution are shown in Figure 2.

The results to date have been analysed using the Gaussian plume approximation for atmospheric dispersion. More complex models do not appear warranted since the input data on the wind field was one-dimensional, the trials were limited to short downwind distances, and only steady-state situations were studied. The following discussion will therefore deal with the Gaussian dispersion parameters $\sigma_y$ and $\sigma_z$, respectively the horizontal and vertical standard deviations of mass within the plume.

The experimentally determined values of $\sigma_y$ and $\sigma_z$ will be compared with values predicted by schemes already in use in the literature. The data were not used to produce a site-specific prediction scheme for two reasons: (i) the data set, although extensive, is not complete enough to provide a reliable prediction scheme under all meteorological conditions; (ii) a new site-specific scheme would simply become one of several such schemes in the literature, and would not further the search for a generalized description of atmospheric dispersion.

## Lateral Dispersion

Many of the ground-level concentration distributions were obtained along roads which did not lie perpendicular to the axis of the plume. It is standard practice under such circumstances to project the measured concentrations onto a line y which does lie at right angles to the axis. The errors produced in $\sigma_y$ through this procedure are small when the angle $\alpha$ between the road and the axis is small, but increase rapidly when $\alpha$ exceeds 25°. In addition, the standard methods for calculating $\sigma_y$ from the projected concentrations result in large errors if the edges of the plume are not well defined by the measurements. A number of the horizontal distributions measured during the AERAD trials were obtained along roads for which $\alpha$ exceeded 25°, and in several of the cases the edges of the plume were not well defined. Rather than discard these data, a new technique to calculate $\sigma_y$ was devised which provides reliable estimates despite these difficulties.

The ground-level concentration in a Gaussian plume at a point (x,y) in a coordinate system with the origin at the source, the x-axis defined by the plume axis and the y-axis perpendicular to the plume axis in the horizontal plane, is given by

$$C = \frac{Q}{\pi \bar{u} \sigma_y \sigma_z} \exp\left[ - \frac{y^2}{2\sigma_y^2} - \frac{H^2}{2\sigma_z^2} \right] \tag{1}$$

where Q is the source strength, $\bar{u}$ an appropriately defined mean wind speed, and H the effective release height. The x-dependence of C is contained implicitly in $\sigma_y$ and $\sigma_z$. Equation (1) can be re-written as

$$C = C_o (x) \exp\left[ - \frac{y^2}{2\sigma_y^2} \right] \tag{2}$$

where $$C_o(x) = Q \exp\left[-H^2 / 2\sigma_z^2\right] / \left[\pi\bar{u}\sigma_y\sigma_z\right]. \tag{3}$$

$C_o(x_o)$ is simply the concentration at the intersection of the plume axis and a sampling road a distance $x_o$ from the source, and is usually well defined experimentally. If the road is perpendicular to the plume, then the lateral distribution of concentration along the road can be written as

$$C = C_o(x_o) \exp\left(\frac{-y^2}{2\sigma_y^2}\right) \tag{4}$$

which is a function of y only. If the road is at an angle to the plume, as in Figure 3, then Equation (2) must be used in full generality. Assume now that there exists a function $\eta(x) = ax^b$ such that

$$C = C_o(x_o) \exp(-y^2 / 2\eta^2) \tag{5}$$

describes the concentration distribution along the oblique road. Note, by comparing Equations (4) and (5), that $\eta(x_o) = \sigma_y(x_o)$. Then, at sampling location i in Figure 3, the concentration is given by

$$C = C_o(x_o) \exp\left[-\frac{y^2}{2a^2(x_o + \Delta x_i)^{2b}}\right]. \tag{6}$$

The values of a and b can be determined by a least-squares fit of (6) to the measured concentration distribution; the desired value of $\sigma_y$ is then obtained by evaluating $\eta(x_o)$. It can be shown that this method produces accurate estimates of $\sigma_y$ even when the sampling string is at large angles to the plume's axis, and when the edges of the plume are poorly defined.

The $\sigma_y$ values obtained in the above way were compared with the prediction schemes of Vogt and Geiss (1964), Briggs (1974), Draxler (1976), Pasquill (1976) and Hay and Pasquill (1959). These schemes were chosen from the many available because they are based to some extent on data obtained under conditions of topography, release height and sampling duration similar to those of the AERAD trials. The $\sigma_y$ values of Vogt and Geiss were derived empirically from tracer releases from a 50-m source over forested terrain with a somewhat greater roughness than is found over the Shield. Briggs combined empirical results from a number of diffusion experiments with various release heights and surface roughnesses. Since both of these schemes are organized in terms of the Pasquill-Gifford (P-G) stability classes (Pasquill 1961; Gifford 1961), it was necessary to assign a P-G class to each of the AERAD trials; this was done through the correspondence (Slade, 1968) between P-G class and $\sigma_A$, the standard deviation in horizontal wind direction, in this case derived from the U-V-W measurements at 60.4 m.

The representations of Hay and Pasquill, of Draxler and of Pasquill for $\sigma_y$ are based upon Taylor's (1921) statistical treatment of the diffusion problem. This treatment provides a Lagrangian description of diffusion in terms of the intensity of turbulence present in the atmosphere and so includes implicitly the effects of surface roughness. Hay and Pasquill reduced Taylor's expression for the lateral diffusion parameter of an ensemble average of particle displacements in a homogeneous, stationary field of turbulence to the form

$$\sigma_y{}^2 = \overline{v'^2}_{\tau\,,T/\beta}\; T^2 \tag{7}$$

where $\overline{v'^2}$ is the variance in the lateral velocity and T is the travel time of the particle. The subscripts on $\overline{v'^2}$ indicate that the variance is formed by first averaging the time series, of length $\tau$, over time intervals $T/\beta$. Here $\beta$ is the ratio of the Lagrangian to Eulerian time scales:

$$\beta = T_L \,/\, T_E$$

where $$T_L = \int_0^\infty R_L\ (\xi)d\xi \text{ and } T_E = \int_0^\infty R_E\ (\xi)d\xi$$

where $R_{L,E}$ $(\xi)$ is the appropriate correlation coefficient at lag time $\xi$. The presence of $\beta$ in E. (7) arises through an assumption made by Hay and Pasquill to relate the Lagrangian formulation of Taylor's original derivation to the more readily measurable Eulerian quantities. Equation (7) is also subject to the restriction $T < \tau$, which was satisfied in all the AERAD trials.

Since $T = x/\bar{u}$ and $\left[\overline{v'^2}\right]^{\frac{1}{2}}/\bar{u} \sim \sigma_A$, Eq. (7) can be written as

$$\sigma_y = \sigma_{A_{\tau,T/\beta}}\; x\ . \tag{8}$$

This is the form in which comparisons were made between the Hay-Pasquill formulation for $\sigma_y$ and the measured values. In practice, $\beta$ was determined from

$$\beta = 0.44/\sigma_A, \tag{9}$$

a relationship suggested by Pasquill (1974), in which $\sigma_A$ is now the unsmoothed standard deviation evaluated over the entire length of record. The travel time T was calculated using the mean wind speed at 60.4 m and the standard deviation $\sigma_{A_{\tau,T/\beta}}$ calculated from the output of the 60.4-m U-V-W sensor over a time interval equal to the $SF_6$ sampling time, but advanced by T.

The formulations of Draxler (1976) and of Pasquill (1976) for $\sigma_y$ are based upon approximations to Eq. (8). Draxler assumes that

$$\sigma_y = \sigma_A\, x\, f_D\ (T/T_L) \tag{10}$$

where $\sigma_A$ is the total standard deviation in the horizontal wind direction, and $f_D$ is a function derived empirically from a wide range of diffusion data.

Although in Draxler's formulation $f_D$ is not a function of stability for elevated releases, it is meant to take into account the averaging of $\sigma_A$ in Eq. (8). Similarly, Pasquill assumes that

$$\sigma_y = \sigma_A \times f_P(x),$$

identical in form with Eq. (10), although $f_P$ differs in functional form from $f_D$, and is a function of downwind distance x rather than travel time T. The functions $f_D$ and $f_P$ can be readily calculated for each AERAD trial.

The comparison between the measured values of $\sigma_y$ and the literature values is given in Table 1 in terms of the statistics obtained from regressing the measured values on the literature values. Table 1 shows that the prediction methods of Vogt-Geiss, of Briggs and of Draxler over-estimate the lateral dispersion observed over the Shield. Pasquill's (1976) method provides quite a good estimate in the mean to the measured $\sigma_y$ values, but the scatter is still quite large, as shown in Figure 4. The Hay-Pasquill method, when applied to the data set as a whole, produced poor results characterized by over-estimation and large scatter. However, as shown in Figure 5, measured versus predicted $\sigma_y$ values tend to group into two classes, termed stable and unstable, for reasons which will become clear. The statistics of the regression lines for these two classes (given in Table 1) indicate that this method of organization results in significantly less scatter than do the other methods. Fourteen of the eighteen $\sigma_y$ values in the stable branch were measured on days characterized by lapse rates (between the 6.6- and 60.4-m levels) greater than the dry adiabatic lapse rate $\Gamma$; in the remaining four cases, very slightly unstable lapse rates were observed. Similarly, lapse rates less than $\Gamma$ were obtained on eight of the eleven days contributing points to the unstable branch, and in the three remaining cases, lapse rates were only slightly stable. The duality apparent in Figure 5 thus appears to be related to atmospheric stability. Equation (8), as applied here, somehow fails to describe the often dramatic changes which occur in the nature and intensity of turbulence as the atmosphere passes through neutrality. The Lagrangian-Eulerian relationship suggested by Hay and Pasquill (1959) may take on different forms in the stable and unstable modes, Eq. (9) for $\beta$ may not be of the correct form in one or the other of the modes, or it may be necessary to use variables measured at different heights when applying Eq. (8) in the different modes.

Results for the five trials conducted over snow-covered ground are indicated by the symbol x in Figures 4 and 5. In both cases, these values show a distribution similar to that of the summer results, indicating that lateral diffusion, when scaled in terms of directly measured turbulence parameters, is independent of the presence of snow cover.

## Vertical Diffusion

The discussion on vertical diffusion will centre on the values of $\sigma_z$ obtained from the directly measured vertical distributions of concentration. Values of $\sigma_z$ have also been determined indirectly from the ground-level distributions by solving Eq. (3) for $\sigma_z$ using experimentally measured values for Q, $\bar{u}$, $\sigma_y$ and $C_o(x_o)$. For the most part, these indirect values order reasonably well when scaled in the traditional ways, but a significant number are much larger, suggesting that the measured ground-level concentrations in these

Table 1. Statistics of the Regression Lines of Measured $\sigma_y$ Values upon Predicted Values for Different Prediction Schemes.

| Scheme | Slope | Intercept | Correlation Coefficient | Standard Deviation of Residuals |
|---|---|---|---|---|
| Vogt & Geiss (1964) | 0.66 | 31.2 | 0.94 | 85.8 |
| Briggs (1974) | 0.82 | 53.0 | 0.93 | 74.1 |
| Draxler (1976) | 0.62 | 44.4 | 0.93 | 97.7 |
| Pasquill (1976) | 0.94 | 24.8 | 0.93 | 63.8 |
| Hay & Pasquill (1959) | 0.66 | 95.4 | 0.82 | 126.8 |
| Stable | 1.21 | 1.0 | 0.98 | 28.8 |
| Unstable | 0.64 | 9.5 | 0.99 | 37.7 |

cases are too low. Since $SF_6$ is an inert gas, it is unlikely that any would be lost through ordinary deposition processes between the source and the samplers. More probably, the lower part of the plume may be entrained in the forest and held up for so long that it is unable to reach the sampling location during the sampling interval. Alternatively, the vertical diffusion in these cases may be sufficiently different from Gaussian that application of Eq. (3) leads to meaningless results. These possibilities and others are currently being investigated and conclusions regarding the indirectly measured $\sigma_z$ values will be reported in the future.

The vertical diffusion parameter is obtained from the vertical distribution of concentration through the relationship

$$\sigma_z = (M_2/M_o - H^2)^{\frac{1}{2}} \qquad (11)$$

where $M_n$ is the $n^{th}$ moment of the distribution about the surface:

$$M_n = \int_0^\infty Cz^n \, dz .$$

Equation (11) will give meaningful results in terms of a Gaussian diffusion parameter only in cases where the atmospheric stability is not a strong function of height. It was therefore necessary to eliminate from further analysis four distributions which were obtained when either a shallow ground-based inversion or a low-level elevated inversion was present. The remaining five profiles were not complete in the sense that the concentration at the highest measurement level was typically still 20% of the maximum concentration. However, the distributions were sufficiently smooth that the profiles could be extrapolated to background levels, with confidence, and reliable $\sigma_z$ values obtained.

The $\sigma_z$ values calculated in the above fashion were compared with the predictions of the literature schemes discussed in the previous section, with a few modifications. Pasquill (1976) did not provide a function analogous to $f_P(x)$ for vertical dispersion, so comparisons with this scheme are not possible. Also, the standard deviations of the time series of vertical velocity, averaged in the appropriate way, are not yet available for the AERAD trials, so comparison with a form equivalent to Eq. (8) is not possible. Draxler's (1976) expression for the vertical diffusion parameter is

$$\sigma_z = \sigma_E \times g_D(T/T_L)$$

where $\sigma_E$ is the total standard deviation in vertical wind direction, measured at the 60.4-m level for these comparisons, and $g_D$ is a function of both stability and travel time. A further scheme, due to Smith (1972) and Hosker (1974), has been included in these vertical comparisons. The Smith-Hosker method is a semi-empirical scheme which allows explicitly for the effect of surface roughness on vertical diffusion; the calculations performed here used a roughness length of 60 cm. This scheme, as well as those of Vogt and Geiss (1964) and Briggs (1974), require specification of the P-G stability class. This was again determined for each AERAD trial through the use of $\sigma_A$ measured at 60.4 m.

The statistics of the regression lines of the measured $\sigma_z$ values on the predicted values are shown in Table 2. These figures should not be given too much significance because of the small sample size, but two results emerge fairly clearly. First, all schemes except that of Smith and Hosker over-estimate the measured vertical dispersion, and secondly, the least scatter is obtained by using either the Smith-Hosker or Draxler method. This latter result is to be expected since these schemes incorporate more of the physics of diffusion than do either of the other two. The Draxler scheme appears to predict the vertical diffusion parameter more reliably than it did the lateral; this may result from the fact that $g_D$ is a function of stability while $f_D$ is not. The individual data points for the Smith-Hosker and Draxler comparisons are shown in Figure 6.

## SUMMARY AND CONCLUSIONS

The AERAD trials have resulted in an extensive set of diffusion and meteorological data representative of the climate and topography of the Pre-Cambrian Shield. This data set includes direct measurements of vertical diffusion, and measurements made in winter over a snow surface, two aspects of diffusion which have received little previous attention. Reports containing a detailed listing of the data collected during the trials are in preparation and will be available shortly.

Gaussian dispersion parameters extracted from the concentration measurements were found to correlate well with predictions which take into account, either implicitly or explicitly, the effects of surface roughness on the dispersion process. This is certainly not an unexpected result, but it is also not particularly useful in generalizing the results to other sites unless correlations can be found between the specialized fast-response measurements required by these theories and meteorological parameters which are more routinely available. Such correlations are presently being sought. A further problem with these methods is their tendency either to overestimate or to underestimate the dispersion parameters in the mean. It would be an easy matter to take these tendencies into account in a site-specific parameter that would lead to accurate predictions for the WNRE site but this again would result in a loss of generality. Work is presently underway to determine

Table 2. Statistics of the Regression Lines of Measured $\sigma_z$ Values upon Predicted Values for Different Prediction Schemes.

| Scheme | Slope | Intercept | Correlation Coefficient | Standard Deviation of Residuals |
|---|---|---|---|---|
| Vogt & Geiss (1964) | 0.38 | 31.0 | 0.77 | 27.4 |
| Briggs (1974) | 0.86 | 38.0 | 0.70 | 31.1 |
| Draxler (1976) | 0.54 | 38.4 | 0.84 | 23.2 |
| Smith (1972) & Hosker (1974) | 1.13 | 14.7 | 0.85 | 22.4 |

the physical reasons for this poor prediction in the mean, so that a more fundamentally based parameterization scheme can be formulated.

## ACKNOWLEDGEMENTS

Edgar Wuschke, John Laporte, Frank Johnston and Carol Szekely of WNRE, and Warren McCormick of the University of Waterloo were responsible for much of the data collection. Warren McCormick and Jiann Sang Al Tang of the University of Waterloo performed much of the data reduction.

## REFERENCES

Arneson M.C. and K.W. Chambers, 1981: "Determination of sulfur hexafluoride in air", WNRE-507, 21 pp.

Briggs, G.A., 1974: "Diffusion estimation for small emissions", in Environmental Research Laboratories, Air Resources Atmospheric Turbulence and Diffusion Laboratory, 1973 Annual Report, USAEC Report ATDL-106, National Oceanic and Atmospheric Administration, December 1974.

Draxler, R.R., 1976: "Determination of atmospheric diffusion parameters", Atmos. Environ., 10, 99-105.

Gifford, F.A. Jr., 1961: "Use of routine meteorological observations for estimating atmospheric dispersion", Nucl. Safety, 2, 47-57.

Hay, J.S. and F. Pasquill, 1959: "Diffusion from a continuous source in relation to the spectrum and scale of turbulence", Advances in Geophysics, 6, 345.

Hosker, R.P. Jr., 1974: "Estimates of dry deposition and plume depletion over forests and grassland", in Physical Behaviour of Radioactive Contaminants in the Atmosphere, IAEA ST1/PUB/354, 291.

Pasquill, F., 1961: "The estimation of the dispersion of windborne material", Meteor. Mag., 90, 33-49.

Pasquill, F., 1974: "Atmospheric Diffusion. John Wiley and Sons, New York.

Pasquill, F., 1976: "Atmospheric dispersion parameters in Gaussian plume modelling, Part 2, Possible requirements for change in the Turner Workbook values", EPA 600/4-76-030b, Washington, D.C.

Sawford, B.L. and P.C. Manins, 1979: "An inexpensive sequential sampler for gas tracer studies", Atmos. Environ. 13, 341-342.

Slade, D.H., Editor, 1968: Meteorology and Atomic Energy, USAEC, Div. Tech. Inf.

Slawson, P.R., G.A. Davidson and C.S. Maddukuri, 1979: "Dispersion modelling of a plume in the tar sands area", Envirrodyne Ltd. Report, 285 pp.

Smith, F.B., 1972: "A scheme for estimating the vertical dispersion of a plume from a source near ground level", Proc. of the Third Meeting of the Expert Panel on Air Pollution Modelling, N.A.T.O. Committee on the Challenges of Modern Society, Paris, France, October 2-3, 1972.

Taylor, G.I., 1921: "Diffusion by continuous movements", Proc. London Math. Soc., Ser. 2, 20, 196.

Vogt, K.J. and H. Geiss, 1964: "Tracer experiments on dispersion of plumes over terrain of major surface roughness", Report Jul-1131-ST, Kernforschungsanlage, Julich, F.D.R., October 1964.

# THE MACGREGOR VINYL CHLORIDE SPILL:

# A PRACTICAL EXERCISE IN DISPERSION

BY

H. M. FRASER
ATMOSPHERIC ENVIRONMENT SERVICE
WINNIPEG, MANITOBA R3C 3V4

Abstract: On March 10, 1980 a train derailment near Macgregor, Manitoba resulted in a spill of some 70,000 litres of vinyl chloride monomer. Relatively flat terrain and the lack of plume rise simplified the application of a ground-based Gaussian dispersion model, but there were large unknowns regarding the source strength. Not only was the rate of discharge of liquid vinyl chloride undefined, the initial release was into an atmosphere about 5 degrees Celsius below the boiling point of vinyl chloride and into snow underlaid by earth some 15 degrees above the boiling point. Estimates are made of the rate of leakage, free surface evaporation and the effect of the earth and the snow to arrive at a dispersion scenario for the 36 hours following the accident. These estimates and the modelled atmospheric concentrations are in broad agreement with the very limited observations and monitoring available. The concentrations at 2 kilometres downwind are estimated to have been of the order of 1 to 5 parts per million during the first 30 hours. The practical difficulties of providing effective warning to nearby residents in situations such as this are also noted.

## INTRODUCTION

As a result of a derailment near MacGregor, Manitoba at 1:40 a.m., C.S.T., March 10, 1980 an estimated 15,538 gallons (70,640 litres) of vinyl chloride monomer (VCM) escaped from two damaged rail tank cars. Because of the high volatility, low boiling point and low solubility of this chemical it is likely that essentially all of it evaporated into the atmosphere.

The object of this study is to estimate rates of emmission of VCM to the atmosphere, its subsequent dispersion and maximum ground level concentrations down wind from the accident site.

## AIR POLLUTION MODELLING

The Gaussian model for dispersion is the one in widest use today mainly because the input parameters for its use are usually available to a reasonable degree of accuracy. For non-buoyant pollutants emitted from a point source at ground level and seeking only the ground level concentrations along the centre line of the plume down wind, the Gaussian formulation simplifies to:

$$C(x,o,o;o) = \frac{Q}{\pi \sigma_y \sigma_z U} \tag{1}$$

C is the concentration
Q is the emission rate
$\sigma_y, \sigma_z$ are dispersion coefficients estimated from the well known Pasquill-Gifford scheme
U is the surface wind

The effect is sketched in Figure 1.

The countryside surrounding the accident site is flat and dotted with bluffs of small trees. This and the restriction of concentration estimates to within a few kilometres of the source makes the Gaussian model appropriate. The assumption of the source as a point will over estimate concentrations close in, since the source was most likely two points and a small area, but at distances of a few hundred metres and beyond the results from a point source or small area would not be significantly different.

### Density Considerations

The dispersion model used is intended for plumes whose density is close to that of air. Since VCM has a molecular weight more than twice that of air such models would not be appropriate for plumes containing a large proportion of VCM. However, except within a few metres of the source the proportion of VCM is small - in most instances a few parts per million (ppm). Density differences between the plume and the ambient air are thus negligible and the neutral bouyancy Gaussian model can be used.

### Weather Inputs

Thirty-five kilometers to the east of the accident site the Portage La Prairie weather station, located at the Department of National Defence Air Base, maintains full weather records 24 hours per day. There are no topographic or landscape features which would lead us to expect significant differences between the two locations. Also, charts of the Winnipeg weather office over the days of interest indicate that there was no appreciable difference in the weather at the two sites caused by the weather patterns moving across the area. Figures 3 and 4 are copied from the surface weather

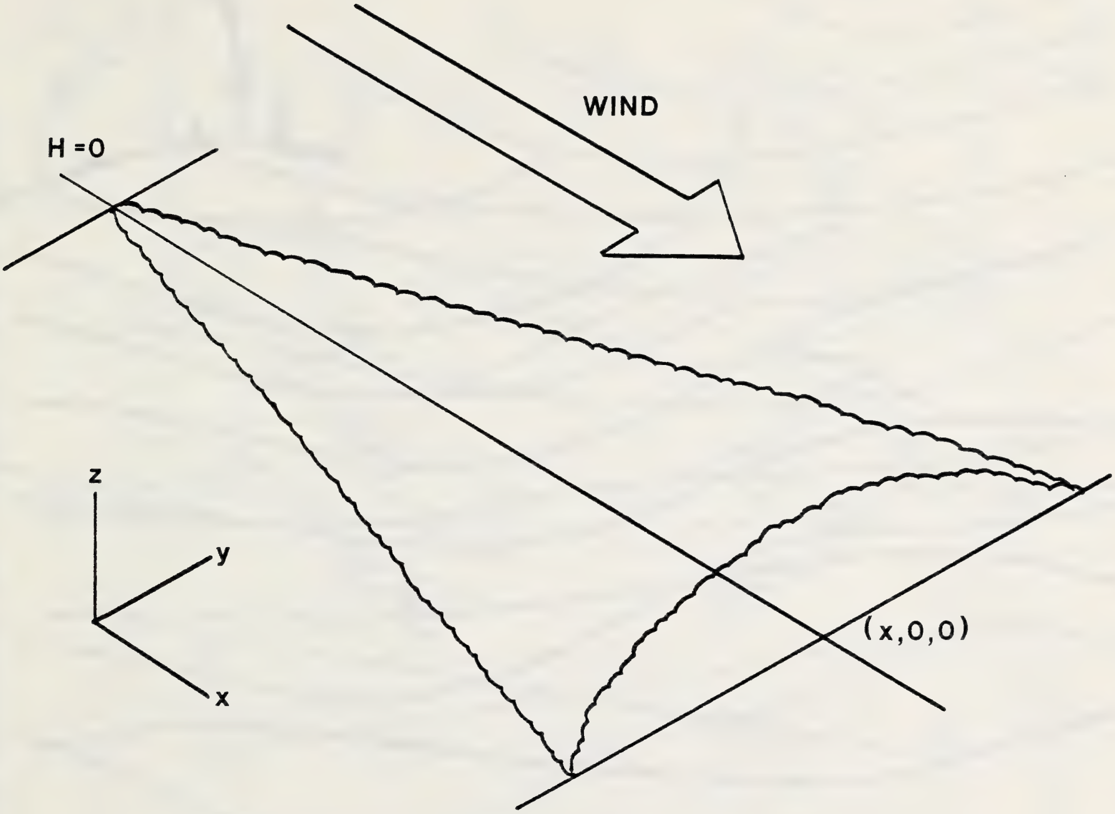

FIG. 1 DISPERSION FROM A GROUND-BASED POINT SOURCE

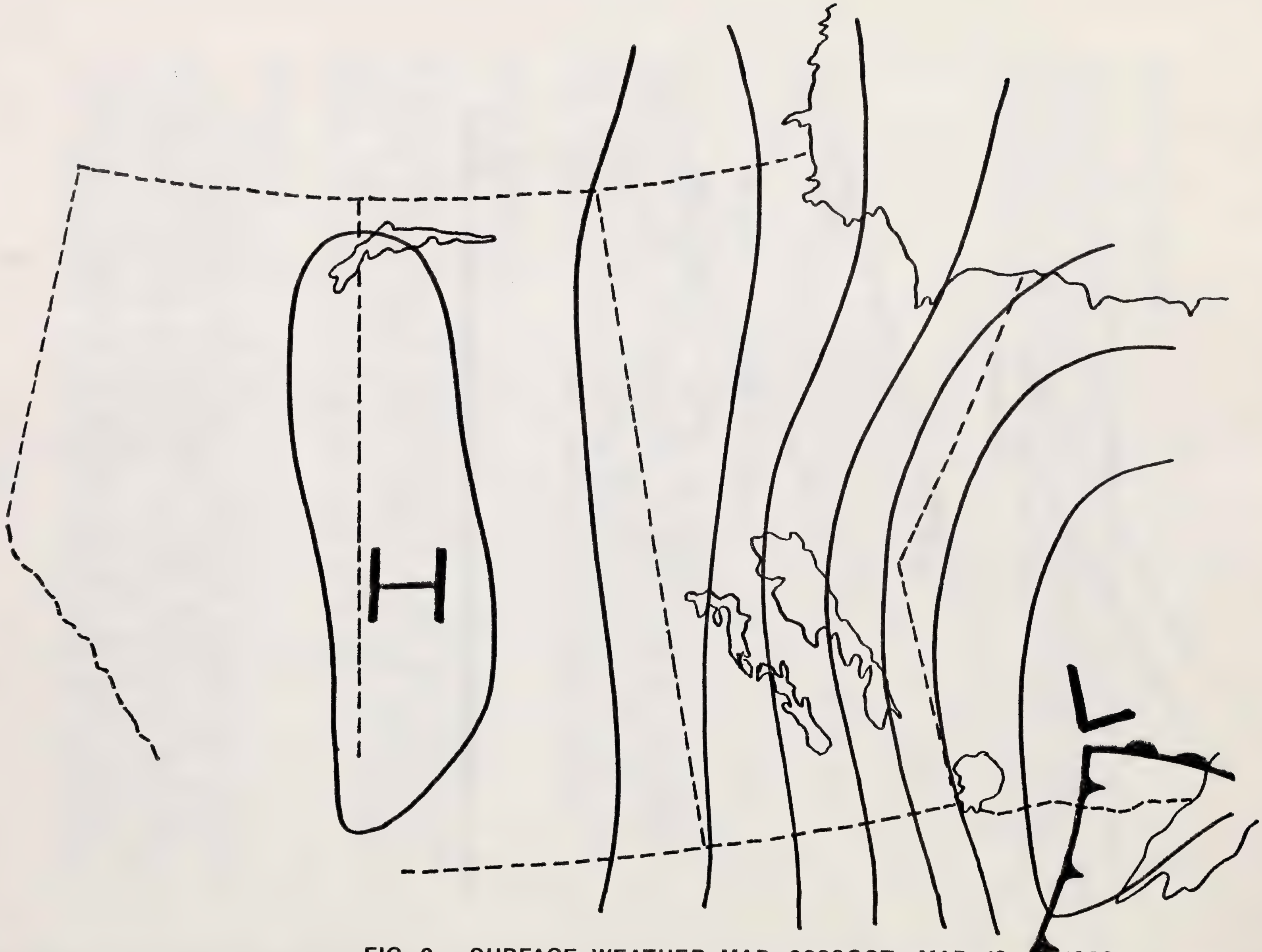

FIG. 2 SURFACE WEATHER MAP, 0000CST, MAR. 10, 1980

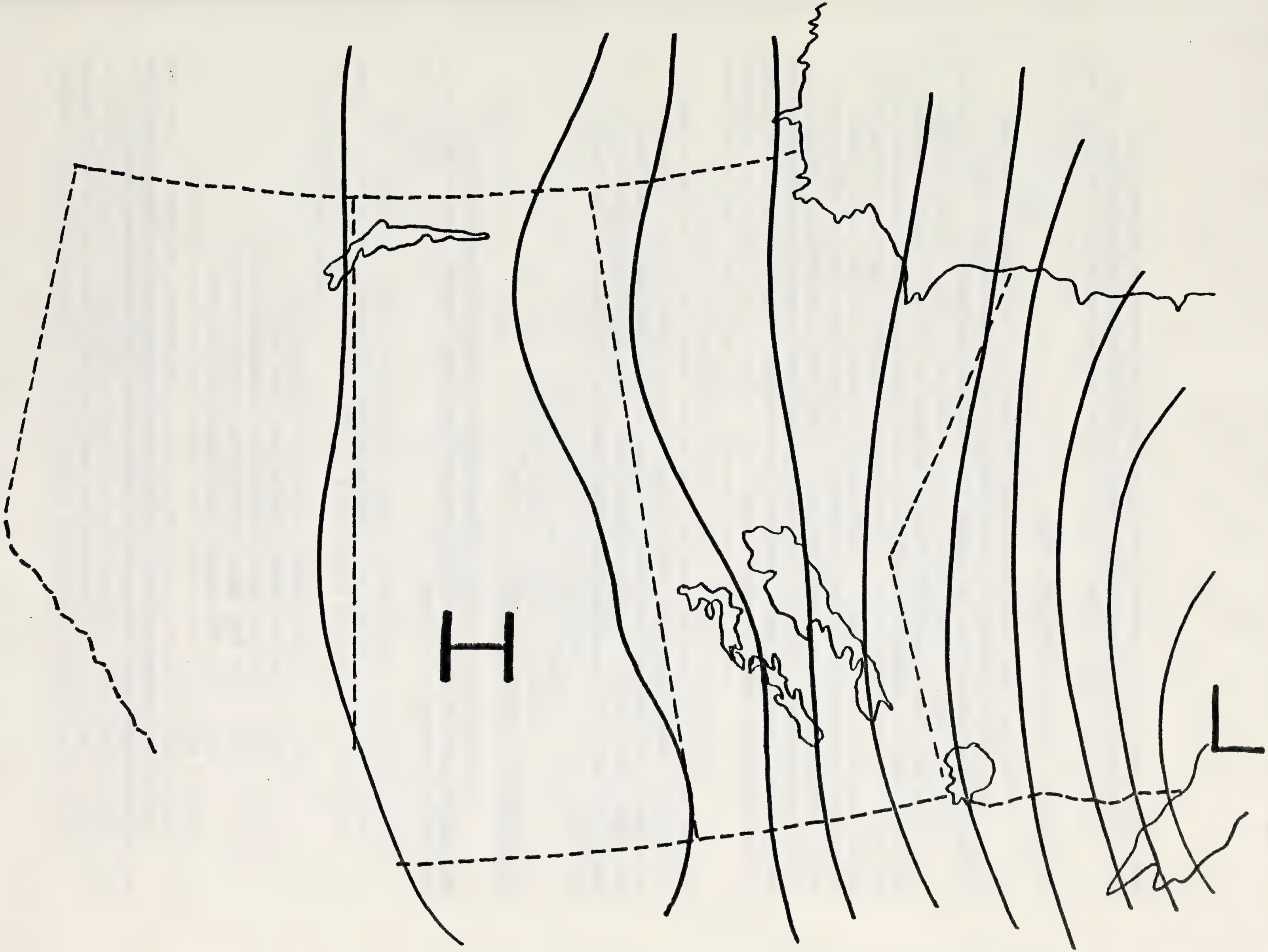

FIG. 3 SURFACE WEATHER MAP, 0600CST, MAR. 10, 1980

maps at midnight C.S.T. March 9 and 6:00 a.m. C.S.T. March 10; they illustrate the consistent pattern over southern Manitoba during that time.

## Discharge of VCM from the Tank Cars

The two cars which discharged VCM came to rest side by side near right angles to the railway with one end near the rails and the other sloping downward into the shallow ditch alongside the roadbed.

The one car, for convenience referred to as Car A, lost 10,447 gallons through a puncture on the down side of the car between the centre and the lower end in the ditch. None of the parameters necessary to calculate the time for the car to discharge this amount are accurately known. However the pressure head can be estimated for various reasonable attitudes of the car (near 15°) and positions of the hole on its underside. Similarily various sizes of orifice - (for example four square inches) can be assumed, and it can be shown that it is possible if not probable that all of the discharge occurred in an hour.

A second car, Car B, lost 5,091 gallons of VCM through a damaged valve. The precise rate of loss is not known but it had decreased to a "drip" when observed on the Tuesday afternoon some 36 hours after the derailment. An average loss would work out to some 140 gallons per hour over that time, but it is more probable that the rate of discharge was higher in the early hours and that the total time of discharge was less than 36 hours.

## Disposition of Discharged VCM

The relevant input to the atmospheric dispersion model is the emission of VCM to the atmosphere not the discharge from the cars. The two can be related as follows:

$$A = D_a + D_b - S = A_s \qquad (2)$$

| | |
|---|---|
| $A$ | is the amount entering the atmosphere |
| $D_a$ | is the amount discharged from Car A |
| $D_b$ | is the amount discharged from Car B |
| $S$ | is the amount going into or onto the snow |
| $A_s$ | is the amount evaporating from the snow |

On the assumption that all of the discharge from Car A occurred in the first hour then during the second hour the following would hold:

$$A = D_a - S + A_s \qquad (3)$$

When Car B ceased to discharge at or prior to hour 36 there is no longer any VCM being discharged or entering the snow. At that point all the VCM entering the atmosphere is that which is evaporating from liquid VCM already in the snow.

$$A = A_s \quad (4)$$

The VCM in the insulated tank cars was estimated too be at a temperature of -6C which is above its boiling point of -14C and above the air temperature of -19C. This would result in an initial rapid boil-off of some 2½% of the VCM; the heat necessary to change the liquid to vapour would be extracted from the liquid itself which in the process would be cooled to its boiling point.

After and during the initial boil-off, VCM would evaporate into the air. It would be very volatile at -19C, in fact, the evaporation may be likened to that of water at 93C and this analogy can be usefully pursued. Over many decades there have been numerous equations developed which quantify the evaporation of water into the atmosphere. They are usually based on Dalton's law of partial pressures and of the form:

$$E = f(u)\ (e_o - e_a) \quad (5)$$

| | |
|---|---|
| $E$ | is the rate of evaporation |
| $f(u)$ | is a function of windspeed |
| $e_o$ | is the saturated vapour pressure at the surface temperature of the liquid |
| $e_a$ | is the partial pressure of vapour in the air |

Since these equations are, although emperical, based on the physical processes, they are useful in assessing the possible evaporation of the VCM.

There was visual evidence of liquid washing over the snow over a semi-circular area of some 900 square metres. An appropriate formula for comarison might be that of Kuzmin (1957) which was derived for reservoirs of 20-100 metres across.

$$E(\text{inches/day}) = .2(1 + .21\ u_g)(e_o - e_a) \quad (6)$$

The estimated evaporation by the Kuzmin method is 5,100 gallons per hour. There are unanswered questions as to the cooling of the liquid surface by evaporation and the effect this would have on the evaporation; 5,100 gallons per hour is not put forward as a reliable estimate but only as an indication of the large evaporative rate possible. Central to this possibility is the assumption that the heat necessary to evaporate the VCM would be extracted from that air which was moving very quickly across the surface. As an example the amount of heat necessary to vaporize 5,000 gallons of VCM in one hour could be supplied by cooling a layer of air one metre in depth by less than one half of one degree C.

The situation within the snowbank is complicated by earth temperatures above the boiling point of VCM. The only soil temperature measurement available in southern Manitoba at the time was from Winnipeg where the temperature at 5 centimetres was reported as -4C with warmer temperatures below. Thus, the top of the snowbank might be near -19C and the bottom near -4C. Liquid VCM percolating down through the snow would vaporize when its temperature rose above -14C; the proportion of vapour and liquid would be governed by the rate at which heat used up in vaporizing the liquid would be replaced by heat transferred from the earth or the atmosphere. The process may be likened to placing a porous sponge containing water at 93C on a surface at 110C and blowing dry air at 93C across it at a high rate. The suggestion is that any restriction to evaporation would not be the lack of heat but the impediment offered by the sponge.

## EVIDENCE OF THE PRESENCE OF VCM

Because of the stormy weather it was a good five hours before emergency personnel could reach the accident site from Winnipeg over 100 kilometres to the east. Initial inspection identified a "sweetish" smell (presumably VCM) immediately adjacent to the wrecked cars but not 150 paces down wind and this was confirmed by crude measurements with an explosimeter. It was about 12 hours after the accident before other experts with more sophisticated monitoring equipment arrived and over the period of several days while clean up was progressing the monitoring results were generally consistent. Between the rail cars, or within a few inches of the cars and snow in the immediate area readings of 1-300 parts per million were sometimes obtained. It should be noted that the amounts of VCM in the snow necessary to produce such readings would be very small and that at no time was liquid VCM encountered in or under the snow. At breathing level even within a few metres of the cars the measured levels were near zero only very occasionally reaching 5 parts per million.

Although the monitoring data is sketchy in both space and time it does lead to the conclusion that by the time monitoring either by instrument or the human nose was possible, most of the VCM was gone into the atmosphere.

## AN EMISSION SCENARIO

Considering the various physical principles discussed and the evidence available it is possible to suggest a scenario for the emission of VCM to the atmosphere. This has been done observing the following:

- All 10,447 gallons from Car A discharged during the first hour;

- 5,091 gallons from Car B began discharging at a rate of 310 gallons per hour and decreased to 10 gallons per hour at hour 31;
- In each hour 2.5% of discharging liquid boiled rapidly into the air;
- Free surface evaporation of 1,250 gallons occurred in the first 15 minutes;
- Evaporation from within the snowbank was 15% of the liquid VCM in the snow in any one hour;
- By hour 36 when the cars had been righted, snow had been moved, and more frequent activity was occurring in the area, liquid VCM in the snow had decreased to some 200 gallons;
- By hour 36 at least 15,000 gallons of VCM had vaporized into the atmosphere.

The estimated emission of VCM to the atmosphere over the first 36 hours is shown in Table 1; column 7 estimates evaporation within the hour, column 8 estimates total evaporation to that time, and column 9 indicates the amount that would be left in the snow at the end of that hour.

## DOWNWIND CONCENTRATIONS

Table 2 uses the emission rates from Table 1 and the hourly weather from the Portage La Prairie weather station as input to Equation 1 and shows estimated ground level concentrations at .1 kilometre, 1 kilometre and 2 kilometres downwind from the accident site for the first 36 hours.

## DISCUSSION OF CONCENTRATIONS

Because at close-in distances we are not dealing with a point source, the estimates at .1 kilometre are not reliable. They can be used in a general way to indicate the increase of concentrations as the source is approached, but in fact would significantly overestimate those concentrations.

During the first hour, when the scenario proposes the highest emissions, maximum concentrations directly downwind are estimated to have been of the order of 15 parts per million at 1 kilometre and 4.8 parts per million at 2 kilometres. Following initial boil-off and free surface evaporation estimates decreased to less than three parts per million (one kilometre) and one part per million (2 kilometres) after seven hours.

The effect of changing weather on atmospheric dispersion and the estimated concentrations is demonstrated in Table 2. For example, through the afternoon the estimates do not change substantially; although the estimated emission was decreasing steadily, so also was the wind and the atmosphere would not disperse the VCM as quickly. The dispersive capability of atmospheric worsened in the evening as the wind decreased to light and

TABLE 1 ESTIMATED EMISSION OF VCM TO THE ATMOSPHERE

| Hr. | Discharge (gals.) this hour at $-6^{o}C$ from |  | Boil-off to Reduce Temp. to $-14^{o}C$ (Gals.) | In/Into Snow This Hour (Gals.) | Evaporation from Snow (Gals.) | Total Vapourization This Hour (Gals.) | Total Vapourization to End Hour (Gals.) | Remaining in Snow at End of Hour (Gals.) |
|---|---|---|---|---|---|---|---|---|
|  | 1010 | 1072 |  |  |  |  |  |  |
| 1 | 10500 | 310 | 265 | 9295 | 2644 | 2909 | 2909 | 7901 |
| 2 | 0 | 300 | 7 | 8194 | 1229 | 1236 | 4145 | 6965 |
| 3 | 0 | 290 | 7 | 7248 | 1087 | 1094 | 5239 | 6161 |
| 4 | 0 | 280 | 7 | 6434 | 965 | 972 | 6211 | 5469 |
| 5 | 0 | 270 | 7 | 5732 | 860 | 867 | 7078 | 4872 |
| 6 | 0 | 260 | 6 | 5126 | 769 | 775 | 7853 | 4357 |
| 7 | 0 | 250 | 6 | 4601 | 690 | 696 | 8549 | 3911 |
| 8 | 0 | 240 | 6 | 4145 | 622 | 628 | 9177 | 3523 |
| 9 | 0 | 230 | 6 | 3747 | 562 | 568 | 9745 | 3185 |
| 10 | 0 | 220 | 5 | 3400 | 510 | 515 | 10260 | 2890 |
| 11 | 0 | 210 | 5 | 3095 | 464 | 469 | 10729 | 2631 |
| 12 | 0 | 200 | 5 | 2826 | 424 | 429 | 11158 | 2402 |
| 13 | 0 | 190 | 5 | 2587 | 388 | 393 | 11551 | 2199 |
| 14 | 0 | 180 | 4 | 2375 | 356 | 360 | 11911 | 2019 |
| 15 | 0 | 170 | 4 | 2185 | 328 | 332 | 12243 | 1857 |
| 16 | 0 | 160 | 4 | 2013 | 302 | 306 | 12549 | 1711 |
| 17 | 0 | 150 | 4 | 1857 | 279 | 283 | 12832 | 1578 |
| 18 | 0 | 140 | 3 | 1715 | 257 | 260 | 13092 | 1458 |
| 19 | 0 | 130 | 3 | 1585 | 238 | 241 | 13333 | 1347 |
| 20 | 0 | 120 | 3 | 1464 | 220 | 223 | 13556 | 1244 |
| 21 | 0 | 110 | 3 | 1351 | 203 | 206 | 13762 | 1148 |
| 22 | 0 | 100 | 2 | 1246 | 187 | 189 | 13951 | 1059 |
| 23 | 0 | 90 | 2 | 1147 | 172 | 174 | 14125 | 975 |
| 24 | 0 | 80 | 2 | 1053 | 158 | 160 | 14285 | 895 |
| 25 | 0 | 70 | 2 | 963 | 144 | 146 | 14431 | 819 |
| 26 | 0 | 60 | 1 | 878 | 132 | 133 | 14564 | 746 |
| 27 | 0 | 50 | 1 | 795 | 119 | 120 | 14684 | 676 |
| 28 | 0 | 40 | 1 | 715 | 107 | 108 | 14792 | 608 |
| 29 | 0 | 30 | 1 | 637 | 96 | 97 | 14889 | 541 |
| 30 | 0 | 20 | 0 | 561 | 84 | 84 | 14973 | 477 |
| 31 | 0 | 10 | 0 | 487 | 73 | 73 | 15046 | 414 |
| 32 | 0 | 10 | 0 | 424 | 64 | 64 | 15110 | 360 |
| 33 | 0 | 10 | 0 | 370 | 56 | 56 | 15166 | 314 |
| 34 | 0 | 10 | 0 | 324 | 49 | 49 | 15215 | 275 |
| 35 | 0 | 10 | 0 | 285 | 43 | 43 | 15258 | 242 |
| 36 | 0 | 10 | 0 | 252 | 38 | 38 | 15296 | 214 |

## TABLE 2 ESTIMATED MAXIMUM DOWNWIND CONCENTRATIONS OF VCM

| Hr. | Date/Hr. CST | Emission Q (Gals./Hr) | Wind Direction (Degrees) | Wind Speed (km/h) | Temp. °C | Stability Class | Estimated Concentration (ppm) .1 km | Estimated Concentration (ppm) 1 km | Estimated Concentration (ppm) 2 km |
|---|---|---|---|---|---|---|---|---|---|
| 1 | 10/02 | 2909 | 300 | 33 | -18 | D | 937 | 15.0 | 4.8 |
| 2 | 03 | 1236 | 310 | 31 | -18 | D | 398 | 6.2 | 2.0 |
| 3 | 04 | 1094 | 310 | 37 | -18 | D | 317 | 5.0 | 1.6 |
| 4 | 05 | 972 | 320 | 37 | -18 | D | 282 | 4.4 | 1.4 |
| 5 | 10/06 | 867 | 310 | 43 | -19 | D | 209 | 3.3 | 1.1 |
| 6 | 07 | 775 | 310 | 37 | -20 | D | 225 | 3.5 | 1.2 |
| 7 | 08 | 696 | 320 | 37 | -20 | D | 202 | 3.2 | 1.0 |
| 8 | 09 | 628 | 320 | 37 | -20 | D | 182 | 2.8 | 0.9 |
| 9 | 10 | 568 | 320 | 33 | -20 | D | 183 | 2.8 | 0.9 |
| 10 | 11 | 515 | 310 | 30 | -19 | D | 187 | 2.9 | 1.0 |
| 11 | 10/12 | 469 | 300 | 31 | -18 | D | 151 | 2.4 | 0.8 |
| 12 | 13 | 429 | 300 | 28 | -17 | D | 155 | 2.4 | 0.8 |
| 13 | 14 | 393 | 290 | 28 | -16 | D | 142 | 2.2 | 0.7 |
| 14 | 15 | 360 | 300 | 20 | -15 | D | 174 | 2.7 | 0.9 |
| 15 | 16 | 332 | 310 | 17 | -15 | D | 193 | 3.0 | 1.0 |
| 16 | 17 | 306 | 320 | 11 | -14 | D | 296 | 4.6 | 1.5 |
| 17 | 10/18 | 283 | 290 | 19 | -15 | D | 164 | 2.6 | 0.8 |
| 18 | 19 | 260 | 280 | 15 | -16 | D | 188 | 2.9 | 1.0 |
| 19 | 20 | 241 | 260 | 15 | -17 | E | 429 | 6.0 | 1.9 |
| 20 | 21 | 223 | 260 | 17 | -18 | E | 317 | 4.4 | 1.4 |
| 21 | 22 | 206 | 280 | 15 | -19 | E | 366 | 5.1 | 1.6 |
| 22 | 23 | 189 | 280 | 9 | -21 | F | 1087 | 18.0 | 5.7 |
| 23 | 11/00 | 174 | 270 | 9 | -22 | F | 1000 | 16.0 | 5.2 |
| 24 | 01 | 160 | 270 | 7 | -24 | F | 1380 | 22.0 | 7.2 |
| 25 | 02 | 146 | - | 0 | -24 | F | Not Applicable When Calm | | |
| 26 | 03 | 133 | - | 0 | -25 | F | | | |
| 27 | 04 | 120 | - | 0 | -26 | F | | | |
| 28 | 05 | 108 | - | 0 | -28 | F | | | |
| 29 | 11/06 | 97 | - | 0 | -25 | F | | | |
| 30 | 07 | 84 | 110 | 9 | -25 | F | 483 | 7.8 | 2.5 |
| 31 | 08 | 73 | 100 | 15 | -25 | D | 53 | 0.8 | 0.3 |
| 32 | 09 | 64 | 110 | 13 | -24 | D | 46 | 0.7 | 0.2 |
| 33 | 10 | 56 | 100 | 15 | -21 | D | 41 | 0.6 | 0.2 |
| 34 | 11 | 49 | 120 | 20 | -20 | D | 24 | 0.4 | 0.7 |
| 35 | 11/12 | 43 | 110 | 20 | -20 | D | 21 | 0.3 | 0.1 |
| 36 | 13 | 38 | 110 | 24 | -18 | D | 16 | 0.2 | 0.1 |

the heat of the sun was lost. By midnight estimated levels at 1 kilometre and 2 kilometres were as high as those in the first hour although the amount of VCM estimated to be entering the atmosphere as the accident site was only one-twentieth as much. Noticeable concentrations are also estimated to have occurred at 7:00 a.m. in the morning following a period of calm winds during the night.

By hour 36 emission and concentrations were estimated to be very low and decreasing.

## THE EFFECT OF OTHER SCENARIOS

The basic pattern of estimated concentrations in the scenario used was that of higher concentrations in the early hours and again during the evening with lower levels between. This pattern is highly weather dependent as discussed. It is possible to construct other emission scenarios which would yield different patterns over the 36 hour period, but clearly the total effect would have to be disperse 15,000 gallons of VMC over some 36 hours.

The relationship between column 3, in Table 3 (emission O) and the estimated concentrations in the same table is linear so that one can estimate some of the changes possible. For example, doubling the emissions in the early hours would double the estimated concentrations, but substantially reduce the amounts left for evaporation and estimated concentrations later. In contrast, substantial reductions in the initial rates would increase later concentrations.

It is the author's opinion that any reasonable variations in the scenario would not change estimated concentrations at specific times by more than a factor of two.

## ADDITIONAL OBSERVATIONS

In the 33 kilometre per hour wind prevailing at the time of the accident the leading edge of any airborne material released would reach 1 kilometre in 1.8 minutes and 2 kilometres in 3.6 minutes. The speed of atmospheric dispersion can thus be seen to be a critical factor in any procedures designed to react to it.

Expert opinion presented at the Canadian Transport Commission hearing on the MacGregor spill was that VCM concentrations of 100-200 ppm over several hours would not constitute a hazard to health. The estimates of this study - even if several times too low - then suggest that a health hazard, if any, could only have existed considerably less than 1 kilometre from the source.

Throughout this report precise statements have been hindered not only because many of the actual events (such as spill rates) could not be defined, but also because the ensuing physical processes in the environment (such as vaporization) were not entirely known. A particular example would be the role that the snow and earth played in the happenings.

# REFERENCES

Briggs, G. A., 1973: Diffusion Estimation for Small Edmissions. Environmental Research Laboratory, Air Resources Atmospheric Turbulence and Diffusion Laboratory, 1973 Annual Report, ATDL-106, USDOC - NOAA.

: Chrisis Manual, U.S. Coast Guard, Dept. of Transport, Washington, D.C.

Gifford, F. A., 1961: Uses of Routine Meteorological Observations for Estimating Atmospheric Dispersion. Nuclear Safety, 2,4, 47-51.

Grey, D. M. (Editor-in-Chief), 1970: Handbook on the Principles of Hydrology, National Research Council of Canada, Ottawa, Ontario.

Leonard, Edward C., 1971: Vinyl and Diene Mononiers, Part 3, John Wiley and Sons, Toronto, Ontario.

Pasquill, F., 1961: The Estimation of Wind Borne Material. Meteorological Magazine, 90, 33-49.

Priestly, C.H.B., 1959: Turbulent Transfer in the Lower Atmosphere, University of Chicago Press, Chicago, IL.

Reimer, A., 1979: The Effect of Wind on Heat Transfer in Snow, Proceedings, Conference on Soil-Water Problems in Cold Regions, September, 1979, Atomic Energy of Canada Ltd., Pinawa, Manitoba.

Sutton, O. G.: The Problem of Diffusion in the Lower Atmosphere. Quarterly Journal of the Royal Meteorological Society, Volume 73, July - October, 1947, 257-281.

Turner, E. B., 1970: Work Book of Atmospheric Dispersion Estimates. U.S. Department of Health, Education and Welfare, National Air Pollution Control Administration, Cincinnati, Ohio.

Uerschuren, Karl, (Editor): Handbook of Environmental Data in Organic Chemistry.

# THE EXTENT OF ACIDIC DEPOSITION IN A REGIONAL CONTEXT OF WESTERN CANADA

by

S.R. Shewchuk
Saskatchewan Research Council
Saskatoon, Saskatchewan, S7N 0X1

Abstract: The wet and dry deposition of sulphur and nitrogen compounds is considered along with future possible emissions for a selected region of northeastern Alberta and northern Saskatchewan. Comparison is made between the deposition values of the project area and other areas within Canada. Major ion composition of the precipitation is considered within the region. A clear absence of alkaline buffer material in precipitation on the Precambrian Shield suggests that any anion material added to the system will show up as a direct acid load to the ecosystems.

## INTRODUCTION

It is well documented (Smith and Jeffrey, 1975) that airborne emissions of gases and particulates can be transported many hundreds or thousands of kilometres. They may be deposited and then interact with the ecosystems at any point along its trajectory. In some cases sulphur and nitrogen compounds, since they are part of the elemental composition of living matter, are utilized in a positive way during the growth processes of living tissue. However, in other cases these substances remain within the ecosystem and are responsible for gradual alteration of the system from its natural state.

The study area comprises 6.46 10" square metres in northern Saskatchewan and northeastern Alberta. In Saskatchewan, it includes the area north of 53°N Latitude, and in Alberta the area east of 118°W longitude and north of a line extending from 53°N Latitude on the east to 56°N Latitude on the west. About 3.69 10" square metres or 57% of the study area, occurs in Saskatchewan and about 2.77 10" square metres or 43% of the area, occurs in Alberta.

In this paper characteristics of the atmosphere will be considered with regard to the deposition and regional transport of pollutants within the study area. The current state of the dry and wet deposition of pollutants will be assessed along with a projection of future trends based upon a given industrial scenario for the region.

The atmosphere is considered as a dynamic pathway for natural and man-influence emission. It is not simply a passive transport mechanism. Emissions of sulphur and nitrogen compounds are transformed by oxidation processes to sulphuric and nitric acids.

The processes whereby the atmosphere passes these substances to other systems is very complex. Direct gaseous absorption or particulate impaction by the various systems is referred to as dry deposition. The gases can be directly absorbed (i.e. water, land, vegetation, etc.) or may be oxidized to an acid by the atmosphere and fall as a dry acidified particle. In the presence of rain the processes of oxidation are much more rapid. In this case the sulphur and nitrogen compounds fall as a direct-added acid constituent of the natural rainfall. Carbon dioxide acts as the main acid control of pure distilled water in the atmosphere, the equilibrium value being approximately a pH of 5.6. Precipitation events with pH values more acidic than this is generally thought to be "acid rain". However this is not correct. Cloud droplets can be formed on many naturally occuring acid aerosols (i.e. $NH_4HSO_4$). A rain drop is formed by a collection of many cloud droplets. The resulting drop may be acidic. The pH of natural (uncontaminated) rain at any location is very difficult to specify. However natural rainfall given the presence of carbon dioxide and natural acid condensation nucleii is at most locations slightly acidic. If the pH value of rain is higher than approximately 5.6, alkaline compounds dominate the precipitation. Alkaline substances in the form of soil dust are common in the atmosphere. If precipitation were to fall in an environment that is very alkaline the precipitation will be alkaline due to the fact that the rain drop will scavenge the alkaline dust from the air. A large amount of alkalinity in the various systems is an indication that the total environment has a high buffering capacity to acid inputs.

Due to the fact that the oxidation times for the sulphur and nitrogen compounds are long, regional and global transport and dispersal of these substances is possible.

## WET DEPOSITION

In order to place the acidic deposition of pollutants within the project area into the context of Canada, analysis of the CANSAP data will be undertaken. Environment Canada has established CANSAP (Canadian Network for Sampling and Analysis of Precipitation), under which rain is collected from across Canada at a number of locations and analysed chemically for its major ion constituents.

In Table I the wet deposition of sulphur as sulphate and nitrogen as nitrate is shown on an annual basis for the year 1978.

The CANSAP data shows that there are marked regional differences in concentration and deposition in Canada.

Wet deposition values for Inuvik, Fort Chimo and Cree Lake represent the lowest values in Canada. They can be considered near the global background for sulphate deposition. Global background levels of wet

Table I. Wet Deposition of Sulphur (as sulphate) and Nitrogen (as nitrate) at Selected CANSAP Stations from Across Canada (1978).

| LOCATION | $\frac{\text{kg } (S\text{-}SO_4)}{\text{hectare . year}}$ | $\frac{\text{kg } (N\text{-}NO_3)}{\text{hectare . year}}$ |
|---|---|---|
| Inuvik | 0.9 | 0.2 |
| Port Hardy | 8.3 | 1.5 |
| Coronation | 4.5 | 1.6 |
| Edson | 4.1 | 0.9 |
| Fort McMurray | 5.2 | 1.4 |
| Cree Lake | 1.8 | 0.5 |
| The Pas | 3.3 | 1.3 |
| Kindersley | 2.2 | 1.1 |
| Atikoken | 4.4 | 2.5 |
| Mount Forest | 23.6 | 10.9 |
| Chibougamau | 10.2 | 3.7 |
| Maniwaki | 9.9 | 5.1 |
| Moosonee | 7.6 | 2.2 |
| Churchill | 4.2 | 0.5 |
| Nitchequon | 3.8 | 1.2 |
| Fort Chimo | 2.6 | 0.7 |
| Gander | 19.7 | 3.5 |
| Sable Island | 40.26 | 1.7 |

deposition of sulphate and nitrate are very difficult to determine, and a value for sulphate of about 2.0 kg-S/hectare year is the best estimate that can be made at this time (Frantisak, 1980). The value of nitrate background is not known.

The sulphate deposition estimates are quite variable however, and since soil is a very important part of the background values, different types of soils and different air mass histories will determine how much sulphate is in wet deposition in a given area.

Anthrogenic or man-induced influences do have a great deal of effect on the sulphate balances in rain, and this of course is the basis of the acid rain problem. At stations that are significantly above the nominal background the influence of man's activities probably is the main source of sulphate.

Since nitrogen is a difficult substance to trace chemically in the atmosphere, the nitrogen deposition as nitrate in the rain is given as a matter of record in Table I as well. In general the stations which were low in sulphate deposition also are low in nitrate deposition. It seems likely that values of nitrogen (as nitrate) in the range of 0.2 to 1.0 kg ($N-NO_3$)/ha yr are at global background values. Again by considering order of magnitude increases in eastern Canada from the project region of this study, it is clear that nitrate deposition from anthropogenic sources is not a major cause for acidity in the project region.

In Table II the major ions are broken into their constituents for various locations in the CANSAP network. Data is tabulated only for the month of July in 1978. The main purpose in presenting these results is to show that pH as a measure of acidity is not direct measure of an anthropogenic influence. While atmosphere carbon dioxide does provide the main control of acidity for "clean rain". The acidity of rain at any one location is in reality a very delicate balance between the atmospheric trace gases ($SO_2$, $NO_x$, $CO_2$ and $NH_3$) and mineral buffering agents that are collected by the rain from the environment. The positive major ions ($NH_4^+$, $Na^+$, $Mg^+$, $Ca^{++}$) all act as agents to neutralize the rains acidity. Kindersley and Fort McMurray are locations where there is a great abundance of major buffer ions in the rain (which were scavenged from the dust particles and trace gas which originated in the environment). At Kindersley for example, the natural acidity of rain has been completely removed by the buffering agents, primarily by alkaline earth substances. Fort Chimo and Cree Lake are examples of locations that have a relative lack of buffering ions in the rain water. This lack of buffering capacity again reflects the entire environment in which the rain drop develops. Ultimately whatever buffering capacity is present in the rain drop must have come from the soil or trace gases in the region.

In order to summarize the approach for the project region under question, as far as sulphate and nitrate deposition is concerned values are near global background values at the present time. If one looks very carefully at the data some influences of anthropogenic components can be found but these are minimal. The significant point is that the region is not homogeneous with regard to its buffering capacity. The western

Table II. Chemical Fractional of Rain from the CANSAP Network (July 1978).

| LOCATION | pH | $SO_4^{=}$ µ eq/ℓ | $NO_3^-$ µ eq/ℓ | $Cl^-$ µ eq/ℓ | $NH_4^+$ µ eq/ℓ | $Na^+$ µ eq/ℓ | $Mg^+$ µ eq/ℓ | $Ca^{++}$ µ eq/ℓ |
|---|---|---|---|---|---|---|---|---|
| Inuvik | 7.5 | 35 | 15 | 18 | 7 | -- | -- | -- |
| Edson | 4.9 | 33 | 4 | 3 | 6 | 4 | 3 | 10 |
| Fort McMurray | 6.2 | 85 | 2 | 8 | 1 | 13 | 53 | 90 |
| Cree Lake | 5.2 | 13 | -- | -- | 1 | 4 | 1 | 3 |
| Kindersley | 7.0 | 40 | 25 | 8 | 12 | 9 | 117 | 180 |
| Simcoe | 4.3 | 213 | 95 | 10 | 99 | 4 | 39 | 110 |
| Fort Chimo | 5.8 | 4 | 1 | 2 | 1 | 9 | 3 | 4 |
| Maniwaki | 4.0 | 144 | 74 | 3 | 31 | 4 | 8 | 26 |
| Sable | 4.6 | 52 | 19 | 72 | 18 | 70 | 16 | 8 |

portion of the project region has a great deal more buffer capacity than the east. The rain at Cree Lake does show some acidification at present. It is difficult to pin the cause of this acidification to an anthropogenic component, particularly as acidity at Cree Lake illustrates very definitely the lack of buffer capacity. If one is to project the increased anthropogenic activities as outlined in other sections of this report, then significant acidity increases in the rain will be documented in the future. They will be due to both the sulphate and nitrate ion increases with the natural buffer of ammonia and other major ions not present.

## DRY DEPOSITION

In dry deposition small particles or gases present in the atmosphere are transferred by turbulent eddy diffusion to the earth surface, where they collect by impaction, adhesion and absorption. Dry deposition velocities of gaseous components are generally very much larger than for particulates. For the Precambrian Shield wet and dry deposition are very important. The determination of dry deposition is very difficult. On a regional basis most estimates of dry deposition are thought to be at least as important as wet deposition. It is more likely that considering the climatic regimes of the project region the ratio of the amount of dry deposition to wet deposition is approximately equivalent to an annual basis. Under current measurement methodologies of the Atmospheric Environment Service dry deposition is not measured. Current data indicates that much of eastern Canada receives precipitation containing elevated levels of hydrogen, sulphate and nitrate ions. There is no reason to assume that this is not the case as well for dry deposition of the same compounds as well.

Dry deposition estimates are possible for the project region if ambient gaseous and particulate sulphur and nitrogen compound levels are known. There has not been a great deal of monitoring for these compounds, however, work done on special projects (Shewchuk, 1979) in the area suggest that the values are near background values. This is not true in isolated cases when wind systems have been known to transport plumes within the project region for hundreds of kilometres. Values as high as 49.3 ug-S/m$^3$ have been reported several tens of kilometres downstream of an oilsands plant (Barrie, 1977). A value of 18 ug/m$^3$ has been reported approximately 150 km from an oilsands plant. Back trajectory seemed to confirm the source as being the tarsands region.

The accumulation of pollutants in a snow pack is a very convenient way to study the deposition (wet and dry) over the period of a season. The snow pack maintains a continuous record of materials accumulated from the atmosphere providing there are no melt periods. It has been shown (Johannessen et al 1978) that laboratory and field measurements of melt water from first snow melt show concentrations of; hydrogen and nitrate ion as much as six times higher than in the bulk snow. Pollutants are leached out of the entire snow pack at first melt. This first melt causes a sudden increase of pollutants to the streams and lakes at run off. In Scandinavia pH drops of more than one unit have been observed; consequently severe physiological stresses were placed upon the fresh water systems. This is responsible for the "acid-shock" effect to the streams and lakes in early spring.

If a snow pack has undergone a series of thaw and refreeze cycles, the concentration of pollutants leached at first melt may be very high. Processes which occur during snow recrystallization are involved in which contaminants accumulate preferentially at the surface of the ice crystals, then are leached out rapidly at spring melt.

Snow packs have a great deal less buffering capacity than other components of the ecosystem because the snow cover prevents re-entrainment of alkaline dust material and natural ammonia.

Table III is a summary of snow quality in various parts of North America. The acidity of a snow pack is thought to be primarily controlled by the sulphate and nitrate concentration as these compounds are believed to exist in a direct acid form. For both Northwestern Quebec and the Adirondack regions the acidity is primarily controlled by nitrogen based ions. However, in northern Saskatchewan and for other areas which are not yet heavily impacted upon by man-made emissions the sulphate ion is the dominant species in the snow pack. The mean concentration values of the ions within the project region are less than in the eastern portions of North America.

## EMISSIONS

Much of the detail of emissions for Alberta has been given (Webber, 1979) to the year 2006 A.D. Forecast emissions from the oil sands industry are to increase from approximately 100 K tonnes of $SO_2$ per year at present to 400 K tonnes of $SO_2$ per year at 2006 A.D. The industrial development scenario of the Energy Resources Conservation Board for this area is as well outlined. Most of this emission increases will take place directly within the Alberta portion of the project region. Sulphur generated by miscellaneous activities of an increased urban population are not given. For the province of Alberta the total emissions of sulphur dioxide are expected to increase to approximately 1168 K tonnes by the year 2000 A.D. This represents more than a doubling of the present emissions. Most of the increase will be from the oil sands heavy oil and power production industries. While the oil sands development will take place within the project region, the power industry-by-way-of an increase in its coal burning facilities will be located primarily in the southeast sections of the province of Alberta.

Emissions for Saskatchewan (Zaidi, 1980) are expected to undergo rapid increase to the year 1990. Sulphur dioxide is expected to go from its present value of 46 K tonnes to 100 K tonnes. This includes the possibility of two heavy oil upgrading plants at a maximum emission of 7 K tonnes per year each. Nitrogen oxides are to have a modest increase from 144 K tonnes to 196 K tonnes per year.

The uranium mining and milling industry is expected to undergo rapid growth increases to the year 2000 with six or seven new sites by 1990. Each site is expected to emit at most 300 tonnes of $SO_2$ per year and negligible amounts of $NO_2$.

Approximate emission scenarios for the project region are given

Table III. Snow Anion Quality from Regional Studies

| Location | pH | Sulphate ppm | | Nitrate ppm | | Source |
|---|---|---|---|---|---|---|
| | Range | Range | Mean | Range | Mean | |
| Adirondack Mountains | 4.2-4.4 | 3.44-1.88 | 1.23±0.50 | 3.23-2.40 | 3.15±4.1 | Galvin (1978) |
| Northwest Quebec | 4.7-4.2 | 1.76-0.48 | 0.90±0.44 | 1.76-0.69 | 1.20±0.40 | Frantisad (1980) |
| Northern Saskatchewan | 5.2-5.6 | 1.23-0.42 | 0.70±0.24 | 0.60-0.19 | 0.42±0.10 | Shewchuk (1981a) |

Table IV. Project Area Emissions Inventories

A. Emission Inventory Summary for Project area at present

| | $SO_2$ K tonnes/yr | $NO_x$ K tonnes/yr |
|---|---|---|
| Oil Sands | 160 | 50 |
| Smelting | 280 | -- |
| Other (urban, uranium) | 3 | 4 |

B. Emission Inventory Summary for Project area at 2000 A.D.

| | $SO_2$ K tonnes/yr | $NO_x$ K tonnes/yr |
|---|---|---|
| Oil Sands | 520 | 200 |
| Smelting | 300 | -- |
| Other | 4 | 4 |

in Table IV. Insufficient information is available to construct a particulate inventory. While Flin Flon is just outside our project region, emissions from industrial sources there were concluded.

Total sulphur oxide emissions at present are 443 K tonnes per year and are expected to increase to 824 K tonnes per year. This value is somewhat conservative, based on the difficulty in assessing the contributions from urban development. Total nitrogen oxides are expected to increase from an estimated 54 K tonnes to 204 K tonnes per year. This is a very difficult figure to estimate and may not be far off reality. The smelting and uranium industries are not the main sources of this oxide. Due to possible increase in the oil sands and associated urbanization, nitrogen oxide emissions may be considerably higher. Nitrogen oxides apparently will increase at a faster rate than sulphur oxides, primarily because the emissions at present are very low and any increase is directly tied to the growth of the oil sands and related industries. If it can be assumed that the additional sulphur stress shows up as increased deposition then the present deposition rates will be increased by 3.2 kg/ha. yr. If all of this sulphur is contained in precipitation as unbuffered anions, the mean pH of the rain will be 4.3 with a hydrogen ion deposition of 20.4 meq/m$^2$.y.

This above estimate assumes that all of the emissions will be deposited within the outlined project region and that the atmospheric environment is lightly buffered. It should be pointed out that neither of these assumptions is correct. Wind patterns will carry the material to preferential locations within the region, hence these estimates could be significantly higher. It is also feasible that certain weather regimes will advect most of the material out of the region, in which case results will be significantly lower.

## CONCLUSIONS

The study forms only part of a major effort (Shewchuk et al, 1981b) to assess the effects of all portions of the ecosystems within the study area. It is shown in this report that increases in the deposition of the order outlined in this paper will result in significant degradation to the highly sensitive systems of the Precambrian Shield within both provinces of Alberta and Saskatchewan.

## References

Barrie, L.A.: "The concentration and deposition of sulphur compounds and metals around the G.C.O.S. oil extraction plant during June 1977". AOSERP sub-project ME 1.5.3.

Frantisak, F., G.H. Pelletier, M. Bedard and G. Castonguay. 1980: "Precipitation quality in the Northwest Quebec-Canada". Air Pollution Control Association, 73rd Annual Meeting, Montreal, Quebec, June 22-27, 1980.

Galvin, P.J. and J.A. Cline. 1978: "Measurement of anions in the snow cover of the Adirondack Mountains". Atmospheric Environment 12, pp. 1163-1167.

Johannessen, M. and A. Henrikson. 1978: "Chemistry of snow meltwater: changes in concentration during melting". Water Resources Research 14, pp. 615-619, August 1978.

Shewchuk, S.R. 1979: "A background study of potential sulphur stresses in west central Saskatchewan". SRC Report No. P 79-6.

Shewchuk, S.R. 1981(a): "Snow surveys in Northern Saskatchewan (unpublished).

Shewchuk, S.R., Z. Abouguendia, F. Atton, J. Dublin, B. Godwin, N. Holowaychuk, R. Hopkinson, W. Liaw, J. Maybank, G. Padbury and B. Schreiner. 1981(b): "Regional transport of air pollutants and associated ecosystem sensitivities". Saskatchewan Research Council Publication No. P-780-1-B-81.

Smith, F.B. and G.H. Jeffrey. (1975): "Airborne transport of sulphur dioxide from the U.K.". Atmospheric Environment 9, pp. 643-659.

Webber, H.J. and G.A. Warne. 1979: "Sulphur emissions - Alberta energy industries". P.N.W.I.S. - A.P.C.A. Annual Meeting 7-9, November 1979, Edmonton, Alberta.

Zaidi, S.A. and R.K. Nath. 1980: "Personal communication".

# METEOROLOGICAL CONTROLS ON AIR POLLUTANTS IN A SELECTED REGION OF WESTERN CANADA

Prepared by

R.F. Hopkinson and J. Dublin
AES, Scientific Services Regina
Regina, Saskatchewan, S4P 3W5

**Abstract**: A study was made of the meterological parameters that influence dispersion, transport, transfromation and deposition of air pollutants over northern Saskatchewan and northeastern Alberta. This involved the investigation of storm tracks and the character of precipitation on a seasonal basis, the construction of precipitation wind roses, and the review of solar radiation and sunshine in the area, and the determination of snow depths and the date of major snowmelt across this region. Annually, the mean transport in the boundary layer is eastward, particularly near the top of the layer. Seasonal variations are more evident at the earth's surface, but the wind roses tend to be dominated by directions with an eastward component.

## INTRODUCTION

As part of a study of the potential for long range transport of air pollutants and in particular,acidic deposition, over Northeast Alberta and Northern Saskatchewan,a general survey of available meteorological data and reports was undertaken. No attempt was made to model transport and deposition in this study but such modelling in conjunction with a monitoring program will be required to provide quantitative deposition patterns. This investigation centred mainly on airflow and precipitation over the study area. In addition reference is made to the maximum afternoon mixing height work of Portelli (1977) and to solar radiation intensities.

The study area includes a portion of the Canadian Shield which covers much of northern Saskatchewan and extreme northeast Alberta. The shield region is relatively uniform in elevation, more than half covered by lakes, and poorly drained. The surface of Lake Athabasca represents the lowest elevation in the study area. In contrast the prairie region to the south and west has a number of significant topographic features superimposed on a general increase in elevation to the south and west. This slope is conducive to orographically induced precipitation for flows from northerly through easterly directions.

## METEOROLOGICAL FACTORS

### Cyclogenesis and cyclone tracks

The lee slopes of the world's major mountain ranges are favoured regions for cyclogenesis. To the west of the study area and in the lee of the Canadian portion of the Western Cordillera, three regions where cyclones are most likely to develop were identified by Chung, Hage and Reinelt (1976). All main synoptic surface maps analyzed in the Regina Weather Office in 1977 and 1978 were re-examined with a view to establishing the origin and tracks of lows crossing the study area. The results supported the findings of Chung et al and indicated that about half of the lows crossing the study area formed or intensified in the Northwest territories in the lee of the MacKenzie Mountains. The tracks of lows were classified as to direction of origin. (See Table 1).

Table 1. Percentage frequency of storm tracks across the study area in 1977-78 classified by direction of origin.

| DIRECTION | FREQUENCY (%) |
|---|---|
| N - NW | 14 |
| NW - W | 46 |
| W - SW | 31 |
| SW - S | 5 |
| S - SE | 3 |
| SE - E | 1 |
| E - N | 0 |

It is interesting to note that the highest frequency of occurrence is for lows tracking from between west and northwest, and that lows tracking from between northwest and southwest account for 77% of all depressions that cross the region. These results are reasonable in view of the prevailing direction of the steering flow, near the middle of the atmosphere at approximately 50 kPa.

The significance of such information lies in the fact that the cyclones and air associated with their origins influence the climate of the region. Most of the storms crossing the region are associated with air which has crossed a major mountain barrier and has had much of its moisture removed by orographic precipitation on the windward slopes. In the wake of these disturbances, injections of air are of arctic origin which in an absolute sense have a low water holding capacity. Incursions of air with high absolute humidity from the Gulf of Mexico are rare. Hence the precipitation over the region is markedly less than over eastern North America. As well, situations which could lead to transport of air with high pollutant loadings from eastern North America are rarely experienced.

Migrating cyclones are also the scale of eddies which are active in the medium and long range dispersion/transport of air pollutants with atmospheric residence times of the order of days (Bolin and Persson, 1975). The wind flow through this region is most likely to be from the northwest at levels above the surface while the frequency of other flows may be viewed as a perturbation imposed on this prevailing direction.

## Wind flow over the Study Area

The study area is thought to be located in the zone of the westerlies both at the surface and throughout the troposphere. Examination of monthly mean charts produced by Harley (1980) for the 50 kPa level supports part of this belief. At this level the mean winds inferred from the direction of the height contours are between west and northwest, with the strongest winds in February and the weakest in June. Migrating depressions generally follow the direction of the 50 kPa flow and the previous section on cyclone tracks provides some information on the frequency of such flows. Almost half the low pressure systems crossing the study area moved in a direction which agreed well with the mean charts of Harley.

Titus (1967) constructed monthly mean geopotential height charts for a number of pressure levels based on data from 1951 to 1960. The lowest such level he considered was 85 kPa. The mean 85 kPa flow ranged from west to northwest and achieved a maximum in strength in December, and a minimum in June. Winds at the 85 kPa level have been used in a number of sulphur transport/deposition models with considerable success. Thus, in a crude sense, such charts imply a net east southeast transport of airborne pollutants across the study region.

A major problem exists with information derived from mean 85 kPa charts. Data averaged over a period of time mask the flow patterns associated with a variety of weather systems and storm tracks, and detail nothing of the frequency and strength of different flows. The wind speed so determined is much less than the mean winds for all directions at that level as opposing flow regimes lead to slack gradients on mean 85 kPa analyses.

In an effort to provide more complete information, 85 kPa winds were examined for one year (March 1971 to February 1972) at Fort Smith, Edmonton and The Pas. Admittedly, this data base was rather short and the resultant wind roses should be regarded as somewhat tentative. The data source was the Monthly Bulletin, Canadian Upper Air Data. Annual wind roses showing percentage frequencies for eight points of the compass and calm are presented in Figure 1.

Winds from the northwest were clearly dominant in all seasons and most strikingly so in winter. East and northeast winds are least frequent at all stations. Some seasonal shifts were observed as directions southeast to southwest were more frequent in seasons other than winter. This provided a quantitative estimate of the likely direction of movement of air parcels at 85 kPa at these stations, and by implication of the frequency of different flow patterns at this level across the study area.

This procedure was employed at the 90 and 95 kPa levels for the same stations. Data at 95 kPa were not available for Edmonton as that pressure level was below ground. The resultant frequency data were very similar to those at 85 kPa. In general, similar observations can be made for these two levels as were made for the 85 kPa level. However, a trend toward greater frequencies for directions with an easterly component is appartent as level of observation approaches the earth's surface. Inversely, the dominance of the northwesterly winds diminishes as one approaches the surface.

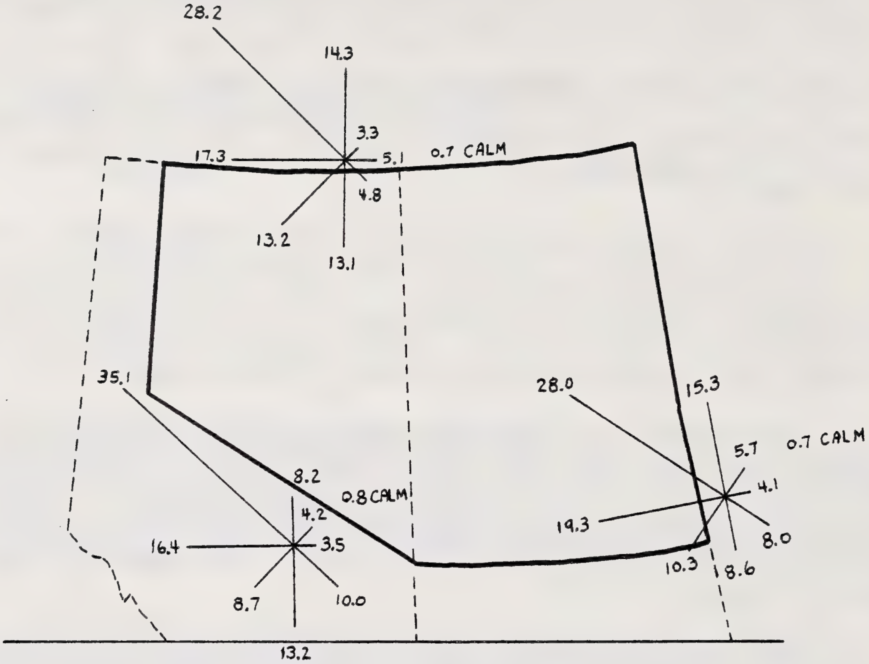

Figure 1. Annual wind rose diagrams for Fort Smith, Edmonton and The Pas at 85 kPa. The figures represent percentage frequency of all observations for the direction indicated.

Mean wind speeds were calculated for all months during the year March 1971 to February 1972 for the pressure levels and stations used in the directional analysis. These mean wind speeds were roughly double the magnitude of the wind speeds determined from the gradient on mean geopotential charts at 85 kPa. The mean speed at all stations increased with height above ground. On an annual basis it ranged from near 6 m/sec at the lowest mandatory level to 8 to 9 m/sec at 85 kPa. The wind speeds over the eastern portion of the study area based on The Pas were noticeably stronger than in the west and perhaps reflect the intensification of cyclones as they track eastward from the Western Cordillera. Wind speeds at all levels tended to be less in magnitude in the spring and summer months and greater in autumn and winter which corresponded to the change in mean flow examined previously.

All hourly and synoptic wind data were processed for 19 surface weather stations within or near the boundary of the study area. The output consisted of tables of percentage frequency of wind direction for 16 points of the compass, and tables of the average wind speed for 16 points of the compass, for each month of the year and on an annual basis. Using these data, wind roses were plotted for January, April, July, October, and the entire year.

These analyses demonstrated the significance that local topography has on the distribution of surface wind directions. There was a general preference for winds with a westerly component at many stations however, at a number of stations east or southeast winds were dominant. Southeast winds showed a seasonal maximum in the spring at most stations. An overall impression that eastward transport near the surface was most frequent was not as strikingly evident in the surface wind roses as it was in the upper level ones.

Joint frequency tables of wind direction and wind speed or mixing height are available as a result of Portelli's (1977) mixing height study. In general the frequency of wind direction using this source agreed well with wind roses computed here, however the clear dominance of northwest winds in winter was not as apparent. The associated wind speeds in winter were also noticeably less. Both these factors are likely a result of the shallowness of the computed mixing height and the increased significance of the surface wind in the calculation of the mixing layer wind speed and direction.

All of the above information indicated that the most frequent direction of air movement over the study region is from northwest to southeast. A secondary maximum was noted in the opposite direction. None of these studies really addressed the persistence and uniformity of flow across the study area that could only be described from synoptic flow and trajectory studies. Denison (1977) constructed trajectories from and to Fort McMurray and compiled a trajectory climatology for that point. The resultant frequency diagrams generally agreed with the wind roses and frequency tables presented here, however, this one point may not presentative of the entire study area. A trajectory climatology for a number of key emission and receptor points would be an asset in evaluating the flow patterns in a more rigorous manner.

## Air pollution climatology

The pollution potential of a region can be assessed by a number of meteorological parameters that determine the rate at which air pollutants are diluted. One of these parameters is the mixing height, which is the vertical height through which dispersion takes place. Another parameter is the mean transport wind speed in the layer specified by the mixing height (Miller, 1967; Holzworth, 1967). Multiplying the mixing height by the mean transport wind speed integrates the two parameters to give a measure of the atmosphere's ability to dilute or ventilate pollutants. This product is referred to as the ventilation coefficient.

In a study by Portelli (1977), mean maximum afternoon mixing heights, mean transport wind speeds, and ventilation coefficients were computed for the period June 1965 to July 1969 using upper-air and synoptic data for 33 Canadian and 13 northern U.S. radiosonde stations. Seasonal averages were computed, mapped, and contoured. The following discussion is based on this study.

Generally speaking, mixing heights decrease with increasing latitude, reflecting the variation in surface heating by solar radiation. For the study area the contours of mean maximum mixing heights are more or less oriented from northwest to southeast for all four seasons. In all seasons except winter, the contours exhibit ridging along a line through Edmonton and Fort Smith, and troughing along a line through The Pas and Churchill. Over the span of a year, the mean maximum mixing heights over the study area range from 200 m in the northeastern corner of Saskatchewan in winter to 1800 m along the southwestern border of the area just north of Edmonton in summer.

In spring, the values of the mean maximum mixing heights range from 700 m in northeast Saskatchewan to 1450 m along the southwestern boundary of the study area. In summer,they attain their highest values, ranging from 1300 m in northeast Saskatchewan to 1850 m to the north of Edmonton. In autumn, the values are lower than in spring and range from 550 m in the northeast to 870 m in the southwest. The winter mixing heights are markedly lower, reflecting the strength of the arctic inversion and the weakness of solar radiation, and range from 210 m in the northeast to 280 m in the southwest.

The mean wind speeds averaged through the maximum mixing layer were determined from the 0000 GMT soundings which corresponds to late afternoon. These wind speeds exhibit a similar pattern in all seasons. The highest wind speeds occur along the eastern boundary of the study area and lowest wind speeds in the northwestern corner. In all seasons except winter, wind speeds range from less than 5 m/s in the northwest to approximately 7 m/s along the eastern boundary. The increase in wind speed as one proceeds eastward is probably a reflection of the increasing intensity of lows to the east of the study area. Most cyclones affecting the study area develop in the lee of the major mountain barriers and intensify as they move eastward. Wind speeds are lowest in winter, ranging from about 2.5 m/s in the northwest to 5.5 m/s in the east. These low wind speeds are partially a result of the arctic high pressure systems which exist over the region for much of the winter. As mentioned in the section on wind flow, winds calculated for the shallow mixing layer in winter are significantly influenced by the surface wind which, for reasons for friction, is substantially less in magnitude than upper level winds.

In the United States, an area is considered to have high pollution potential if the afternoon ventilation coefficient does not exceed 6000 $m^2/s$ (Stackpole 1967; Gross, 1970). The mean summer afternoon ventilation coefficients exceed 6000 $m^2/s$ for the entire study area. In spring, the mean afternoon ventilation coefficients are below 6000 $m^2/s$ for approximately the northeastern quarter of the area. In the fall and winter, the coefficients are below 6000 $m^2/s$ for the entire area, with lowest values in winter when figures range from approximately 1000 to 1600 $m^2/s$. Using the criterion given above, the entire study area has high pollution potential in the fall and winter, and the northeastern quarter of the area has high pollution potential in spring for pollutants released with in the mixing layer.

Although the concept of ventilation coefficient is not entirely suitable to long range transport, it does provide an indicator of the atmosphere's dispersive capability over the study area. The mean maximum mixing height is used to define the layer through which released emissions will be mixed for the purpose of some transport/deposition models. Some models use seasonal estimates for the height of the well mixed layer which could mask significant episodic events. In addition, there will be cases, when the mixing height concept is inappropriate to emissions from elevated sources such as the case of emissions above the well mixed layer or in the case of the absence of a well mixed layer. This could be of particular concern in winter and any model chosen to assess deposition should be capable of addressing such cases.

## Precipitation over the study area

Winter, which for computational convenience is defined as the period of December through to February, is the season with least precipitation. Amounts range from approximately 50 mm over most the Saskatchewan portion of the region to in excess of 75 mm in the Birch Mountains and Cheecham Hills of Alberta (Longley, 1972). Frontal systems moving across the region account for only a small fraction of the precipitation events but their contribution to total winter precipitation is significant. A few well developed frontal lows may contribute the bulk of the snow pack in a given winter. Light continuous snow or snowflurries in low level circulations ranging from northerly through to southeasterly occur over much of the region for extended periods of time and appear to contribute significantly to total winter precipitation. Through the range of low level circulations above, the air moves upslope over much of the region. This so-called circulation weather occurs to the east and south of persistent arctic highs. Ice crystals and intermittent light snow are frequently reported in stagnant arctic air masses but account for very little of the total snowpack.

Precipitation patterns associated with frontal lows bear little resemblance to the textbook models. The only generalization that can be made is that for a well developed frontal low, the continuous precipitation associated with the frontal wave extends well to the west of the wave because of the circulation phenomenon discussed above.

Spring precipitation (that for March through May) ranges from less than 50 mm in extreme northeastern Saskatchewan to in excess of 90 mm in the Cheecham Hills area of Alberta. The number of frontal systems crossing the region increases and most of the spring precipitation is produced by these systems. Circulation weather, which is still common in March, decreases in frequency of occurrence as the season progresses. In May, convective weather begins to make a significant contribution to precipitation over the study area.

The summer (June through July) is the wettest time of the year. Precipitation amounts range from a minimum of less than 125 mm to the north of Lake Athabasca to in excess of 250 mm in the Birch Mountains and Cheecham Hills. Almost all precipitation is showery in nature, being almost equally divided between activity on frontal systems and airmass weather. This is in marked contrast to areas in Saskatchewan and Alberta to the south of the study area where airmass weather (convective storms not associated with fronts) is more common than frontal weather in summer. This appears reasonable in view of the fact that most of the lows and associated frontal waves track across the northern halves of Alberta and Saskatchewan in this season. The precipitation minimum to the north of Lake Athabasca in summer appears to result from the stabilizing effect that the relatively cold lake water has on air masses moving across the lake from the south.

Fall precipitation amounts range from a minimum of less than 75 mm in the Lloydminster-North Battleford area to a high of 125 mm along the Manitoba-Saskatchewan border to the east of Wollaston Lake. Showery weather decreased as the season progressed. Frontal systems appear to account for most of the precipitation. Circulation weather increased in frequency and importance late in the season.

Another way to view the nature of the precipitation was to look at the ratio of rainfall to total precipitation. This was done by taking a sample of long period station across the study region from Canadian Normals 1941-1970. The normal monthly and annual rainfall were divided by the corresponding normal total precipitation. In general the percentage rainfall at all stations is insignificant in the months November to March inclusive. In April, rainfall represents roughly one third of the total precipitation while in October about one-half of the precipitation falls as rain. Through the remaining months, May to September, rainfall is dominant.

## Snow depth and snowmelt

Throughout the winter, sulphates and nitrates accumulate in the snowpack. When the snowpack melts in spring, the accumulated pollutants suddenly enter the streams and lakes causing the acidity to increase sharply for a short period of time. The phenomenon is referred to as the "acid shock". The timing of the first major runoff can be determined by examining hydrometric data, which are scarce for much of the north. An alternate but less precise method of determining the time of the first major runoff is obtained by examining the depletion of the snowpack. Time series of the snow depth on the ground as reported on the 1200 GMT synoptic reports for all weather reporting stations in or near the study area were examined. As the days begin to warm in spring, the water equivalent of the snow gradually increases as snowdepth decreases until the snow is ripe. Slow decreases in snow depth were ignored and the date of the first major runoff was assumed to be the middle of period when snow depth decreased rapidly over a period of several days.

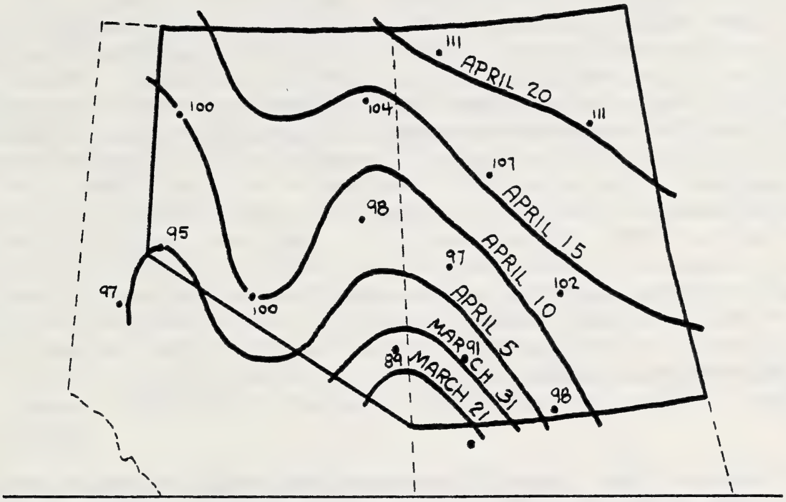

Figure 2. Mean date of the first major snow melt (plotted figures - Julian day).

Plotted and contoured average dates of the first major snowmelt are shown in Figure 2. The variation of these dates was much less over the forested portions of Alberta and Saskatchewan than over the prairie region to the south as evidenced by standard deviations of 5 to 7 days and several weeks repectively.

The mean depth of snow on the ground at the end of February and March was calculated for the same stations. The greatest snow depth extended across the northern portion of the study area which agreed well with earlier work by Potter (1965). Somewhat more detail was evident in these analyses than in Potter's study but the local influence of topography was not well depicted. None of the stations was located at the higher elevations of the major ranges of hills where it could be anticipated that snow depths would be noticeably greater.

Solar radiation and bright sunshine

Yorke and Kendall (1972) presented the normal hours of bright sunshine for the years 1941 to 1970. On an annual basis, there is a large degree of uniformity across the study with a very gradual decrease from 2200 hours in the south to about 2000 hours in the north. Although much farther south, southern Ontario and southern Quebec experience only 2000 hours of bright sunshine a year, reflecting the greater frequency of cloud cover in eastern Canada. A partial season (May to September) comparison indicates a greater number of hours of bright sunshine are observed over most of the study area than in southern Ontario and southern Quebec.

Solar radiation normals have recently been updated (Phillips and Aston, 1980). Monthly and annual mean daily charts as well as tabular data were assembled. The charts were produced using radiation normals for the 57 stations in the radiation network and derived data for 50 stations based upon a method outlined by McKay and Won (1979). On an annual basis, the mean daily global solar radiation decreases gradually across the study area from 12 megajoules per square metre in the south to about 11 $MJ/m^2$ in the north. These values are somewhat less than over southern Ontario where the annual mean daily figure exceeds 13 $MJ/m^2$. For comparison of monthly values of mean daily solar radiation, data for Toronto Meteorological Research Station, Cree Lake and Fort Smith were examined. The values for Cree Lake were interpolated from the monthly charts while those for Fort Smith and Toronto were provided in tabular form (Philips and Aston, 1980). Except for April, May, and June, global solar radiation is greatest at Toronto and substantially so from October to February. From April to June the three curves are almost coincident. Despite a comparable or even a greater number of hours of bright sunshine over the study area, the difference in sun elevation angle leads to higher values of energy received at Toronto on an annual basis.

## CONCLUSIONS

The concept that the airflow across the study region is most frequently from the northwest is generally supported by the information surveyed. The maximum depth of the well mixed layer during the seasons other than winter is of the order of kilometer. Thus, a model using the 85 kPa wind field as the transport wind would likely demonstrate skill for much of the year. More sophisticated procedures may be required during the winter season.

The annual precipitation over the study area is much less than over eastern North America or Western Europe, reflecting the drier origins of the air masses affecting northern Alberta and Saskatchewan. Rain is the significant or dominant form of precipitation from April to October. The major snowmelt and the associated release of pollutants accumulated in the snowpack commence near the spring equinox in the south progressing to late April in northeast Saskatchewan.

Solar radiation is near the same intensity over the study area as in southern Ontario except in the late fall and winter months. Thus during the warm months, any difference in oxidation rates may be attributable to other factors such as humidity.

## Acknowledgements

We gratefully acknowledge the assistance of P. Kociuba of AES Western Region, Scientific Services Division for the computer processing of data required for the surface wind frequency tables and snow depth tabulations. R. Angle of the Pollution Control Division of Alberta Environment offered constructive criticism of the initial findings. R.K. Smith of Scientific Services Regina helped prepare the diagrams and assisted in much of the data reduction.

## References

Bolin, B. and C. Persson, 1975: Regional dispersion and deposition of atmospheric pollutants with particular application to sulphur pollution over western Europe. Tellus Vol. 17, 281-310.

Chung, Y.S. K.D. Hage and E.R. Reinelt, 1976: On lee cyclogenesis and airflow in the Canadian Rocky Mountains and East Asian Mountains. Mon. Wea. Rev., Vol. 104. 879-891.

Denison, P.J., 1977: A climatology of low level trajectories in the Alberta oil sands area. Alberta Oil Sands Environmental Research Program, Project ME 3.4. AOSERP Rept. No. 15. 118 pp.

Environment Canada, 1975: Canadian Normals: 1941-1970. Precipitation, Volume 2SI. Downsview, Ontario. 333 pp.

____________, Monthly: Monthly Bulletin, Canadian Upper Air Data. Downsview, Ontario.

Gross, E., 1970: The national air pollution potential forecast program. ESSA Tech. Memo. WBTM-NMC 47, National Meteorological Center. Suitland, Maryland. 28 pp.

Harley, W.S.; 1980: Northern hemisphere monthly mean 50 kPa and 100 kPa Height charts. Environment Canada, Atmospheric Environment Service, circular CLI-1-80. 30 pp.

Holzworth, G.C. 1967: Mixing depths, wind speeds, and air pollution potential for selected locations in the United States. J. Appl Meteor., Vol.6, 1039-1044.

Johnson, W.B., D.E. Wolf and R.L. Mancuso, 1976: The European-regional model of air pollution (EURMAP) and its application to transfrontier air pollution. Seventh International Tech. Meeting on Air Pollution Modelling and its Application. NATA/CCMS Air Pollution Pilot Study. 30 pp.

Longley, R.W. 1972: The climate of the Prairie Provinces. Environment Canada, Atmospheric Environment Service. Climatological Studies No. 13. Toronto, Ontario. 79 pp.

McKay, D.C. and T.K. Won, 1979: Expansion of the Canadian solar radiation data base by estimation. Paper 79-102 presented at solar Energy Society of Canada Inc. Conference, Charlottetown, P.E.I. 12 pp.

Miller, M.E., 1967: Forecasting afternoon mixing depths and transport wind speeds. Mon. Wea. Rev., Vol. 95, 35-44.

Phillips, D.W. and D. Aston, 1980: Canadian solar radiation data. Environment Canada, Atmospheric Environment Serive, circular CLI-2-80. 110 pp.

Portelli, R.V., 1977: Mixing heights, wind speeds, and ventilation coefficients. Environment Canada, Atmospheric Environment Service. Climatological Studies No. 31. 87 pp.

Potter, J.G., 1965: Snow cover. Canada Department of Transport, Meteorological Branch. Climatological Studies No. 3. 69 pp.

Stackpole, J.D., 1967: The air pollution potential forecast program. Weather Bureau Tech. Memo. WBTM-NMC 43, National Meteorological Center. Suitland, Maryland. 8 pp.

Titus, R.L., L967: Upper air climate of Canada 1951-1960. Charts of monthly geopotential, temperature and humidity. Canada, Department of Transport, Meteorological Branch. Toronto, Ontario. 103 pp.

Yorke, B.J. and G.R. Kendall, 1972: Daily bright sunshine 1941-1970 Environment Canada, Atmospheric Environment Service, circular CLI-6-72. 9 pp.

# SENSITIVITY OF SOILS TO ACIDIC DEPOSITION IN A SELECTED REGION OF WESTERN CANADA

by

N. Holowaychuk
Alberta Research Council
4445 Calgary Trail South
Edmonton, Alberta

G. Padbury
Saskatchewan Institute of Pedology
University of Saskatchewan
Saskatoon, Saskatchewan

B. Schreiner
Saskatchewan Research Council
University of Saskatchewan
Saskatoon, Saskatchewan

## ABSTRACT

The relative sensitivity of acidic deposition of the soils of northern Saskatchewan and northeastern Alberta was evaluated. Three categories of relative sensitivity were established based on the buffering capacity of the soils as interpreted from their cation exchange capacity and reaction, and where pertinent, from other soil attributes.

Approximately 40 to 50 percent of the soils in the study area were found to be in the most sensitive category, about 17 percent in the intermediate sensitivity category, and about 15 percent in the least sensitive category. The remaining part of the study area is comprised of lakes and rock outcrops.

The bulk of the soils in the most sensitive category are classified in the Podzolic and Brunisolic Orders and occur on coarse textured sandy and gravelly sediments of the Canadian Shield. Large tracts of relatively sensitive organic soils also occur in the northern regions of Alberta.

## INTRODUCTION

The paper presents interpretative ratings and general areal distribution of the relative sensitivity of the soils of the selected region to likely effects of acidic depositions. As used in the discussion, the term sensitivity refers primarily to the degree of susceptibility of the different kinds of soils recognized in the region to change in soil pH and base saturation in response to effects of depositional acid inputs. Some consideration is also given to the possible modifying influences the soils may have on the quality of effluent water. A review and the interpretations of what information was available regarding the chemical and physical properties and other pertinent attributes of the soils of the region, serve as the basis for estimating their relative sensitivity.

The soils recognized in the region to date are classified into three broad relative categories of sensitivity. Because of the large number of different kinds of soils present in the region, the soils within each of the broad categories are grouped into subcategories to facilitate more specific consideration of the pertinent properties. The general areal distribution of subcategories is shown on a small scale map.

The paper reports on an initial attempt at assessing the sensitivity of the soils of this region to effects of acidic deposition. Because of the overall scarcity of both inventory and analytical data on the soils, this study is regarded as a first approximation rather than a sophisticated conclusive evaluation.

## GENERAL DESCRIPTION OF THE SELECTED REGION

### Location and Extent

The location and extent of the selected region are shown in Figure 1. It comprises an area of about 70 million hectares of which about 60 percent occur in Saskatchewan and 40 percent in Alberta.

### Geology

A basement complex of ancient Precambrian rocks, mainly granites and sandstone, comprise the Canadian Shield section outlined in Figure 1. Numerous rock outcrops, accounting, in places, for as much as 80 percent of the land surface, are one of the prevalent features. A narrow belt of Devonian limestone, dolomite and evaporites borders the Canadian Shield on the south and west. In the remaining extensive portion of the region, the bedrock consists almost entirely of nearly horizontally bedded Cretaceous shales, sandy shales and sandstones. Remnants of Tertiary gravels are found in Alberta in the Caribou and Pelican Mountains and in the Swan Hills.

All of the region has been overridden by continental glaciers so a very large proportion of the bedrock is covered by glacial drift that ranges from a thin veneer to several hundred metres in thickness.

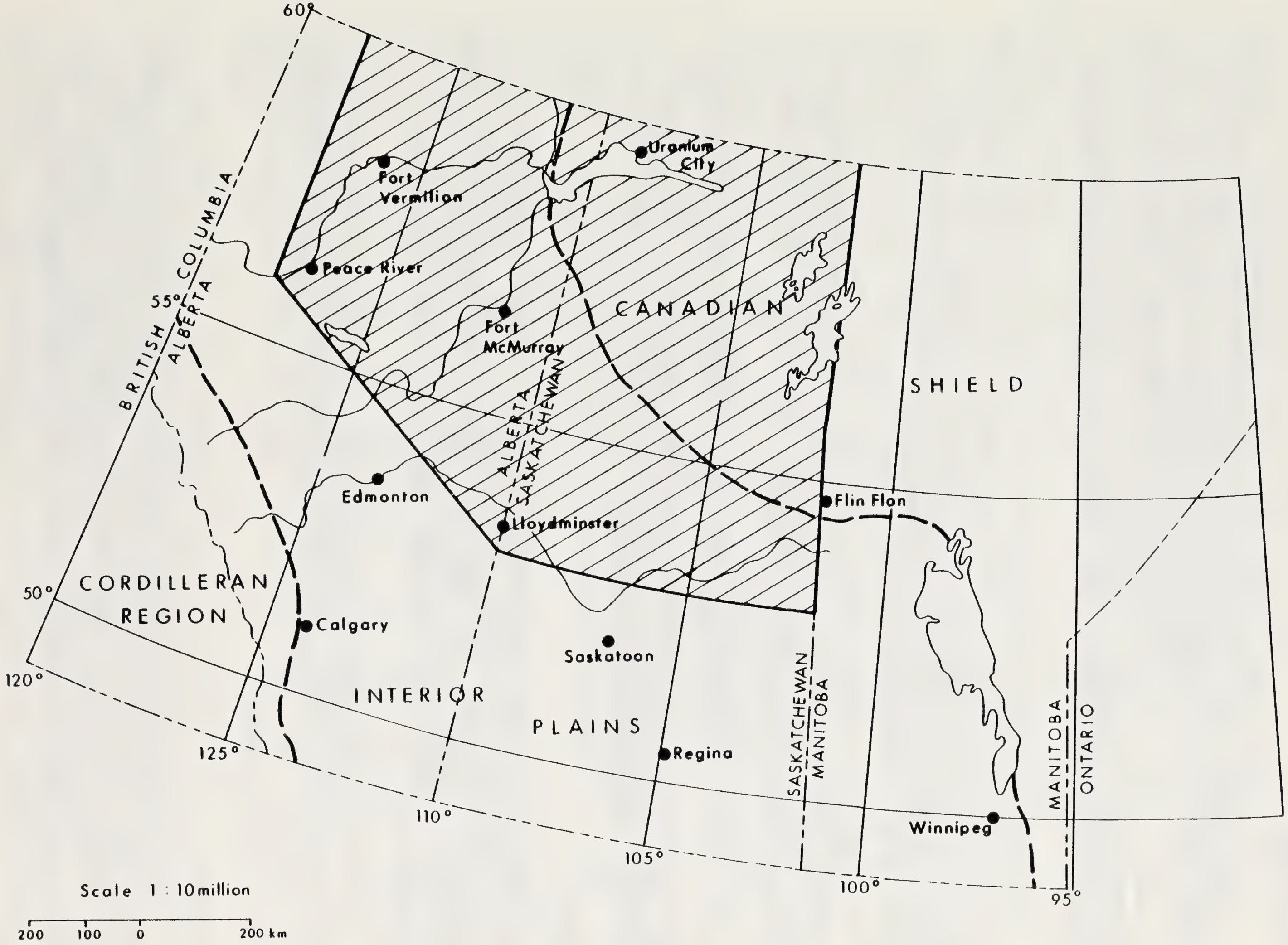

Figure 1. Location and the major physiographic divisions of the selected region.

## Physiography

The selected region spans two major physiographic regions, the Canadian Shield and the Interior Plains (Bostock, 1970) as shown in Figure 1. The Canadian Shield comprises about 60 to 70 percent of the selected region in Saskatchewan, but only a minor portion extends into the northeastern corner of Alberta. There are two physiographic divisions within the Canadian Shield, the Kazan Upland and the Athabasca Plains. The latter borders the Interior Plains south of Lake Athabasca and extends across northern Saskatchewan to Wollaston Lake.

The Interior Plains includes several physiographic divisions within the selected region: the Manitoba, the Saskatchewan and the Alberta Plains in the southern parts and the Alberta Plateau, the Peace River Lowlands, the Hay River Lowlands and the Great Slave Plain in the northern portion of Alberta. A somewhat more extended resume of the physiography is given by Clayton *et al*. (1977a, pp 29-39 and 42-49).

In general the surface of the region has a general downward slope from the west or southwest to the east and northeast, ranging from about 1200 metres in the Swan Hills area to about 500 metres in eastern Saskatchewan and 200 to 300 metres near Lake Athabasca.

The region is drained by stream systems flowing northward to the Arctic Ocean and eastward to Hudson Bay. Many parts of the region have restricted surface drainage due to the weakly expressed stream systems in such areas. There are myriads of small and a number of larger lakes in a considerable portion of the Canadian Shield section.

## Climate

The climate of the area is cold continental characterized by long, cold winters and short, warm summers. Considerable variations in climatic conditions do, however, occur from one place to another due both to the latitudinal expanse and to differences in elevations. The latter is documented in a study carried out by Longley and Janz (1978) in the Fort McMurray-Lake Athabasca area.

Average monthly temperatures range from a low of about -15 to -30°C in January to a high of about 15 to 20°C in July. The mean annual temperature ranges from 2 to -4°C. Average annual precipitation is about 300 to 400 mm, with about 50 to 70 percent of the annual total occurring during the growing season, May to September.

## Vegetation

According to Rowe (1972) the selected region occurs within the Boreal Forest region. The southern fringe of the region and parts of the Peace River Lowland represent a transitional zone between the Boreal Forest and the Grasslands to the south. This is referred to by Rowe as the Aspen Grove section. A somewhat comparable zone, the Boreal Forest-Tundra transition, prevails in the northern portion of the Canadian Shield in the selected region. More extended discussions of the Boreal Forest or parts of it in the region, are given by Clayton et al. (1977, pp 85-89), Kabzems et al. (1976) and North (1976). The publications by Jeglum (1972) and Stanek (1977) are additional sources of information on the vegetation of the poorly or very poorly drained landscapes such as bogs and fens.

Considerable farming is carried on in much of the area along the southern border of the region and in the Peace River basin as far north as Fort Vermillion.

## Surficial Materials

Directly or indirectly the invasions by continental glaciers during the Pleistocene Epoch have strongly influenced or determined the characteristics and distribution of the surficial materials of the region. Unsorted glacial deposits (glacial till), consisting of admixtures of materials derived from local bedrock with materials transported from more distant sources, are widespread throughout the region. Usually the bulk of the till material is derived locally so its composition is strongly influenced by the nature of the indigenous bedrock. This influence is reflected in the texture, mineralogy and carbonate content of the till. Throughout most of the Canadian Shield section the till is coarse textured and noncalcareous due to the prevalence of igneous, metamorphic and sandstone bedrock.

Glaciation also resulted in deposition of sorted materials. These consist of clayey, silty, and in some cases sandy glaciolacustrine sediments and sandy or gravelly glaciofluvial deposits. Postglacial aeolian and alluvial sediments occur sporadically throughout the region but are of relatively minor extent.

There is appreciable terrain in the region where the mineral materials are overlain by peat accumulations of varying thickness. These deposits occur mainly in the poorly drained, low-lying, level areas or depressions but they are also found in some gently sloping uplands especially those of higher elevations. There are two major types of organic terrain, the bogs and the fens. In general the bogs consist of peat derived mainly from moss whereas the peat of fens is derived largely from sedge vegetation. Organic terrain occurs extensively in areas south of the Canadian Shield in Saskatchewan and is of wide extent northward from Lesser Slave Lake in Alberta.

## Soils

The region encompasses a variety of soils that differ widely in texture, organic matter content, chemical and physical properties, soil moisture regimes and other attributes. They range from dark colored grassland soils in the south and west to some of the more northerly areas that are permanently frozen in the subsoil. According to the taxonomic classification of soils (Canada Soil Survey, 1978) all of the 9 Orders: Brunisolic, Chernozemic, Cryosolic, Gleysolic, Luvisolic, Organic, Podzolic, Regosolic and Solonetzic are represented in the region by one or more Great Groups. The principles and criteria employed in the taxonomic classification of soils and the general characteristics of soils in each of the 9 Orders are discussed by Clayton et al. (1977a, pp 100-243). A map, scale 1:5,000,000, that is included with the companion publication (Clayton et al. 1977b), shows the general distribution in the region of the soil Orders and of subgroup combinations.

More detailed information on the occurrence and distribution of soils is available for a minor portion of the selected region. Reconnaissance and detailed reconnaissance soil surveys, scale 1:50,000 to 1:250,000, have been completed for the strip between latitude 53°N and 55°N in the south, in the Peace River valley northward to vicinity of Fort Vermillion and for a sizeable block in the Fort McMurray-Lake Athabasca area. A large portion of the remaining area has been covered by very general exploratory surveys, and a sizeable section is still unexplored. The information accrued to date suggests that soils of Brunisolic, Gleysolic Luvisolic, Organic and possibly Podzolic Orders are the more extensive in the region.

## SOIL SENITIVITY

A clarification of soil acidity parameters will be helpful in the discussion of soil sensitivity. Bache (1980a) states: "Three different parameters are involved in defining soil acidity: the total acidity, the degree of activity, and the manner in which the degree of acidity varies when total acidity is varied i.e. the 'buffering capacity'." Total acidity represents the quantity of acidity that has to be neutralized to raise the pH of the soil to some specified level, usually pH 8.0 and is reported in units like milliequivalents. The total acidity dissociates to a small extent thus generating active hydrogen ions (actually hydronium $H^3O^+$ ions) and the resultant hydrogen ion concentration constitutes the degree of acidity whose magnitude is expressed as pH. The following terminology is commonly used to denote the classes of active acidity (or alkalinity) found in soils.

| Class | pH Values |
|---|---|
| Extremely acid | <4.6 |
| Very strongly acid | 4.6-5.0 |
| Strongly acid | 5.1-5.5 |
| Medium acid | 5.6-6.0 |
| Slightly acid | 6.1-6.5 |
| Neutral | 6.6-7.3 |
| Mildly alkaline | 7.4-7.8 |
| Moderately alkaline | 7.9-8.4 |
| Strongly alkaline | >8.4 |

Another parameter frequently employed, the exchangeable acidity refers to the portion of total acidity that can be extracted from a soil with an unbuffered concentrated (usually 1.0 molar) salt solution such as KCl or $NH_4Cl$. The buffering capacity (BFC) is the amount of acid or base required to change the pH of a given quantity of soil by one pH unit or some other selected increment of pH.

Sensitivity is an expression of the susceptibility of a soil to the degree of change in its pH, base saturation and mobilization of exchangeable bases (Ca, Mg, K, etc.) in response to a given input of acidity.

A review of literature indicates that the BFC of a soil is considered to be the most important parameter that determines its sensitivity. In general, sensitivity is inversely related to BFC. The magnitude of BFC, however, changes with changes in pH. According to Bache (1980a), Fieldes (1962) and Wiklander (1979) the BFC of a negatively charged mineral soil is greater in the very strongly to strongly acid range than it is at higher pH. Holowaychuk and Lindsay (1980) report that upon acidification of medium acid to neutral soils, the pH decreases more markedly relative to the noted decrease in base saturation. In more acid soils the rate of decrease is relatively small compared to the decrease in base saturation as shown in Figure 2.

Pertinent literature indicates that BFC is positively related to a number of soil parameters such as clay content, loss on ignition, base saturation, sum of exchangeable bases and cation exchange capacity (CEC). Holowaychuk and Lindsay (1980) used CEC as an index of BFC and this parameter is also employed in this project to estimate the BFC of the soils of the region.

The level of sensitivity of a soil reflects the integrated result of several factors of which BFC and pH are the most significant. In addition to those two parameters other soil properties or attributes influence the degree to which the soil responds to acidity inputs. Such properties as permeability and moisture holding capacity determine the rate and extent of movement (percolation) of transient soil solutions within the soil and thus may affect the time of contact or degree of miscibility and equilibration between the soil particles and the solution. As an example, in a porous sandy soil equilibration may be minimal because of the rapid movement of solution through the soil as at times of heavier rainfall. The soil moisture regime is likewise a factor that may influence the sensitivity of a soil. Imperfectly, poorly and very poorly soil drainage classes reflect periods of excessive moisture within the soil that may be due to abnormal additions of water supplied surficially or by precipitation or by inflow from subsurface sources. Since the water from the latter sources is often minerotrophic, it may ameliorate the effects of acidic depositions.

The mineralogy of a soil is another factor that may affect its sensitivity. If the more readily weatherable minerals are present, their weathering abets the buffering properties of the soil and in addition may replenish some of the nutrients mobilized by acidifcation.

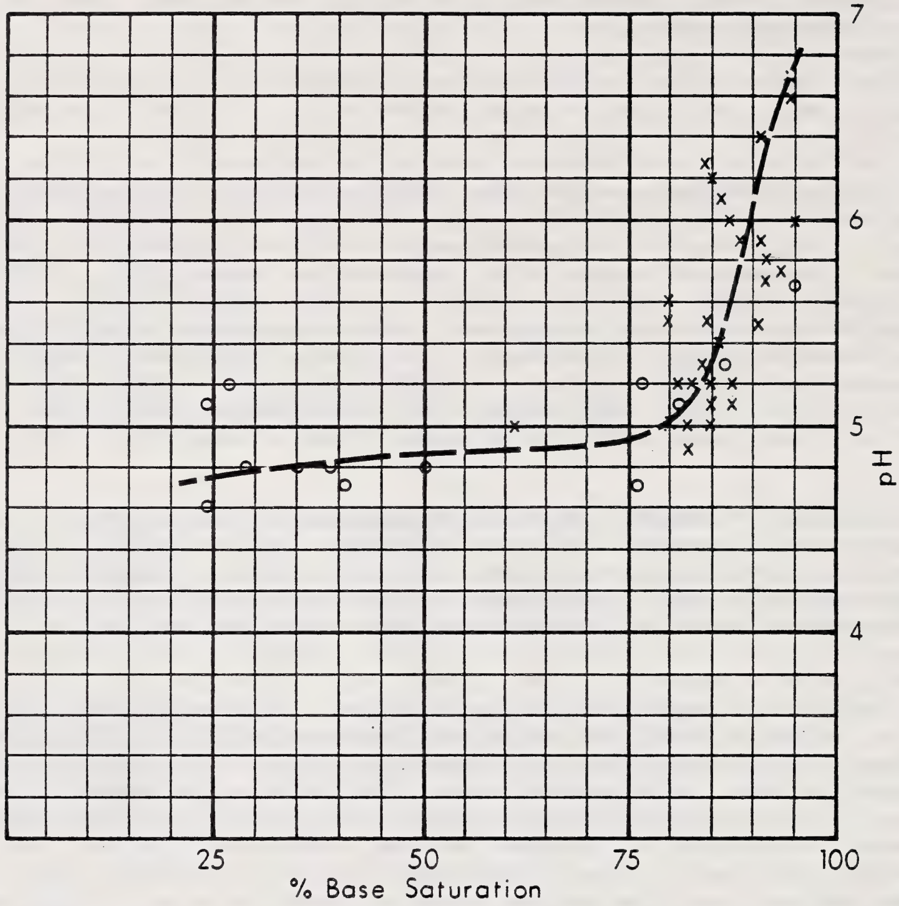

Figure 2. Relationship between pH ($H_2O$) and percent base saturation of Orthic Gray Luvisolic AB horizon samples from Sand River (x) and Fort McMurray (o). Percent base saturation is based on CEC and exchangeable bases measured at pH 7.0. (From Holowaychuk and Lindsay, 1980)

## SENSITIVITY CLASSIFICATION OF SOILS

### Broad Categories and Criteria

The soils of the selected region are classified according to the following three broad relative categories of sensitivity:

1. Most sensitive soils

2. Soils of intermediate sensitivity

3. Least sensitive soils

The three broad categories of sensitivity are based mainly on the BFC of soils but soil reaction (pH) and, where deemed pertinent, the other attributes of soils mentioned previously are also considered. Since the sensitivity of a soil and its BFC are inversely related, soils with low BFC are considered to be the most sensitive while those with high BFC are least sensitive. Three ranges of BFC, low, medium and high, characterize the three broad categories of sensitivity. The relationship between BFC and soil CEC reported by Holowaychuk and Lindsay (1980) and McFee (1980) is used to define low, medium and high ranges of BFC in terms of CEC of mineral soils as follows:

Low BFC - CEC 6 or less meq/100 g soil

Medium BFC - CEC 6 to 15 meq/100 g soil

High BFC - CEC 15 or more meq/100 g soil

In organic soils the BFC is estimated on volume rather than weight basis because of the low bulk density of these soils and their very high CEC if it is expressed on weight basis. Despite the very high CEC of most organic soils their estimated BFC is comparable to that of mineral soils for a given volume of soil when differences in bulk density are taken into account.

### Role of Sensitivity Subcategory

The large number of different kinds of soils that are present in the region emphasizes the need for a scheme and criteria for assembling the soils into groupings that simultaneously would facilitate the following:

1. Classification of the soils within a group into an appropriate category of sensitivity

2. Discussion of the pertinent properties and behaviour of the soils

3. Development of mapping units for showing the areal distribution of soils by sensitivity categories

These objectives are met in the approach used in this project. Soils with similarities in sensitivity – pertinent properties or attributes are assembled into like groups and on the basis of their pertinent properties are classified as to their broad relative category of sensitivity. Subsequently these groupings are used to generate and characterize mapping units for showing the general areal distribution of sensitivity categories in the region. A grouping of like soils with respect to their sensitivity pertinent properties and attributes and their category of sensitivity is referred to as a sensitivity subcategory in this report.

The definitive criteria for each of the subcategories reported in this paper is relatively broad for two reasons. Firstly, the general scarcity of data for soils in considerable portions of the region would not substantiate the application of subcategories with too restrictive limits. Secondly, narrow or too exacting criteria would be conducive to a proliferation of subcategories established to such an extent that the preparation of a regional sensitivity map would be complicated.

## CLASSIFICATION OF SOILS BY SENSITIVITY SUBCATEGORIES

Seventeen sensitivity subcategories are employed to classify the soils of the region in regards to their relative sensitivity and to characterize the soils in each subcategory as to its sensitivity-pertinent properties and attributes. Each subcategory is identified by a numerical symbol consisting of two digits, the first digit denoting the broad relative category of sensitivity. The subcategories are described briefly and listed in numerical sequence. The list also includes three miscellaneous groups that consist of undifferentiated organic soils and of rock outcrops.

1. Most sensitive soils

    1.1 Very strongly to slightly acid soils with low BFC.

    This subcategory includes the deep sandy or gravelly, rapidly pervious soils that have low CEC and low or very low moisture holding capacity. Most of the soils are in the Brunisolic Order.

    1.2 Very strongly to medium acid soils with low BFC in upper horizons and medium BFC in lower horizons.

    The upper horizons of these soils are sandy, rapidly pervious and have low CEC and moisture holding capacity. The lower horizons are finer in texture (loam and sandy loam), are somewhat less pervious and have medium CEC. Most of the soils in this subcategory are in the Luvisolic Order.

    1.3 Very strongly to extremely acid soils with low BFC.

    Soils in this subcategory are sandy, rapidly pervious and have low CEC and base saturation and very low moisture holding capacity. Included in this subcategory are soils of the Brunisolic and Podzolic Orders that have developed on very sandy glacial till, glaciofluvial and aeolian deposits.

1.4 Extremely to medium acid soils with low BFC in surface horizons and low to medium BFC in lower horizons.

Included in this subcategory are sandy soils of the Brunisolic and Podzolic Orders and weakly expressed soils of the Luvisolic Order.

1.5 Very strongly to extremely acid, very poorly drained organic soils.

This subcategory includes the very acid sphagnum dominated organic soils. Because of their low pH and low bulk density they have low effective CEC and low BFC when these properties are considered on volume rather than a weight basis.

2. Soils of intermediate sensitivity

2.1 Slightly to very strongly acid soils with medium BFC in upper Horizons and medium to high BFC in the lower horizons.

Soils that are included in this subcategory are generally loamy in texture in the upper horizons and loamy to clayey in the subsoil. They are moderately to slowly pervious and have medium to high moisture holding capacity. Soils in this subcategory are largely of the Luvisolic Order but some soils of the Solonetzic Order are included. Most of the soils are calcareous within about a metre of the surface.

2.2 Slightly to medium acid soils with medium to high BFC in upper horizons and high BFC in the lower horizons.

The upper horizons of the soils in this subcategory are loamy in texture and contain appreciable organic matter. The lower horizons are generally finer in texture. These soils are moderately to slowly pervious and have medium to high moisture holding capacity. Most of the soils in this subcategory are in the Dark Gray subgroup of the Luvisolic Order.

2.3 Medium to very strongly acid soils with low BFC in the upper horizons and medium to high BFC in the lower horizons.

The upper horizons of these soils are sandy loam or loamy sand in texture, are rapidly pervious and have low to medium moisture holding capacity. The lower horizons are generally loam or clay loam in texture. These horizons are moderately to slowly pervious and have medium to high moisture holding capacity. Most of these soils are in the Luvisolic Order.

2.4 Extremely acid to neutral soils with medium to high BFC.

This subcategory includes soils of the Luvisolic Order that have developed on silty and clayey glaciolacustrine deposits and glacial till in the Agassiz Basin in the Canadian Shield.

## General Areal Distribution of Relative Categories of Sensitivity in the Region

Sixteen mapping units are employed to depict the areal distribution of the relative categories of sensitivity in the region as shown in Figure 3. The relative category of sensitivity of each mapping unit is included in Table 1 and is based on the relative category of sensitivity of its primary component as subsequently defined.

The term primary component of a mapping unit refers to a particular sensitivity subcategory or a miscellaneous group that is more prominent in extent when compared to the other sensitivity subcategories or miscellaneous groups of significant extent that are included in the mapping units delineated. These inclusions of sensitivity subcategories or miscellaneous groups are designated as secondary components of the mapping units.

The sensitivity subcategories and/or the miscellaneous groups that constitute the primary and secondary components of each of the mapping units employed in developing the small-scale map shown as Figure 3, are given in Table 1. It should be emphasized, however, that the composition of the mapping units shown in this table is most likely over-simplified. To begin with, the individual subcategories delineated in the original preliminary map of somewhat larger scale (1:2,000,000) undoubtedly contain appreciable inherent inclusions that are unspecified due to the dearth and general nature of the source information available for much of the region. The small-scale map shown as Figure 3 represents a further generalization.

2.5 Very strongly to strongly acid soils with medium BFC in upper horizons and medium to high BFC in the lower horizons.

The soils in this subcategory are similar to those of subcategory 2.1 in physical properties but are generally more acid. They are in the Luvisolic Order.

3. Least sensitive soils

3.1 Slightly acid to mildly alkaline, poorly to very poorly drained soils with medium to high BFC.

This subcategory includes soils of the Gleysolic Order and the sedge-dominated Organic soils.

3.2 Slightly acid to neutral soils with high BFC.

These soils have thick, dark colored surface horizons with a high organic matter content and high CEC and base saturation. They are in the Chernozemic Order.

3.3 Recent alluvium and rough broken land.

3.4 Slightly acid to neutral soils with high BFC in the upper horizon and low to medium BFC in the lower horizons.

This subcategory includes Chernozemic soils that are rapidly pervious in the lower horizons.

3.5 Medium to slightly acid soils with high BFC.

These soils have a relative, thick surface horizon with considerable organic matter and high CEC. The lower horizons have high CEC and are very slowly pervious. Soils in this subcategory are in the Solonetzic and Chernozemic Orders.

3.6 Neutral to mildly alkaline calcareous soils.

3.7 Very strongly to medium acid soils with high BFC.

This subcategory includessoils that are fine textured with high CEC. They are slowly or very slowly pervious.

Miscellaneous Groups

| | |
|---|---|
| OR | Organic soils with undetermined proportions of subcategories 1.5 and 3.1 and minor inclusions of mineral soils of subcategories 1.1, 1.2, 2.1 and 2.5. |
| R1 | Plutonic rocks — mainly granite, granodiorite, and quartz monzonite. |
| R2 | Plutonic rocks — mainly granite, granodiorite, and quartz monzonite with abundant metasediments, metavolcanics and some mafic and ultra mafic rocks. |

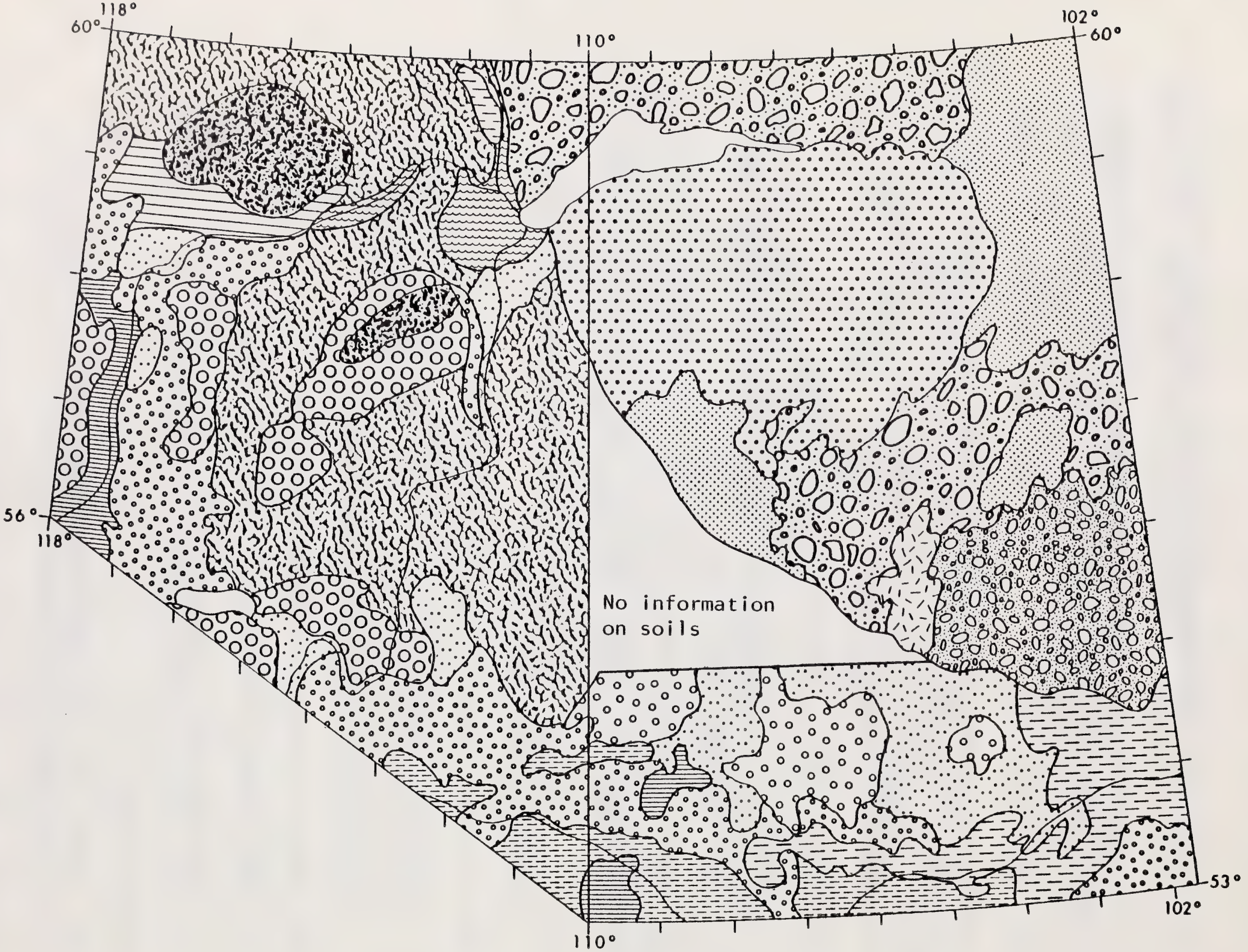

Figure 3. General areal distribution of soil sensitivity subcategories, see Table 1 for legend.

Table 1. Relative category of sensitivity and the primary and secondary sensitivity components of the mapping units (see footnote for explanation of composition of primary and secondary components)

| Mapping Unit | Primary Component | Secondary Components |
|---|---|---|
| | Most Sensitive Soils | |
| ░ | 1.1 | 1.2, 1.5, 2.1, 2.5, 3.1, 3.2, OR |
| ░ | 1.3 | |
| ▒ | 1.4 | R1, OR |
| | Soils of Intermediate Sensitivity | |
| ⁘ | 2.1 | 1.1, 1.5, 2.2, 3.1 |
| ○ | 2.3 | 1.1, 1.2, 3.1 |
| ◯ | 2.5 | 1.1, 3.1, OR |
| | Least Sensitive Soils | |
| ☰ | 3.2 | 1.1, 2.1, 3.4, 3.5 |
| ☰ | 3.3 | |
| ☰ | 3.5 | 2.1, 2.2, 3.2, 3.3 |
| ☰ | 3.6 | 1.5, 3.1, 3.2 |
| ☰ | 3.7 | 3.1, 3.2 |
| | Miscellaneous Groups | |
| ▓ | OR | |
| ▨ | OR | 1.1, 1.2, 1.3, 2.1, 2.5, 3.7 |
| ▨ | R1 | |
| ▨ | R1 | 1.4 |
| ▨ | R2 | 1.4, 2.4 |

---

One sensitivity subcategory or one miscellaneous group characterize the primary component. The secondary component may consist of several of the more significant inclusions of sensitivity subcategories or miscellaneous group. The subcategories are identified by the two digit number symbols and the miscellaneous group by capital letters as these are defined in the preceding section.

## DISCUSSION

It is estimated that about 23 million hectares, or 38 percent of the area, is in the most sensitive category, about 10 million hectares, or 17 percent in the moderately sensitive category, and about 9 million hectares, or 15 percent in the least sensitive category. The remaining area is comprised of lakes, rock outcrop and undifferentiated organic terrain. Roughly 3.4 million hectares, or 5 percent of the area, located north of 55°N latitude and south of the Shield in Saskatchewan, are omitted because of lack of data and inventory information for the area.

The bulk of the soils in the most sensitive category occur in the northern part of the region, mainly in the Precambrian Shield area and to a lesser extent in the forested regions to the south and west of the Shield. The soils are classified mainly in the Brunisolic and Podzolic soil Orders and are developed on coarse textured, sandy or gravelly materials. In addition to these soils, however, large tracts of organic terrain occur throughout the region. These organic soils vary widely in terms of their sensitivity to acidic deposition, ranging from relatively sensitive, weakly decomposed sphagnum-dominated materials to relatively nonsensitive sedge-dominated materials. Although many of the present soil resource inventories do not differentiate between these types of organic materials, it is reasonable to assume that a significant proportion is comprised of those in the most sensitive category. Approximately 9.6 million hectares, or 16 percent of the region, are designated as organic terrain. If it is assumed that 50 percent of this area is comprised of shpagnum-dominated organic materials, then the total area of most sensitive soil approximates 27.5 million hectares, or 46 percent of the region. A summary of the extent of the various categories and subcategories is given in Table 2.

It is important to note that since the bulk of the soils in the most sensitive relative category are in the medium to extremely acid range, acidic depositions are not expected to have a pronounced effect upon the soils themselves. However, since these soils are highly pervious and have a very low buffering capacity, it is anticipated that they will have little buffering effect upon acidic depositions which will result in an acidifying effect on the effluent and groundwater and hence possibly on nearby lakes and streams as well. It is largely for this reason that they are considered to be in the most sensitive category.

Included in the moderately sensitive relative category are mainly Luvisolic soils developed on loam to clay loam textured glacial till and glaciolacustrine deposits. These soils occur mainly in the forested regions of the area to the south and west of the Shield. The effects of acidic deposition on these soils will likely consist of a mobilization of exchangeable bases and a moderate rate of decline in pH for those soils that are in the medium to slightly acid range. These effects are likely to be confined to the upper horizons as the lower horizons are relatively impervious and have a medium to high buffering capacity. For those soils in the strongly to extremely acid range, acidic depositions are not expected to have a significant effect on the soils themselves, but due to the low buffering capacity and pervious nature of the upper horizons, lateral movement of water through these horizons may have an acidifying effect on the groundwater, particularly in sloping terrain.

Most of the soils in the least sensitive category occur in the southern parts of the study area and are classified in the Chernozemic, Solonetzic and Gleysolic soil Orders, although significant areas of Organic soils designated as miscellaneous groups OR in Figure 3, also fall into the least sensitive category. It should be mentioned that most of what observations were made on organic soils of the region were conducted about two decades ago. At that time the minimum thickness of peat was 30 cm to qualify a soil as being organic. Currently the thickness limit is 40 to 60 cm so some of the soils formerly considered to be organic are now classified as peaty Gleysols. In general, soils in the least sensitive category have relatively high levels of organic matter and/or are moderately fine to fine in texture. Some also have free carbonates throughout the profile.

It should be emphasized also that this paper represents an initial attempt at assessing the sensitivity of the soils in this large region in northern Saskatchewan and northeastern Alberta to acidic deposition, and that it should be regarded as a first approximation rather than a sophisticated evaluation. This approach is dictated in large part by an overall scarcity of both inventory and analytical data about many of the soils of the area and also by the dearth of information regarding the direct and indirect effects of acidification on certain types of soils. For example, soil resource inventories vary widely throughout the region ranging from detailed reconnaissance surveys throughout most of the southern sections and in the Fort McMurray-Lake Athabasca area, to broad exploratory surveys throughout much of the northern areas in Alberta and the Shield area of Saskatchewan. In some areas, virtually no soil inventory is available. Moreover, adequate characterization of many of the soils is nonexistent, consisting in some of the more northern areas of about one site per 2 to 3 million hectares or more.

The constraints on the evaluation sensitivity of soils on basis of data available should be recognized. The scarcity of data has been mentioned but the kinds of data likewise should be considered. For example, CEC data employed in estimating BFC were largely obtained by extractants buffered at pH 7.0. CEC, however, is pH dependent and especially so in organic soils or soils having a high organic matter content. This means that in acid soils the actual CEC at field pH is lower than the values obtained at pH 7.0. This decrease in CEC is markedly pronounced in organic soils that are acid. In view of these constraints and general scarcity of pertinent laboratory data, it is stressed that if serious attempts are made in the future to refine the sensitivity evaluations of the soils of this region, they should be premised on ample appropriate research.

Table 2. Area Summary of Soil Sensitivity Categories

| Sensitivity Category | Sensitivity Subcategory | Area (hectares x $10^6$) | Percent |
|---|---|---|---|
| 1 | | 22.7 | 38.2 |
| | 1.1 | 4.5 | 7.6 |
| | 1.2 | 1.0 | 1.7 |
| | 1.3 | 8.1 | 13.6 |
| | 1.4 | 7.6 | 12.8 |
| | 1.5 | 1.5 | 2.5 |
| 2 | | 10.2 | 17.0 |
| | 2.1 | 5.3 | 8.9 |
| | 2.2 | 0.2 | 0.3 |
| | 2.3 | 1.1 | 1.8 |
| | 2.4 | 0.9 | 1.5 |
| | 2.5 | 2.7 | 4.5 |
| 3 | | 8.9 | 15.0 |
| | 3.1 | 2.7 | 4.5 |
| | 3.2 | 2.4 | 4.1 |
| | 3.3 | 0.7 | 1.1 |
| | 3.4 | 0.4 | 0.7 |
| | 3.5 | 0.7 | 1.1 |
| | 3.6 | 1.1 | 1.9 |
| | 3.7 | 0.9 | 1.6 |
| Miscellaneous Groups | | | |
| OR | | 9.6 | 16.1 |
| $R_1$ | | 6.6 | 11.1 |
| $R_2$ | | 1.4 | 2.5 |
| Unclassified | | 3.4 | |

## REFERENCES

Bache, Byron W. 1980: The acidification of soils; pp 183-202; In Effects of Acid Precipitation on Terrestrial Ecosystems. T.C. Hutchinson and M. Havas editors; Plenum Press, New York, 654 p.

Bache, Byron W. 1980: The sensitivity of soils to acidification, pp 569-572; In Effects of Acid Precipitation on Terrestrial Ecosystems. T.C. Hutchinson and M. Havas editors; Plenum Press, New York, 654 p.

Bostock, H.S. 1970: A provisional physiographic map of Canada; Geological Survey of Canada Map 1245A.

Canada Soil Survey Committee, Subcommittee on Soil Classification, 1978: The Canadian System of Soil Classification; Supply and Services Canada, Ottawa, Ontario, 164 p.

Clayton, J.S., W.A. Erlich, D.B. Cann, J.H. Day and I.B. Marshall 1977a: Soils of Canada, Volume I Report; The Soil Research Institute, Research Branch, Canada Department of Agriculture, Ottawa, Ontario, 243 p.

Clayton, J.S., W.A. Erlich, D.B. Cann, J.H. Day and I.B. Marshall 1977b: Soils of Canada, Volume II; The Soil Research Institute, Research Branch, Canada Department of Agriculture, Ottawa, Ontario, 239 p.

Fieldes, M. 1962: The nature of the active fraction of soil, pp 62-78, In Transactions of Joint Meeting of Commissions IV and V, International Society of Soil Science. Palmerston, New Zealand. G.J. Neale editor, 916A.

Holowaychuk, N. and J.D. Lindsay 1980: Distribution and relative sensitivity to acidification of soils of Sand River area, Alberta. Alberta Research Council, Edmonton.

Kabzems, A., A.L. Kosowan and W.C. Harris: Mixed wood section in an Ecological Perspective Saskatchewan. Forestry Branch DTRR, Technical Bulletin, 118 p.

Kalisz, P.J. and E.L. Stone, 1980: Cation exchange capacity of acid forest humus. Jour. Soil Sci. Soc. Amer. 44: 407-413.

Longley, Richmond W. and B. Janz 1978: The climatology of Alberta Oil Sands Environmental Research Program, Study Area. Project M.E. 10, AOSERP, Alberta Environment, Edmonton.

McFee, William W. 1980: Sensitivity of soil regions to acid precipitation, EPA-600/3-80-013. U.S. Environmental Protection Agency, Environmental Research Laboratory, Corvallis, Oregon.

North, Margaret A. 1976: A Plant Geography of Alberta. Department of Geography, University of Alberta, Edmonton, 147 p.

Pawluk, S. and L.A. Bayrock 1969: Some characteristics and physical properties of Alberta tills, Bulletin 26. Alberta Research Council, Edmonton.

Rowe, J.S. 1972: Forest Regions of Canada. Canadian Forestry Service Publication No. 1300, Department of Environment.

Wiklander, L. 1979: Leaching and acidification of soils, pp 1-24, In Ecological Effects of Acid Precipitation, M.J. Wood editor. Electric Power Research Institute, Palo Alto, California, U.S.A.

# POTENTIAL EFFECTS OF ACIDIC DEPOSITION ON PLANTS WITH SPECIAL REFERENCE TO N. SASKATCHEWAN

by

Z.M. Abouguendia and R.C. Godwin
Saskatchewan Research Council
Saskatoon, Saskatchewan, S7N 0X1

Abstract: This paper provides a review of the literature pertaining to the effects of acidic deposition on plants and attempts to assess the potential ecological significance of the projected increases in air pollutant emissions and subsequent elevation of acidic deposition rates in northern Saskatchewan. Tentative relative sensitivity analysis of the natural terrestrial and wetland ecosystems of the area is presented.

## INTRODUCTION

The present levels of acidic deposition in northern Saskatchewan are generally low and considered to represent the natural background levels. These levels, however, are likely to change significantly during the next 10-20 years (Shewchuk *et al* 1981).

The major objective of this paper is to provide an ecological overview of the potential effects of acidic deposition on plants, with particular reference to northern Saskatchewan. The paper examines the available literature pertaining to the possible direct and indirect effects on individual plants or plant parts and then considers their ecological consequences. The ecological regions in the study area are described briefly and their sensitivity to acidic deposition is assessed on the basis of the available literature. Further research needed to provide greater understanding of the potential impact of acidic deposition on individual plants and plant communities in the area is indicated.

More detailed treatment of the above subjects can be found in Abouguendia and Godwin (1980).

## POTENTIAL EFFECTS ON INDIVIDUAL PLANTS OR PLANT PARTS

Acidic deposition can affect plants in two basic ways: (1) the direct damage to leaves or other parts of the plant; and (2) the soil-mediated effects resulting from alteration of soil biological, physical and chemical properties.

## Direct Effects

Acidic precipitation may cause injury to (or erosion of) the protective surface structures of plants such as the cuticle (Tamm and Cowling 1977; Shriner 1980). The commonest form of direct injury is the development of small necrotic lesions. Acid precipitation can also cause disturbance of normal metabolism or growth processes such as photosynthesis, without visible necrosis of plant cells (Shriner 1980). This could lead to abnormal development or premature senescence of leaves or other organs.

Other direct effects include: (1) interference with normal functions of guard cells leading to loss of control of stomata and subsequent altering of the gas exchange and transpiration (Cowling 1978; Tamm and Cowling 1977); (2) interference with reproduction processes such as seed production, germinability and seedling establishment (Abrahamsen *et al* 1977; Abouguendia and Redmann 1979); and (3) acceleration in the rate of leaching of nutrients from foliage, twigs, branches and stems (Abrahamsen *et al* 1977; Niborg *et al* 1977 and Lakhani and Miller 1980).

The direct effects discussed above often result in a number of "indirect" effects such as increased susceptibility to other environmental stress factors such as other pollutants, drought, pathogens and insects (Tamm and Cowling 1977; Shriner 1977; Shriner and Cowling 1980).

Most investigators assume that the free hydrogen ion concentration of acidic precipitation is the component most likely to produce direct, harmful effects on plants and experimental studies have supported this assumption (Jacobson 1980 and Shriner 1980).

The plant dose-response to acidic precipitation appears to be governed by a large number of factors. These include wettability of leaf surfaces (Jacobson 1980 and Schriner 1980), the presence or absence of sensitive morphological features such as trichomes (Evans *et al* 1977), the effectiveness of plant tissues at buffering against pH changes (Small and Jackson 1949; Sholz and Reck 1977; Redmann and Abouguendia, unpublished data), stomatal frequency and factors affecting their opening (Tamm and Cowling 1977) and the general morphological characteristics of leaves, such as patterns of venation and leaf shape.

The threshold level for damage (visible injury and growth effects) of vascular plants ranges from pH 1.0 to 4.0 (Table 1). Coniferous trees appear to be more tolerant to high precipitation acidity than broad-leaved deciduous species. Within the herbaceous species grasses appear to be fairly tolerant. Within species variations are common. Growth effects may occur before the development of any symptoms of visible injury (Jacobson 1980; Lee *et al* 1980; Shriner 1980; Hindawi *et al* 1980). Although no data are available regarding the threshold for damage of mosses and lichens it is always assumed that they are more sensitive than vascular plants.

It should be noted, however, that under field conditions the response of plants to acidic deposition is influenced by a large number of fac-

Table 1. Threshold Levels for Damage (visible injury and growth effects) of Some Vascular Plants From Simulated Acidic Precipitation Experiments

| | Threshold (pH level) | Source |
|---|---|---|
| Coniferous Trees | | |
| Pine (*Pinus strobus*) | 1.0 | Haines *et al* (1980) |
| | <3.0 | Lee and Weber (1979) |
| | 3.2 | Shriner 1980 |
| Scotch Pine (*Pinus sylvestris*) | 2.6-3.4 | Jacobson and van Leuken (1977) |
| Deciduous Trees | | |
| Yellow birch (*Betula alleghaniensis*) | 4.0 | Lee and Weber (1979) |
| | 3.1 | Wood and Bormann (1977) |
| Hybrid poplar (*Populus* sp.) | 3.4 | Evans *et al* (1978) |
| Grasses | | |
| Oats, Wheat and Barley | <3.0 | Lee *et al* (1980) |
| Cultivated perennial grasses | 3.0-4.0 | Lee *et al* (1980) |
| Non graminoid Herbs | | |
| Carrot | 4.0 | Lee *et al* (1980) |
| Alfalfa | 3.5 | Lee *et al* (1980) |
| Radish and beet | 3.5 | Lee *et al* (1980) |
| Sunflower and beans | 3.1 | Evans *et al* (1977) |

tors (Cowling 1978 and Shriner 1980). These include: (1) precedent conditions (e.g. soil nutrient status, plant nutrient requirements, growth stage); (2) total loading, or deposition of critical loading ($H^+$, $NO_3^-$, $SO_4^=$); and (3) duration and frequency of exposures.

Soil-Mediated Effects

Acidic precipitation can affect many soil processes and properties. Among the major effects are the following:

- Alteration of soil chemistry characteristics such as: lowering soil pH, accelerating leaching of plant nutrients and other ions, increased aluminum mobility and associated toxicity, and reduced phosphorous availability (Abrahamsen *et al* 1977; Baker *et al* 1977; McFee *et al* 1977; Mayer *et al* 1977; Norton 1977 and Nyborg *et al* 1977).

- Inhibition of litter decomposition and associated release of plant nutrients (Freeman and Hutchinson 1980).

In general, higher plants can tolerate a pH level as low as 4.0 (Arnon and Johnson 1942). Lower substrate pH can be directly toxic to plants, particularly during the critical seedling establishment stage (Abouguendia and Redmann 1977; Redmann and Abouguendia 1979). Root development in many species is adversely affected at pH 3.2-3.5 or lower (Ellenberg 1958; Marchner *et al* 1966; Wind 1967).

The relative tolerance of a number of plant species to pH is given in Table 2. Only a few species are considered highly sensitive to low pH substrate. Many northern species are tolerant to low acidity.

POTENTIAL EFFECTS AT THE ECOSYSTEM LEVEL

The ecological effects of acid precipitation on forest ecosystems are potentially significant. Forests provide large surfaces for deposition and potential assimilation of both beneficial nutrients and injurious substances dispersed in the atmosphere. Because trees persist for many years or decades in the same environment, they are subject to long-term changes in the chemistry of the atmosphere and precipitation. Furthermore, because tree growth is directly related to base saturation (a widely accepted indicator of soil fertility) adverse effects of acid precipitation could be expected. Base saturation is inversely related to acidity (Tamm 1976).

Wittaker *et al* 1974 suggested that the abrupt and significant decrease in forest growth which occurred in the Hubbard Brook Experimental Forest in New Hampshire in 1961-65 was mainly due to the increase in the acidity of the rain. Analysis of forest growth in southern Sweden showed a 2 to 7% decrease in tree growth between 1950 and 1965 (Jonsson 1977). Jonsson "found no good reason for attributing this reduction in growth to any cause other than acidification". A similar analysis was attempted in eastern North America (Cogbill 1977). However, due to the unknown initiation date of acid precipitation and to the large variations of tree growth estimates, a correlation of forest growth and acid precipitation could not be established.

Table 2. Estimated Relative Sensitivity of Some Vascular Plant Species to Low Soil pH*

| Highly Sensitive (Miminum Substrate pH for Good Growth: >5.5) | Moderately Sensitive (Minimum Substrate pH for Good Growth: 4.5-5.5) | Less Sensitive (Minimum Substrate pH for Good Growth: 3-4.4) |
|---|---|---|
| Alfalfa (*Medicago sativa*) (1) | Barley (*Hordeum vulgare*) (1) | Willows (*Salix* spp.) (1) |
| Sweetgale (*Myrica gale*) (2) | Red Clover (*Trifolium pratense*) (1) | Wild Rose (*Rosa woodsii*) (1) |
| Flat-Leaved Willow (*Salix planifolia*) (2) | Most Cultivated and Native Grasses (1) | Saskatoon berry (*Amelanchier alnifolia*) (1) |
|  | Oats (*Avena sativa*) (1) | Aspen (*Populus tremuloides*) (1) |
|  |  | Labrador Tea (*Ledum groenlandicum*) (2) |
|  |  | Sphagnum Moss (*Sphagnum* spp.) (2) |

* These values may vary depending on other soil characteristics.

(1) Nyborg 1974

(2) Abouguendia *et al* 1979

Height and diameter growth were stimulated by increased "rain" acidity in a Scots pine sapling stand (Tveite and Abrahamsen 1980) and eastern white pine (Wood and Bormann 1977). The growth increase in both cases was attributed to fertilizing effect of N and S added in the rain. It should be noted, however, that N can only stimulate growth when supplies of available cations are not limiting. The increased leaching losses of K, Mg and Ca accompanying the acidification process indicate that the stimulatory effect might not be permanent. Similar experiments resulted in growth reduction of yellow birch seedlings; Norway spruce and lodgepole pine were largely unaffected by the treatment.

Substantial changes in bryophyte species composition, attributable to sulphur pollution, have taken place in *Sphagnum*-rich bog communities in the Southern Pennines within the last 200 years (Ferguson and Lee 1978, 1980). Field studies showed that sulphate and bisulphate applications, even when they occur as short-lived episodes, can severely reduce the growth of *Sphagnum* species, while having no apparent effect upon the angiosperm component of the vegetation (Ferguson and Lee 1980). Application at higher levels completely inhibited *Sphagnum* growth. Marked reduction in photosynthesis of mosses resulted from simulated acid precipitation (Sheridan and Rosentreter 1973).

Acidic precipitation appears to affect aquatic plant communities more drastically than terrestrial communities. Significant alteration in species composition of aquatic macrophytes has taken place in some Swedish lakes as a result of pollution with acidic substances (Grahn 1977). *Lobelia littorella* and *Isoetes* were driven out of large littoral areas which have been overgrown by thick mats of *Sphagnum*. These successional changes, which appear to have occurred over a short period, were correlated with increasing acidity of the lake water. The *Sphagnum* expansion caused the lakes to change from an equilibrium system to a biologically accumulating system similar to acid bogs. This accumulating system may cause an acceleration of the acidification processes leading to further disorder in the lake ecosystem. The number of submerged and floating macrophyte species in 29 ponds and lakes in the Sudbury region were inversely related to dissolved sulphates (Gorham and Gordon 1963).

Soil degradation, such as that caused by acidic precipitation, is a long-term process that is not easily measured, due to naturally-occurring temporal and spatial fluctuations in soil properties (Seip and Freedman 1980; McFee *et al* 1977). For example, natural intraseasonal and interseasonal fluctuations in pH of up to ± 1.3 units are not uncommon in natural habitats (Vézina 1965). Short-term fertilizing effect, as a result of N and S content of precipitation, may take place, particularly in sulphur-deficient soils such as the gray-wooded soils of Saskatchewan (Bettany 1972). Nyborg *et al* (1977) estimated that the soils of central Alberta are being acidified at a rate of one pH unit in 10 to 20 years at the present sulphur loading. Norton (1977) estimated that in initially-impoverished or unbuffered soils, the removal of soil cations may be significant on the scale of 10 to 100 years.

The question of whether the direct effects on plants or the soil-mediated effects are of greater significance to plants and ecosystems has not been answered. McFee (1978) suggested that soils in general are much more resistant to damage from acid precipitation than vegetation. Hornbeck *et al*

(1977) found that as summer precipitation passes through the forest canopy, H ion concentrations are lowered by an average of 90%, primarily as a result of exchange with other cations. They suggested that this exchange in the canopy lessens the potential impact of acid precipitation and increases the nutrient content of rainfall reaching the forest floor and thus will become largely available for plant use. Contrary to the findings of Hornbeck *et al* (1977), Baker *et al* (1977), in a study of a forested area in Alberta, found that the $H^+$ concentrations in the throughfall were consistently higher than that of open rain. Analysis of throughfall and stemflow water in Norway revealed that the total deposition of $H_2SO_4$ beneath spruce and pine is approximately two times the deposition in open terrain (Abrahamsen *et al* 1977).

It is apparent from the above discussions that while the ecological impacts of acidic precipitation on aquatic and wetland plant communities are striking and well documented, direct evidence of ecological impacts on terrestrial plant communities (e.g. forests) is lacking. The lack of field evidence, however, might be attributed to: (1) the unavailability of adequate pre-pollution baseline data for comparison purposes; (2) the high degree of spatial and temporal variations in these complex systems; and (3) the possibility of temporary fertilizing effects. The lack of direct ecological evidence does not, therefore, mean that acidic precipitation is not ecologically detrimental to terrestrial ecosystems.

## NATURAL VEGETATION OF THE STUDY AREA

The natural vegetation of the study area ranges from a grassland - forest transition in the south to a subartic lichen-woodland in the northeast (Figure 1). The Aspen Parkland Region is a mosaic of grassland (mainly fescue prairie dominated by rough fescue *Festuca scabrella*) occupying the drier sites and aspen (*Populus tremuloides*) dominating the moister sites. Lying to the north of the Aspen Parkland Region is the Mixedwood Ecological Region. The Mixedwood Region encompasses the most productive forests in the area and is characterized by a mixed coniferous (jack pine, *Pinus banksiana*; white spruce, *Picea glauca*; black spruce, *Picea mariana*) - deciduous (aspen, balsam poplar, *Populus balsamifera*) forest types that are highly diverse both structurally and floristically. Forest productivity appears to generally decrease in a northeastern direction due to the rigorous climatic conditions; the thin, coarse-textured soils and the frequency of forest fires. The proportion of hardwoods appears to follow the same trend. In the northern regions productive forests are generally restricted to the more favourable habitats such as riparian landscapes and deeper soils.

Peatlands and other wetlands are present in all regions. Two major types of peatlands can be recognized. Fens are found along streams and seepages where mineral-rich water flushes the peat intermittently. They are characterized by nearly neutral or slightly acid pH and support mainly aquatic plants, brown mosses and sedges. Willows and larch may grow profusely in such areas. Bogs are nourished primarily by precipitation and are relatively nutrient poor. This environment favours the growth of acid *Sphagnum* mosses with hydrophytic and mesophytic ericoid shrubs and black spruce.

Aquatic macrophytes occur in all ecological regions. Composition and abundance of these communities, however, vary considerably from one

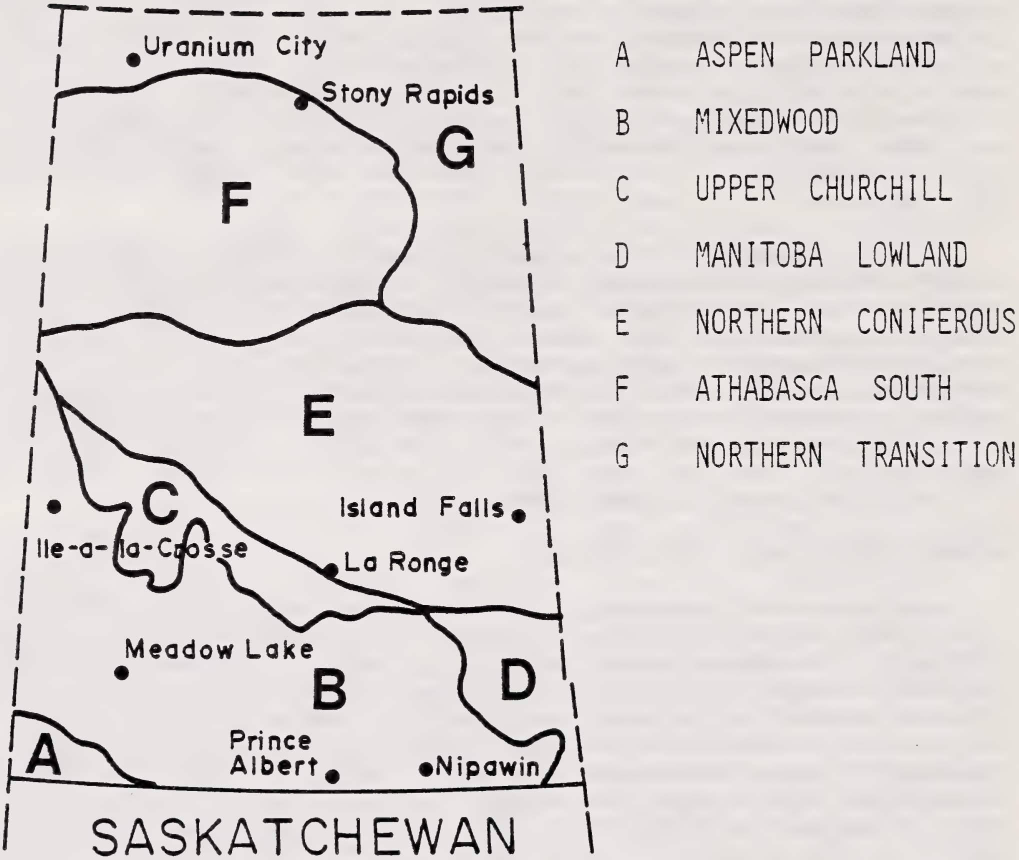

Figure 1. Ecological Regions of the Study Area (Rowe 1977).

region to another. Generally, productivity appears to decline in a northeastern direction. In the northern regions, dense and diverse communities are largely restricted to narrow and sluggish streams; small, shallow, protected lakes; and seepage lagoons.

## RELATIVE SENSITIVITY ANALYSIS

The task of assessing the relative sensitivity of plants and ecosystems of the study area is made extremely difficult due to the following factors: (1) the effects of acidic precipitation on plants and ecosystems are numerous and extremely complex, and are not well understood; (2) most of the available literature deals with results obtained from short-term treatments under controlled laboratory conditions. Extrapolation from such studies to actual field situation is not always possible. Furthermore, none of the main species found in the study area were studied with respect to their response to acidic precipitation; (3) most available studies employ $H_2SO_4$ in the simulated acid rain experiments and the interactions with the other pollutants or other environmental stresses are rarely considered; (4) while a great deal of information is available regarding the effects of $SO_2$ on plants (no attempt was made to review these effects in this report), there is no basis for equating such effects with those of acidic deposition; and (5) detailed regional information on soils and vegetation of the study area is lacking. Therefore, only a tentative, relative sensitivity analysis is possible at present.

The analysis developed in this paper (Tables 3 and 4) considers the following: (1) the expected relative level of acidic deposition (Shewchuk *et al* 1981); (2) the sensitivity of the soils and water to acidification (Shewchuk *et al* 1981); and the sensitivity of the major groups of plants to acidic precipitation (preceding sections). A great deal of variations in sensitivity are apparent both within and between ecological regions. However, the following general comments can be made: (1) the deposition rates are expected to be moderate to high in all regions except the southernmost region (Aspen Parkland) where it is low; (2) the buffering capacity of the atmosphere appears to decrease in a northward direction; (3) the buffering capacity of soils appears to generally decrease in a northward direction; (4) both aquatic macrophytes and organic-terrain communities are most sensitive in the northern regions (Northern Coniferous, Athabasca South and Northern Transition); and (5) the deciduous forests, common mainly in southern regions are more sensitive to direct effects than the coniferous forests, the dominant communities in the north.

Within any of the ecological regions considered the following sensitivity rating could be assumed starting with the most sensitive component or community: aquatic macrophytes > organic terrain (mainly bogs) communities = lichens > deciduous forests > coniferous forests.

## CONCLUSIONS

From the above assessment it can be concluded that: (1) the potential detrimental and beneficial effects of acidic precipitation on plants and ecosystems are numerous and extremely complex, and are not well understood; (2) the present level of available information permitted only a tentative sensitivity analysis; (3) the various ecosystems possess natural buffering

Table 3. Relative Magnitude of Expected Acidic Deposition, Relative Degree of Atmospheric Buffering Capacity and Relative Sensitivity of the Soils in the Study Area*

| Ecological Regions | Expected Relative Level of Acidic Deposition | Atmospheric Buffering Capacity | Soil Sensitivity |
|---|---|---|---|
| A. Aspen Parkland | Low | High | Low to High |
| B. Mixedwood | Moderate to High | Moderate | Low to High |
| C. Upper Churchill | Moderate to High | Moderate | Moderate to High |
| D. Manitoba Lowland | Moderate to High | Moderate to High | Low |
| E. Northern Coniferous | Moderate to High | Low to Moderate | Moderate to High |
| F. Athabasca South | Moderate to High | Low | High |
| G. Northern Transition | Moderate to High | Low | Moderate to High |

*Based on Shewchuk *et al* 1981

Table 4. A Comparison of the Relative Sensitivity of the Major Plant Communities in the Study Area*

| Ecological Region | Aquatic Macrophytes | Organic Terrain Communities | Upland Forest Communities | | |
|---|---|---|---|---|---|
| | | | Deciduous | Coniferous | Lichens |
| A. Aspen Parkland | 1 | 1 | 3 | | |
| B. Mixedwood | 1-2 | 1-2 | 3 | 1 | |
| C. Upper Churchill | 2-3 | 2-3 | 3 | 1 | 3 |
| D. Manitoba Lowland | 1 | 1 | 3 | 1 | |
| E. Northern Coniferous | 3 | 3 | | 1 | 3 |
| F. Athabasca South | 3 | 3 | | 1 | 3 |
| G. Northern Transition | 3 | 3 | | 1 | 3 |

* 1 Less Sensitive
2 Moderately Sensitive
3 Highly Sensitive

mechanisms against the effects of acidification, the degree of effectiveness of such protection varies substantially both within and between ecosystems; (4) the aquatic macrophytes in the northern part of the study region are likely to be the most vulnerable communities to acidic precipitation; (5) approximately 10-fold to 100-fold increase in hydrogen ion concentration of precipitation (depending on the type of ecosystem and the ecological region) would be required to produce significant detrimental effects on plant communities of the study area; (6) detailed multidisciplinary studies are needed to provide a more accurate sensitivity analysis and to identify potential ecological and economical effects of acidic deposition on the plant communities and ecosystems of the study area; (7) a detailed chemical and ecological monitoring program is necessary to permit detection of changes in ecosystem parameters before any irreversible damage takes place.

## References

Abouguendia, Z.M. and R.C. Godwin. 1980: "The effects of acidic precipitation on plants with special reference to N. Saskatchewan and N.E. Alberta". SRC Publication No. C-805-28-E-80.

Abouguendia, Z.M. and R.E. Redmann. 1979: "Germination and early seedling growth of four conifers on acidic and alkaline substrates". Forest Sci. 25: 358-360.

Abrahamsen, G., R. Horntvedt and B. Tveite. 1977: "Impacts of acid precipitation on coniferous forest ecosystems". Water, Air and Soil Pollution 8: 57-73.

Altshuller, A.P. and G.A. McBean. 1979: "The LRTAP problem in North America: a preliminary overview". United States-Canada Research Consultation Group on the long-range transport of air pollutants.

Arnon, D.I. and C.M. Johnson. 1942: "Influence of hydrogen ion concentrations on the growth and development of higher plants under controlled conditions". Plant Physiology 17: 525-539.

Bettany, J.R. 1972: "The status of sulphur in Saskatchewan soils". Ph.D. Thesis, Dep. of Soil Science, University of Saskatchewan, 150 p.

Baker, J., D. Hocking and M. Nyborg. 1977: "Acidity of open and intercepted precipitation in forests and effects on forest soils in Alberta, Canada". Water, Air and Soil Pollution 7: 449-460.

Cogbill, C.V. 1977: "The effects of acid precipitation on tree growth in eastern N. America". Water, Air and Soil Pollution 8: 89-93.

Cowling, E.B. 1978: "Effects of acid precipitation and atmospheric deposition on terrestrial vegetation", p. 46-63 In: A Report to the Council on Environmental Quality (U.S.A.), National Atmospheric Deposition Program, NC-141.

Denison, R., G. Caldwell, B. Bormann, L. Eldred, C. Swanberry and S. Anderson. 1977: "The effect of acid rain on N-fixation in Western Washington Coniferous forests". Water, Air and Soil Pollution 8: 21-34.

Ellenberg, H. 1958: "Bodenreaktion (einschliesslich kalkfrage)". In Handbuck der Pflanzenphysiologic Bd. IV (W. Ruhland, ed), p. 638-708. Springer-Verlag, Berlin.

Evans, L.S., N. Gmur and F. Da Corta. 1977: "Leaf surface and histological perturbations of leaves of *Phaseolus vulgaris* and *Helianthus* after exposure to simulated acid rain". Amer. J. Botany 64: 903.

Ferguson, P. and J.A. Lee. 1978: "Effects of sulphur pollutants on the growth of *Sphagnum* species". Envir. Pollution 16: 151-162.

Ferguson, P. and J.A. Lee. 1980: "Some effects of bisulphite and sulphate on the growth of *Sphagnum* species in the field". Envir. Pollution (Ser. A) 21: 59-71.

Freedman, B. and T.C. Hutchinson. 1980: "Smelter pollution near Sudbury, Ontario, Canada, and effects on forest litter decomposition", p. 395-434 In: T.C. Hutchinson and M. Havas (eds). Plenum Press, New York.

Gorham, E. and A. Godrdon. 1963: "Some effects of smelter pollution upon aquatic vegetation near Sudbury, Ontario". Can. J. Bot. 41: 371-378.

Grahn, O. 1977: "Macrophyte succession in Swedish lakes caused by deposition of airborne acid substances". Water, Air and Soil Pollution 7: 295-305.

Hornbeck, J.W., G.E. Likens and J.S. Eaton. 1977: "Seasonal patterns in acidity of precipitation and their implications for forest stream ecosystem". Water, Air and Soil Pollution 7: 355-365.

Jacobson, J.S. 1980: "Experimental studies in the phytotoxicity of acidic precipitation: the United States experience", p. 151-160 In: T.C. Hutchinson and M. Havas (eds). Effects of Acid Precipitation on Terrestrial Ecosystems. Plenum Press, New York.

Jonsson, B. 1977: "Soil acidification by atmospheric pollution and forest growth". Water, Air and Soil Pollution 7: 497-501.

Lakhani, K.H. and H.G. Miller. 1980: "Assessing the contribution of crown leaching to the element content of rainwater beneath trees", p. 161-172 In: T.C. Hutchinson and M. Havas (eds). Effect of Acid Precipitation on Terrestrial Ecosystems. Plenum Press, New York.

Lee, J.J. 1979: "The effect of acid rain on seedling emergence and growth of eleven woody species". Forest Science 25: 393-398.

Lee, J.J., G.E. Neely and S.C. Perrigan. 1980: "Sulfuric acid rain effects on crop yield and foliar injury". U.S. Environmental Protection Agency, Corvallis, Oregon.

Likens, G.E., F.H. Bormann, J.S. Eaton, R.S. Pierce, and N.M. Johnson. 1976: "Hydrogen ion impact to the Hubbard Brook Experimental Forest, New Hampshire, during the last decade". Water, Air and Soil Pollution 6: 435-445.

Marschner, H., R. Handley, and R. Overstreet. 1966: "Potassium loss and changes in the fine structure of corn root tips induced by $H^+$ ions". Plant Physiology 41: 1725-1735.

McFee, W.W. 1978: "Effects of acid precipitation and atmospheric deposition on soils", p. 64-73 In: A Report to the Council on Environmental Quality (U.S.A.), National Atmospheric Deposition Program, NC-141.

McFee, W.W., J.M. Kelly and R.H. Bek. 1977: "Acid precipitation effects on soil pH and base saturation of exchange sites". Water, Air and Soil Pollution 7: 401-408.

Norton, S.A. 1977: "Changes in chemical processes in soils caused by acid precipitation". Water, Air and Soil Pollution 7: 389-400.

Nyborg, M. 1974: "Reclamation of soils and waters made acid by windblown dust", p. 55-75 In: D. Hocking (ed) Proceedings Workshop on reclamation of disturbed land in Alberta. Alberta Environment.

Nyborg, M., J. Crepin, D. Hocking and J. Baker. 1977: "Effect of $SO_2$ on precipitation and on the sulphur content and acidity of soils in Alberta, Canada". Water, Air and Soil Pollution 7: 439-448.

Redmann, R.E. and Z.M. Abouguendia. 1979: "Germination and seedling growth on substrates with extreme pH - laboratory evaluation of buffers". J. Appl. Ecol. 16: 901-907.

Rowe, J.S. 1977: "Forest Regions of Canada". Can. Forestry Public. No. 1300-1972. 172 pp.

Scholz, F. and S. Reck. 1977: "Effects of acids on forest trees as measured by titration in vitro, inheritance of buffering capacity in *Picea abies*". Water, Air and Soil Pollution 7: 41-45.

Seip, H.M. and B. Freedman. 1980: "Effect of acid precipitation on soils", p. 591-596 In: T.C. Hutchinson and M. Havas (eds). Effect of Acid Precipitation on Terrestrial Ecosystems. Plenum Press, New York.

Sheridan, R.P. and R. Rosenstreter. 1973: "The effect of hydrogen ion concentration in simulated rain on the moss *Tortula ruralis* (Hedw.) Sm." The Bryologist 76: 168.

Shewchuk, S.R. 1979: "A background study of potential sulphur stresses in west central Saskatchewan". SRC Report No. P 79-6.

Shewchuk, S., Z. Abouguendia, F. Atton, J. Dublin, B. Godwin, N. Holowaychuk, R. Hopkinson, W.K. Liaw, J. Maybank, G.A. Padbury, B. Schreiner. 1981: "Regional transport of air pollutants and associated ecosystem sensitivities". SRC Publication No. P-780-1-B-81.

Shriner, D.S. 1977: "Effects of simulated rain acidified with sulfuric acid or host-parasite interactions". Water, Air and Soil Pollution 8: 9-14.

Shriner, D.S. 1980: "Terrestrial vegetation-air pollutant interactions: non-gaseous pollutants, wet deposition". A paper presented at International Conference on Air Pollutants and their Effect on the Terrestrial Ecosystem, Banff, Alberta, Canada, May 10-17, 1980.

Shriner, D.S. and E.B. Cowling. 1980: "Effects of rainfall acidification on plant pathogens", p. 435-442 In: T.C. Hutchinson and M. Havas (eds), Effect of Acid Precipitation on Terrestrial Ecosystems. Plenum Press, New York.

Small, J. and T. Jackson. 1949: "Buffer index values in relation to soil-pH tolerances". Plant Physiol. 24: 75-83.

Tamm, C.O. 1976: "Acid precipitation: biological effects in soil and on forest vegetation". Ambio 5: 235-238.

Tamm, C.O. 1977: "Acid precipitation and forest soils". Water, Air and Soil Pollution 7: 367-369.

Tamm, C.O. and E.B. Cowling. 1977: "Acidic precipitation and forest vegetation". Water, Air and Soil Pollution 7: 503-511.

Tveite, B. and G. Abrahamsen. 1980: "Effects on artificial acid rain on the growth and nutrient status of trees", p. 305-318 In: T.C. Hutchinson and M. Havas (eds), Effects of Acid Precipitation on Terrestrial Ecosystems. Plenum Press, New York.

Vézina, P.E. 1965: "Methods of pH determination and seasonal pH fluctuations in Quebec forest humus". Ecology 46: 752-755.

Whittaker, R.H., F.H. Bormann, G.E. Likens and T.G. Siccama. 1974: "The Hubbard Brook Ecosystem Study: forest biomass and production". Ecol. Monographs 44: 233-252.

Wind, G.P. 1967: "Root growth in acid soils". Neth. J. Agric. Sci. 15: 259-266.

Wood, T. and F.H. Bormann. 1977: "Short-term effects of a simulated acid rain upon the growth and nutrient relations on *Pinus strobus*". Water, Air and Soil Pollution 7: 479-488.

# A USER-ORIENTED CLIMATOLOGICAL DISPERSION MODEL FOR THE ALBERTA OIL SANDS

by

D.S. Davison, E.D. Leavitt, R. McKenna
and R. Rudolph
INTERA Environmental Consultants Ltd.
Calgary, Alberta. T2H 1X9

Abstract: A climatological air quality dispersion model was developed to permit much more powerful analyses capabilities than are available on traditional CDM-type models. One of the major structural features is the efficient generation of a time series of GLC values utilizing a pre-calculated random access file. The user can then construct GLC statistics based upon user-selected criteria for inclusion/exclusion or weighting of time series realizations depending upon ambient meteorological conditions.

The dispersion formulation consisted of a Gaussian framework with plume sigmas defined by a modification to the statistical theory. Effective downwind distances were utilized to allow for source effects and to simplify the analytic downwind dependence of the plume sigmas. The standard deviations of the azimuthal and elevation wind fluctuations were estimated from a planetary boundary layer parameterization involving similarity theory and empirical results.

## INTRODUCTION

The end users of air quality models often desire results in a form which most air quality models are not structured to provide. A review of user needs in the Alberta Oil Sands (Davison and Lantz 1979) identified many of the major needs of such users as land-use planners and biological and forestry scientists. Two major concerns were the need to allow for the susceptibility of a receptor and the time relationships between pollution episodes. For example, a high ground-level-concentration (GLC) might have a serious impact upon parts of an eco-system if it occurred on a warm June morning, but might have no effect at all if the same GLC value occurred on a cold day in winter. Timing between events is also important since time for recovery is important for biological systems.

Traditional air quality models usually incorporate one of two basic approaches. One approach is a simple case study, often a "worst case" scenario. The second approach is climatological. A frequency distribution of dispersion classes is generated using available meteorological data. The climatological average GLC values are then calculated by weighting the GLC predicted for each dispersion class by the frequency of its occurrence. Neither of these approaches addresses the concerns outlined above.

The present study was commissioned by the Research Management Division of Alberta Environment in order to develop a more effective model for airshed management. Specifically, the model was to incorporate a measure of the susceptibility of a receptor which could be simply expressed by a user in terms of the meteorological conditions present at the time. The model was to be suitable for wet and dry deposition calculations. Finally, the model was to be of a basic Gaussian formulation, but it was to involve a plume sigma specification scheme reflecting the work previously done in the AOSERP study area. Much of this previous work was summarized by Davison and Leavitt (1979) including the results from the three intensive field studies in which AES had extensive participation and by Slawson et al. (1978), which documented much of the work sponsored by Syncrude Canada Ltd.

The RMD project also involved several other developments. A time series of meteorological data was needed to drive the model. Western Research and Development took a lead role in developing a wind and mixing height climatology (Leahey and Hanson, 1980); INTERA Environmental Consultants developed the time series of surface heat flux values and other meteorological parameters and synthesized the data files. A second phase of the project involved sensitivity and verification studies (Davison et al. 1981b).

The present paper outlines the major innovative features of the model formulation itself with some illustrative examples from the sensitivity and verification studies portion of the study. The detailed model description and documentation is in a draft report (Davison et al. 1981a).

## TIME SERIES APPROACH

The present model incorporated a time series approach in order to satisfy the identified user needs. This approach is shown schematically in Figure 1. A matrix of dispersion classes is chosen and the Gaussian model estimates of the GLC values for each source receptor pair are calculated and stored in a random access file. The user then operates a second program (FRQDTN) which reads a time series of meteorological data and looks up on the GLC file the appropriate GLC values, with an option to "weight" the GLC values according to the importance selected for that particular meteorological condition.

If the user elects to have no weighting then the model produces a time series of GLC values. This time series can then be analyzed to produce a frequency distribution as would arise from a traditional climatological dispersion model. However, the time series of GLC values permits many additional types of analyses including the statistics of return periods.

The use of weighting can involve a selection of specified conditions for which GLC statistics are desired. For example, the GLC values selected could be those occurring only when there is positive net

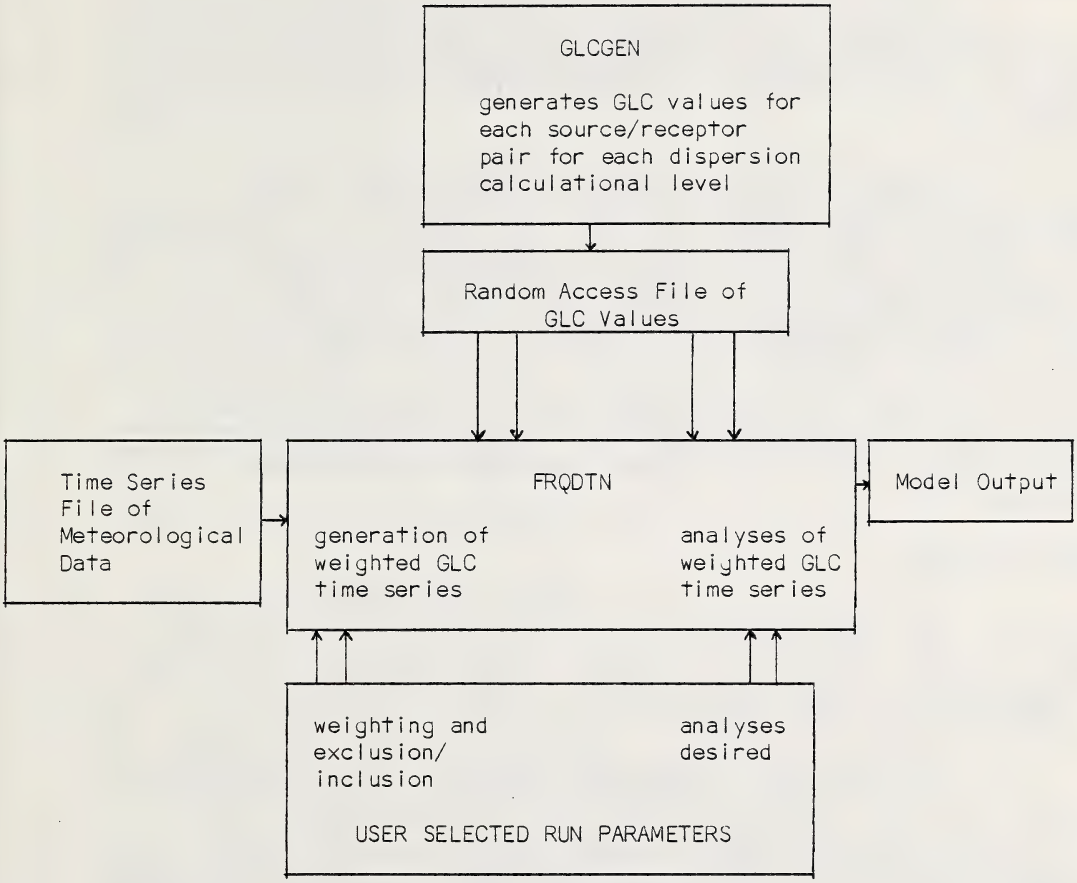
GLCGEN
generates GLC values for each source/receptor pair for each dispersion calculational level
Random Access File of GLC Values
Time Series File of Meteorological Data
FRQDTN
generation of weighted GLC time series
analyses of weighted GLC time series
Model Output
weighting and exclusion/inclusion
analyses desired
USER SELECTED RUN PARAMETERS

Figure 1. A schematic outline of the model components. The time series file of meteorological data includes meteorological data that may be of use in selecting time series events that are to be included or excluded from the analysis. The program GLCGEN calculates the GLC values according to user-selectable calculational levels of wind speed, heat flux and convective mixing height; thus, the discrete dispersion classes can be optimized for a particular region or application. The program FRQDTN utilizes the time series file and the GLC file depending upon the input instructions.

radiation and temperatures above 5°C. In this way subsets of the total population of events can be analyzed conveniently.

Weighting can also be used to generate an effective GLC time series. The previous inclusion/exclusion of values represents a weighting of unity or zero. The model includes the option of any linear weighting function for any of the meteorological variables on the time series file.

The basic feature of the time series approach is the calculation of a GLC time series which can be weighted. In the traditional CDM-type approach, a single realization in the time series of meteorological conditions is classified according to dispersion class and the bin corresponding to that class in a frequency distribution is incremented by one. After all of the time series is analyzed in a CDM-type model, the resulting distribution is used to weight the GLC values for each dispersion class. In the time series approach, a single realization is similarly classified, but that classification index is used as the index of a random access file to provide the corresponding GLC values for each source-receptor pair. The resulting time series of GLC values can then be used for more effective airshed management analyses.

## MODEL STRUCTURE

The model structure is largely determined by the time series approach. The three components are the time series file, the program used to generate the GLC file (GLCGEN) and the central analysis program (FRQDTN) which defines the analyses for a particular run and reads the other two files.

The time series file of meteorological values includes the parameters needed to define the dispersion class. It also includes a variety of other meteorological parameters that can be used to select subpopulations of conditions to be analyzed or to define the GLC weighting parameters. The data include temperature, relative humidity, net radiation, precipitation, snow cover, opaque cloud cover, wind speed and direction and estimated convective mixing height. Most of these parameters are available from an AES Surface Weather Record station. The net radiation, convective mixing height and plume level ( 400 m) wind speed and direction were derived through separate analyses.

The program used to derive the GLC file (GLCGEN) incorporates the dispersion formulations. For the present model, the plume sigma specification scheme used involved wind speed, surface heat flux and convective mixing height. The details are presented in a following section. The pre-calculation of GLC values and their storage on a random access file requires a discretization of the dispersion formulations into dispersion classes but results in about an order of magnitude decrease in computing time compared to calculation at each time step for typical numbers of sources and receptors and lengths of time series.

The analysis program FRQDTN is designed for ease of operation for the user. If the GLC file and the time series file exist, then the user can proceed to consider various scenarios. The source rates are set in FRQDTN and so various sources can be turned off or on and various strengths of emissions can be assigned. Thus different chemical species can be examined readily without having to redo the dispersion calculations (which are usually the most expensive part of the model). The user can specify what types of analyses are desired and can also decide upon what weighting parameters, if any, are desired.

## DISPERSION FORMULATION

The basic model structure could incorporate a variety of dispersion formulations. A simple Gaussian framework was adopted in the present version of the model due to the large number of calculations involved and the implicit averaging over many realizations. Because of the rather extensive field studies undertaken in the Athabasca Oil Sands area, however, it was felt that a plume sigma scheme that was more consistent with observations and with similarity theory should be utilized.

The basic plume sigma formulations were adopted from the statistical theory of dispersion.

$$\sigma_y = \sigma_A \, (2\, \ell_v)^{\frac{1}{2}} \, X_{ey}^{\frac{1}{2}}$$

$$\sigma_Z = \sigma_E \, (2\, \ell_w)^{\frac{1}{2}} \, X_{ez}^{\frac{1}{2}}$$

where $\ell_V$ and $\ell_W$ are the Lagrangian integral length scales in the lateral and vertical directions, $\sigma_A$ and $\sigma_E$ are the wind azimuthal and elevation angle standard deviation and $X_{ey}$ and $X_{ez}$ are effective downwind distances for lateral and vertical dispersion.

The effective downwind distances were used to account for initial source effects and were defined by a plume sigma matching technique at the transition zone from source to environmentally dominated dispersion. The transition zone was defined by dissipation matching similar to the technique presented by Briggs (1975). The use of effective downwind distances also permits the adoption of a simple power law formulation in the model. The source effects are most evident for $\sigma_Z$ in stable conditions where the large initial expansion in the source region results in a slow rate of increase of $\sigma_Z$ with distance beyond the transition zone, which is in qualitative agreement with observations.

The value for both of the Lagrangian integral length scales was chosen as 500 m. This value is consistent with measured values in the region (Davison and Grandia 1979) and with the implicit value adopted by Pasquill (1976) and recommended by an AMS review group (Hanna et al. 1977).

The representation of $\sigma_Z$ by the statistical theory formulation has significant limitations. It is well established that the rate of vertical mixing changes with height and so the assumption of homogeneous turbulence within the statistical theory is not met. The Gaussian formulation, however, has already enforced a vertical homogeneity and so utilizing statistical theory introduces no new assumptions about vertical homogeneity.

Representative values of $\sigma_A$ and $\sigma_E$ are required to complete the plume sigma specification. It would be most preferable to use measured values of $\sigma_A$ and $\sigma_E$ provided that these are representative of the turbulence encountered by the plume. Unfortunately, such representative measured values did not appear to be available over an extensive period of time in the Athabasca Oil Sands area. Thus, the value of $\sigma_A$ and $\sigma_E$ were estimated using empirical results from other regions within the context of similarity theory.

The basic input data needed to generate the dispersion parameters $\sigma_A$ and $\sigma_E$ are similar to data needed to specify other empirical plume sigma classes. The data include wind speed, surface heat flux and convective mixing height. The major advantages to using a formulation guided by similarity theory, compared to other empirical sigma curves, are that transferability from other areas is on a much more secure basis and the various components of the parameterization are, in general, measurable physical quantities.

The input data together with an adopted value of the surface roughness length were used to generate various scaling parameters used in the similarity theory representation:

$$w_* = \left(\frac{g}{T}\,\overline{w\theta}\,Z_i\right)^{1/3}$$

$$L = -\frac{u_*^3}{K\,\frac{g}{T}\,\overline{w\theta}}$$

$$\mu_* = \frac{u_*}{fL}$$

where $\overline{w\theta}$ is the surface heat flux,
$Z_i$ is the convective mixing height,
$K$ is von Karman's constant,
$u$ is the friction velocity
$f$ is the Coriolis parameter

The estimation of the friction velocity, $u_*$, involved a similarity formulation consistent with Carson and Richards (1978), Businger et al. (1971) and Leavitt et al. (1977).

The values of $\sigma_A$ and $\sigma_E$ were then estimated using a variety of empirical results. For convective (i.e. positive heat flux) conditions,

$$\sigma_E = \mathrm{MAX}\ (0.6\ w_*/U,\ 1.3\ u_*/U)$$

$$\sigma_A = u_*/U\ (12 - 0.5\ Z_i/L)^{1/3}$$

The $\sigma_E$ value adopted is the maximum of a free convective and a mechanical estimate. The coefficient, 0.6, for the free convective formulation is a value consistent with most data. However, McBean (1976) found a systematic change with height from about 0.4 to 0.68 at mid-level in the mixed layer and decreasing to 0.4 towards the top of the layer. Caughey and Palmer (1979) found a maximum of 0.4. Subsequent senstivity studies of this model indicated that the coefficient uncertainty was not a major source of error for the averaged GLC values. The expression for $\sigma_A$ was recommended by Panofsky et al. (1977). For free convection, it reduces to,

$$\sigma_A = 0.6 \frac{w_*}{U}$$

which is the same for $\sigma_E$, consistent with airborne measurements by Davison and Grandia (1979).

In stable conditions, there is no firmly established parameterization. The stability parameter utilized was $\mu_*$ as recommended by Deardorff (1978). Values for $\sigma_A$ and $\sigma_E$ were estimated in terms of an empirical power law fit of observations to the stability parameter. The data for this fit were derived from Weber et al. (1975), Luna and Church (1972) and Leavitt et al. (1978),

$$\sigma_E = 11.8\ \mu_*^{-0.64}$$

$$\sigma_A = 19.8\ \mu_*^{-0.55}$$

The uncertainties in the $\sigma_A$ and $\sigma_E$ specifications reflect some of the inadequacies of our knowledge of turbulent dispersion. The approach to specifying the dispersion through results of similarity theory, nevertheless, has some significant advantages over a purely empirical plume sigma curve approach. The transferability criteria are defined by expressing empirical results within the context of similarity theory.

The use of the friction velocity $u_*$ rather than the mean wind speed as a scaling parameter is a clear example of the transferability advantages. In rougher terrain, there will be enhanced mechanical mixing. This enhanced mixing is due to the larger surface roughness length, $Z_o$, which relates the friction velocity to the mean wind speed. The roughness length can be measured and so the enhanced terrain-induced mixing can be accounted for directly.

The mixing in convectively dominated conditions involves a sensitivity to convective mixing height which is not included in most empirical schemes. Figure 2 shows an example of the sensitivity of sector-averaged GLC values as a function of convective mixing height. In GLCGEN a unit value for source strength is used, this simulation involved

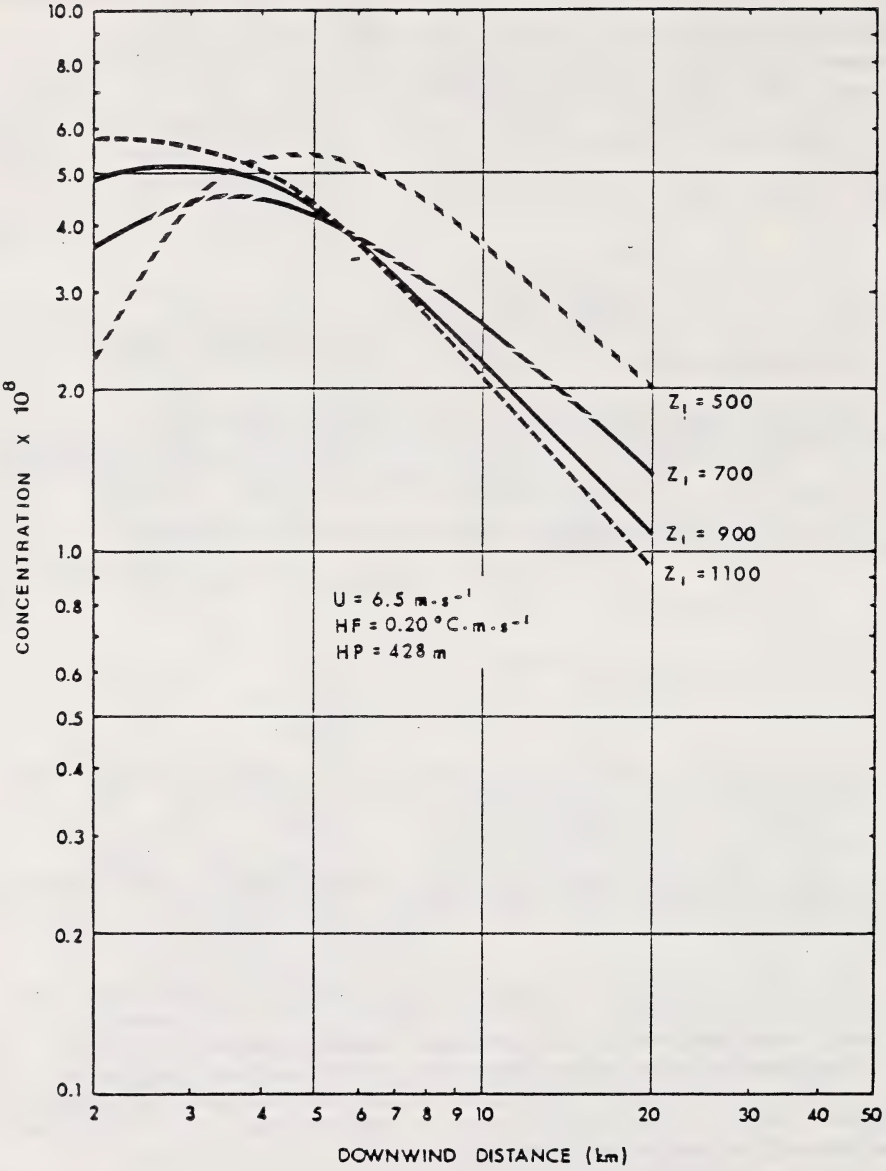

Figure 2. Sensitivity of sector-averaged GLC values to convective mixing height for a wind speed of 6.5 $ms^{-1}$, a heat flux of 0.20°C $ms^{-1}$ and a plume height of 482 m.

a final plume rise from the Suncor main powerhouse stack of 428 m AGL. Note that at larger downwind distances the GLC values scale according to the depth of the mixed layer, as expected. Close to the source, however, the larger values of $Z_i$ result in greater vertical mixing and so GLC values are larger for the "unlimited" mixing of $Z_i$ = 1100 m compared to the trapped situation where $Z_i$ = 500 m. At downwind distances of 4 or 5 km, there is little sensitivity to mixing height.

## MODEL TESTING AND VERIFICATION

Sensitivity studies and initial testing of the model with observed air quality data have been undertaken. The air quality data are from stations about 5 km from the Suncor plant in the Athabasca Oil Sands. The studies have been presented in a draft report (Davison et al. 1981b); some of the major results are the following:

1. Uncertainties in wind direction are the major source of error for comparison of observed and predicted values at specified times and locations.

2. Air quality records are often dominated by a small number of episodes in a given month. The monthly averages show a high statistical variability indicating that one month is too short an averaging time for valid model comparisons.

3. Signal-to-noise problems limit the reliability of observed monthly averages beyond 5 to 10 km from existing sources.

4. Spatially averaged results over 12 months show a model underprediction compared to observed data, the discrepancy appears to occur mostly in mechanically mixed situations.

5. A change in roughness length from 0.3 to 0.9 m could account for the discrepancy.

6. An allowance for terrain effects due to Suncor source being lower than most of monitors could also account for discrepancy. The spatially and temporally averaged residuals would become minimal if the physical stack height were reduced from 107 m to about 84 m.

7. Existing uncertainties in plume rise coefficients can lead to significant changes in GLC values. For example the change of the $C_1$ coefficient in the neutral plume rise formulation (Briggs 1975) from 1.4 to 1.6 can decrease the maximum GLC by 25% and move the maximum 1.5 km further out under typical meteorological conditions.

## CONCLUSIONS

The model described in this paper was developed as part of a larger airshed management program sponsored by Alberta Environment. The model developed is a user-oriented climatological dispersion model which permits much more extensive time domain analyses of GLC values than traditional CDM-type models. The key structural difference is the generation of a time series of GLC values rather than a frequency distribution of dispersion classes. The user can easily define subsets of meteorological conditions for which GLC values are desired based upon the susceptibility of the particular type of receptor of concern. The user can also examine the statistics of timing between episodes.

The model includes a plume sigma specification scheme linked to wind fluctuations and then to more easily measured meteorological conditions through empirical observations guided by similarity theory scaling. The attempt at parameterization of the planetary boundary layer to produce wind fluctuation standard deviations showed that major uncertainties remain. The approach is promising, nevertheless, since dispersion is being described by physical quantities that can be independently measured. Thus step-by-step component evaluation becomes possible. The use of similarity theory provides a much more reliable basis for transferability of results from and to other locations.

## ACKNOWLEDGEMENTS

This work was funded by the Research Management Division of Alberta Environment.

## REFERENCES CITED

Briggs, G.A. 1975. Plume rise predictions. Pages 59-111 in D.A. Haugen, ed. Lectures on Air Pollution and Environmental Impact Analyses. Amer. Met. Soc., Boston.

Businger, J.A., J.C. Wyngaard, Y. Izumi, and E.F. Bradley. 1971. Flux profile relationships in the atmospheric surface layer. J. Atmos. Sci. 28:181-189.

Carson, D.J. and P.J.R. Richards. 1978. Modelling surface turbulent fluxes in stable conditions. Bound.-Layer Met. 14:67-81.

Caughey, S.J. and S.G. Palmer. 1979. Some aspects of turbulence structure through the depth of the convective boundary layer. Quart. J. Roy. Met. Soc. 105:811-828.

Davison, D.S. and K.L. Grandia. 1979. Plume dispersion measurements from an oil sands extraction plant, June 1977. Prep. for Alberta Oil Sands Environmental Research Program by INTERA Environmental Consultants Ltd. AOSERP Report 52. 194 pp.

Davison, D.S. and R.B. Lantz. 1979. Review of requirements for air quality simulation models. Prep. for Alberta Oil Sands Environmental Research Program by INTERA Environmental Consultants Ltd.

Davison, D.S. and E. Leavitt, 1979. Analysis of AOSERP plume sigma data. Prep. for Alberta Oil Sands Environmental Research Program by INTERA Environmental Consultants Ltd. AOSERP Report 63. 251 pp.

Davison, D.S., E.D. Leavitt, R.F. McKenna, R.C. Rudolph and M.J.E. Davies. 1981a. Airshed Management Systems for The Alberta Oil Sands, Part I, a Gaussian frequency distribution model. Draft report to Alberta Environment. 131 pp.

Davison, D.S., M.J.E. Davies, R.C. Rudolph, M.C. Hansen. 1981b. Airshed Management System for the Alberta Oil Sands, Part III, Validation and Sensitivity Studies. Draft report prepared for Alberta Environment. 120 pp.

Deardorff, J.W. 1978. Observed characteristics of the outer layer. Chapter in A.K. Blackadar, ed. The Planetary Boundary Layer. To be published by the Amer. Met. Soc.

Hanna, S.R., G.A. Briggs, J. Deardorff, B.A. Egan, F.A. Gifford, and F. Pasquill. 1977. AMS workshop on stability classification schemes and sigma curves - summary of recommendations. Bull. Amer. Met. Soc. 58:1305-1309.

Leahey, D.M. and M.C. Hansen. 1980. Wind and mixing height climatologies for the Athabasca Oil Sands area. Prep. for the Research Management Division of Alberta Environment by Western Research and Development.

Leavitt, E., D. Bell, M. Clarke, R. Anderson, and C.A. Paulson. 1977. Computation of air stress and sensible heat fluxes from surface layer profile data, AIDJEX 1975. AIDJEX Bull. 36:157-174.

Leavitt, E., M. Albright, and R. Baumann. 1978. Variations in planetary boundary layer parameters observed during AIDJEX. AIDJEX Bull. 39:149-164.

Luna, R.E. and H.W. Church. 1972. A comparison of turbulence intensity and stability ratio measurements to Pasquill stability classes. J. Appl. Met. 11:663-669.

McBean, G.A. 1976. Scaling turbulence in the planetary boundary layer. Atmosphere. 14:254-226.

Panofsky, H.A., H. Tennekes, D.H. Lenschow, and J.C. Wyngaard. 1977. The characteristics of turbulent velocity components in the surface layer under convective conditions. Bound.-Layer Met. 11:335-361.

Pasquill, F. 1976. Atmospheric dispersion parameters in Gaussian plume modelling. Part II. Possible requirements for change in Turner Workbook values. U.S. EPA Report EPA - 600/4-76-0 Research Triangle Park, North Carolina. 12 pp.

Slawson, P., G. Davidson, W. McCormick, and G. Raithby. 1978. A study of dispersion characteristics of the GCOS plume. Prep. for Syncrude Canada Ltd., Edmonton. 112 pp.

Weber, A.H., J.S. Irwin, J.P. Kahler, and W.B. Petersen. 1975. Atmospheric turbulence properties in the lowest 300 meters. U.S. Envir. Prot. Agency Rep. EPA-600/4-75-004. 152 pp.

# AN ANALYSIS OF PRECIPITATION CHEMISTRY IN THE OIL SANDS AREA OF NORTHERN ALBERTA

by

R.R. Peters and H.S. Sandhu,

Alberta Department of the Environment, Edmonton, Alberta

and

W.D. Hume,

Atmospheric Environment Service, Edmonton, Alberta

## ABSTRACT

Rain samples were collected on an event basis during the months of May to October for the period 1976 to 1979. Preliminary analysis of the data has indicated a seasonal cycle of chemical constituents in rainfall. Sample collection procedures, limitations of the chemical techniques, and the reliability of the data without a quality assurance program are discussed. The 1981 project is described in which new methods and procedures are used to overcome limitations of previous experiments.

## INTRODUCTION

Atmospheric pollutants are subjected to various processes, such as diffusion, chemical transformation and advection, from the time they are emitted into the atmosphere until they are deposited. It is important to know the rate of their removal from the air in order to understand their impact on the environment. Airborne and deposited sulphur and nitrogen compounds are the most important man-made constituents in relation to ecological impact of acid precipitation.

In order to measure the rates of wet deposition in the Oil Sands area, Alberta Environment (AE) and Atmospheric Environment Service (AES) in 1976 jointly initiated a program for the collection and analysis of event rain samples. This network was operated up to 1979. A thorough review of the collection and analysis procedures has been carried out to determine the confidence in the 1976-1979 values of chemical constituents in rainfall. This paper discusses the preliminary analysis of this data and describes the 1981 project.

Project Region: The study area, known as the Athabasca Tar Sands, is located in northeastern Alberta between 56° and 59° north latitude (see Figure 1). Major topographical features of the region are the Athabasca River valley running in a north-south direction, Birch Mountain in the northwest, Muskeg Mountain in the east-central area and, Stoney Mountain in the south-central portion of the region. Vegetation in the region consists of white and black spruce.

Wind flow characteristics are important to the dispersion of emissions in the region (see Figure 2). Upper winds are predominantly from the west as indicated at the three mountain sites. The river valley sites reflect the influence of topography by veering the winds to a north-south direction. The effect of these wind patterns has been observed in snow surveys which show a north-south and easterly bulge in deposition patterns (Barrie 1980).

Emissions: Centrally located in the region are two oil sands plants, Suncor (formerly Great Canadian Oil Sands) and Syncrude. Emissions from these plants totalled 110,000 tonnes of $SO_2$ and 20,000 tonnes of $NO_x$ in 1978 (Sandhu 1979, Peters and Sandhu 1980). These emissions are about 1/5 and 1/11 of the total Alberta emissions. Because of the larger emissions of $SO_2$ from the sources compared to $NO_x$, one would expect higher levels of sulphur containing compounds in precipitation.

## SAMPLING AND CHEMICAL ANALYSIS

Sites: Fifteen sampling sites were chosen at Alberta Forestry Stations (AFS) in the region (see Figure 1). The sites were ideal in that they are isolated, radially distributed with respect to the two emission sources and, most importantly, manned during the project period from May through September (Barrie, Nespiak, and Arnold 1978).

Sampling: Rain samples were collected with a plastic funnel (approximately 6" diameter) and a 250 ml polyethylene bottle. The bottle and funnel were set inside a plastic container and another plastic container covered the top of the funnel to prevent contamination by dust.

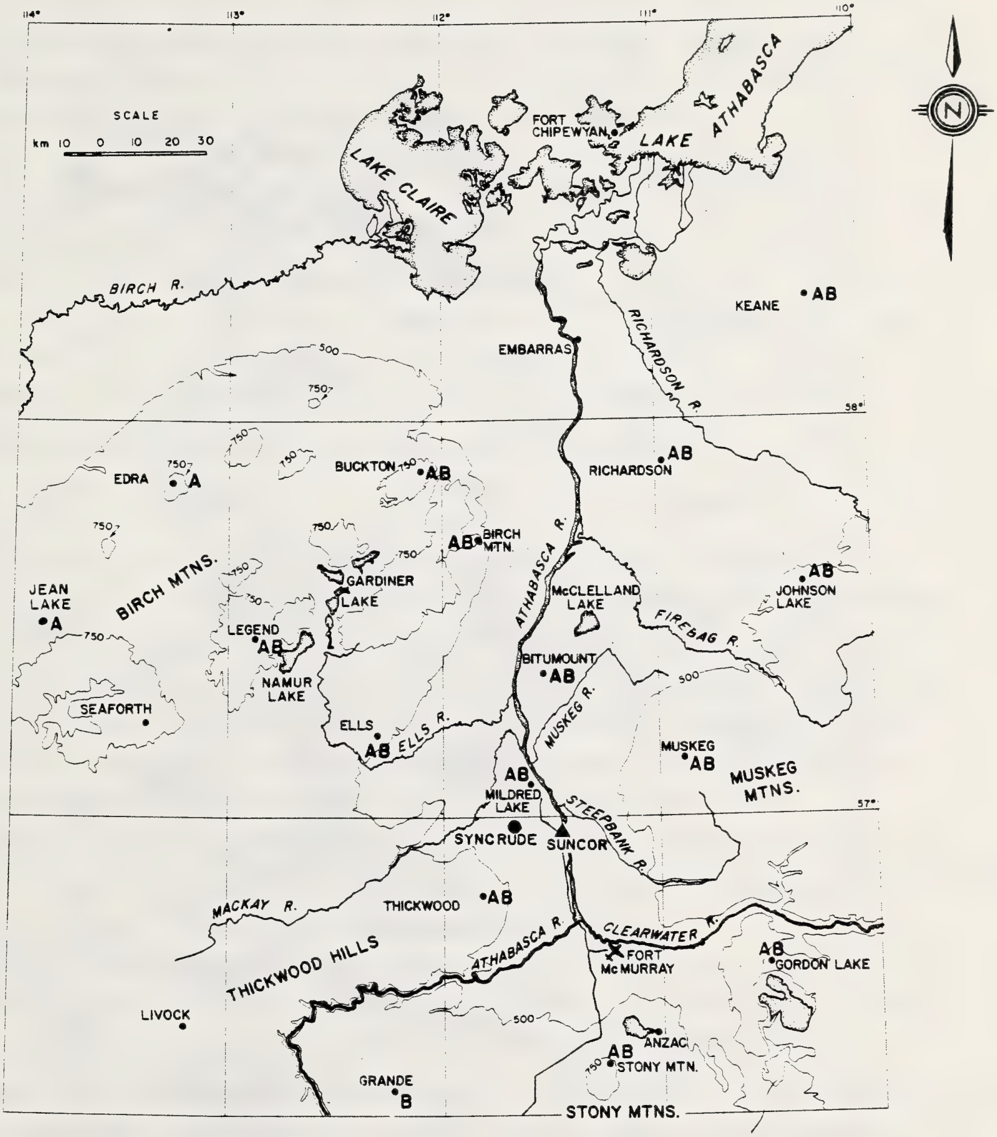

1976-79 RAIN SAMPLING STATIONS - A
1981 RAIN SAMPLING STATIONS - B
EMISSION SOURCES SYNCRUDE - ● SUNCOR - ▲

FIGURE 1. EVENT RAIN SAMPLING SITES IN THE AOSERP STUDY AREA

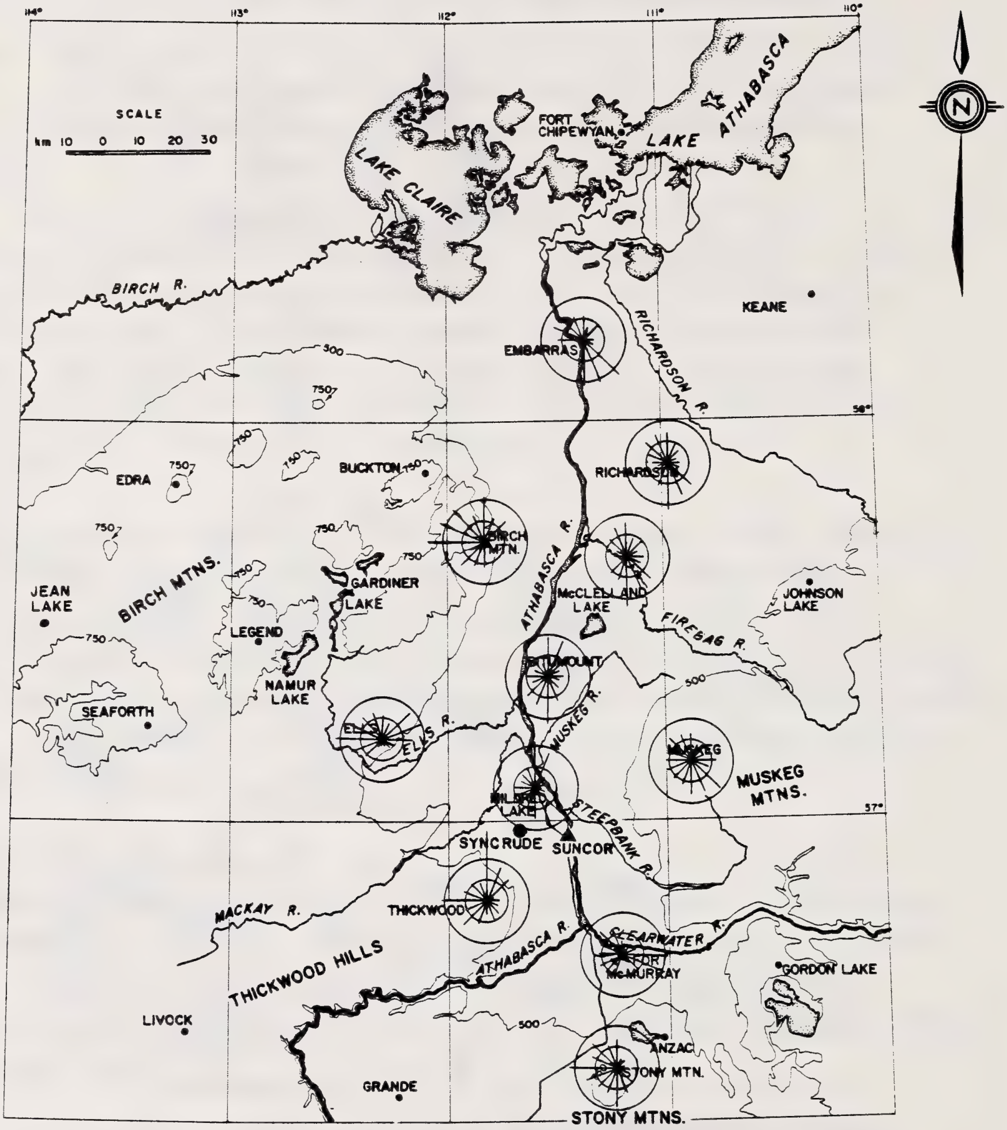

ANNUAL WINDS: CIRCLES REPRESENT 5 + 10% FREQUENCY

FIGURE 2. WIND ROSES IN THE PROJECT REGION

Samples were collected by removing the lid covering the funnel when rain started then removing the sample when it stopped. The funnel was rinsed with distilled water and a new bottle installed to receive the next sample. Samples taken during a month were stored in a refrigerator. At the end of the month the samples were picked up and sent to a laboratory.

Chemical Analysis: During the four years of the project, chemical analysis of samples was performed by one laboratory during 1976-77 and by another during 1978-79. The parameters measured were pH, $SO_4^{2-}$, $NO_3^-$-N, $Cl^-$, $PO_4^{3-}$-P, $NH_4^+$, $Ca^{2+}$, $MG^{2+}$, $NA^+$, $K^+$, alkalinity and conductivity. In 1976 and 1977, pH and conductivity were mainly measured in the field with some pH's taken in the laboratory. In 1978 and 1979 this practice was stopped and only lab measurements were made (Parkhurst, Bittman, and Kelly 1980).

## ANALYSIS OF DATA

The quality of the data has been evaluated in terms of an ionic coefficient "R". R. is equal to the total number of positive molar equivalents divided by the total number of negative molar equivalents of the principal ions measured (as listed in the previous paragraph) in each sample. Each sample is identified as one "count" for the R coefficient. A value of 1 for R indicates all parameters have been accurately analysed. The histogram of R values in Figure 3 demonstrates the variability of the analysis.

Monthly means of several parameters have revealed the occurance of a seasonal cycle. The cycle usually shows a maximum in May, a minimum in July, and again rises in September (see Figures 4-7).

Figure 4 shows that pH varies considerably in the 4 year period from 5.3 (1976), 5.2 (1977), 4.7 (1978) and to 4.6 (1979). As mentioned previously, two different laboratories and somewhat different procedures (field pH measurements versus laboratory pH measurements) were employed. The decrease of 0.5 to 0.6 pH units is difficult to rationalize in terms of the procedure changes (Barrie 1980; Baker, Caniparoli, and Harrison 1980). A similar but reverse pattern is seen for $SO_4^{2-}$ concentrations increase over the four years.

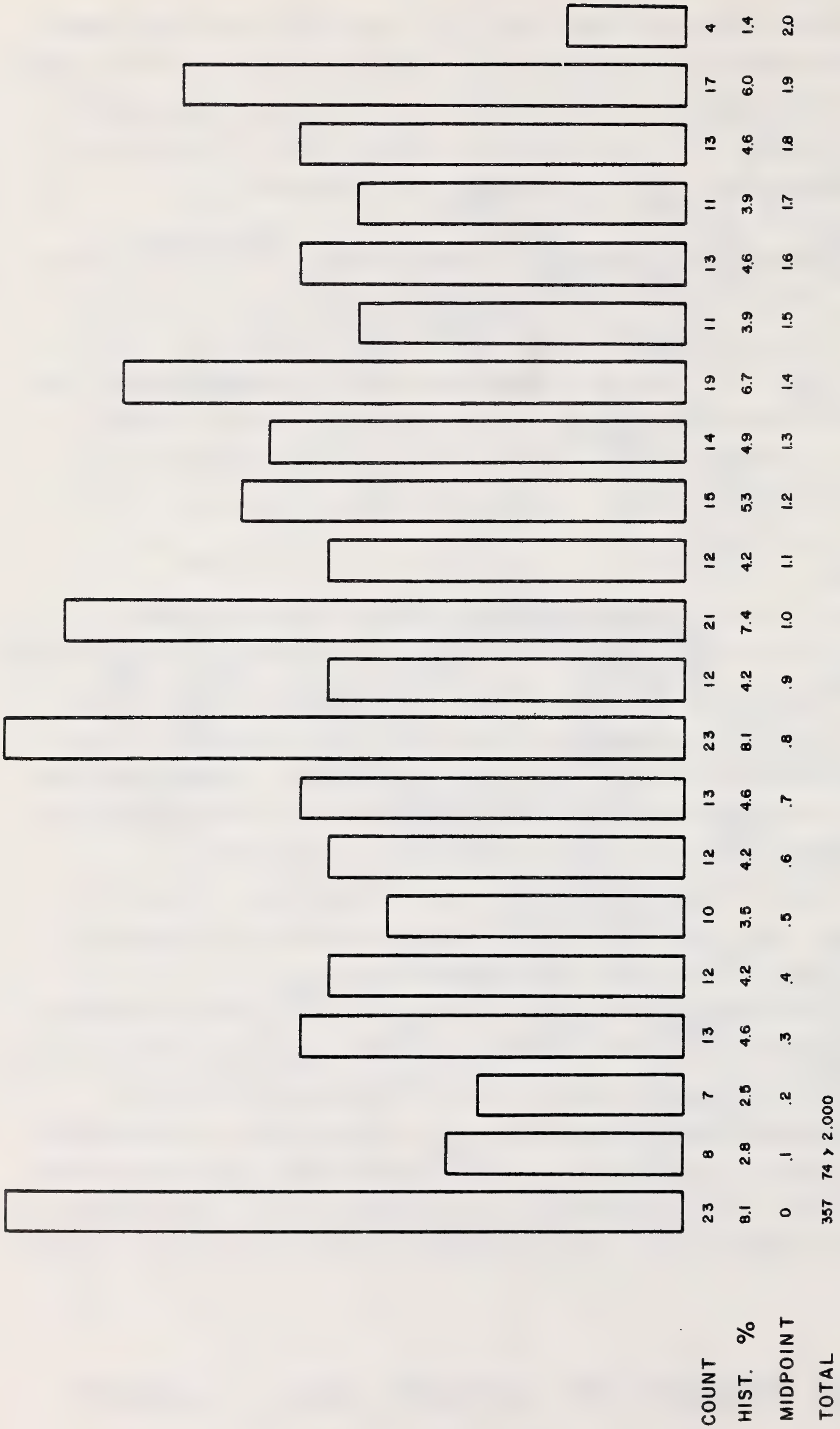

FIGURE 3. HISTROGRAM OF R COEFFICIENT

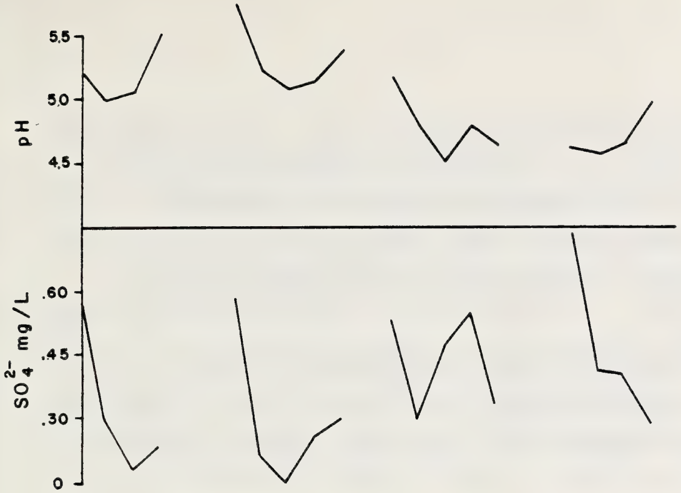

Figure 4. pH and $SO_4^{2-}$ monthly means

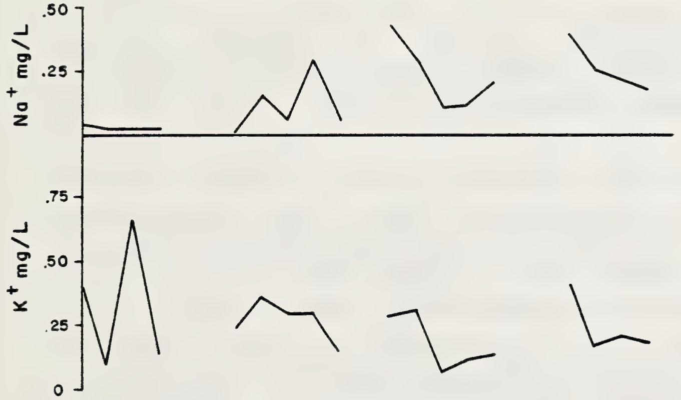

Figure 5. $Na^+$ and $K^+$ monthly means

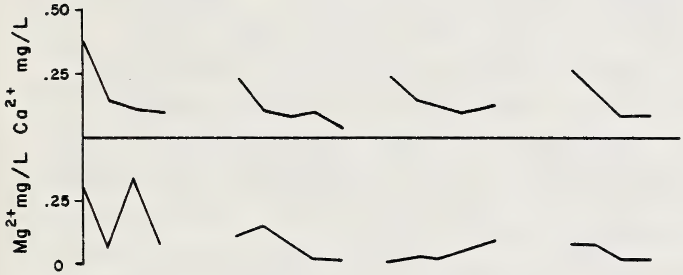

Figure 6. $Ca^{2+}$ and $Mg^{2+}$ monthly means

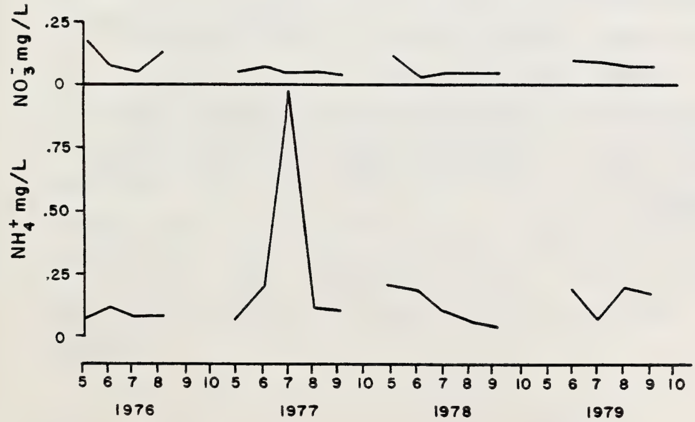

Figure 7. $NO_3^-$ and $NH_4^+$ monthly means

Overall, no correlation was found between pH and $SO_4^{2-}$. No correlations were found between $NO_3^-$ and pH or $SO_4^{2-}$. The possible contamination of rain samples by calcareous materials in the atmosphere predominates over any correlations that could exist (Barrie 1981), Site characteristics and their relative positions to each other and emission sources are being evaluated in a continuing case study analysis.

The $Na^+$ and $K^+$ ions (see Figure 5) show a large amount of seasonal variability. $Ca^{2+}$ and $Mg^{2+}$ ion concentrations (see Figure 6) are low and these are attributed to regional sources rather than originating from the Pacific Ocean.

Concentrations of $NH_4^+$ and $NO_3^-$ given in Figure 7 are relatively low. The possibilities of changes in the ion concentrations during the two month period between collection and analysis could be quite large.

## DISCUSSION

Western Canada has ionic concentrations in precipitation many times less than eastern Canada or the United States. Special concern for any possibilities of contamination must be evaluated (Tyree 1980). Field measurements of pH and conductivity, at low concentrations and small sample volumes, are influenced by contaminants present in the samples. Contamination of the wet surface by dry deposition can result from rinsing funnels with distilled water in the field. The reuse of sample bottles after washing is always a risk, with possibilities of soap remaining in the bottles and contaminating the samples. A check of wash bottles, under laboratory conditions, revealed that one sample was contaminated and one had no change in the concentrations of all measured parameters (GRAY, M. 1979).

Overall, the greatest concern is for sample and data compatibility and comparability with other rain event sampling projects using different chemical techniques (Parkhurst, Bittman, and Kelly 1980). The techniques used in this project had two problems: (1) detection levels were not low enough for measuring constituents, and (2) techniques employed are not widely used in analysing event rain samples.

With regards to the questions on pH cycle, this could have been better addressed if the pH had been analysed fully in terms of contributions due to strong or weak acids (Parkhurst, Bittman, and Kelly 1980).

Field observations are important in assessing a site characteristic which might be exhibited in the analysis. Additional data, such as the times of beginning and ending of the sampling period, winds during those times, airborne dust or smoke in the area due to forest fires, would have helped in assessing the quality of measured parameters.

An ongoing program including spiked and standard samples and participation of other laboratories are needed to assess a laboratory's bias and accuracy (Madsen 1980). Conditions and environment are different for each new project. An assessment of sample change with time should be made if long periods of time are going to occur between collection and analysis. Throughout the project only a few spiked and standard samples were reported. No substantial check was made on sample change during the period between collection and analysis for the period of the project.

## 1981 PROJECT

In view of the above concerns, literature has been reviewed for procedures and techniques used in the sampling and analysis of event rain samples. A project has been initiated in 1981 in the Tar Sands region employing similar techniques to that of Ontario Ministry of the Environment (Vet and Chan 1980).

Two main objectives of this project are (1) to study and measure background concentrations, and (2) to study and measure effects of point source emissions on wet deposition. AFS sites are suitable for sampling to address both of these objectives. Man power is available to operate the equipment and obtain field observations.

A 44 imperial gallon plastic garbage can with a tightly sealing lid along with polyethylene sample bags is used to collect the event rain samples. The lid prevents dust from entering the sample bag or depositing on the lip of the sample container. The sample bags are modified with a diagonal seam that funnels the rain into the bottom of the bag to prevent any losses due to evaporation. These bags are only used once. Chemical characteristics of these bags have already been identified (Vet and Chan 1980) and will be investigated further.

Analyses of the rain samples are being done by Alberta Environmental Centre. A quality assurance program with several private labs has also been established.

## ACKNOWLEDGEMENTS

The authors are thankful to the many persons both in Alberta Environment and Atmospheric Environment Service for useful discussions.

## REFERENCES

Baker, M.B., Caniparoli, D., and Harrison, H. 1980: "An Analysis of the First Year of MAP3S River Chemistry Measurements". Atmospheric Environment, Vol. 15, pp. 43-55.

Barrie, L.A. 1980: "The Prediction of Rain Acidity and $SO_2$ Scavenging in Eastern North America". Atmospheric Environment, Vol. 15, pp. 31-41.

Barrie, L.A. 1980: "A Wintertime Investigation of the Deposition of Pollutants Around an Isolated Power Plant in Northern Alberta". Alberta Oil Sands Environmental Research Program, Edmonton, Alberta, Canada. Report AS 3.2.

Barrie, L.A., Nespiak, V., and Arnold, J. 1978: "Chemistry of Rain the Athabasca Oil Sands Region" Summer 1977". Atmospheric Environment Service, Downsview, Ontario, Canada. Report ARQT 3-78. Various paging.

Gray, M., 1979. Private communication. Alberta Research Council.

Madesen, B.C. 1980: "Some Aspects of Quality Assurance in Acid Precipitations Studies". Presented at American Chemistry Society Meeting, San Francisco, California, August 24-29, 3 pp.

Parkhurst, W.J., Bittman, R.M., and Kelly, J.M. 1980: "Atmospheric Wet/Dry Deposition Measurement and Sampling Variability". Presented at 73rd Air Pollution Control Association Meeting, Montreal, Quebec, June 22-27, 16 pp.

Peters, R., and Sandhu, H.S. 1980: "Nitrogen Oxides Emissions for Alberta". Alberta Department of the Environment, Research Management Division, Edmonton, Alberta, 12 pp.

Sandhu, H.S. 1979: "Industrial Sulphur Emissions for Alberta. 1974 to 1978". Alberta Department of the Environment, Research Secretariat, Edmonton, Alberta, 21 pp.

Tyree, S.Y. Jr. 1980: "Rainwater Acidity Measurement Problems". Atmospheric Environment, Vol. 5, pp. 57-60.

Vet, R.J., and Chan, W.H. 1980: "The Acidic Precipitation in Ontario Study (APOS)". Air Resources Branch, Ministry of the Environment, Toronto, Ontario. Various paging.

# ION AND METAL CONTENT OF THE SNOW COVER OF THE AOSERP STUDY AREA

by

W. A. Murray
Promet Environmental Group Ltd.
Calgary, Alberta, T2E 6T6

Abstract: Snow samples were collected at 60 sites around the existing oil sands plants in the Athabasca Oil Sands region of Alberta in mid-January and late February, 1981. The snowpack depth was measured and snow cores were taken at all 60 sites. Snow sample collectors were set out at six of the sites in mid-January and removed in late February. Quantitative chemical analysis of the core and collector samples was carried out by a commercial laboratory. Duplicate samples from nine of the sites were analyzed by a second laboratory as an independent cross-check. The amounts of sulphate and nitrates deposited in the snow within 25 km of the existing oil sands plants has increased by 88 and 27 percent, respectively, since a study in 1978. However, the amounts of insoluble metals deposited has decreased markedly.

## INTRODUCTION

The fate of pollutants emitted into the atmosphere is a complex problem which has been under intensive scrutiny over the past few years. This effort has been spurred by the possible implications for lake or soil acidification, and the possible effects on vegetation.

An important aspect of the problem is the study of the processes that remove pollutants from the atmosphere. Snowpack sampling and analysis provide a convenient method of investigating the removal processes of wet and dry deposition. Provided there is not substantial thawing, the snow cover retains a good part of the annual precipitation and the chemical contaminants.

Two previous studies of pollutant deposition to the snowpack have been conducted in the Alberta Oil Sands Environmental Research Program (AOSERP) study area. Sulphur and hydrogen deposition patterns were determined by a survey of 55 sites in the area in 1976 (Barry and Whelpdale 1978). An 1978 study (Barrie and Kovalik 1980) surveyed 60 sites with an extension of the chemical analysis to include major ions and trace metals.

Since the 1978 study, the Syncrude extraction and upgrading plant has become operational, and consequently, the industrial emissions of contaminants into the atmosphere has increased by up to a factor of two in the study area. The main purpose of the current study is to determine how the snowpack loadings have changed in response to the added emissions.

## METHODS

### Sample Collection

The snowpack in the Athabasca Oil Sands was sampled twice, from 10 to 13 January, and from 20 to 23 February 1981. Snow cores were collected at 60 sites, shown in Figure 1, within a 100 km radius of the existing oil sands plants. The sites were visited by helicopter except for those along Highway 63, by truck. Snow cores were obtained with a half-cylindrical, acrylic tube, 1 m long and 80 $cm^2$ in cross-section. The coring procedure described by Barrie and Kovalik (1980) was followed. Two samples of three cores were bagged at 51 of the sites. At the remaining 9 sites, four samples were taken to allow a duplicate analysis. Snow collectors, trays 12 x 36 x 49 cm, were deployed at six sites on 16 January and retrieved on 23 February. Both the core and collector samples were bagged and shipped in the frozen state to Chemex Laboratories in Calgary for chemical analysis. The nine duplicate samples were analyzed by Barringer Magenta Ltd. in Mississauga, Ontario.

### Chemical Analysis

The chemical analysis of the snow was performed by two commercial laboratories: Chemex Laboratories (all samples) and Barringer-Magenta (the nine duplicates). Concentrations of the following trace constituents were determined:

1. Major Ions: $SO_4^=$, $Cl^-$, $NO_3^-$, $NH_4^+$, $K^+$, $Na^+$, $Mg^{++}$, $Ca^{++}$, as well as pH and alkalinity.

2. Particulates and heavy metals: Al, Fe, Ni, V, Mn, and Ti.

Blank samples were analyzed to determine detection limits and as a quality control measure. Chemex Laboratories used the same analytical methods as Barrie and Kovalik (1978). Barringer Magenta used ion chromatography for the major ions, and the inductively coupled plasma for the metals.

## RESULTS

### Meteorological History of the Snowpack

The early winter of 1980-81 was cold with a mean temperature of -22.9°C in December compared to the long term normal (Environment Canada 1973) of -16.9°C at Fort McMurray airport. However, January and February were very mild with mean temperatures of -9.4 and -10.9°C, compared to the normals of -21.5 and -16.9°C, respectively. The trends of air temperature and snowpack depth over the winter of 1980-81 are shown in Figure 2.

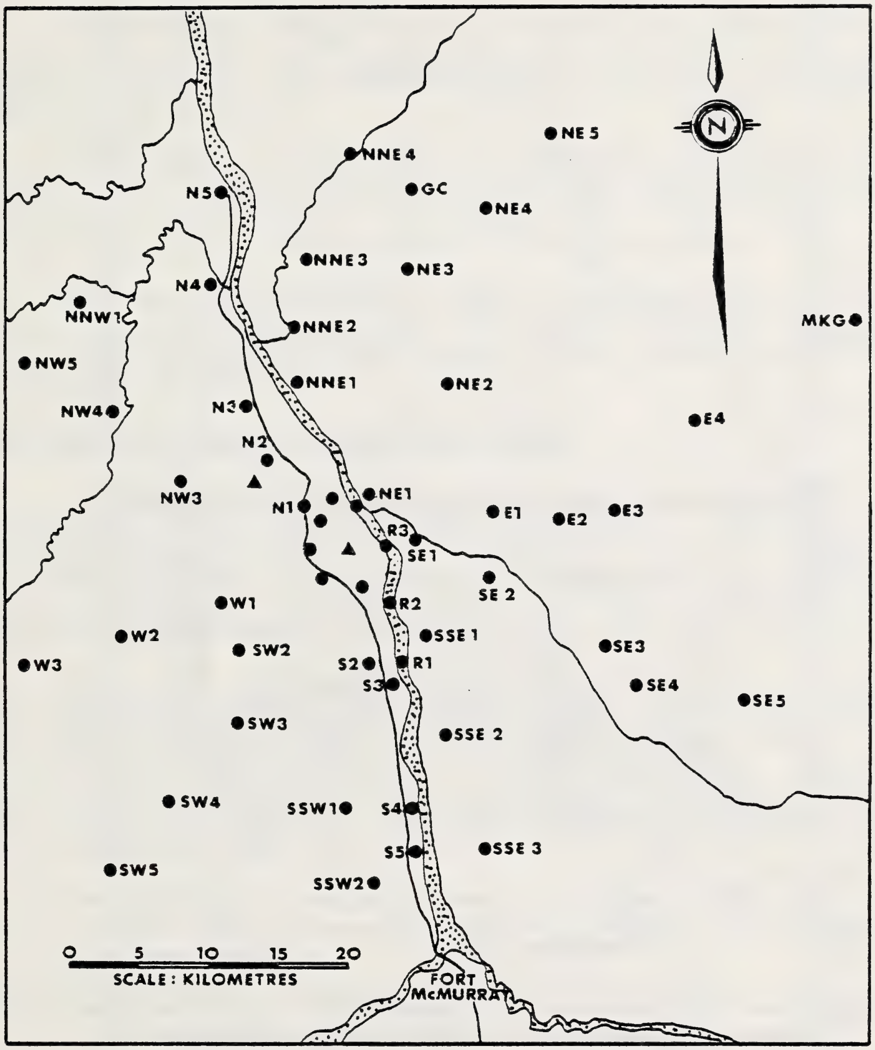

Figure 1. Map of the study area. Dots mark the locations at which snow was sampled. Triangles indicate the Suncor and Syncrude extraction plants. Map scale prevents the inclusion of outlying sample locations at Stoney Mountain AOSERP tower, Ells tower, Birch Mountain tower, Firebag River hydrometric gauge, the Alberta-Saskatchewan border, and Gordon Lake tower.

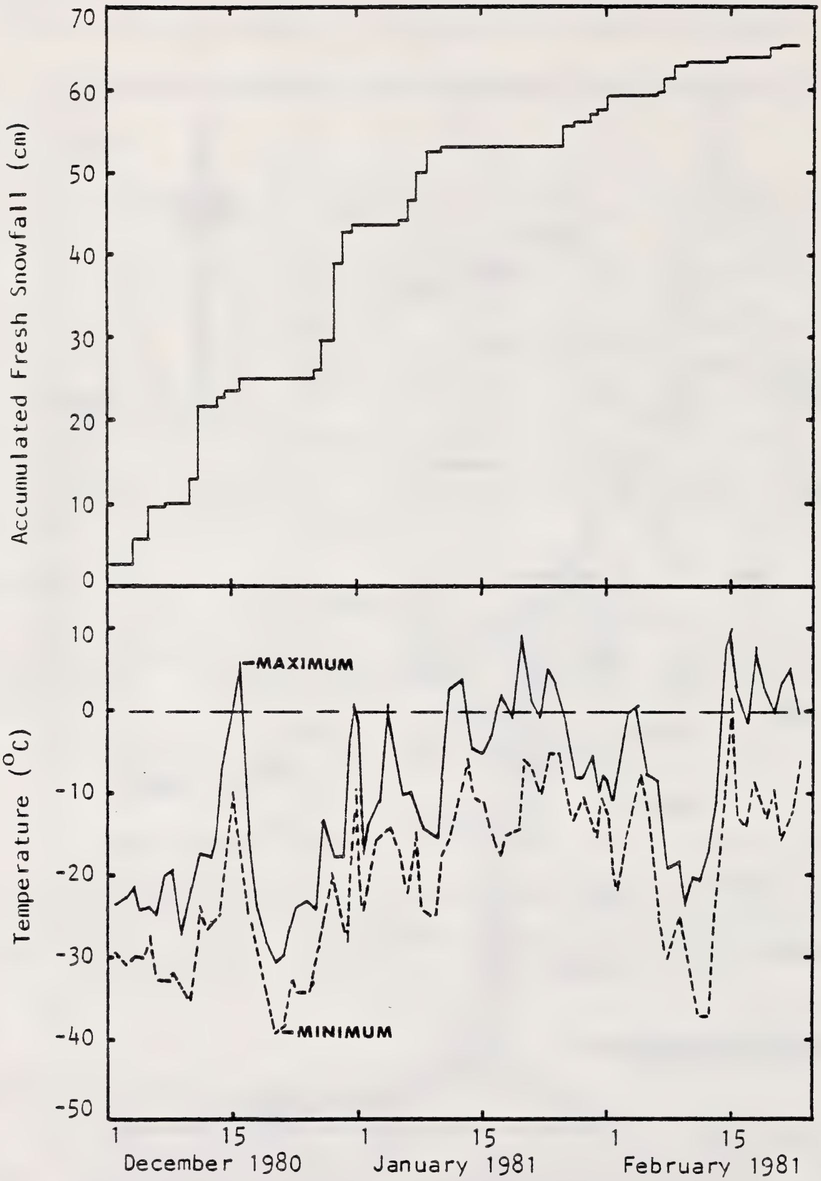

Figure 2. Accumulated fresh snowfall and air temperatures for the study area from 1 December 1980 to 23 February 1981.

There was not significant thawing prior to the first study but between the two studies there were eleven days with positive temperatures. The snow depth data indicate that there was significant melting on 14 and 15 February when the maximum temperatures were 7.5 and 9.9°C, respectively. The melt water trickling through the snowpack would tend to leach out the contaminants.

The frequency distributions of surface wind direction at Mildred Lake in the study area prior to the first study, and between the two studies are shown in Figure 3. The prevalent directions during both periods were southeasterly and northerly.

The average snow depth over the study area was 32 cm in the January study and 31 cm in February. The variability over the network was 10 percent in the first, and 8 percent in the second study. The variability between cores at a given site was about 2 percent of the mean depth.

Snow densities averaged 0.17 and 0.23 over the network in the January and February surveys, respectively. The variability over the network was typically about 9 percent. The standard deviation about the mean at a site was typically 0.006 g/cm$^3$.

## Snowpack Loading of Major Ions and Trace Metals

The snowpack loadings of the major ions and trace metals which originate at the oil sands plants are mapped in Figure 4. Generally, the patterns reflect the wind roses shown in Figure 3. Maxima of loading occur to the northwest and south of each source. Spatial distributions of the metals show a much more rapid decrease with distance from the sources than do the sulphate and nitrate ions.

The amounts deposited within 25 km of the sources were calculated from the deposition patterns and compared to the 1978 results (Barrie and Kovalik 1978) in Table 1. With the additional Syncrude source, sulphates and nitrates were higher by 88 and 27 percent, respectively. The amounts of insoluble metals were much lower than in 1978. Electrostatic precipitators were not installed on the power plant chimney at Suncor in the 1978 study, so particulate emissions were relatively high.

Table 1. Average mass of substances deposited per day (T/d) within 25 km of site N1 (midway between Syncrude and Suncor) from 6 November 1980 to 10 January 1981.

| | $SO_4^=$-S | $NO_3^-$-N | Al | Mn | V |
|---|---|---|---|---|---|
| 1978* | .33 | .15 | 2.97 | 0.024 | 0.41 |
| 1980 | .62 | .19 | 0.78 | 0.0065 | 0.058 |

*Based on deposition amounts reported by Barrie and Kovalik (1980).

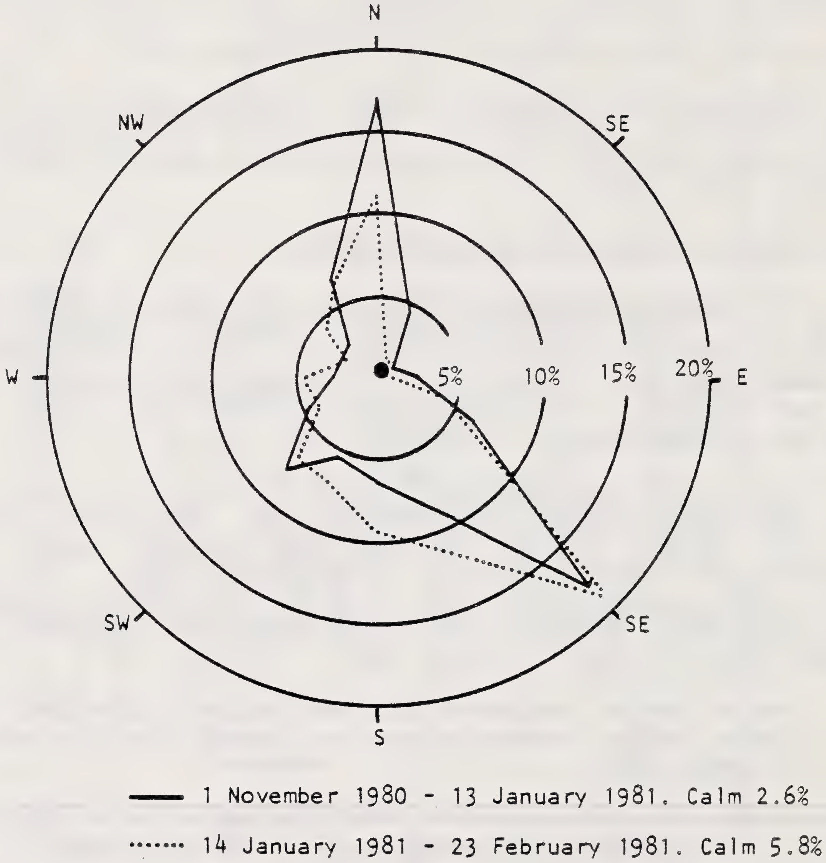

Figure 3.. Wind roses showing the frequency distribution of wind direction at the Mildred Lake station during the lifetime of the snowpack. Data were provided by Alberta Environment.

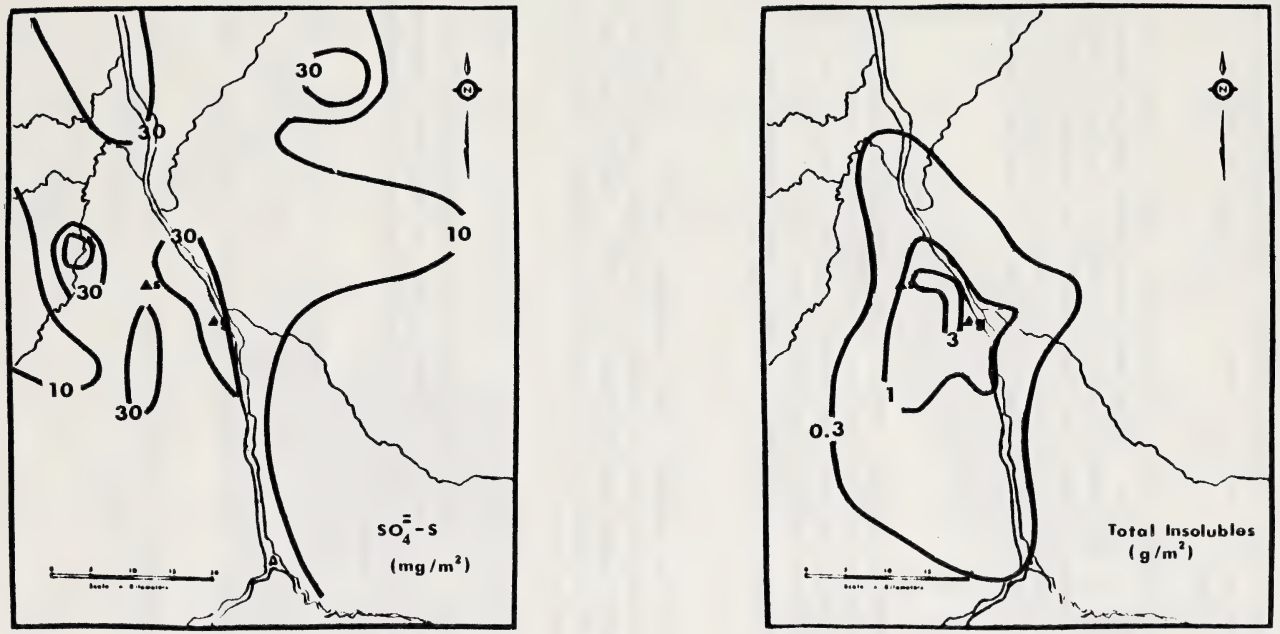

Figure 4. The spatial distribution of snowpack loading of sulphate ion (mg/m$^2$) and total insolubles (g/m$^2$) in the AOSERP study area on 10 January 1981.

## Comparison With 1978 Study

The changes in the major ion and metal loadings from January 1978 to January 1981 are mapped in Figure 5. The sulphate loadings show increases to the northwest and south of the Syncrude plant, the prevailing direction of emission transport. The metals tend to show a decrease in the same directions centred on the Suncor plant.

A mapping of snowmelt pH for the study area is shown in Figure 6. Areas of relatively high pH occur to the west-northwest and north-northeast of the sources. The pH falls off rapidly with distance in other directions. The changes in pH of the snowmelt from the results of the January 1978 survey are shown in Figure 7. The increases of pH to the north-northeast and west-northwest appear to be correlated to increased calcium ion loadings also shown in Figure 7.

## Snow Collector Results

The contaminant loadings determined from the snow collectors in general showed little correlation with the loadings calculated from the difference between the concentrations observed on 10 January and 20 February 1981. In fact, the soluble metals and the ions $SO_4^=$, $Na^+$, $K^+$, $Ca^+$, and $Mg^{++}$ showed apparent decreases in loadings at some sites between the two surveys.

## CONCLUSIONS

The results of the January 1981 snowpack survey in the AOSERP study area showed that there has been an increase in sulphate and nitrate loadings since the Syncrude plant became operational in 1978. Metal loading have decreased dramatically from January 1978 when electrostatic precipitators were not in use at the Suncor plant.

## REFERENCES

Barrie, L.A., and J. Kovalik 1980: "A wintertime investigation of the deposition of pollutants around an isolated power plant in Northern Alberta." Prep. for the Alberta Oil Sands Environmental Research Program by Atmospheric Environment Service. AOSERP Report 90. 115 pp.

Barrie, L.A., and D.M. Whelpdale 1978: "Background air and precipitation chemistry." pages 124 to 159 in Fanaki, R. Meteorology and air quality field study in the AOSERP study area, March 1976. Prep. for the Alberta Oil Sands Environmental Research Program by Atmospheric Environment Service. AOSERP Report 27. 499 pp.

Environment Canada, Atmospheric Environment Service 1973: "Canadian normals, temperature, 1941-1970." 186 pp.

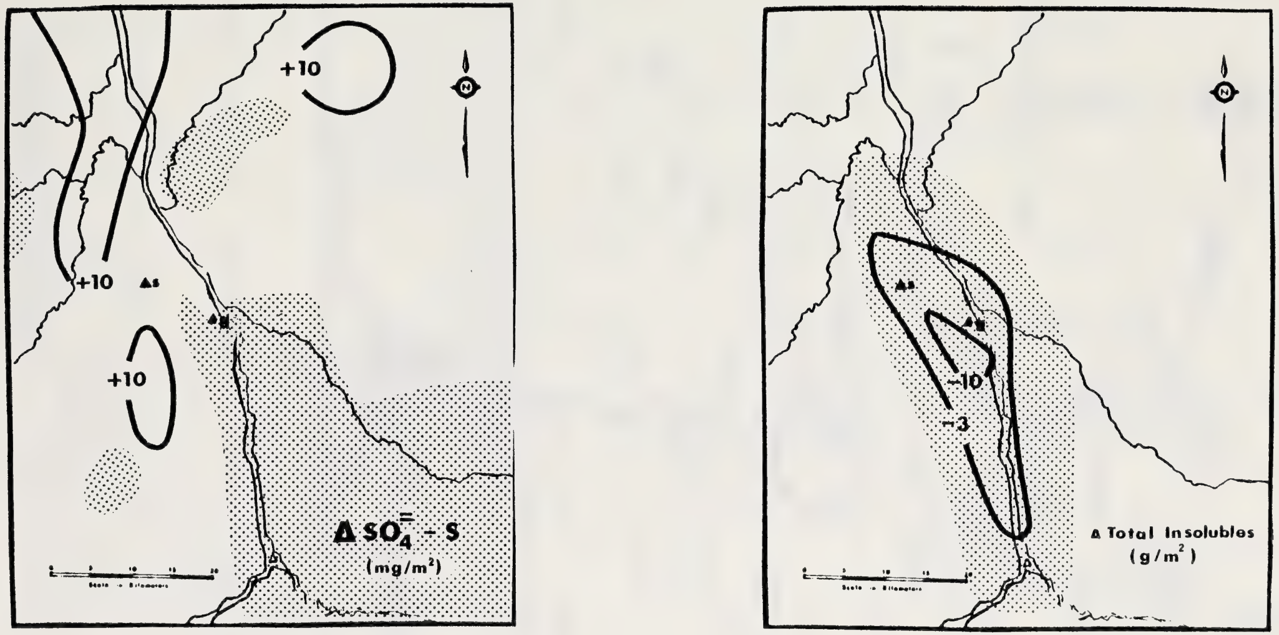

Figure 5. The spatial distribution of the change in sulphate and total insoluble loadings in the AOSERP study area between January 1978 and 1981. Shading indicates areas of decreased loading.

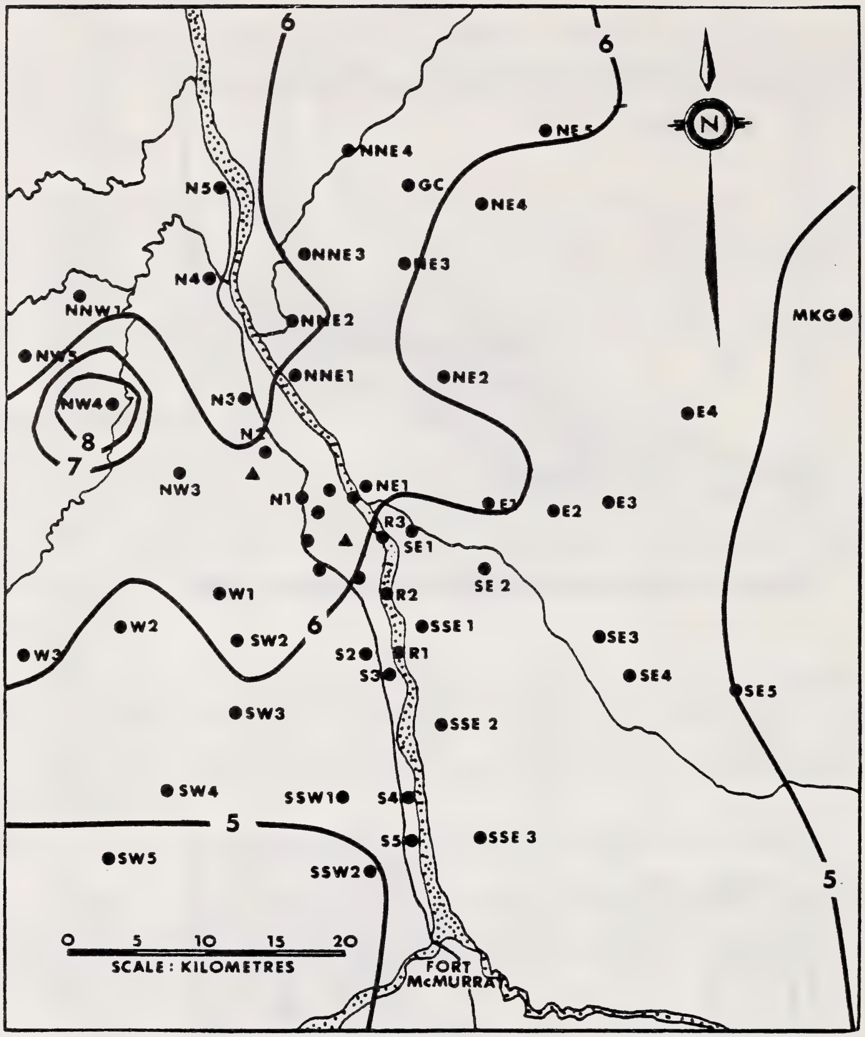

Figure 6. The spatial distribution of snowpack pH in the study area on 10 January 1981.

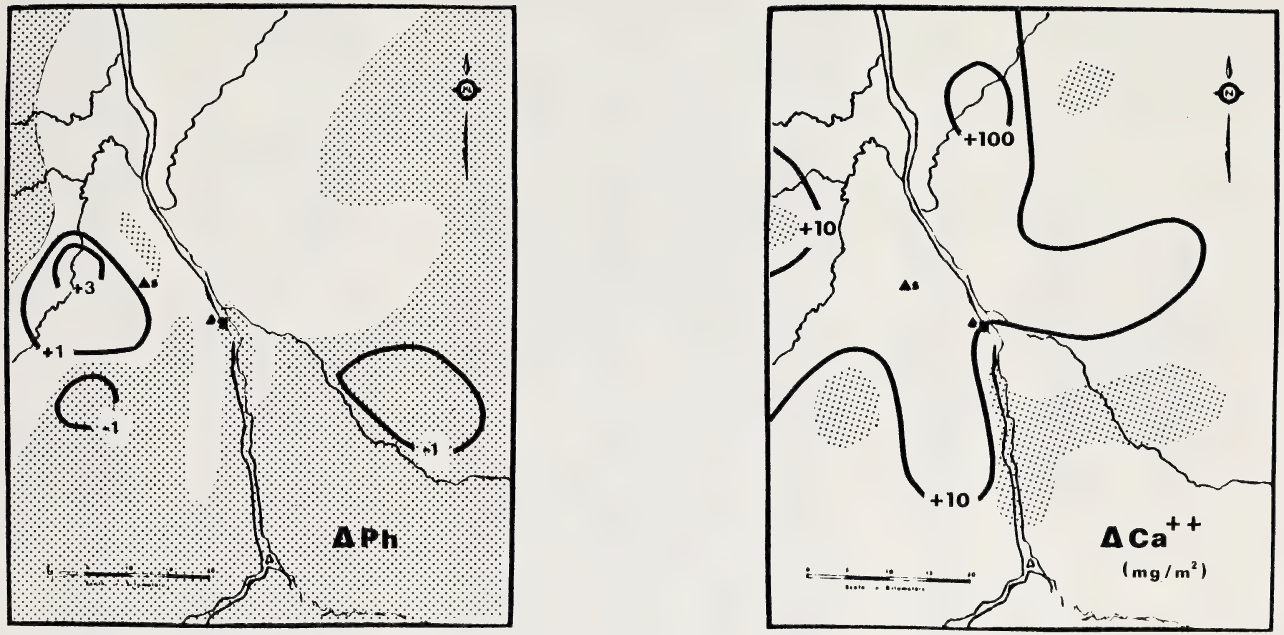

Figure 7. The change in pH and calcium ion loadings in the AOSERP study area between January 1978 and 1981. Shading indicates areas of decrease.

# USER CONSIDERATIONS

# IN

# AIR QUALITY MODELLING

by

R. P. Angle
Air Quality Control Branch, Alberta Environment
Edmonton, Alberta, T5K 2J6

Abstract: The achievement of satisfactory air quality entails the adoption of one or more air pollution control strategies. Of the four basic strategies available, only air resource management requires the use of air quality models. Atmospheric dispersion models are a subset which can be employed either for fundamental research or for practical decision making. The characteristics of user oriented atmospheric dispersion models are simplicity, clarity, appropriateness, practicality, flexibility and reliability. Model performance is determined with reference to accuracy, skill, sensitivity, consistency, generality, integrity, and mechanism. For the successful application of air quality models to the decision process, there must be close co-operation between modellers and users.

## INTRODUCTION

The term "model" may be defined as "a representation of the important properties of any phenomenon". A model cannot have all the properties of the phenomenon, otherwise it would not be a model - it would be the phenomenon itself. A model is an abstraction or simplification of reality that may be used in: (1) description - integrating observations and theories (2) prediction - looking beyond recorded experience (3) optimization - allocating resources to achieve desired ends.

Air quality managers use models within the context of an air pollution control strategy, that is, a master plan containing long term objectives and principles of action which govern the choice of tactics or detailed implementation procedures. Four distinctly different air pollution control strategies have been identified: (1) Emissions standards - limiting the quantities of pollutants emitted (2) Emissions taxes - imposing financial penalties on polluters (3) Cost/Benefit - selecting only tactics where the benefits exceed the costs (4) Air Resource Management - regulating emissions so as to meet ambient air quality standards. The first three strategies require economic models of varying complexity, whereas the fourth makes use of physical or mathematical models of the atmosphere, commonly called "air quality models".

## AIR RESOURCE MANAGEMENT

The elements of an air resource management strategy are:

- air quality objectives - goal specification in terms of short or long term concentrations of pollutants
- emissions inventory - the total amount and time variation of pollutants
- predictive methodology - a means of relating air quality to emissions
- monitoring system - measurements of air quality and a record of changes
- air pollution control tactics - alternative actions required to attain or maintain the air quality objectives
- enforcement procedures - the authority to implement the pollution control plan

Figure 1 shows the information inputs and their relationships.

Four general classes of predictive methodologies are available (see Angle 1979 for a fuller description and references):

1. Proportional relations (or rollback) - assumes that ambient concentrations are a linear function of total emissions.
2. Fluid simulations - using miniatures in a wind tunnel or water channel.
3. Empirical analysis - applying various types of statistical methods to describe observations and relate variables.
4. Atmospheric dispersion models - mathematical methods that aim to provide a quantitative cause-effect link between the intensity and spatial distribution of the sources of air pollution and the measured distribution of air quality.

### Atmospheric Dispersion Modelling

An atmospheric dispersion model, sometimes called an air quality simulation model, can be defined as a numerical technique or methodology, based upon physical principles, for estimating pollutant concentrations in space and time as a function of the emission distribution and the attendant meteorological and geophysical conditions.

A clear distinction ought to be made between "models" and "computational algorithms". As defined above a model is a set of mathematical relation-

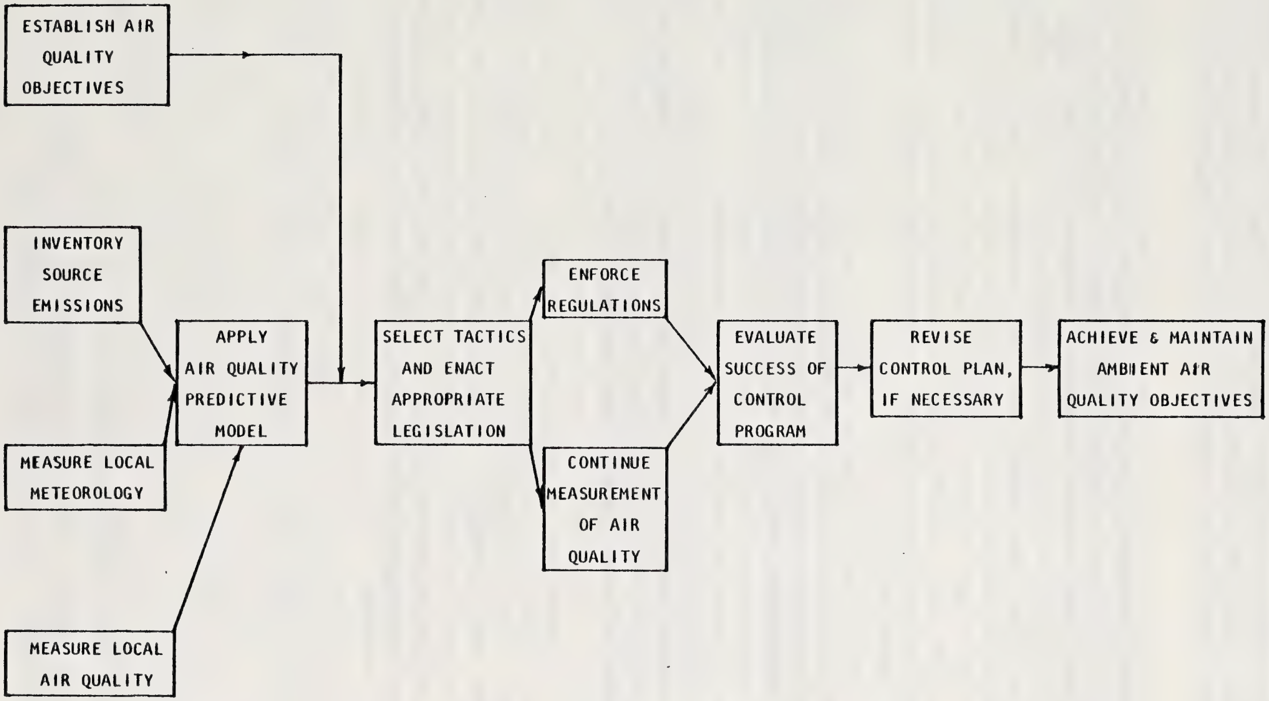
ESTABLISH AIR QUALITY OBJECTIVES
INVENTORY SOURCE EMISSIONS
MEASURE LOCAL METEOROLOGY
MEASURE LOCAL AIR QUALITY
APPLY AIR QUALITY PREDICTIVE MODEL
SELECT TACTICS AND ENACT APPROPRIATE LEGISLATION
ENFORCE REGULATIONS
CONTINUE MEASUREMENT OF AIR QUALITY
EVALUATE SUCCESS OF CONTROL PROGRAM
REVISE CONTROL PLAN, IF NECESSARY
ACHIEVE & MAINTAIN AMBIENT AIR QUALITY OBJECTIVES

Figure 1. Air resource management requirements.

ships based on physical principles. A computational algorithm is a set of detailed instructions for implementing a model, that is, a computer program or computer code (Roberts 1977). Thus, there can be many algorithms (computer programs) that implement the same basic model. Given identical input data all algorithms must yield the same results if they are a faithful rendition of the underlying model. The term "computer model" is often used when basic models are combined with submodels in a manner which does not lend itself to hand calculations.

Atmospheric dispersion models serve two very different purposes (Stern 1970; Hanna 1973). In fundamental research models serve to test our understanding of the physical and chemical processes involved in air pollution. If we cannot model a system, then we do not understand it. In the past, scientists tended to say that they understood the phenomena, back lacked the computational and statistical capabilities to solve the understanding problems. Now, the situation is reversed; enormous computer power is available, but scientists are finding that they lack the physical knowledge to exploit if fully. A research-grade model serves to test ideas by providing detailed representations of the phenomena under study.

In practical applications, models are called upon to provide quick, reasonable answers to the host of questions routinely faced by the decision maker. Applications-grade models allow the exploration of hypothetical situations and their consequences for air quality. Quantitative answers to "what if" questions facilitate the evaluation and assessment of air pollution control tactics and, to some extent, of air pollution control strategies. Model results provide the foundation for decisions that govern many day-to-day activities. Such models are tools which decision makers employ to obtain some of the many information inputs that enter into their deliberations.

## Model Usage

A "user" of a computer model is a decision maker whose actions will be affected by the model results. Despite the demonstrated uses (see Rote 1976), potential benefits and the proliferation of available computer models, not all decision makers may be regarded as "users". The Holcomb Research Institute (1978) identified four major factors that influenced the acceptance of computer models by decision-makers:

- Limited resources: Time, money, and personnel are generally scarce and their allocation affects the implementation of programs and policies.
- Political pressure: The power structure and the conflicting viewpoints of different special interest groups must somehow be accommodated.
- Problem complexity: Solutions to one set of problems regularly create unmanageable new problems.
- Unfamiliarity: There is considerable professional risk in a methodology that is new and often unproven.

Once computer models have been accepted as decision-making tools, it becomes necessary to determine what is required of a model. This is not an easy task for a decision maker. Generally his training, experience, perspectives, goals, methodologies, values, and reward systems will be quite dissimilar from those of a modeller. The great differences often pose a barrier to communication and effective interaction. In such circumstances, an intermediary who is conversant with both technical modelling matters and the pragmatic realities of decision making can be called upon. Such a "policy analyst" has the capacity to translate the goals and constraints of decision making into tangible modelling specifications.

A systematic approach to the evaluation of alternative computer models has been prepared by the staff of Argonne National Laboratory (Rote et al. 1977). The methodology combines technical, importance and pragmatic ratings to arrive at a final comparative judgment as to which of two or more models best suits the application. An application of a similar procedure is described by Davison and Lantz (1980).

## USER CONCERNS

### Simplicity

The principle of simplicity has always guided physical scientists in their quest for explanations of natural phenomena. This same principle applies in the consideration of competing models for practical decision making. A user will choose the simplest possible model that meets the performance specifications.

Many atmospheric scientists today speak disdainfully of "simple" models and express a clear preference for more "sophisticated" models. It has been pointed out that "simple" is not the opposite of "sophisticated" but rather of "complex". The antonym of "sophisticated" is "naive". Simple models are not necessarily naive and may in fact represent the essence of sophistication (Gifford and Hanna 1975). Complex models are not necessarily tied to any deep understanding of physical and chemical processes, and hence can be naive.

### Clarity

The user of an air quality model needs to understand the components of the "tool" he is using. He should know, in general terms, how the model works, what its limitations are, where problems may arise, and what to do before calling in the specialist, that is, the modeller. It is not intellectually satisfying to rely upon a mysterious "oracle" or "black box" about which nothing can be comprehended. Only if the user is comfortable with the general concepts and terminology--if he feels that he understands the model--will he have confidence in the results.

Clarity is related to simplicity only to the extent that a simple model can probably be explained more easily than a complex model. However, even complex models can be explained adequately if enough care and attention are directed towards the documentation. Too often modellers write their documentation for other modellers, with all the emphasis on theoretical and numerical aspects. Even the informed user may find such detail next to unintelligible. This inevitably leads to a wholesale rejection of modelling.

### Appropriateness

The time, space, information, and resource scales of a computer model ought to be appropriate to the problem at hand. A computer model suited to one purpose will not necessarily be suited to a second purpose even on the part of the same user. Different applications will entail different performance goals, different levels of accuracy, different inputs, and different outputs. No one computer model can serve all purposes equally well. Of necessity a decision maker will require a number of computer models, each optimally suited to a particular function. Like a craftsman, the decision maker must have the right tool for the job. Otherwise he may be guilty of the proverbial "killing a fly with a sledge hammer"!

Model developers need to specify the limitations of their models so that they are not used out of context. Ideally, a model would be designed and tailored to the requirements of the user. Often, however, existing research grade models are merely converted into a working format. There are many difficulties with such conversions.

## Practicability

Resource constraints are very real and must always be kept in mind when developing or adapting a computer model. Questions such as the following must be asked: What size computer installation is to be used? What are the qualifications of the staff who will be operating the program? Are the requisite data readily available? Can runs be set up and executed within a reasonable period of time? Is the output in the most appropriate format? Are diagnostic test available? Unsatisfactory answers to any of these questions will probably result in rejection of the computer model.

Research-grade models almost always fail in this regard because they tend to take too much computer time, have exorbitant data requirements, produce reams of irrelevant output, and demand the attention of several system's analysts and programmers.

## Flexibility

The user desires models that are adaptable to a wide variety of situations, investigations, scenarios, input data and formulations. As knowledge advances he wants to be able to upgrade his models/algorithms with minimum effort. As different data become available he wants to be able to maximize his use of it.

## Reliability

Perhaps the greatest single barrier to extensive model use has been a general lack of confidence in their capabilities. This is due, in part, to the fact that detailed knowledge about many of the basic meteorological and chemical process operating on pollutants in the lower atmosphere is still incomplete. However, perhaps equally as important is the fact that few models have been adequately evaluated and verified. This, in turn, has resulted from both the paucity of suitable data and the absence of performance goals.

In the absence of an appropriate data base, many modellers have simply compared model calculations with observed pollutant concentrations. Unmeasured variables or empirical "constants" are then adjusted to provide the best overall agreement. Such a procedure is a calibration and does not contribute to general confidence in the model. It is entirely possible that the model may have several defective but compensating elements which together yield results that are fortuitously in agreement with observations. Other modellers have merely used whatever was available to them, data bases which are, by and large, hopelessly inadequate owing to small size, limited conditions of measurement, poor quality, absence of measurements of important variables, and other factors. Still other model developers have resorted to comparison with other models and have never tested their models against the real world, an unthinkable practice to the user.

A true verification program must involve the careful appraisal and confirmation of the individual model elements on the principle that the whole cannot be better than the weakest part. And the weakest part is often the emissions submodel, which is frequenly overlooked by air quality modellers. Hourly source strengths in urban areas are typically known to about ±50% (Hanna 1973). This imposes a severe limitation on the accuracy of air quality predictions even if the diffusion and transport submodels were perfect.

While the terms validation and verification are often used synonymously, there is a subtle difference which has important ramifications (Angle, 1979):

> "Verification" refers to establishing or proving the correctness of the model by rigorous scientific methods.
>
> "Validation" implies the formal approval or official acceptance of the model.

Thus validation goes beyond verification and takes into account performance goals and user applications. Similar definitions were also put forward by Turner (1979).

Only when model results can be trusted within known tolerances will a user feel comfortable in applying that model as a problem-solving tool. Confidence limits must accompany any estimate or prediction.

## CONCEPTS IN MODEL PERFORMANCE

### Accuracy

Accuracy refers to the deviation of a model's predicted value from the value actually measured in the field. The agreement between observations and predictions can be expressed in various ways (see, for example, Bowne, 1980. Besides correctness of predicted magnitudes, an air quality model may also need to be capable of predicting hour-to-hour variations. For some applications it may be necessary to predict the frequency distribution of pollutant concentrations. The requirements of the user will determine the appropriate objective measure of agreement between predictions and observations.

### Skill

Skill refers to the relative success of a model. Measures of accuracy by themselves have little meaning. To interpret the results of a verification there must be some standard for comparison. Simple models usually provide such standards.

In air quality modelling no clear standards have yet emerged although box models have been suggested for the urban modelling standards (Gifford and

Hanna 1975) and Gaussian models are generally recognized for the diffusion of non-reactive pollutants from point sources. The usefulness of any complex model will depend entirely upon its ability to predict better than any given simple model. If a complex model cannot estimate observed conditions better than some simple model, then in a practical sense it shows no skill. In such a case, the development of complex models for applied purposes is not only unnecessary but unprofitable.

Also of relevance here is the issue of predictability of the atmosphere both in principle and in practice. Stern (1970) noted that computers had gained a generation on air quality modellers and he warned that "it gains us naught to apply better programming to inadequate physical input data and inadequate physical concepts". Hanna (1973) observed that after a decade of air quality model development there was little indication of improved forecasting ability. Gifford (1976) commented that, while we are on the threshold of basic new insights into theoretical aspects of the turbulence problem, little progress can be expected in practical diffusion modelling. Venkatram (1980) showed that the stochastic nature of concentration fields limits the predictability of models.

### Sensitivity

Sensitivity refers to the magnitude of change in a predicted value that occurs as a result of an incremental change in an input value. Sensitivity analysis of a model determines the expected error and uncertainty in predicted quantities due to error and uncertainty in input parameters. Random errors will be present in all observations and knowledge of model sensitivity will essentially define the accuracies required of various measurements. Systematic errors are most likely to be present when input parameters are estimated. The magnitude of the variations introduced will indicate whether or not effort must be expended to correct the estimation procedure.

Sensitivity analysis obviously needs to be done prior to the design of any field studies. Each submodel needs to be evaluated separately and as one component of the complete air quality model. This will isolate the key model elements and provide guidance as to the allocation of resources for field verification. Special attention can be focused upon conditions that stress the model, that is, combinations of variables to which the model is very sensitive as these may reveal a basic flaw or shortcoming in the formulations.

### Consistency

Consistency refers to the interrelationship between various submodels. If certain assumptions are made in one submodel, they should not be violated in another. Internal consistency is necessary if a model is to be realistic, that is, if it is to be based on the physics and chemistry of the phenomena rather than in some fortuitous combination of conflicting formulations.

Ideally, consistency also requires that the level of sophistication of each submodel be comparable and that the complexity of each submodel match the physical concepts and physical inputs involved. In practice, discrepancies must be allowed, but satisfactory tradeoffs can often be made after examining sensitivities.

### Generality

Generality refers to the range of applicability of the model. The underlying assumptions, both explicit and implicit, of a model will place certain limitations upon the situations in which the model can be expected to perform well. These restrictions may be expressed in terms of time scale, space scale, climatic type, terrain features, or source characteristics. A proper verification will examine all conditions to which the model is expected to apply and perhaps some to which, in principle, it does not apply. Often a verification is done for only one small set of possible conditions. This may provide confidence in the model's use for those particular conditions but lends no support to the potential for more general usage of the model. It is especially important to test models under those conditions that may reveal hidden flaws or shortcomings.

### Integrity

Integrity refers to the quality of the data used in a model verification. Assurances need to be provided that the data are sufficiently precise, accurate, repeatable, and generally trustworthy to allow a proper verification to be performed. Care in the acquisition of the measurements is only the first step. Hypotheses which address the data base itself ought to be formulated and tested (Rote 1976). It must be clearly demonstrated that a particular data base is, in fact, adequate for the verification of any given model. If this step is ignored the verification effort will be inconclusive. The modeller will tend to blame the data for the model's poor performance whereas the user is apt to reject the model. If good agreement is obtained it may only be accidental and ought not be considered supportive of model reliability.

This is closely related to maximum utilization of a data set. Most researchers fail to extract more than a small portion of the wealth of information contained in a data set. Much of the knowledge present could be revealed by data analysis techniques quite removed from the air quality model for which the data may have been gathered in the first place. While helping to establish data integrity, such procedures are also cost effective since large sums of money are often expended to obtain these data.

### Mechanism

Mechanism refers to the extent to which the physics and chemistry of the phenomena are embodied in the model, as opposed to statistical summaries or tabular data. This is really nothing more than the distinction between cause-effect relationships and variance reduction relationships. It is generally accepted that equations expressing causality are superior to those that merely describe a connection between two variables. At present it is not possible to model atmospheric systems entirely with mechanistic equations. Invariably field data which are not well understood must be used in various model components. Models differ in the degree to which this is the case.

## CONCLUDING REMARKS

The interaction between the decision process and the air environment may include as an intermediate step the activity of air quality modelling. This relationship is shown schematically in Figure 2. Also shown are the links with fundamental scientific research and practical applications, or policy analysis. As the diagram indicates, modelling for applications will reflect the decision maker's perspective whereas modelling for research will focus upon basic knowledge and understanding of the air environment.

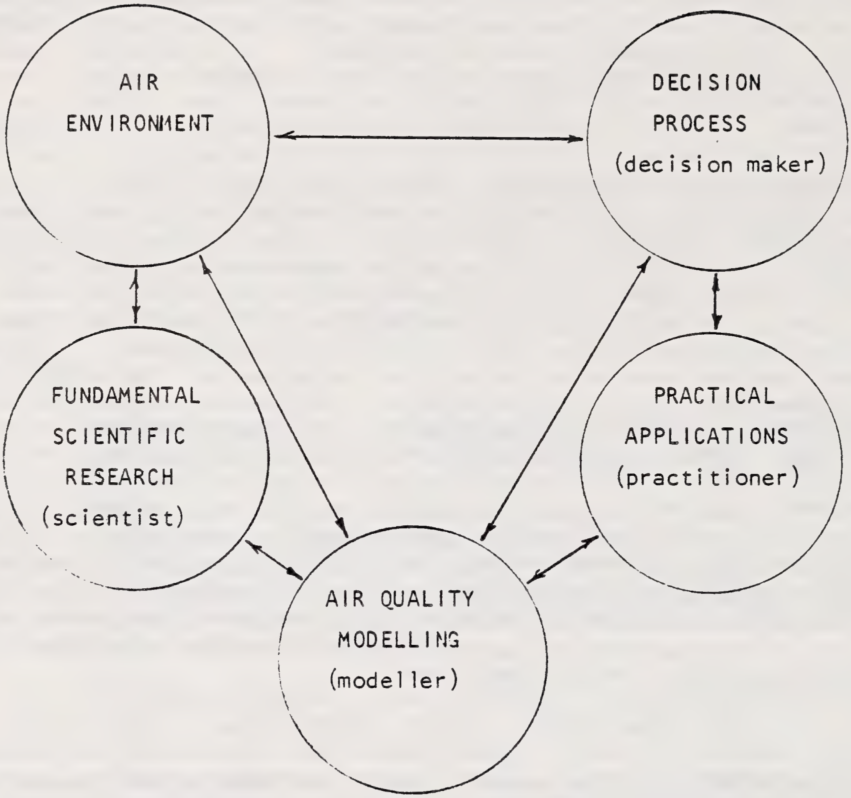

Figure 2. The air environment and interrelationships with various activities (after Holcomb Research Institute, 1978).

After examining the United States experience with environmental modelling and decision making, the Holcomb Research Institute (1978) concluded that:

> Modelling undertaken in an application-oriented, integrative context (i.e., the synthesis and integration of current knowledge) has a better chance of facilitating decision making than modelling undertaken as basic research. This is not to belittle the role of basic scientific research, but to suggest that modelling applied to environmental management must be undertaken with different and perhaps more pragmatic objectives.

The differences between research and applications are also displayed in the attitudes of atmospheric scientists. Tucker (1976) described the two archetypes and the working associations between them. He concluded that the most effective association involves continuous interaction and discussion such that fundamental research is kept relevant, new ideas can enter operational development without delay, and feedback can suggest new lines of research. In order to establish this he recommended that:

> A mutual recognition is necessary of the need for two types of scientists with different attitudes to tackle different jobs of similar importance ... The gap between these must be bridged, but not narrowed, in such a way that an interchange and flow-on can occur without neutralizing the effectiveness of either.

Air quality modelling is potentially of great use in the decision process that directs and controls man's impacts upon the air environment. For that potential to be realized, the modelling activity must address the needs of the deicision maker. Hence, the model user should be directly involved in each stage of model development. Before undertaking any model development, the modeller and user should agree as to the objectives of the project and as to its scope in terms of available resources. Performance goals and documentation standards should also be established. To work in other than a fully cooperative manner squanders human resources and imperils the attainment of our clean air objective.

## REFERENCES

Angle, R.P. 1979: Air quality modelling and user needs. Prep. for the Alberta Oil Sands Environmental Research Program by Alberta Environment, Air Quality Control Branch. AOSERP Report 74. 34 pp.

Bowne, N.E. 1980: Validation and performance criteria-air quality models. Conference pages, pages 614-626. Second joint conference on Application of Air Pollution Meteorology, March 24-27, 1980, New Orleans, American Meteorological Scoeity.

Davison, D.S. and R.B. Lantz 1980: Review of Requirements for air quality simulation models. Prep. for the Alberta Oil Sands Environmental Research Program by INTERA Environmental Consultants Ltd. AOSERP Report 104. 56 pp.

Gifford, F.A. 1976: Atmospheric dispersion models for environmental pollution applications. Chapter 2, pages 35-58. Lectures on air pollution and environmental impact analyses, American Meteorological Society, Boston, Mass.

Gifford, F. and S.R. Hanna. 1975. Modeling urban air pollution. Discussions Atmospheric Environment 9, 267-270.

Hanna, S.R. 1973. Urban air pollution models--why? ATDL, Oak Ridge, Tennessee. Presented at Nordic Symposium on Air Pollution Modelling, October 3-5, 1973. Vedbeek, Denmark.

Holcomb Research Institute. 1978. Environmental modelling and decision making, the United States experience. Report for the Scientific Committee on Problems of the Environment. Praeger Publishers, New York.

Roberts, J.J. 1977. Report to the U.S. EPA of the specialists conference on the EDA modeling guideline. Argonne National Laboratory, Chicago.

Rote, D.M. 1976. Current uses and requirements for air quality models. Argone National Laboratory. Prepared for NATO/CCMS Expert Panel on Air Quality Simulation Modeling.

Rote, D.M., K.L. Brubaker, A.E. Smith, R.R. Cirillo, and J. McHenry. 1977. Methodology for evaluating air quality modeling approaches for particular applications. Proceedings of 4th International Clean Air Congress, Japanese Union of Air Pollution Prev. Association. Tokyo, Japan.

Stern, A.C. 1970. The utilization of air pollution models. Chapter 13, pages 13-1 to 13-8. Proceedings of Symposium on Multiple Source Urban Diffusion Models. U.S. Environmental Protection Agency, Research Triangle Park, N.C.

Tucker, G.B. 1976. Research and services: differing attitudes within the science of meteorology. Weather 31, 104-112.

Turner, D.B. 1979. Atmospheric dispersion modelling-a critical review. J. Air Pollution Control Association 29, 502-519.

Venkatram, A. 1980. Model predictability with reference to concentrations associated with point sources. Conference pages, pages 658-662. Second joint conference on Applications of Air Pollution Meteorology, March 24-27, 1980, New Orleans, La., American Meteorological Society.

# MIXED LAYER STATISTICS DISPERSION MODEL

by

C.S. Matthias
Atmospheric Environment Service
Downsview, Ontario, M3H 5T4

Abstract: This model calculates the range of hourly-averaged ground-level concentrations at a point beneath the plume centerline for each season of the year. The results are presented as seasonal and annual cumulative frequency distributions for a given downwind distance. They can be used to estimate the probability of exceeding a given concentration within an arbitrary time period within a given compass sector, or to estimate the highest, second highest, etc., hourly concentrations likely to be experienced within any sector during any time period.

The model is deterministic, using a Gaussian equation to calculate concentrations, and using climatological mixed layer data describing wind speeds and maximum mixing heights. Incorporated in the model are sub-models describing the diurnal variation of surface heat flux, surface shear stress, mixing height, turbulence intensity, and stability class. The use of mixed layer data generated from the sparse radiosonde network across Canada makes the model more suitable for elevated plumes rather than for surface plumes. The model may be applied to a variety of seasonal and surface conditions.

## INTRODUCTION

The Mixed Layer Statistics Dispersion Model (MLSDM) is designed to estimate the higher hourly-averaged surface concentrations during a season or a year downwind from a single point source. The meteorological data requirements are modest and consist of the joint frequency distribution of maximum mixing heights $z_{max}$ versus mixed layer wind speeds U for the required time period (season or year). These have been generated for each radiosonde station in Canada and in the northern United States. Although they form a sparse data set across the country, mixed layer properties do not in general vary too strongly from one radiosonde station to another and are strongly linked to the geostrophic flow. Surface winds on the other hand are strongly linked to the highly variable surface characteristics. For this reason, MLSDM is most suitable for application to elevated plumes rather than to surface plumes. No distinction need be made at large downwind distances when the plume thickness is comparable to the mixed layer height.

MLSDM is a model in which both the meteorology and the diffusion processes are modelled. For each U, $z_{max}$ combination, the mixing height $z_i$ is allowed to vary between $z_{min}$ and $z_{max}$ during a 24 hour period. A Gaussian dispersion model then calculates the ground-level concentrations at each hour of the day at a receptor located beneath the plume centerline. The concentration calculations will therefore always exceed (or equal) the values experienced at a stationary receptor. Although the results are not comparable to those at a fixed monitor, they are indicative of the highest concentrations experienced somewhere within a sector.

The dispersion curves and stability categories used in Gaussian models have been developed in temperate zones over surfaces of given roughness length and albedo. To use the well-known Pasquill-Gifford-Turner (PGT) scheme, for example, one determines a stability category which depends on meteorological observations and then chooses the corresponding sigma or dispersion curve to use in the Gaussian equation. Strictly speaking, the PGT scheme is most applicable over surfaces having a roughness length of 3 cm, and an albedo comparble to grass (about .15).

To be more general in application, MLSDM uses surface layer and planetary boundary layer similarity relations in order to estimate the lateral turbulence intensity $u_2$ for arbitrary surface roughness and albedo. Near the source, it can be shown that $\sigma_y \approx (u_2/U)\ x$ where $\sigma_y$ is the lateral dispersion coefficient. The ratio $u_2/U$ can be estimated from any set of dispersion curves. By comparing the ratio $u_2/U$ calculated by MLSDM with the ratios estimated from the dispersion curves, the appropriate $\sigma_y$ curve can be chosen. Associated with this $\sigma_y$ curve is a stability class and a vertical dispersion coefficient $\sigma_z$. The dispersion curves used in this report are formulated by Briggs (Gifford, 1975) and are an amalgamation of several dispersion studies.

Another input to the model, besides the surface roughness and the seasonal surface albedo, is the mean seasonal gradient of the morning potential temperature profile. This is the gradient that must be eroded away during the daytime heating hours as the mixed layer grows from $z_{min}$ to $z_{max}$. All these features make the model quite adaptable to a variety of surface and climatic conditions.

The mixed layer is that part of the planetary boundary layer which is bounded below by the earth (or water) and above by a stable layer. It is assumed that first order meteorological variables, such as wind speed, wind direction, and potential temperature, are reasonably uniform with height within the mixed layer. This assumption is a good one on sunny days when there is a large sensible heat flux upwards from the surface. The mixed layerbecomes less uniform as the heat flux diminishes but is still a useful concept since the height to which significant turbulence extends can be estimated for stable and neutral flows as well as for unstable flow. The availability of maximum mixed layer heights along with wind statistics which are representative of regional flow provide a data set well suited for regional diffusion calculations of elevated plumes.

The complete model consists of several sub-models which describe a Gaussian concentration distribution, plume rise, plume depletion, mixing height development, surface heat flux development, atmospheric turbulence, characteristic plume thickness or sigma curves, and stability class determination. The model is subject to the limitations of all Gaussian plume models, which require, ideally, homogeneity and stationarity of meteorological conditions, and level terrain having uniform roughness.

MLSDM is currently being run on an interactive computer system in which a series of questions is put to the user requesting information on the emission characteristics, pollutant depletion rates, surface characteristics, and meteorology. The meteorological information is prepared ahead of time for the region of interest and is stored on a data file. This meteorological input is derived from percentage joint frequency distribution (JFD) tables of daily mixed layer wind speed U, wind direction $\alpha$, and maximum mixing height $z_{max}$. This analysis is discussed in more detail in a report by Protelli (1977).

After receiving all the input information, the program begins computations. To calculate hourly concentrations at a downwind distance x, the Gaussian plume formula needs hourly values of wind speed, sigmas, and mixing height. Since we are not using actual sequential hourly meteorological data, the program must model the above hourly variables for each day that we anticipate to find in each season.

Consider a certain combination of U and $z_{max}$ from the JFD table for a given season. The table gives the percent frequency of occurrences of days during the season that have this U - $z_{max}$ combination. These joint frequencies have been prepared by summing over all directions. Ideally, we should use the joint frequencies for a particular direction. Since these are not available, we will assume that the JFD is independent of direction. Considering all the sources of uncertainty that feed into the dispersion model, this is probably not a bad assumption.

For a given season, we pick the mid-point in days in order to establish the sunrise and sunset times for a mean day. The mixed layer wind speed is assumed to remain constant for the entire day. Wind direction diurnal variability does not affect the present model since the receptor is always located beneath the plume centerline. The mixed layer height is assumed to vary monatonically from a minimum value established during thenight to the maximum value $z_{max}$ at one hour before sunset. After calculating the concentration for 24 successive hours in the day defined by a given U-$z_{max}$ combination, the results are stored.

This process of calculating hourly concentrations is repeated for each of the different U-$z_{max}$ combinations within the season. Then the concentrations are ordered and counted so as to form a cumulative frequency distribution (CDF). When plotted on a graph, the CFD indicates the frequency with which a given concentration is exceeded.

This process is repeated for each season. Lastly, all the results are combined to form an annual CFD.

Briefly then, the model simulates a single point source operating continuously for a year under a variety of meteorological conditions as described by joint frequency distribution tables of wind speed and maximum mixing heights. Hourly concentrations are calculated for each season and are arranged into seasonal and annual frequency distribution tables and cumulative frequency distribution tables. The concentrations are calculated at any given downwind distance x and for an unspecified angular location. The CFD's can be used to estimate 1) the frequency with which a concentration is exceeded and 2) the highest, second highest, etc., concentrations to be experienced within a given time period within a given compass sector.

Although the model uses statistical or climatological data as input, it is a deterministic model since the concentrations are calculated directly using a Gaussian equation rather than inferred from a statistical formula. Depletion of the plume is described by a constant dry deposition velocity $v_d$ and a constant first order chemical decay rate $k_c$. Wet deposition is not considered since the model does not employ any rainfall statistics at present.

## THE GAUSSIAN MODEL

The standard Gaussian bi-normal equation is used for all calculations (Turner, 1970). When used under conditions of limited mixing (i.e., dispersion in the vertical direction is limited by an elevated stable layer), an infinite series expansion may be used (Turner, 1970,). It has been found that a truncated expansion may be used as long as $\sigma_z < z_i$, and the limited mixing equation for $\sigma_z > z_i$, resulting in a maximum deviation of 2% from the exact solution. These two equations, written so as to give the ground level concentration beneath the plume center-line, are;

$$C = \frac{D\,Q}{\pi U \sigma_y \sigma_z}\left[\exp\left(-\frac{h^2}{2\sigma_z^2}\right) + \exp\left(-\frac{(h-2z_i)^2}{2\sigma_z^2}\right) + \exp\left(-\frac{(h+2z_i)^2}{2\sigma_z^2}\right)\right] \quad (\sigma_z < z_i) \qquad (1)$$

$$C = \frac{D\,Q}{(2\pi)^{1/2}\, U \sigma_y z_i} \quad (\sigma_z > z_i) \qquad (2)$$

where

$$D = \exp\left(-\frac{k_c x}{U} - \frac{v_d x}{U z_i}\right)$$

where C is the concentration, Q is the source strength, $v_d$ is the dry deposition velocity, $k_c$ is the chemical decay rate, $\sigma_y$ and $\sigma_z$ are the horizontal and vertical standard deviations of the plume concentration distributions, h is the height of the plume centerline, and $z_i$ is the mixed layer height. These equations are used only if the plume is within the mixed layer, this condition being defined by $h < z_i$. If $h > z_i$ the plume is assumed to be trapped within the elevated stable layer, resulting in zero concentration levels at the ground. There is no treatment of partial trapping in which some plume material is above, and some below, the mixing height $z_i$. This results in a dearth of low concentration calculations, and an unrealistic tail at the low concentration end of any cumulative frequency distribution (CFD).

The plume height h is the sum of the stack height $h_s$ and the plume rise $\Delta h$. The dispersion coefficients $\sigma_y$ and $\sigma_z$ are expressed as functions of downwind distance x. These are discussed in later Sections.

PLUME RISE

Effluents are often emitted into the atmosphere with a finite vertical velocity and a temperature in excess of the ambient value. These effects cause the plume to rise a distance $\Delta h$ above the physical source height $h_s$. There are many competing expressions to represent the plume rise and they all exhibit considerable scatter when compared with measured data.

The plume rise expressions depend upon whether the atmosphere is unstable or stable. For unstable conditions (and for neutral stability), we use the Briggs formula (1971) for height of final rise occurring at a downward distance 3.5 $x^*$:

$$\Delta h = 1.6 \frac{F^{1/3}}{U} (3.5 x^*)^{2/3} \tag{3a}$$

where

$$\begin{aligned} x^* &= 14 F^{5/8} \text{ (m)} \qquad F < 55 \text{ m}^4 \text{ s}^{-3} \\ &= 34 F^{2/5} \text{ (m)} \qquad F > 55 \text{ m}^4 \text{ s}^{-3} \end{aligned} \tag{3b}$$

$$F = \frac{g V_s d_s^2}{4} \frac{(T_s - T_a)}{T_s} \tag{3c}$$

were F is the buoyancy flux from the stack, g is the gravitational acceleration, $V_s$ is the stack exit velocity, $d_s$ is the exit diameter, $T_s$ is the exit temperature, and $T_a$ is the ambient temperature at the stack exit.

If the source is emitting into a stable atmosphere, the Briggs plume rise formula is given by;

$$\Delta h = 2.4 \left(\frac{F}{US}\right)^{1/3} \tag{3d}$$

where

$$S = \frac{\gamma g}{T_a} \tag{3e}$$

where $\gamma$ is the gradient of the ambient potential temperature.

The circumstances under which these are used are as follows. Typically, during the daytime, we have an unstable, surface-heated mixed layer of height $z_i$. This requires the use of Equation (3a). If h exceeds $z_i$, the plume is assumed to be totally trapped in the elevated stable layer, contributing no pollution to the surface.

Typically, during the nighttime, we have a statically stable or positive potential temperature gradient extending to the surface. However, there still exists a mixed layer whose height $z_{min}$ is determined by the height to which shear-generated turbulence is generated. For these statically stable conditions, Equation (3d) is used. If h exceeds $z_{min}$, the plume is assumed to be totally trapped in the elevated dynamically stable layer.

SURFACE HEAT FLUX

Since the climatological input meteorological data represent daily mean conditions, a diurnal model is required to supply hourly conditions. No attempt is made to model a non-homogeneous or non-stationary atmosphere such as in a baroclinic atmosphere or during a frontal passage. It is assumed that the wind speed, the cloud cover, and the air mass remain the same during a 24 hour period. These conditions permit a uniform variation of solar radiation input R during the day, which in turn leads to a smoothly varying vertical heat flux H from the surface.

Although an accurate determination of H requires a surface heat budget model, there is sufficient data to show that the daytime variation of H from a dry surface is approximately sinusoidal, and the nighttime heat flux is downwards and constant (Wyngaard, 1973). The condition of a clear sky that leads to a large daytime heat flux will permit maximum surface radiation loss at night, leading to a large nighttime negative heat flux. The nighttime heat flux will be of opposite sign and in general, proportional to the daytime maximum heat flux $H_o$. The variation can be modelled by;

$$H = Ho \sin \frac{\pi t}{2\tau} \qquad \text{(during daylight)} \tag{4a}$$

$$= -\beta \, Ho \qquad \text{(at night)} \tag{4b}$$

Hence $\beta$ is taken as .1. Measurements indicate that there is a time lag between the time of sunrise and positive heat flux (upwards) and between the termination of positive heat flux and sunset. The time lag is frequently of the order of 1 hour. Therefore if t' is the time of day, and $t_{rise}$ and $t_{set}$ are sunrise and sunset times, then $\tau = t_{set} - t_{rise} - 2$ and $\tau = t' - t_{rise} - 1$ (times in hours).

These heat flux estimates are required in order to determine the lateral turbulence intensity $u_2$, which allows an appropriate sigma curve to be chosen. They are also used to determine the minimum mixed layer height which is maintained at night by mechanical turbulence.

## DAYTIME MIXING HEIGHT

The mixing height varies each day from a minimum value $z_{min}$ estabished at night to a maximum value $z_{max}$ during the day. The minimum value at night is the height above which turbulence, generated by wind velocity shear, falls to some arbitrarily small value. If there is no sunshine, and hence no surface heating during the day, the mixing height will be maintained at the minimum value for the entire day. With surface heating, the mixed layer may grow beyond the minimum value.

In general, as nighttime progresses and as the surface cools, the PBL tends to develop a positive potential temperature gradient throughout. Assume this gradient $\gamma$ to be invariant with height prior to sunrise. Then as the ground temperature $\theta_g$ increases, a turbulent isothermal layer of temperature $\theta_m$ develops and erodes away the positive gradient $\gamma$. In this mixed layer model, the turbulence is intense enough to cause an overshoot in the elevated statically stable air, resulting in downward heat flux into the mixed layer. The downward heat flux is approximately proportional to the surface heat flux and can be given as (Tennekes, 1973);

$$H_i = -A_i H \tag{5}$$

The same paper describes the growth rate of the thermal boundary layer (TBL) as;

$$\frac{\gamma dZ_i}{dt} = \frac{-\gamma H_i}{\Delta\theta} = \frac{d\,(\Delta\theta)}{dt} + \frac{H}{Z_i} - \frac{H_i}{Z_i} \tag{6}$$

Since the temperature jump $\Delta\theta$ at the top of the TBL can be written approximately as;

$$\Delta\theta = f_o \gamma Z_i \tag{7}$$

Equations (5), (6), and (7) can be re-written as;

$$\frac{dZ_i}{dt} = \frac{H}{\gamma Z_i\ (1-2f_o)} \tag{8}$$

$$A_i = \frac{f_o}{1-2f_o} \tag{9}$$

Using the sinusoidal heat flux of Equation (4a), Equation (8) can be integrated to give;

$$Z_i^2 = \frac{4H_o\ \tau}{\pi\gamma(1-2f_o)}\ \left(1-\cos \frac{\pi t}{2\tau}\right) \tag{10}$$

The maximum height of the TBL occurs when $t = 2\tau$, and is given by;

$$Z_{max}^2 = \frac{8\ H_o\tau}{\pi\gamma(1-2f_o)} \tag{11}$$

If the surface heating is so weak that the TBL does not grow as high as $z_{min}$ established during the night by mechanical turbulence, then the mixing height $z_i$ remains constant all day and is equal to $z_{min}$.

If the surface heating is strong enough so that $Z_i$ exceeds $z_{min}$ at some time, then the mixing height $z_i = Z_i$ from that time until near sunset. More generally;

$$z_i = \text{Max}\ (Z_i,\ z_{min}) \tag{12A}$$

$$z_{max} = \text{Max}\ (Z_{max},\ z_{min}) \tag{12b}$$

If we refer back to Portelli (1977), we find that the maximum mixing heights which he determined, and which form part of the JFD data input, are also thermal boundary layer heights. Hence, Equation (11) can be conveniently used with the JFD maximum mixing height values to determine the maximum heat flux $H_o$. An estimate of $H_o$ is necessary in order to calculate $z_{min}$ and turbulence intensities, which are done in succeeding sections.

The value of $f_o$ can be taken as .14 (Tennekes, 1973). A mean potential temperature gradient $\gamma$ can be calculated from the monthly average temperatures of radiosonde ascents, and averaged further to give a seasonal $\gamma$. It has been found quite suitable to calculate a monthly $\gamma$ from temperature and height data at 800 mb and 950 mb to give.

$$\gamma = \frac{\theta_{800} - \theta_{950}}{Z_{800} - Z_{950}}$$

In reality, $Z_{max}$, $H_o$, and $\gamma$ all vary from day to day. The gradient $\gamma$, however, is represented by the seasonal mean value, allowing $H_o$ to be calculated using Equation (11) for each $z_{max}$ of the JFD input. There is a limiting value of $H_o$, which is determined by the solar radiation input R when the sun is at its maximum solar angle $\theta_{max}$ (noon) during clear skies. Using expressions form Briggs (1975) and Duffie (1974), we have;

$$R_{max} = 2/3\ S \sin \theta_{max} (1 - a_s) \tag{14a}$$

$$\theta_{max} = 90 - \phi + \delta \text{ (deg.)} \tag{14b}$$

$$\delta = 23.45 \sin\left(\frac{360}{365} (284 + n)\right) \text{ (deg)} \tag{14c}$$

$$H_{o_{max}} = .55\ R_{max} \tag{14d}$$

where the solar constant $S = 1.05°K\ m\ sec^{-1}$, $\phi$ is the latitude, $\delta$ is the solar declination angle, $a_s$ is the surface albedo, and n is the number of the day of interest in the year, beginning with January 1 as 1. The units of the solar constant, commonly used in atmospheric physics, are derived by dividing watts per square meter by $\rho C_p$, the product of atmospheric density and specific heat. Since $H_o$ as calculated from Equation (11) is not permitted to exceed $H_{o_{max}}$ given by Equation (14d), then for each $z_{max}$,

$$H_o = \text{Min } (H_o \text{ from Equation 11, } H_{o_{max}}) \tag{15}$$

NIGHTTIME MIXING HEIGHT

Well before sunset, the mixed layer should still be growing, with the rate of growth tending towards zero. About 1 hour before sunset, the surface heat flux H changes sign and becomes negative, flowing from the atmospheric surface layer into the soil. The heat flux falls quickly to its minimum value and remains fairly constant all night.

When H becomes negative, there is no further thermal turbulence to support the mixed layer at its present height. As the turbulence aloft dissipates, a mixed layer of shallower depth is still maintained by mechanically generated turbulence (assuming the day had been sunny with moderate winds). Mixed layer properties continue to evolve during the night as surface temperatures continue to fall. However the depth of the turbulence seems to remain fairly constant (Mahrt et al, 1979). Within the model, we will assume that the transition to nighttime conditions is rapid, i.e., $z_i$ transfers from $z_{max}$ to $z_{min}$ in one hour.

The mixed layer adjacent to the surface does not have the same degree of uniformity of wind speed, wind direction, and turbulent mixing as does the unstable daytime mixed layer. In order to utilize the Gaussian formula, we must assume that there is some mean height, mean turbulence, and mean wind speed that will give reasonable agreement between measured and modelled results. A typical means of choosing the mixed layer or boundary layer height is to define it as the height at which some variable of interest drops to 10%, or 5%, or 1% of the value it has at the surface. For the present model, it is taken as the height at which the shear stress u'w' falls to $e^{-1}$ or .37 of its surface value. The stress profiles which are used are taken from a theoretical study of the stable boundary layer by Businger and Arya (1974). Although the solutions were found numerically, a good analytical fit which describes the variation of stress versus height for $T_x > .05$ is given by;

$$z = -\frac{u_* k \, T_x^{\alpha} \, \ell n \, T_x}{f \, B_*} \qquad (16)$$

where

$$B_* = 1.21 \; \mu^{1/2} + 1.2$$

$$\mu = \frac{u_*}{fL} \qquad (16b)$$

$$L = -\frac{u_*^3 \, T_a}{k \, g \, H} \qquad (16c)$$

$$T_x = -\frac{\overline{u'w'}}{u_*^2} \qquad (16d)$$

$$f = 2\Omega \sin \phi \qquad (16e)$$

In these expressions, $u_*$ is the friction velocity, $\mu$ is a stability parameter, L is the Monin Obukhov length, $T_a$ is the ambient temperature, f is the Coriolis parameter, $k = .35$ (von Karman constant), $\Omega = 7.29 \times 10^{-5}$ radians per second (earth's rotational speed), $g = 9.81 \text{ m sec}^{-2}$ (gravitational acceleration) and $\alpha = .29$ (calibration constant). Defining the nighttime mixed layer height $z_{min}$ as the height at which $T_x = e^{-1}$,

$$z_{min} = \frac{.26 \, u_*}{f B_*} \qquad (17)$$

$$= .22 \, \frac{u_*}{f} \quad (\mu = o\text{:neutral}) \qquad (17a)$$

$$= .21 \left( \frac{u_* L}{f} \right)^{1/2} \quad (\mu >> 1\text{:very stable}) \qquad (17b)$$

The constant .21 in the asymptotic expression given by Equation (17b) is comparable to those determined by other authors: .27, .55, .22, .40 (Rao and Snodgrass, 1979). Their numbers are higher since they are taken from expressions which describe a deeper mixed layer, defined as the height at which $T_x$ is between .1 and .01

In order to use Equation (17) for $z_{min}$, an expression for the friction velocity $u_*$ is required. The friction velocity can be related to the geostrophic wind speed through the use of PBL similarity theory. The geostrophic wind speed is close enough to the mixed layer wind speed u that we can use the latter. The similarity relations, which are expressed in terms of mixed layer variables by Yamada (1976), are

$$u_* = C_u U \tag{18}$$

$$C_u = \frac{k}{\left( \left( \ln \left(\frac{z_i}{zo}\right) - A\right)^2 + B^2\right)^{1/2}} \tag{18a}$$

For unstable conditions ($z_i/L < o$),

$$A = 10.0 - 8.145 \, (1.0 - .008376 \, z_i/L)^{-1/3}$$

$$B = 3.02 \, (1.0 - 3.29 \, z_i/L)^{-1/3}$$

For stable conditions ($z_i/L > o$),

$$A = \begin{cases} 1.888 - .38 z_i/L & \text{for } 0 < z_i/L < 35 \\ -2.94 \, (z_i/L - 19.94)^{1/2} & \text{for } 35 < z_i/L \end{cases}$$

$$B = \begin{cases} 3.02 + .30 \, z_i/L & 0 < z_i/L < 35 \\ 2.85 \, (z_i/L - 12.47)^{1/2} & \text{for } 35 < z_i/L \end{cases}$$

In using Equation (17) and associated equations to calculate $z_{min}$, they must be solved by iteration since the mixing height is contained in the expressions for $u_*$ and $B_*$. At the same time, the nighttime and peak daytime heat fluxes are calculated using Equations (4b) and (11). Equation (18) is used at hourly intervals in the daytime layer in the calculation of turbulence intensities as will be described in the next section.

MIXED LAYER TURBULENCE

In the present model, the lateral component of turbulent velocity, $u_2$, is calculated in order to determine the appropriate stability category and sigma curve. All the components can be expressed concisely using expressions derived from surface layer and mixed layer similarity theory. A surface layer is defined as a layer within which the shear stress u'w' at any height remains fairly close to the surface shear stress value ($T_x = 1$).

At night, or for stable conditions in general (H negative, or L positive), turbulence and shear stress levels decrease with height beyond the surface layer. The nighttime mixed layer, arbitrarily defined as the height at which $T_x = e^{-1}$, is of the same order but slightly thicker than the surface layer. Experiments within the surface layer show that;

$$\frac{u_2}{u_*} = C_2 \qquad \text{(stable)} \qquad (19)$$

where $C_2$ is reasonably constant. Ariel and Nadezhina (1976) compare results of several experiments and find that $C_2 = 1.9 \pm .23$, where .23 is the standard deviation of the estimates.

During the daytime, the PBL generally varies from neutral to convective. The lateral turbulence within the mixed layer is described well by (Panofsky et al, 1977)

$$\frac{u_2}{u_*} = (a_2 - .5 \frac{z_i}{L})^{1/3} \qquad (20)$$

where the Monin-Obukhov length L is negative and where $a_2$ is chosen so as to agree with Equation (19) in the limit of neutrality, i.e., $a_2 = 6.9$.

PLUME SIGMA CURVES

There is unfortunately no single definitive expression for the plume dispersion widths $\sigma_y$ or $\sigma_z$ as a function of easily available meteorological parameters. A commonly-used set of sigma curves is that of Briggs (Gifford, 1975). They are an amalgamation of results of several field experiments having different averaging times and over surfaces of different roughnesses. To apply them, one need only determine the stability class of the atmosphere. The stability condition is a measure of the atmosphere's ability to disperse a plume within a given distance, with A stability causing the most dispersion and F stability causing the least (Turner, 1970). Briggs' curves are given in the table below:

Table 1. Horizontal and Vertical Dispersion Curves for Rural Terrain (Gifford, 1975)

| Stability Category | $\sigma_{yB}$(m) | $\sigma_{zB}$(m) |
|---|---|---|
| A | $.22\ x\ (1 + .0001x)^{-1/2}$ | $.20x$ |
| B | $.16\ x\ (1 + .0001x)^{-1/2}$ | $.12x$ |
| C | $.11\ x\ (1 + .0001x)^{-1/2}$ | $.08x\ (1 + .0002x)^{-1/2}$ |
| D | $.08\ x\ (1 + .0001x)^{-1/2}$ | $.06x\ (1 + .0015x)^{-1/2}$ |
| E | $.06\ x\ (1 + .0001x)^{-1/2}$ | $.03x\ (1 + .0003x)^{-1}$ |
| F | $.04\ x\ (1 + .0001x)^{-1/2}$ | $.016x(1 + .0003x)^{-1}$ |

The most commonly used stability class scheme is that of Pasquill and Turner (Turner, 1970) which requires information describing wind speed, cloud cover, and solar angle. This stability scheme is restrictive in that it relates meteorological conditions to dispersion conditions for a particular type of surface having a roughness and albedo characteristic of short grass. The dispersion curves are capable of more general application since they themselves describe the plume growth as a function of turbulence intensity, wind speed, and Lagrangian time $\tau_L$. Taylor's theory of single particle dispersion in homogeneous turbulence expresses the root-mean-square (RMS) displacement, or sigma, as a product of turbulence intensity and time t from release as given by (Pasquill, 1974),

$$\sigma_y = u_2\, t = \frac{u_2\, x}{U} \qquad (t \ll \tau_L) \tag{21}$$

where the travel time t is small compared to the Lagrangian time scale $\tau_L$. The dispersion equations of Table 1 in the limit of small x are identical in form to Equation (21), allowing us to associate a range of the ratio $u_2/U$ to each stability class. From Table 1, if $u_2/U = .16$ is taken as the mean ratio for stability class B, then the upper and lower limits for B can be arbitrarily assigned as .19 and .135 respectively. Similarily, corresponding $u_2/U$ ratios and stability classes can be determined for the remainder and are given below:

Table 2. Turbulence Ratios $u_2/U$ and corresponding stability categories.

| Stability Category | Turbulence Ratio $\frac{u_2}{U}$ |
|---|---|
| A | $u_2/U > .19$ |
| B | $.19 > u_2/U > .135$ |
| C | $.135 > u_2/U > .095$ |
| D | $.095 > u_2/U > .07$ |
| E | $.07 > u_2/U > .05$ |
| F | $.05 > u_2/U$ |

Within the program, each value of $u_2/U$ is compared with the limits established in Table 2 from which the appropriate stability category and sigma curve are chosen.

This stability class determination scheme is suitable for surfaces of any roughness length $z_o$. The effect of a $z_o$ larger than 3 cm is to increase the turbulence level $u_2$. For meteorological conditions which describe a class D stability category using the Paquill-Turner scheme, the roughness may be large enough to generate a value of $u_2/U$ corresponding to a class C in Table 2. A similar transition to a more stable category can occur if $z_o$ is much smaller than 3 cm.

In the near field, an additonal important factor in plume growth is the turbulence associated with the plume rise $\Delta h$ resulting from plume buoyancy and momentum. The additional spreading can be described as (Hanna et al, 1977).

$$\sigma_{y\,\Delta h} = \sigma_{z\,\Delta h} = .32\ \Delta h$$

Since the plume-rise-generated turbulence and the ambient atmospheric turbulence are independent of one another, the net plume growth can be described by;

$$\sigma_i^2 = \sigma_{iB}^2 + \sigma_{i\,\Delta h}^2$$

where i is either y or z. No additional plume-broadening features are included in the present model.

## CONCLUSIONS

Input to the model consists of stack parameters, surface roughness length, latitude, deposition velocity, reaction rate coefficient, downwind distance x, and a meteorological data file. The latter contains joint frequency distribution information on the mixed layer wind speeds and maximum mixing heights, ambient temperature, albedo, morning inversion strength, and wind direction distribution.

Output from the model for each season consists of 1) the relative frequencies of different stability classes for daytime and nighttime conditions, 2) the frequency distribution, and 3) the cumulative frequency distribution of the range of hourly concentrations.

This model is a mechanism by which the range of variation of hourly concentrations during a season or a year due to a point source can be estimated. The concentrations are measured at ground level below the plume centerline and hence are an estimate of the maximum concentration at any time and downwind distance. The model can be applied to terrain of arbitrary surface roughness and albedo.

The accuracy of the model estimates has not yet been determined. After first relating the ground-level, plume-centerline concentrations to fixed monitor concentrations, it is hoped that the model evaluation can be done in the near future.

## ACKNOWLEDGEMENT

I would like to express my sincere appreciation to Dr. A. Venkatram for his informative discussions on the physics of mixed layer development.

REFERENCES

Ariel, N.Z., and Y.D. Nadezhina 1976: "Dimensionless turbulence characteristics under various stratification conditions," Izv., Atmospheric and Oceanic Physics, 12, 802 - 809.

Briggs, G.A. 1971: "Some recent analyses of plume rise observation," Proceedings of the Second International Clean Air Congress, Academic Press, New York. 1029 - 1032.

Briggs G.A. 1975: "Plume rise predictions," Lectures on Air Pollution and Environmental Impact Analyses, AMS, Boston, 59 - 111.

Businger, J.A., and S.P.S. Arya 1974: "Height of the mixed layer in the stability stratified planetary boundary layer," Advances in Geophysics, 18A, Academic Press, New York, 73 - 92.

Duffie, J.A., and W.A. Beckmann 1974: "Solar Energy Thermal Process," J. Wiley and Sons, New York.

Gifford, F.A. 1975: "Atmospheric dispersion models for environmental pollution applications," Lectures on Air Pollution and Environmental Impact analyses, AMS, Boston, 35 - 58.

Hanna, S.R., G.A. Briggs, J. Deardorff, B.A. Egan, F.A. Gifford and F. Pasquill 1977: "AMS Workshop on stability classification schemes and sigma curves - summary of recommendations," Bull. Amer. Meteor. Soc., 58, 1305 - 1309.

Holzworth, G.C. 1964: "Estimates of mean maximum mixing depths in the contiguous United States," Mon. Wea. Rev., 92, 235 - 242.

Mahrt, L., R.C. Heald, D.H. Lenschow, B.B. Stankov, and I.B. Troen 1979: "An observational study of the structure of the nocturnal boundary layer," Boundary Layer Meteor. 17, 247 - 264.

Panofsky, H.A., H. Tennekes, D.H. Lenschow, and J.C. Wyngaard 1977: "The characteristics of turbulent velocity components in the surface layer under convective conditions," Boundary Layer Meteor., 11, 355 - 361.

Pasquill, F., 1974: "Atmospheric Diffusion," 2nd ed., J. Wiley and Sons, New York, 429.

Portelli, R.V. 1977: "Data on Mixing Heights, Wind Speeds, and Ventilation Coefficients for Canada," Climatological Studies No. 31, Atmospheric Environment Service, Department of the Environment, Canada.

Rao, K.S., and H.F. Snodgrass 1979: "Some parameterizations of the nocturnal boundary layer," Boundary Layer Meteor., 16, 15 - 27.

Tennekes, H. 1973: "A model for the dynamics of the inversion above a convective boundary layer," J. Atmos. Sci., 30, 558 - 567.

Turner, D.B. 1970: "Workbook of Atmospheric Dispersion Estimates," U.S. Public Health Service Publication, 999 - AP-26, 84 p.

Wyngaard, J.C. 1973: "On surface layer turbulence," Workshop on Micrometeorology, AMS, Boston, 392 p.

Yamada, T. 1976: "On the similarity functions A,B and C of the planetary boundary layer," J. Atmos. Sci., 33, 781 - 793.

# CROSSWIND DISPERSION FUNCTIONS OVER SUBURBAN TERRAIN FROM TURBULENT ENERGY SPECTRA VIA THE STATISTICAL THEORY OF DIFFUSION

by

D. G. Steyn
Department of Geography
The University of British Columbia
Vancouver, B.C., V6T 1W5

Abstract: The nondimensional crosswind dispersion function $S_y(t^*) = \sigma_y/\sigma_v t$ may be detemined directly from the statistical theory of diffusion if the form of the Eulerian turbulent energy spectrum is know. Such an analysis has been applied to empirically determined spectra from an unstable suburban surface layer, the resulting dispersion function having the form: $S_y(t^*) = (1.0 + 0.16\sqrt{t^*})^{-1}$ .
This function is shown to be consistent with previously estimated forms.

## INTRODUCTION

The spread of pollutants in turbulent flows is intimately linked to the turbulence. This spread may be conveniently represented by a non-dimensional dispersion function $S_y=\sigma_y/\sigma_v t$ (Pasquill (1971), Hanna et. al. (1977), Randerson (1979) for crosswind spread) where $\sigma_y$ is the standard deviation of crosswind material distribution, $\sigma_v$ is the standard deviation of the crosswind velocity component and t is the travel time. This dispersion function must depend on travel time (Pasquill (1974), Pasquill (1975), Draxler (1976) and Sawford (1979)) and atmospheric stability (Doran and Horst (1978) and Steyn (1981a)). This last mentioned work shows how the statistical theory of diffusion with the Hay-Pasquill form of the Eulerian-Lagrangian transform applied to turbulence spectra in nondimensional frequency space results in Sy depending on $t^* = t\sigma_u/z$ where $\sigma_u$ is the standard deviation of the alongwind component and z is the height at which diffusion is taking place. This method produces stability dependent dispersion functions when applied to stability dependent spectra (Steyn, 1981a).

The present study will apply the method of Steyn (1980, 1981a) to turbulent spectra measured over suburban terrain under unstable conditions (Steyn, 1981b) in order to derive Sy(t*) for those atmospheric conditions. Currently, applications of the Gaussian plume model over urban or suburban surfaces are based on, at best, the tentative Pasquill-Gifford curves for urban surfaces (Gifford, 1976) or the same curves as derived from flat-land tracer observations.

## COMPUTATION OF THE DISPERSION FUNCTION

Steyn (1981a) showed that Sy(t*) may be derived from the Eulerian crosswind spectral function $\Phi_{v,E}$ by performing the integration of:

$$S_y^2(t^*) = \int_0^\infty \Phi_{v,E}(f)\,\{\sin(2\pi f t^*)/(2\pi f t^*)\}^2\,df \tag{1}$$

where f is the nondimensional frequency. This form is in general not amenable to integration in a closed form, but presents no problems to numerical quadrature routines. Numerical integration will require tabulated values of the chosen spectral function $\Phi_{v,E}$.

A recent study of atmospheric turbulence in an unstable surface layer over a suburban surface (Steyn, 1980 and Steyn 1981b) has provided a fairly complete knowledge of turbulent energy spectra under these conditions. Of interest in this context is the spectrum of the crosswind component, (Fig.1) which exhibits a somewhat broad peak and distinct rolloff at both high- and low-frequency ends. The shading indicates the range of amplitudes encountered, and the dashed roloff at low frequencies indicates the dependence of this spectral region on atmospheric stability. The range of stabilities represented by this spectrum is $-0.2 < z/L < -140$ where L is the Monin-Obukhov stability length, but the details of stability dependence within this range were obscured by scatter in the data (Steyn, 1981b).

In order to determine Sy(t*) from Eq. (1) with this spectral function, the curve was digitized at 50 uniformly spaced points in log space, multiplied by the sampling function appropriate to the travel time being considered, and the integration performed with a standard numerical quadrature package. Integrals of Eq. 1 were determined every three units of t* from 1 to 150. This upper limit corresponds to a travel time of 60 min (the length of the time series used to derive Fig.(1)) and a $\sigma_u$ of 0.8 m s$^{-1}$ at z = 20 m (representative of the conditions encountered.)

The crosswind dispersion function determined in this way is shown as curve a on Fig.(2). The integral of the spectrum shown in Fig.(2) is 0.950, indicating a 5% loss of total variance. This loss is assumed to occur at the low-frequency end, where the cutoff is only half an order of magnitude below the peak amplitude, while the high-frequency cutoff is two orders of magnitude down. To correct this, the spectrum was extended linearly (in log-log space) to an amplitude of -1.75 at a frequency of -4.00. This extension results in an increase of the spectral integral to 1.002. The crosswind dispersion function corresponding to this extended spectrum is shown as curve b in Fig.(2). Further low frequency extension of the spectrum produces very little change in the shape of Sy(t*).

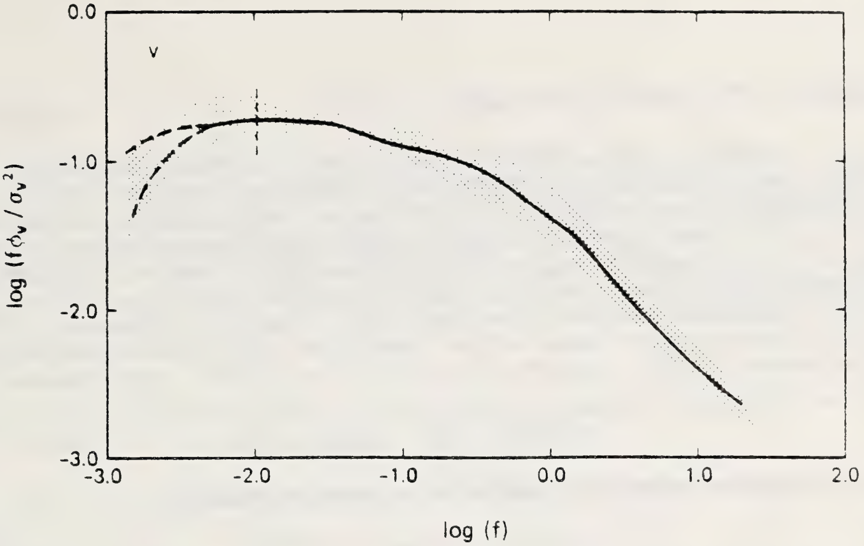

Figure 1. Turbulent energy spectrum of crosswind component in unstable atmospheric conditions over a suburban surface from Steyn (1981b).

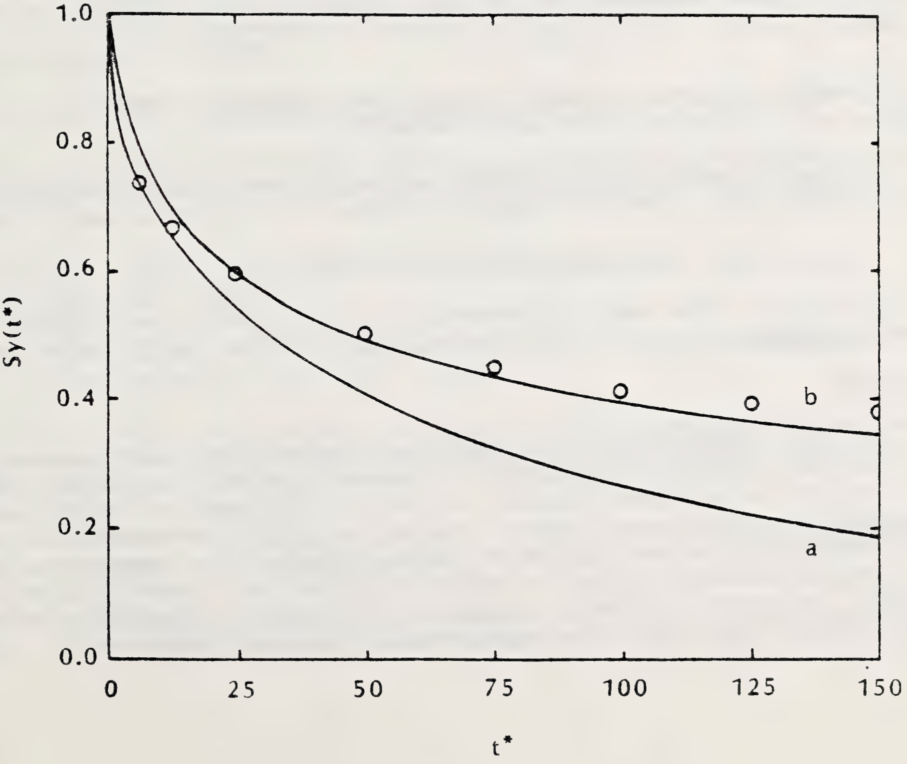

Figure 2. Crosswind dispersion function. Points are Draxler's (1976) function. Curve b is for the extended spectrum.

## COMPARISON WITH PREVIOUS ESTIMATES OF Sy(t*)

Draxler (1976) compiled a large body of data representing tracer studies over a wide range of atmospheric conditions, and was able to fit a single function to the widely scattered data, thus deriving a form for Sy. Sawford (1979) used a method closely related to the present one to derive a form for Sy that agrees well with Draxler's (1976) results. Neither of the two above authors derive an internal scaling time such as $t_s$ or the closely related Lagrangian integral time scale ($t_L$) suggested by Pasquill (1971), but scale their travel times by the time after which the dispersion function has decreased to 0.5. From Fig.(2), S(47.17) = 0.5000, which means that

$$t_i = 47.17\ t_s \qquad (2)$$

Using Eq. (2) to transform Draxler's recommended function

$$S(t/t_i) = (1.0 + 0.9\sqrt{t/t_i})^{-1}$$

at selected points produces the symbols shown on Fig. 2. The agreement between these points and curve b is excellent, with only very slight relative skewing. It must be emphasized that $t_i$ is an entirely artificial time, and Draxler's (1976) and Sawford's (1979) attempts to relate it to $t_L$ serve only to highlight its inadequacy in this context. Their relationships between $t_i$ and $t_L$ result in unrealistically large values for $t_L$ and are unable to show any of the known stability dependence of $t_L$. The scaling time $t_s$ suffers from none of these disadvantages and can be shown (Steyn, 1981a) to be related to $t_L$ by:

$$t_s = 1.58\ t_L\ .$$

The Lagrangian integral time scale is the most appropriate scale in this context, but is in general not easily measured.

Least squares fitting techniques may be used to show that curve b in Fig. 2 fits very closely the analytic form

$$Sy(t^*) = (1.0 + 0.16\sqrt{t^*})^{-1}$$

This form has the advantage of preserving the long travel time parabolic asymptote suggested by the Taylor theory, and is easy to apply operationally.

## CONCLUSION

This analysis has shown that the crosswind dispersion function Sy(t*) may be determined from extended crosswind spectral functions. The form of Sy(t*) is strongly dependent on the spectral shape at low frequencies, particularly for long travel times. The form of Sy(t*) presented here is in agreement with previously presented forms, but should be regarded as tentative until further knowledge of low frequency spectra allows a more detailed re-analysis. The method presented is capable of producing a dispersion function for any surface type, given the representative spectral function.

## ACKNOWLEDGEMENTS

This work formed part of my doctoral studies under the able guidance of Dr. T. R. Oke. Research grants by the Natural Science and Engineering Research Council of Canada and a Scientific Subvention from the Atmospheric Environment Service of Environment Canada funded the field work. I was personally supported by a Killam Predoctoral Fellowship and latterly a Killam/ N.S.E.R.C. Postdoctoral Fellowship from The University of British Columbia.

## REFERENCES

Doran, T.C., and T.W. Horst, 1978: Variations in measured values of lateral diffusion parameters. J. Appl. Meteor., 17, 825-831.

Draxler, R.R., 1976: Determination of Atmospheric Diffusion Parameters. Atmos. Env., 10, 99-105.

Gifford, F.A., 1975: Atmospheric Dispersion Models for Environmental Applications. In Lectures on Air Pollution and Environmental Impact Analyses, ed. D.A. Haugen, Amer. Meteorol. Soc., Boston, Mass.

Hanna, S.R., G.A. Briggs, J. Deardorff, B.A. Eagen, F.A. Gifford and F. Pasquill, 1977: A.M.S. Workshop on Stability Classification Schemes and Sigma-curves Summary of Recommendations, Bull. Amer. Meteorol. Soc., 58, 1305-1309.

Pasquill, F., 1971: Atmospheric Dispersion of Pollution. Quart. J. Roy. Meteorol. Soc., 97, 369-395.

Pasquill, F., 1974: Atmospheric Diffusion (2nd Ed.), Ellis Horwood, 429 pp.

Pasquill, F., 1975a: Some Topics Relating to Modelling of Dispersion in the Boundary Layer, EPA-650. 4-75-015, U.S. Environmental Protection Agency, Research Triangle Park, N.C., 1975.

Randerson, D., 1979: Review Panel on Sigma Computations. Bull. Amer. Meteorol. Soc., 60, 682-683.

Sawford, B.L., 1979: Wind Direction Statistics and Lateral Dispersion. Quart. J. Roy. Meteorol. Soc., 105, 841-848.

Steyn, D.G., 1980: Turbulence, diffusion and the daytime mixed layre depth over a coastal city. Unpublished Ph.D. thesis, The University of British Columbia, Vancouver. 161 pp.

Steyn, D.G., 1981a: Crosswind dispersion functions from turbulence spectra. Submitted to Quart. J. Roy. Meteoro. Soc.

Steyn, D.G., 1981b: Turbulence in an unstable surface layer over suburban terrain. Submitted to Boundary Layer Meteor.

# THE APPROPRIATE CHOICE OF $\sigma_Z$ AND $\bar{u}$ FOR PREDICTING SURFACE CONCENTRATION USING THE GAUSSIAN MODEL

by

John D. Reid

Air Quality Research Branch
Atmospheric Environment Service
4905 Dufferin Street
Downsview, Ontario, M3H 5T4

Abstract: Predictions of surface concentration resulting from surface and elevated pollution sources obtained with a Monte Carlo dispersion model are interpreted in terms of the Gaussian model parameters $\sigma_Z$ and $\bar{u}$. For neutral stratification $\sigma_Z$ can be made independent of source height if the mean wind speed is chosen as a function of downwind distance, approximately the wind at $0.6\sigma_Z$ or $0.6 *$ source height, whichever is greater. Comparisons with the Brookhaven and TVA experimental results and Briggs curves are given.

## INTRODUCTION

An important question that has to be addressed in air quality assessment modelling is "What is the appropriate mean wind speed to choose in this situation". In fact most problems require a knowledge of more than a single wind speed since wind plays multiple roles. The source strength may be dependent on wind speed as for fugitive dust sources. Near source effects such as plume rise and wake effects are significantly related to wind speed. The stability class parameterizing the turbulence levels and, implicitly, certain wind structure vertical variation, is importantly related to wind speed. Since dispersion is fundamentally a time dependent process wind speed also enters the Gaussian equation for concentration to relate the transit time between source and receptor to their separation. Finally, wind speed may also influence the strength of sinks as it does in disturbing a water surface to change the effective deposition rate.

In general, the appropriate wind speed for each role is different. This paper examines only one aspect, that of $\bar{u}$ appearing directly in the Gaussian equation for concentration.

Consider, for the sake of simplicity, the Gaussian concentration equation applied for crosswind averaging. Surface concentration is given by:

$$C(x) = \frac{A}{\sigma_z \bar{u}} \exp\left(-\frac{h^2}{2\sigma_z^2}\right) \tag{1}$$

where

$A = Q(2/\pi)^{1/2}$

Q is the point source emission rate $[MT^{-1}]$

x is the downwind distance $[L]$

$\bar{u}$ is the mean wind speed $[LT^{-1}]$

$\sigma_z$ is the vertical spread parameter $[L]$

h is the effective source height $[L]$

Note that although this study does not explicitly treat lateral dispersion this is also true of many practical models, for example, the sector averaged CDM and ATDL models.

Inspection of (1) shows that for given A and h the same C value can occur for various combinations of $\sigma_z$ and $\bar{u}$. $\sigma_z$ values for given surface concentration values are only determined when a unique specification for $\bar{u}$ is given. Similarly in applying (1), or any Gaussian model, an unbiased C value can only be calculated if the correct specification for $\bar{u}$ accompanying the $\sigma_z$ curves is employed.

The above fact is frequently overlooked. For example, the Turner workbook instructs on page 7 that "a mean through the vertical extent of the plume should be used, $h - 2\sigma_z$ to $h + 2\sigma_z$, or surface to $h + 2\sigma_z$ if $2\sigma_z > h$." The further comment is made that surface wind values are frequently all that is available and that the surface wind is most applicable to surface or low-level emissions. These comments lack justification. In view of the fact that a substantial effort is often made to produce the "correct" $\bar{u}$ this investigation was undertaken to put on a firmer basis the best selection of $\bar{u}$ in the Gaussian equation.

## THE MONTE CARLO MODEL

It has now been adequately shown that the Monte Carlo technique for predicting dispersion of air pollution gives excellent agreement with observation for vertical dispersion in the atmospheric surface layer for all stabilities; Reid (1979), Wilson et al. (1981 a,b,c). The Monte Carlo technique involves following markers through a statistically correct boundary-layer flow field and computing dispersion from the distribution of these markers. For more detail on the technique readers are referred to the references above.

Extension to the total planetary boundary layer depth, H, required here is hampered by uncertainty as to profiles of wind, turbulent fluctuations and Lagrangian time scales applicable in the upper PBL. Reid and Crabbe (1980) modelled a neutral PBL by extending the surface logarithmic wind profile throughout the PBL.

$$\bar{u} = \frac{u_\star}{k} \ln \left( \frac{z}{z_0} \right) \tag{2}$$

where $u_\star$ is the friction velocity and $z_0$ the surface roughness length. The standard deviation of vertical velocity, $\sigma_w$ was constant with height,

$$\sigma_w = 1.25\, u_\star \tag{3}$$

A form for the Lagrangian time scale profile,

$$T_L = 0.4 \frac{z}{u_\star} \exp \left( - 3 \frac{z}{H} \right) \tag{4}$$

was selected, where H is set to its Ekman value in this study,

$$H = 0.3\, u_\star / f, \tag{5}$$

and f is the Coriolis parameter. A sensitivity study indicated that for the release heights examined in this study, the exact choice of H, and in fact the entire absence of the exponential term in (4), made little difference to $\sigma_z$ and $\bar{u}$ predictions to ∿10 km downwind of the source.

Figure 1 shows, for neutral stratification and vertical dispersion only, normalized surface concentration against downwind distance for $z_0$ = 3 cm and four different source height, 10, 50, 100 and 150 m. The trend for the maximum concentration to be lower and occur further downwind for more elevated sources is evident.

## CHOICES OF $\bar{u}$ AND $\sigma_z$

The Monte Carlo results for surface concentration together with an appropriate specification for $\bar{u}$ can be entered into (1) which may then be solved numerically for $\sigma_z$. As no *a priori* specification for $\bar{u}$ is available we experiment with various choices.

### Choice A

Suppose, as is commonly assumed, that the appropriate $\bar{u}$ is that at the source height. For an elevated source and given concentration away from the maximum two roots for $\sigma_z$ occur on either side of the maximum.

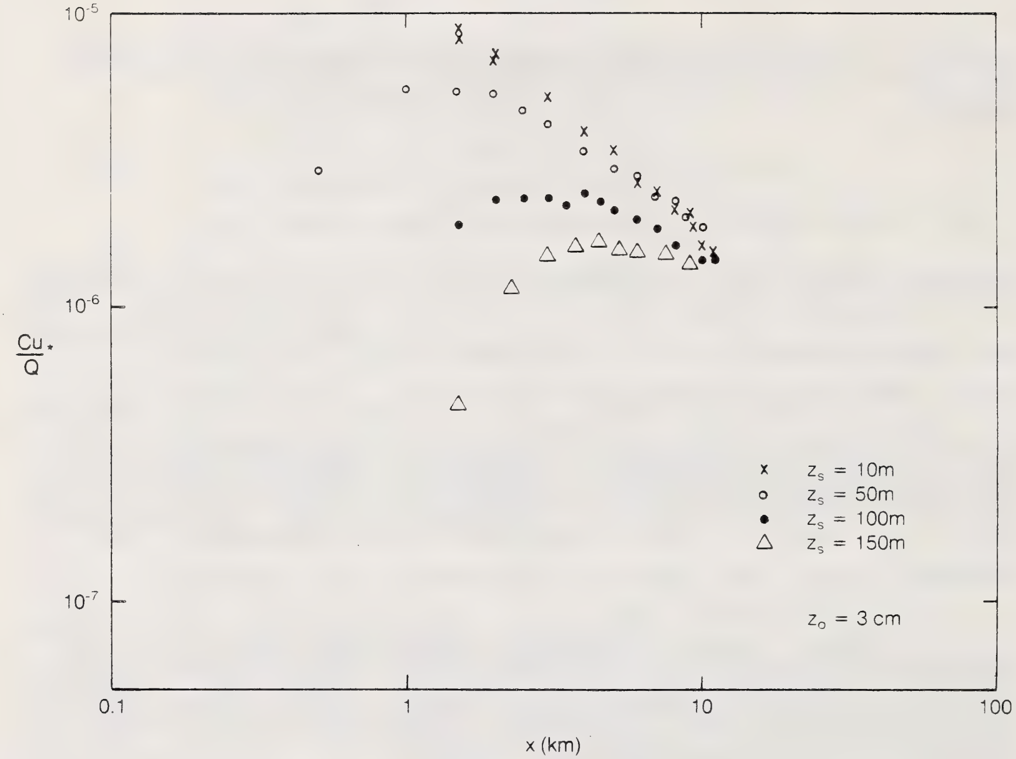

Figure 1: Normalized surface concentration against downwind distance for $z_0$ = 3 cm and four source heights in neutral conditions.

However, for concentrations near the maximum no real roots exist and a gap exists in the resulting $\sigma_z$ vs x curve (fig. 2a). The form of (1) supports a maximum concentration for $\sigma_z = h$ given by:

$$C = \frac{A}{\bar{u}h} \exp\left(-\frac{1}{2}\right) \qquad (6)$$

Choice A for $\bar{u}$ gives $C\bar{u}$ near the maximum larger than $Ah^{-1} \exp\left(-\frac{1}{2}\right)$ and so no real root for $\sigma_z$ can be found.

Choice B

Another assumption commonly used is that the appropriate $\bar{u}$ is that at 10 m, standard anemometer height. This gives real roots for $\sigma_z$ at all concentrations, however a range of $\sigma_z$ values near h are excluded for elevated sources (Fig. 2b) and a discontinuity exists in the $\sigma_z$ vs x curve. The product $C\bar{u}$ never achieves the maximum value $Ah^{-1} \exp\left(-\frac{1}{2}\right)$.

Choice C

Results for the choices above show that a casual selection of $\bar{u}$ can cause problems. To avoid discontinuities and gaps a choice of $\bar{u}$ which gives $\sigma_z = h$ at $C = C_{(max)}$ must be made. Let this $\bar{u}$ be $\bar{u}_c$, the critical windspeed, and the height at which this occurs $h_c$; $h_c$ and $\bar{u}_c$ are related by (2). Using the maximum concentration calculated by the Monte Carlo model for five different source heights figure 3 shows the ratio $h_c/h$, as a percentage, for these five h values. Statistical variations in the Monte Carlo calcuated concentration arise because only a small number of markers were followed. This uncertainty is shown by the error bars. All values of $h_c$ are less than h and greater than 0.2h. In view of the scatter and statistical uncertainty an average $h_c = 0.6h$ is appropriate.

With this selection we are now in a position to compute $\sigma_z$ for various source heights and downwind distances. Figure 4 shows $\sigma_z$'s and their uncertainties 1, 3, 5 and 10 km downwind and for source heights 10, 50, 100, 150 m. Clearly $\sigma_z$'s become progressively more dependent on source height with downwind distance for this choice.

Choice D

It would be convenient if $\sigma_z$ were not a function of source height and examination of figure 4 shows that for this to be the case $\bar{u}$ in the Gaussian equation must increase with downwind distance. Far downwind all memory of the source height must be lost; an appropriate scale height for $\bar{u}$ is then $\sigma_z$ itself. Some experimentation yields the rule; $\bar{u} = \bar{u}\ (0.6h)$ or $\bar{u}\ (0.6\sigma_z)$, whichever is greater. The impact of 10 km is shown in Figure 5, $\sigma_z$ is sensibly independent of source height. These $\sigma_z$'s are the present predictions shown in figures 6 and 7.

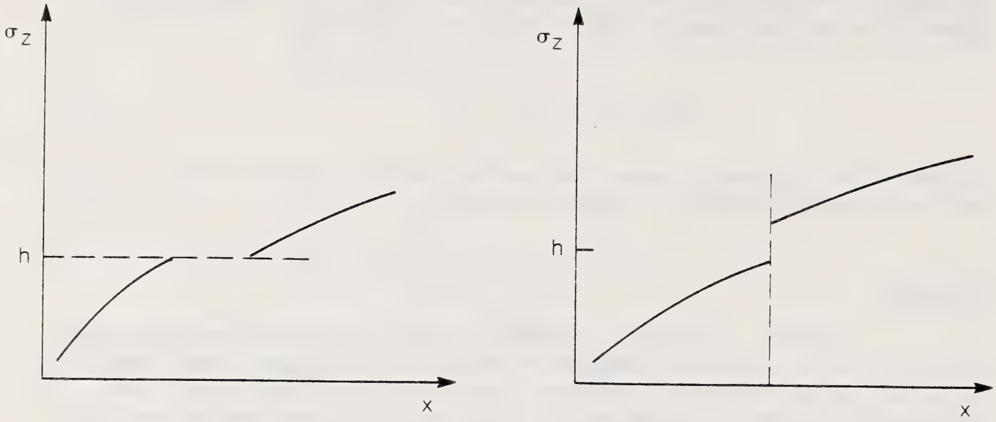

Figure 2a, b: Schematic variation of $\sigma_z$ with downwind distance for choices A and B respectively.

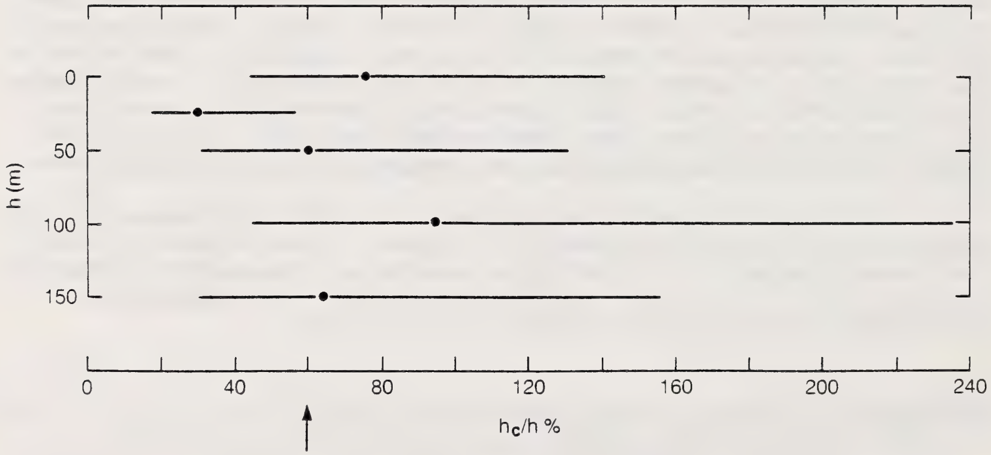

Figure 3: Variation of the height $h_c$ as a percentage of source height for source heights to 150 m. Error bars are the uncertainties owing to a 10% concentration uncertainty. The best estimate of the optimum $h_c/h$ ratio, 60%, is indicated by the arrow.

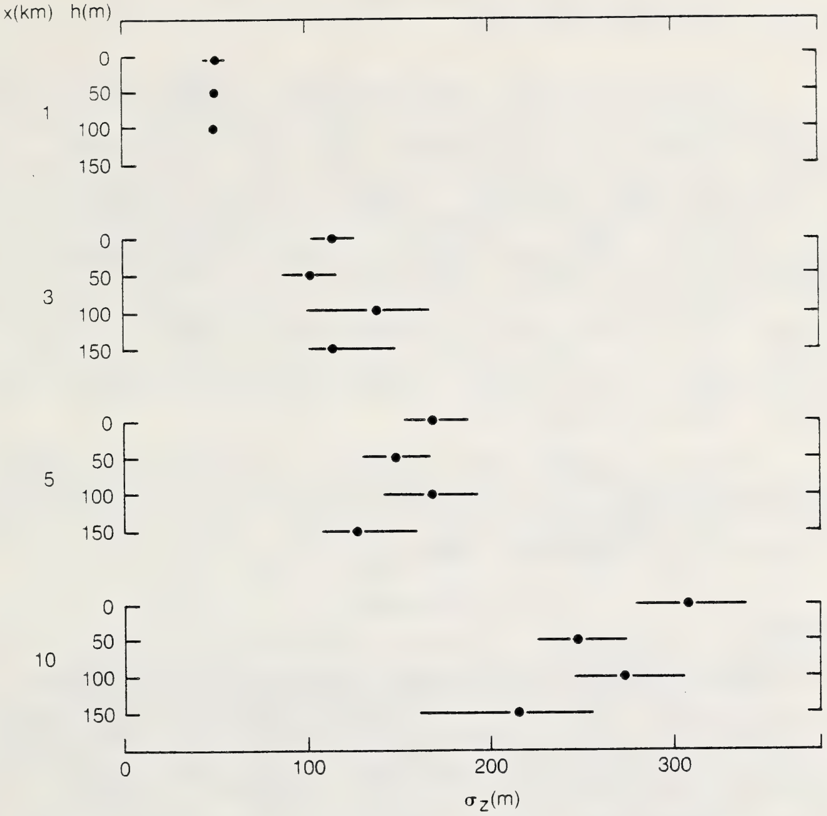

Figure 4: $\sigma_z$ and its uncertainty for downwind distances 1, 3, 5, 10 km and four different source heights with $z_0$ = 3 cm and choice C specification of $\bar{u}$. Note the indication of a systematic trend for $\sigma_z$ to decrease with increasing source height at the further downwind distances.

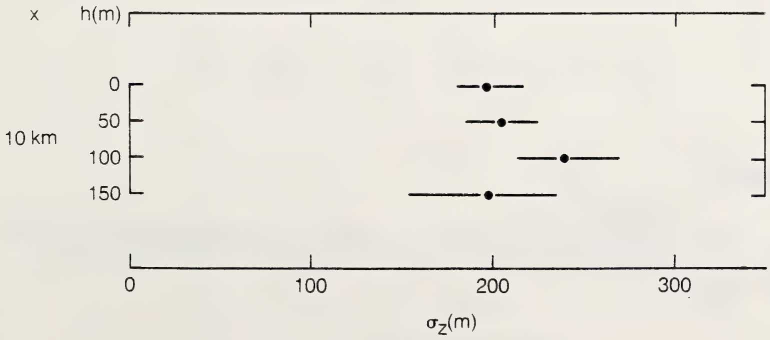

Figure 5: $\sigma_z$ for various source heights at 10 km downwind with choice D specification of $\bar{u}$ and $z_0$ = 3 cm. Note there is no trend for $\sigma_z$ variation with source height.

## COMPARISON WITH OTHER $\sigma_Z$ VALUES

The two most widely recognized sets of experimental data that have yielded dispersion parameters for downwind distances of general industrial interest are the Brookhaven (BNL) and TVA data sets. In addition Briggs has produced interpolation curves for the dispersion parameters which are widely employed. A good review of the above is given by Gifford (1976). Figure 6 compares the $\sigma_Z$ predictions using the Choice D method for selecting $\bar{u}$ and $z_0$ = 3 cm to these standard results. The present predictions are in good agreement with the Briggs (Open Country) curve except at 10 km. The BNL points are substantially above the present curve; note however that the best estimate for $z_0$ at Brookhaven is 1m. The TVA curve is even further above the present curve, and particularly at short range. This is undoubtedly because of the buoyancy of these industrial sources.

Figure 7 compares the standard $\sigma_Z$ results to the present $\sigma_Z$'s using Choice D and $z_0$ = 1m. The present predictions lie between the BNL and TVA data but favoring the TVA. The Briggs (Urban) curve is substantially above any of the other three.

## CONCLUSION

The arguments presented above show that it is important to make an appropriate selection of the mean windspeed $\bar{u}$ in the Gaussian model if unbiased surface concentration estimates are to be obtained. For the neutral stratification conditions investigated, a specification of $\bar{u}$ as that at the height 0.6h or $0.6\sigma_Z$, whichever is greater, is shown to give $\sigma_Z$ independent of source height (h) for h up to 150 m and downwind distance up to 10 km. Figures 6 and 7 compare the $\sigma_Z$ values resulting with standard data and show comprehensible trends. The present $\sigma_Z$ values can be reasonably well represented as power law curves. With $\sigma_Z$ and x expressed in metres:

$$\begin{aligned} \sigma_Z &= 0.20\ x^{0.75} \quad (z_0 = 0.03\ \text{m}) \\ \sigma_Z &= 0.27\ x^{0.78} \quad (z_0 = 1\ \text{m}) \end{aligned} \tag{7}$$

## ACKNOWLEDGEMENT

The author is particularly pleased to acknowledge helpful discussions with his colleague Dr. C. Matthias of the Atmospheric Environment Service.

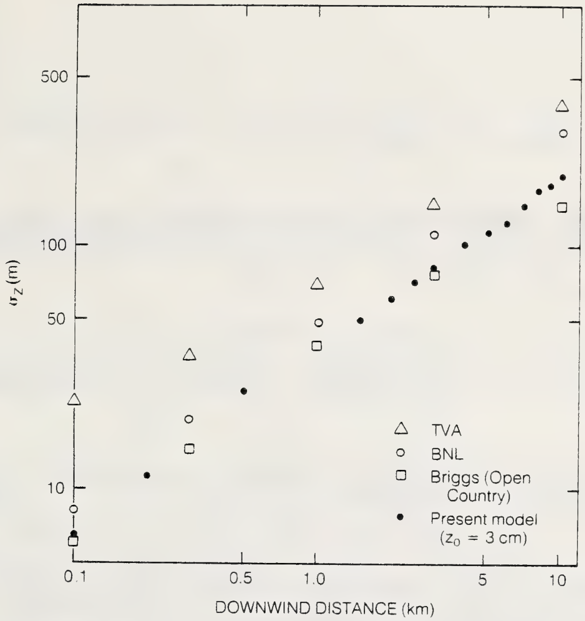

Figure 6: $\sigma_z$ variation with downwind distance for neutral conditions and $z_0$ = 3 cm for the model compared with TVA and Brookhaven data analyses and Briggs analyses.

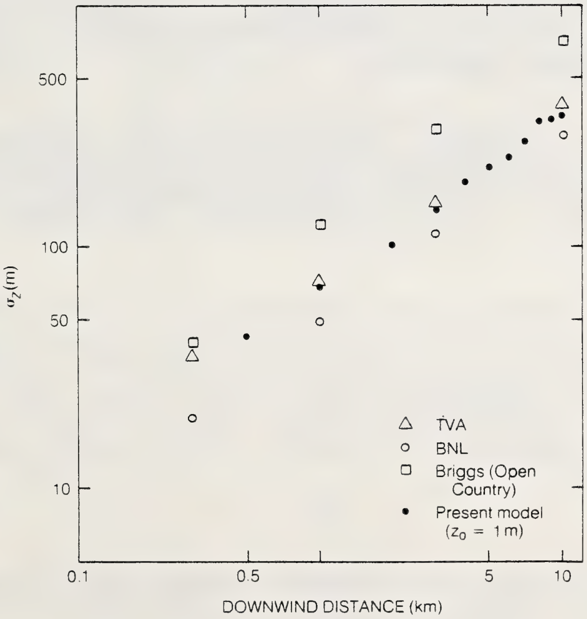

Figure 7: As for figure 6, but for $z_0$ = 1 m.

## REFERENCES

Gifford, F.A., 1976: Turbulent diffusion - typing schemes: A review. Nuclear Safety, 17, 68-86.

Reid, J.D., 1979: Markov chain simulations of vertical dispersion in the neutral surface layer for surface and elevated releases. Boundary-Layer Meteorol., 16, 3-22.

Reid, J.D., and R.S. Crabbe, 1980: Two Models of Long-Range Drift of Forest Pesticide Aerial Spray. Atmospheric Environment, 14, 1017-1025.

Turner, D.B., 1979: Workbook of atmospheric dispersion estimated. U.S. EPA Publication AP-26, 84.

Wilson, J.D., G.W. Thurtell, and G.E. Kidd, 1981a: Numerical simulation of particle trajectories in inhomogeneous turbulence, I: Systems with constant turbulent velocity scale. To appear in Boundary-Layer Meteorol.

Wilson, J.D., G.W. Thurtell, and G.E. Kidd, 1981b: Numerical simulation of particle trajectories in inhomogeneous turbulence, II: Systems with variable turbulent velocity scale. To appear in Boundary-Layer Meteorol.

Wilson, J.D., G.W. Thurtell, and G.E. Kidd, 1981c: Numerical simulation of particle trajectories in inhomogeneous turbulence, III: Comparison of predictions with experimental data for the atmospheric surface layer. Submitted to Boundary-Layer Meteorol.

# A MODEL FOR URBAN AREA SOURCE CO CONCENTRATIONS

by

K. D. Hage and P. Hopps
Meteorology Division
University of Alberta
Edmonton, Alberta T6G 2H4

Abstract: High surface concentrations of motor vehicle pollutants in urban areas occur in periods of stable air and stagnant air flow when wind speeds often drop below the threshold of standard 10 m anemometers. In order to assess the relative importance of wind speed, vertical dispersion and source strength variations, a numerical model is formulated for carbon monoxide concentrations near city centre. Surface-layer profile equations from the Kansas and Minnesota experiments, as modified recently by Wieringa, are used to calculate the parameters of Roberts' solution to the diffusion equation for a surface line source. Contributions from line sources at some distance from the receptor are obtained by summation with allowance for time changes in source strength, wind speed, and wind direction. The model requires temperature observations at two levels and wind observations at a single level on an urban tower. Computed and observed carbon monoxide concentrations are compared using data from Edmonton.

## INTRODUCTION

The most important physical factors that influence the concentration $\psi$ of pollutants emitted by motor vehicles and measured near street level at some central urban monitoring station are revealed by the simple urban dispersion model used by the Air Resources Atmospheric Turbulence and Diffusion Laboratory of the National Oceanic and Atmospheric Administration in the United States (Hanna, 1971). According to this model

$$\psi = \frac{Cq}{U} \qquad (1)$$

where q is the area source strength in amount of pollutant per unit area per unit time, U is wind speed, and C is a dimensionless parameter which depends strongly on atmospheric stability and weakly on city size.

In steady wind speeds and near-neutral stability conditions $\psi$ varies in time in accordance with variations in source strength Q exhibiting maxima during morning and afternoon traffic peaks and minima in midday and in the early morning hours. However, on many clear evenings observations show that C/U can increase sufficiently rapidly so as to overcome the effect of declining source strengths producing one or more evening concentration maxima. In order to explain such complex changes in $\psi$ it will be necessary to examine the influence of stability and wind speed changes in more detail.

## MODEL DEVELOPMENT

The model to be described utilizes a known gradient-transfer mathematical solution for crosswind line sources together with recent similarity-theory summaries of wind and temperature profiles in the atmospheric surface layer. The shortcomings of gradient-transfer theory are well known but the fact is that it works well for short-range diffusion from ground-level line and area sources, evidently because the scales of vertical turbulence are severely constrained by the earth's surface (Pasquill, 1975). For this reason the diffusive growth of the plume is accomplished by vertical scales of turbulence that are comparable to or smaller than the vertical scale of the plume.

A solution to the two-dimensional diffusion equation for concentration $\psi$:

$$U \frac{\partial\psi}{\partial x} = \frac{\partial}{\partial z}\left(K \frac{\partial\psi}{\partial z}\right), \qquad (2)$$

subject to power-law representation of vertical variations of wind speed U and vertical eddy diffusivity K,

$$U = U_1\left(\frac{z}{z_1}\right)^m, \qquad K = K_1\left(\frac{z}{z_1}\right)^n \qquad (3)$$

was first presented by Roberts (unpublished, see Sutton, 1953). In (3) $U_1$ and $K_1$ are the values of U and K at $z = z_1$. The boundary conditions are:

$$\psi \rightarrow 0 \quad \text{as} \quad x,z \rightarrow \infty$$

$$\psi \rightarrow \infty \quad \text{as} \quad x = z = 0$$

$$K\frac{\partial\psi}{\partial z} \rightarrow 0 \quad \text{as} \quad z \rightarrow 0, x > 0$$

The equation of conservation of mass is:

$$\int_0^\infty U\psi dz = Q \qquad x>0 \qquad (4)$$

The solution to (2), subject to conditions (3) is:

$$\psi = \frac{Qr}{U_1\Gamma(s)} \left(\frac{U_1}{r^2K_1x}\right) z_1^{\frac{1}{1+2m}} \exp - \left(\frac{U_1}{r^2K_1}\right) \frac{Z_1^{1-2m}}{x} z^{2m+1} \qquad (5)$$

where $r = m - n + 2 > 0$

$s = m+1/r$

$n = 1 - m$

The condition $n = 1 - m$ implies conjugate power laws for U and K. However, as will be seen later, the numerical value of $K_1$ is taken to be that for heat rather than momentum.

In the present application the principal sources of carbon monoxide (CO) are gasolene-powered motor vehicles. Emissions are buoyant and mechanically stirred by moving vehicles at low levels. Therefore, it is assumed that concentrations are uniform in the layer between the earth's surface and the height of the air sample intake in downtown Edmonton (8.5 m). The heights z and $z_1$ in (5) are taken to be 0 and 8.5 m, respectively. In this case (5) reduces to:

$$\psi = \frac{Qr}{U_1\Gamma(s)} \left(\frac{U_1}{r^2K_1x}\right)^s z_1^{1/r} \qquad (6)$$

## Source Data

The urban area source can be interpreted as a succession of elementary crosswind line sources having strength:

$$\Delta Q = q(x)\Delta x$$

where q(x) is the area source strength for a crosswind strip of width $\delta x$. The daily average area source strength appropriate for a receptor in central Edmonton is shown in Figure 1. Figure 1 was derived from traffic flow data for 1977 in Edmonton and represents an average for all wind directions. The observed source strength variations with distance were simulated by the step functions shown by the solid line in Figure 1. With this approximation (6) becomes:

$$\psi = \frac{r}{U_1\Gamma(s)} \left(\frac{U_1}{r^2K_1}\right)^s z_1^{1/r} \int_0^X \frac{q(x)}{x^s}\,dx \qquad (7)$$

where X is the distance from the receptor to the city boundary, taken to be 7 km. The integral in (7) is:

$$\int_0^X \frac{q(x)}{x^s}\,dx = \frac{(1000)^{1-s}}{(1-s)} \left(7.5 + 2(3)^{1-s} + 5.3(7)^{1-s}\right) \times 10^{-7} \qquad (8)$$

The receptor data available for testing were hourly mean concentrations $\psi$.

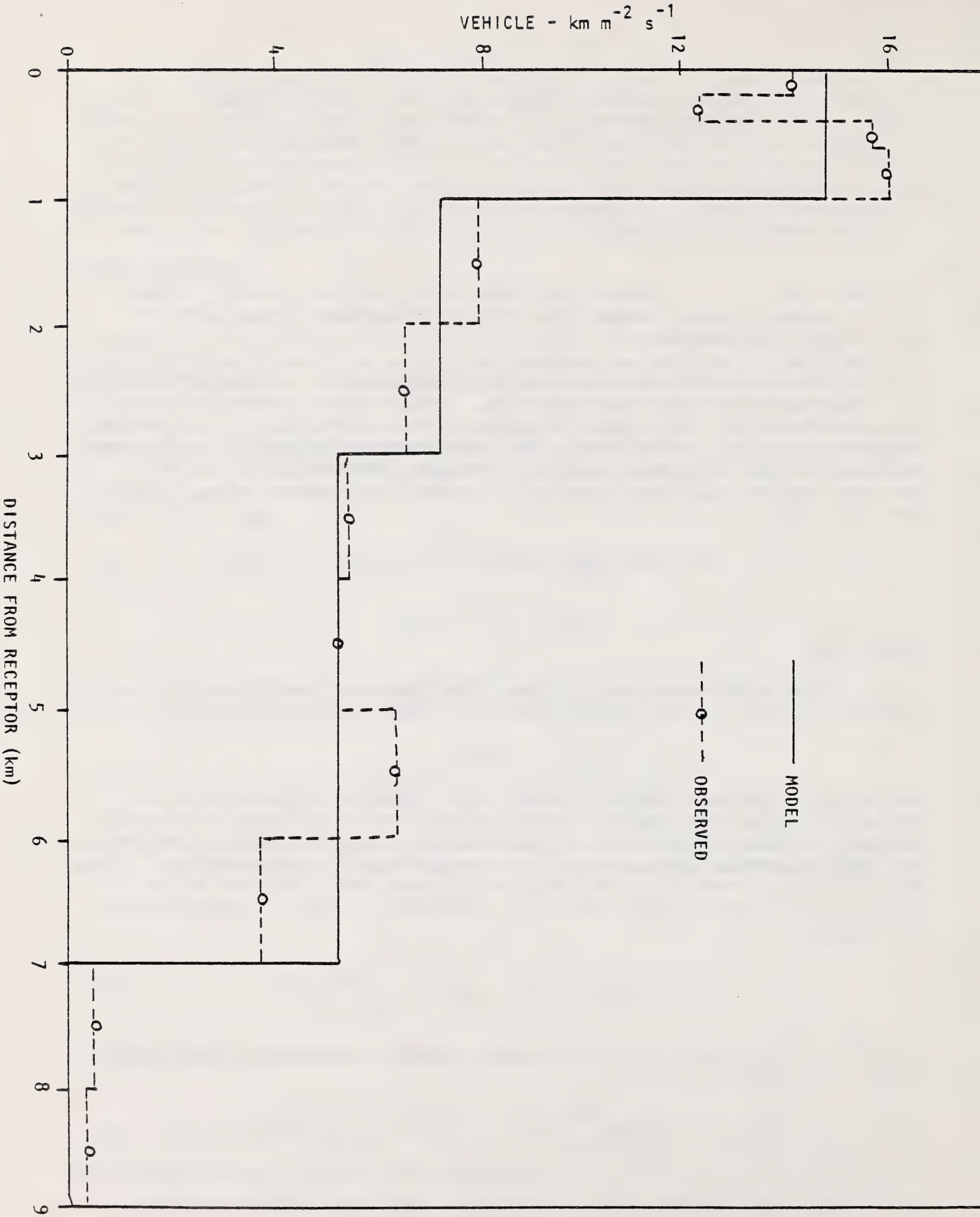
VEHICLE - km m$^{-2}$ s$^{-1}$
0
4
8
12
16
0
1
2
3
4
5
6
7
8
9
DISTANCE FROM RECEPTOR (km)
MODEL
OBSERVED

Therefore, the model equation (7) was applied to hourly mean values of wind speed, diffusivity, and source strengths. Equation (8), which is valid for mean daily traffic flow, was multiplied by a factor $N/\bar{N}$ where N is the percentage of traffic at any hour and $\bar{N}$ is the mean hourly percentage. Values of N valid for Edmonton in 1977 are listed in Table 1.

Table 1. Mean Hourly Percentages of Daily Traffic, Edmonton, 1977.

| Hour Ending | Percent | Hour Ending | Percent |
|---|---|---|---|
| 0 | 2.4 | 12 | 5.5 |
| 1 | 1.3 | 13 | 5.7 |
| 2 | 0.6 | 14 | 5.9 |
| 3 | 0.4 | 15 | 6.0 |
| 4 | 0.3 | 16 | 6.8 |
| 5 | 0.3 | 17 | 8.4 |
| 6 | 0.7 | 18 | 7.3 |
| 7 | 3.3 | 19 | 5.4 |
| 8 | 7.4 | 20 | 5.0 |
| 9 | 6.4 | 21 | 4.1 |
| 10 | 4.9 | 22 | 3.9 |
| 11 | 4.9 | 23 | 3.3 |

For $\psi$ in parts-per-million (ppm), (7) must be multiplied by an emission factor E for CO (g vehicle$^{-1}$ km$^{-1}$) and by a conversion factor (g m$^{-3}$ to ppm). With these the working equation is:

$$\psi(\text{ppm}) = 0.218 \times 10^{-4}\, W\, N\, E\, \frac{(1000)^{1-s}}{(1-s)} \left(7.5 + 2(3)^{1-s} + 5.3(7)^{1-s}\right) \qquad (9)$$

where

$$W = \frac{r z_1^{1/r}}{U_1 \Gamma(s)} \left(\frac{U_1}{r^2 K_1}\right)^s$$

with $z_1 = 8.5$ m, $U_1$ in m s$^{-1}$, and $K_1$ in m$^2$ s$^{-1}$.

## Meteorological Data

The meteorological data available for the evaluation of unknown parameters in (9) consisted of temperature differences between 3 levels $z_3 = 91.4$ m, $z_2 = 45.7$ m, and $z_1 = 10$ m, along with wind speeds at $z_3$, on a tower within the city of Edmonton about 3 km northwest of the city centre. From these data hourly mean bulk Richardson Numbers B were computed, where:

$$B = \frac{g}{T} \frac{\partial\theta/\partial z}{U_3^2} \bar{z}^2 \qquad (10)$$

where g is the acceleration of gravity, T is mean temperature, $\partial\theta/\partial z$ is the vertical gradient of potential temperature, U is wind speed at $z_3$, and $\bar{z}$ is the geometric mean height between $z_1$ and $z_3$. The vertical temperature gradient of $\theta$ was approximated by (Panofsky, 1965):

$$\frac{\partial\theta}{\partial z} \doteq \frac{\theta_3 - \theta_1}{(z_1 z_3)^{\frac{1}{2}} \ln z_3/z_1}$$

In these calculations all heights were converted to $z' = z - z_o$ where $z_o$ is the roughness length.

According to Golder (1972) the bulk Richardson Number B is related to the nondimensional height $\zeta' = \bar{z}'/L$, where L is the Monin-Obukhov length, by:

Unstable

$$B = \frac{\zeta'}{y^2 \, (\ln \bar{z} / z_o - \psi)^2} \tag{11}$$

where $\psi = 2 \ln (1+y)/2 + \ln (1+y^2)/2 - 2\tan^{-1}y + \pi/2$ and $y = (1 - \beta_m \zeta')^{\frac{1}{4}}$

Stable

$$B = \frac{\zeta'(1 + \beta_m \zeta')}{(\ln \bar{z} / z_o + \beta_m \zeta')^2} \tag{12}$$

where $\beta_m = 22$ (unstable) or $\beta_m = 6.9$ (stable) according to Wieringa (1980). Given B, equations (11) and (12) were solved for L. Given L the required wind speed $U_1$ was obtained from

Unstable

$$\frac{U_1}{U_3} = \frac{\ln z_1/z_o - \psi(\zeta_1')}{\ln z_3'/z_o - \psi(\zeta_3')} \tag{13}$$

Stable

$$\frac{U_1}{U_3} = \frac{\ln z_1/z_o + \beta_m \zeta_1'}{\ln z_3/z_o + \beta_m \zeta_3'} \tag{14}$$

The exponent m in the wind power law (2) was obtained by fitting the power law to the wind speeds $U_1$ and $U_3$. The remaining parameter $K_1$ was derived by assuming that the eddy diffusivity for mass was equal to that for heat. Then

$$K_1 = \frac{k \, u_* \, z}{\phi_H} \tag{15}$$

where $\phi_H = (1 - \beta_H \zeta')^{-\frac{1}{2}}$ (unstable)

or $\phi_H = (1 + \beta_H \zeta')$ (stable)

with $\beta_H = 13$ (unstable) or $\beta_H = 9.2$ (stable) according to Wieringa (1980).

The friction velocity $u_*$ was computed from:

$$u_* = \frac{kU_3}{\ln z_3/z_o - \psi(\zeta_3')} \qquad \text{(unstable)} \qquad (16)$$

or

$$u_* = \frac{kU_3}{\ln z_3/z_o - \beta_m \zeta_3'} \qquad \text{(stable)} \qquad (17)$$

A two-layer version of the model which permits different values of $L$ and $u_*$ in the upper and lower layers can be formulated in a similar way by utilizing the observed vertical potential temperature differences $(\theta_3 - \theta_2)$ and $(\theta_2 - \theta_1)$. In this version it is necessary to compute $U_2$ at $z_2'$ by first evaluating $B$ and $L$ for the top layer. Given $U_2$ the computations proceed as before based, however, on $B$ and $L$ for the lower layer.

## Critical Richardson Number

As $L \rightarrow 0$, $B \rightarrow 1/\beta_m = 0.145$, and $K_1 \rightarrow 0$. In this limit the wind profile becomes linear $(m=1)$ and it is still possible to compute $U_1$ from the observed wind speed $U_3$. The implication is that turbulent vertical diffusion is non-existent. However, because of the urban heat island effect, and because of plume buoyancy and mechanical mixing by moving vehicles it seems reasonable to assume that a shallow mixed layer exists over the city. In practice when $L \leq \bar{z}'$, concentrations were computed from a box model for which

$$\psi = \frac{0.218 \times 10^{-4} NE}{HU_1} \int_0^X q(x)dx \qquad (18)$$

where $H$ is the depth (assumed constant) of the shallow mixed layer. The depth $H$ was obtained by matching (9) and (19) using the smallest allowed value of $L$ in (9).

## Time Variations

When $U_1$ in (9) or (19) is so small that more than 1 h travel time is required for air to reach the receptor from the city boundary, the time-dependent parameters in (9) and (19) were replaced by appropriate averages over past hours. The parameters in question are $r$, $U_1$, $K_1$, $s$, and $N$. Alternatively, and more accurately, one may sum the separate contributions from individual preceding hours, provided that time changes in $\psi$ can be interpreted properly as sums of successive steady states. Tests indicated that the final results were quite insensitive to this choice of procedure and, therefore, the first and simplest procedure was followed.

## Unknown Parameters

The two unknown parameters in the model are the emission factor $E$ and the roughness length $z_o$. A survey of previous studies in the United States and Canada suggested that $E$ could range from 20 g vehicle$^{-1}$ km$^{-1}$ to

80 g vehicle$^{-1}$ km$^{-1}$ for Edmonton in 1977. It depends on many factors such as mean vehicle speed, vehicle ages, vehicle mix, altitude, pollution control equipment, maintenance, vehicle operating temperature, and air temperature.

In an attempt to estimate $z_0$ ten samples of neutral or near-neutral wind profiles were selected using the tower temperature differences ($\theta_3 - \theta_1$) and $U_3$. For lack of low-level tower wind speeds it was necessary to use 10 m wind speeds from the Municipal Airport some 2 km distant. Needless to say, the results showed considerable scatter with a range of $0.3 \text{ m} \leq z_0 \leq 1.4 \text{ m}$ and a mean value of 1.0 m. Even if this range is accepted there is some question as to whether or not it includes the desired mean value for air moving from the city boundary to city centre.

## PRELIMINARY RESULTS

Out of 15 cases with maximum hourly mean CO concentrations in excess of 8 ppm in 1977, two were selected for preliminary tests of the model. One criterion for selection of both cases was that no major wind direction change (>90°) occurred with light wind speeds. Such meandering can result in a significant increase in the path length of the air over the city - a factor which is not included in (9) or (19). In addition it was desired to have one test case in which the critical value of the bulk Richardson Number was not exceeded in 24 hours and a second test case with a late evening CO concentration maximum.

The results for October 12-13, 1977 are shown in Figure 2 for a mean roughness length of 1.0 m. The critical value of B was not exceeded in this case. The unknown emission factor E was eliminated by dividing hourly concentrations by the 24 h mean predicted or observed concentration. Wind speeds at 91.4 m were averaged from 10 min readings. Occasional below-threshold values were replaced by a speed of 0.7 m s$^{-1}$ (50 percent of the anemometer threshold speed).

The correlation between predicted and observed relative concentrations in Figure 2 exceeded 0.85. The principal error in both timing and magnitude occurred by premature overprediction of the first concentration maximum.

The results for May 20-21, 1977 are shown in Figure 3 for a roughness length of 1.0 m. In this case L dropped below the mean tower height at 0130 on 21 May. The box model was matched to the diffusion model at 0030 resulting in a box of effective depth 26 m which was held constant for the remaining hours. The diffusion model (9) appeared to underestimate concentrations during the daytime convective period (1000-1600) and overestimated concentrations in the late afternoon and early evening. However, since these errors were not apparent on October 12-13 more testing will be needed to establish whether or not such systematic errors are characteristic of the model. The correlation between predicted and observed concentrations exceeded 0.8.

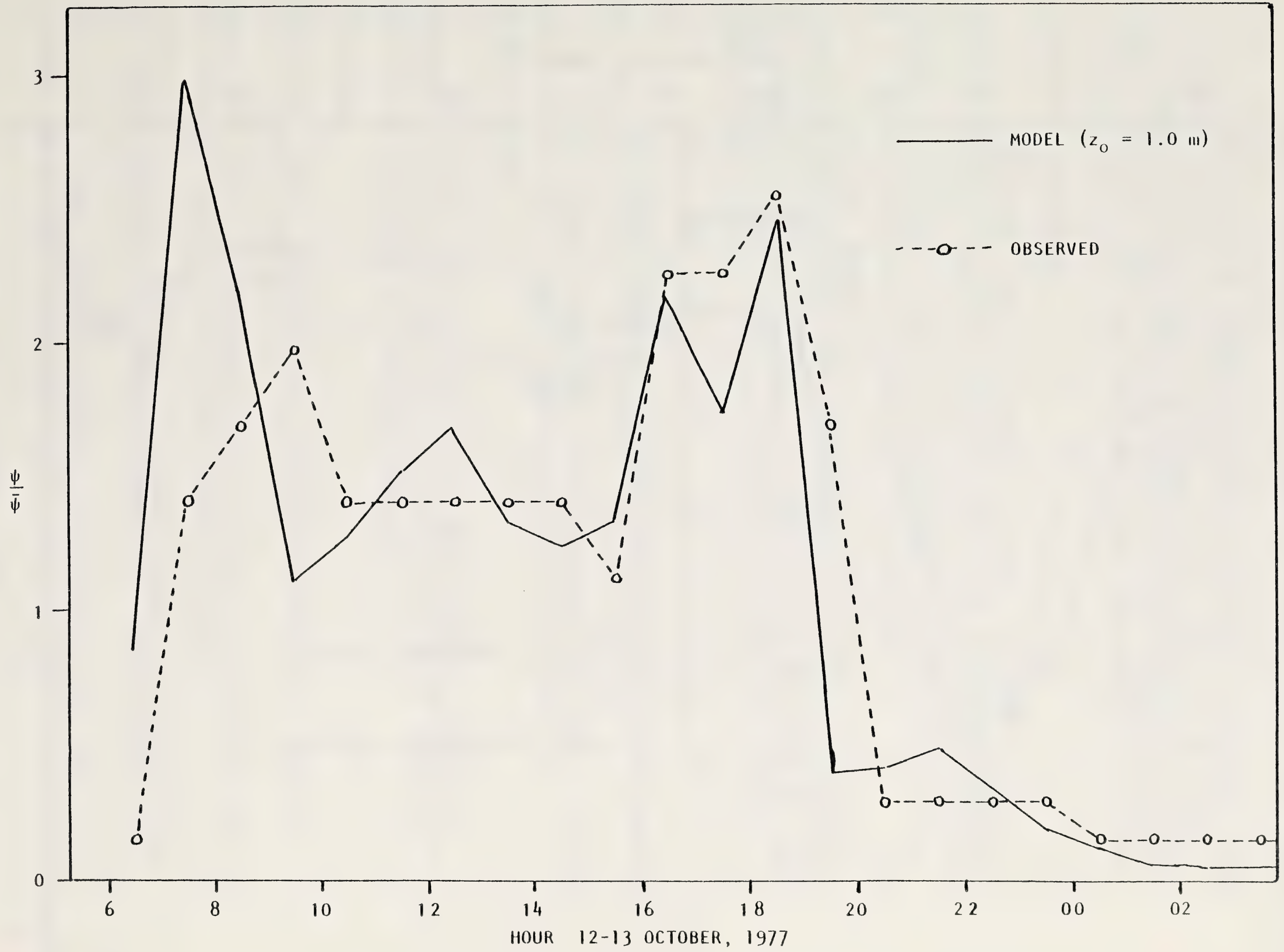

Figure 2. Observed and Predicted CO Concentrations $\psi/\bar{\psi}$ for October 12-13, 1977.

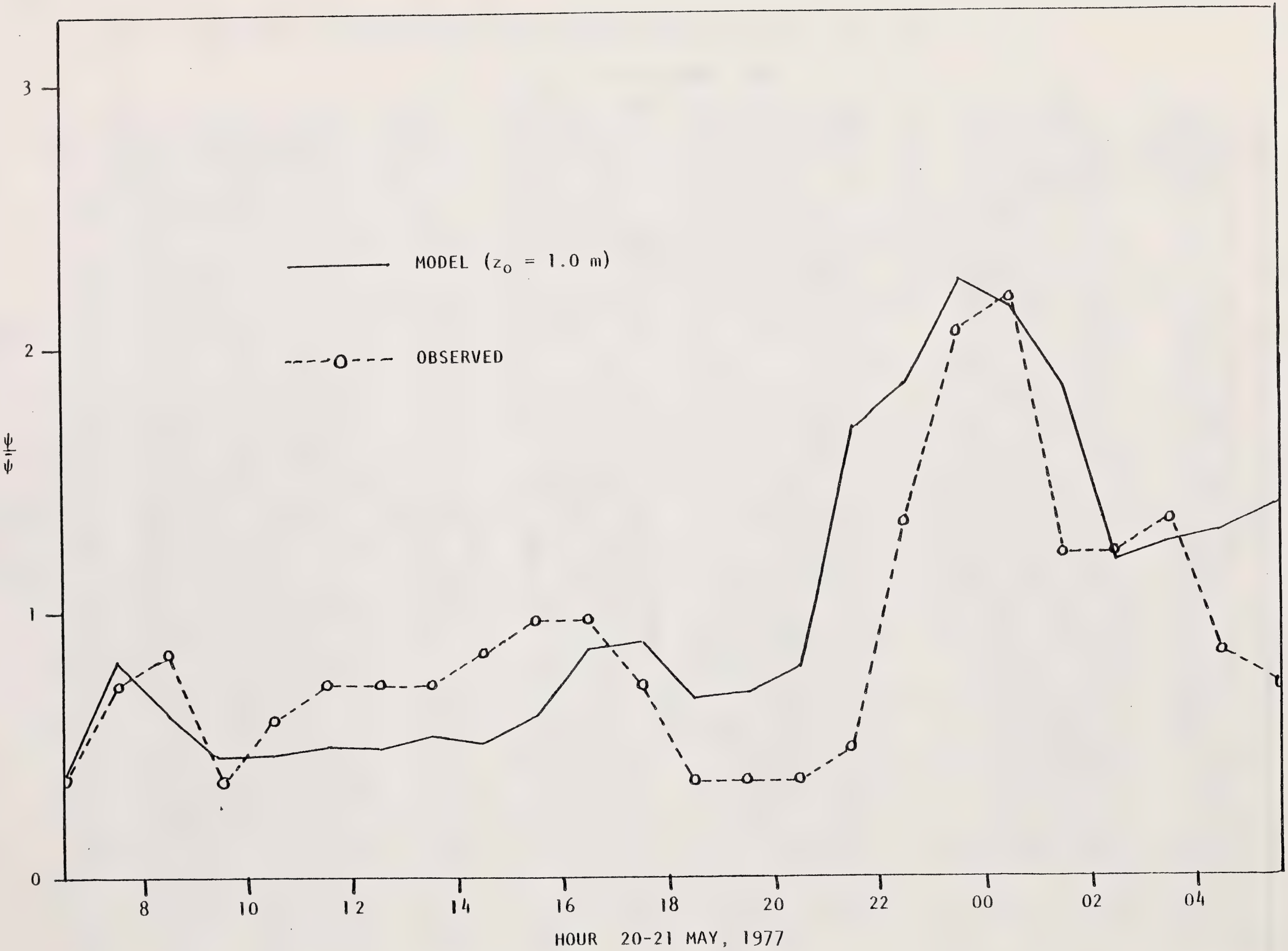

Figure 3. Observed and Predicted CO Concentrations $\psi/\bar{\psi}$ for May 20-21, 1977.

Sensitivity of the model predictions to changes in roughness length are shown in Figure 4 for October 12-13. Roughness length changes from 0.3 m to 3.0 m resulted in rather large changes in mean concentration but had little impact on the correlation between predicted and observed relative concentrations. For example, on October 12-13, a change in roughness length from 0.3 m to 3.0 m more than doubled the implied emission factor E from 42 to 87 g vehicle$^{-1}$ km$^{-1}$.

## SUMMARY AND CONCLUSIONS

Preliminary tests of a mathematical model for estimating hourly mean CO concentrations from an urban area source show considerable promise, but more tests are needed to establish whether or not appreciable systematic errors are present in the model. In the course of model development two parameters having major uncertainties were identified: the emission factor E for CO, and the roughness length $z_0$ for the urban area.

The model requires only one temperature difference and one wind speed from a meteorological tower and it appears to be capable of predicting a realistic low-level wind speed on most occasions when such speeds are below the threshold of standard anemometers. It will fail, however, when the wind speed at tower top is also below the anemometer threshold for periods in excess of about 30 min.

The greatest weaknesses of the model are believed to be:

(a) The application of similarity theory with its implied assumptions to a 90 m layer over an urban area in all stability conditions.

(b) The need to match the diffusion model to a box model of constant depth when the bulk Richardson Number exceeds a critical value.

## ACKNOWLEDGEMENTS

The authors wish to express their appreciation to the Research Management Division of Alberta Environment and to the Natural Sciences and Engineering Research Council of Canada for financial support. Thanks are due also to Laura Smith for typing the manuscript.

## REFERENCES

Golder, D., 1972: "Relations Among Stability Parameters in the Surface Layer," Boundary-Layer Meteorol., 3(1), 47-58.

Hanna, S.R., 1971: "A Simple Method of Calculating Dispersion from Urban Area Sources," J. Air Pollution Control Assoc., 21, 774-777.

Panofsky, H.A., 1965: "Reanalysis of Swinbank's Kerang Observations," Flux of Heat and Momentum in the Planetary Boundary Layer, Pennsylvania State University, 66-76.

Pasquill, F., 1975: "Atmospheric Diffusion," 2nd Edition, John Wiley, Toronto, 429 pp.

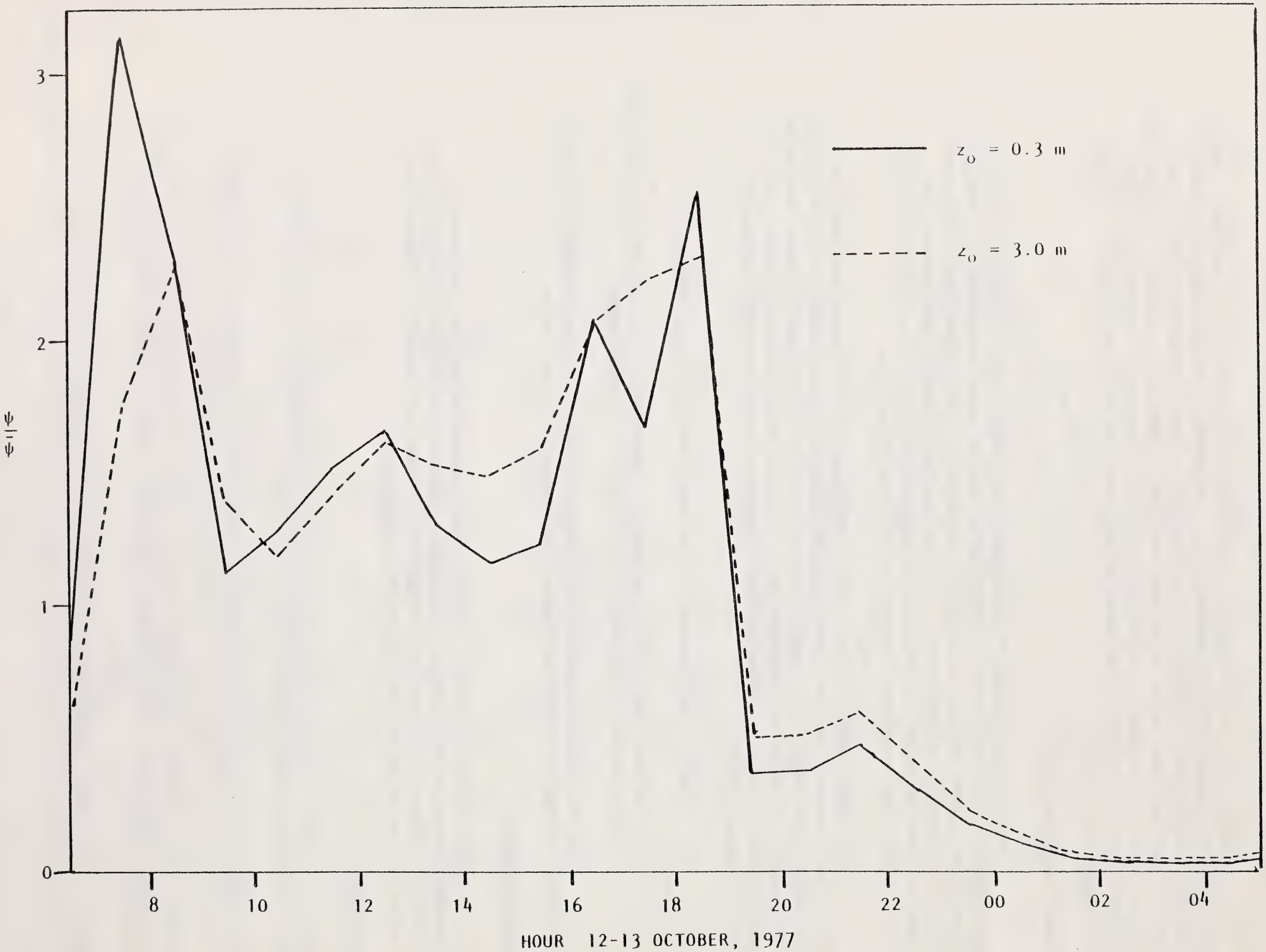

Figure 4. Predicted CO Concentrations $\psi/\bar{\psi}$ Using Roughness Lengths of 0.3, 1.0, and 3.0 m for October 12-13, 1977.

Sutton, O.G., 1953: "Micrometeorology," McGraw-Hill, Toronto, 333 pp.

Wieringa, J., 1980: "A Revaluation of the Kansas Mast Influence on Measurements of Stress and Cup Anemometer Overspeeding," Boundary-Layer Meteorol., 18(4), 411-430.

# INCOMPATIBILITY BETWEEN AIR QUALITY MODEL PREDICTIONS

# AND

# REGULATORY REQUIREMENTS: ATTEMPT AT SOLUTION

by

S. G. Djurfors
Syncrude Canada Ltd.
Edmonton, Alberta
T5J 3E5

Abstract: Atmospheric dispersion models are able to predict average concentrations only for time periods greater than those given by the short term (1/2-hr. and 1-hr.) air quality standards. Because government and industry are both committed to the use of such models, an air quality standard consistent with model ability must be adopted. The shortest compatible "modeling standard" appears to be a 3-hr. standard. The adoption of such a standard must be accomplished without loss of regulatory stringency. A 3-hr. sulfur dioxide air quality standard is developed which indicates that a 3-hr. value of 0.12 ppm is equivalent to the Alberta 1-hr. base value of 0.17 ppm. In addition, the 24-hr. standard is shown to be the most stringent of all the short term air quality standards.

## INTRODUCTION

An atmospheric dispersion model is a mathematical tool which provides a quantitative link between emissions of pollutants and the observed distribution of air quality. Industry and government alike are increasingly making use of such models in an effort to control an area's air quality. The dispersion model, therefore, has become an important tool in air resource management. Dispersion modeling has reached a high level of maturity and sophisticated models are now being developed and proposed for routine application. However, even if the model is an ideal representatation of the dispersion process and even if the model input is accurate, predictions will be in error because short term observed concentrations are incompatible with concentrations predicted by the model. This problem arises because the model relates the dispersion of pollutants to their ensemble mean concentration rather than to the time average concentration, which is what we measure. The ensemble mean concentration, being largely a theoretical concept, is inherently difficult to determine experimentally. The simplest physical situation in which the ensemble mean concentration may be satisfactorily approximated experimentally is the continuous release of a tracer at constant rate into a steady, homogeneous field of turbulence of constant mean velocity. Under these conditions, the ensemble mean concentration at a given location equals the time average concentration, obtained by averaging the concentrations observed in a single experiment over a sufficiently long period. In other words, the time average is expected to converge to a constant value, the ensemble mean value.

The main practical use of the dispersion model, therefore, lies in its ability to provide an approximate but acceptable model for the realized time average concentration (accessible by direct measurement) provided always that the observed concentration is averaged over a sufficiently long time period. The question is of course, how long is sufficiently long?

## THE ERROR CAUSED BY FINITE AVERAGING TIME

Because it would be impractical to average a concentration record $\tilde{c}(t)$ over an infinitely long time interval, our task must be to consider the error caused by finite averaging time. The realized time average concentration is given by:

$$\bar{C}_T = \frac{1}{T}\int_0^T \tilde{c}(t)\,dt \qquad (1)$$

where T is the time interval over which the averaging process is carried out and the origin of time was taken to be zero for convenience. This of course can be done without loss of generality. The difference between the time average concentration $\bar{C}_T$ and the ensemble mean value $\bar{C}$ is then:

$$\bar{C}_T - \bar{C} = \frac{1}{T}\int_0^T c(t)\,dt \qquad (2)$$

where now c(t) is the difference between the instantaneous realized value and the ensemble mean value. To be useful, Eq. (2) must be expanded into its mean square form, i.e.

$$\frac{\overline{(\bar{C}_T - \bar{C})^2}}{\bar{C}^2} \equiv \varepsilon^2 = \frac{2\overline{c^2}}{\bar{C}^2 T}\int_0^T \left(1 - \frac{\tau}{T}\right) R_E(\tau)\,d\tau \qquad (3)$$

where $\overline{c^2}$ is the ensemble concentration variance, $R_E$ the Eulerian auto-correlation function, which depends only on the lag-time τ* and overbar denotes a simple arithmetic ensemble averaging process. In addition, Eq. (3) was normalized by the ensemble mean concentration. Thus, ε is the expected rms error caused by finite averaging time, expressed as a fraction of the ensemble mean concentration $\bar{C}$.

---

[*] In steady conditions, $R_E$ is independent of what instant t is chosen as the base for its computation, any release time being equivalent to any other.

It is instructive to study Eq. (3) for a moment. From a maximum value of unity at very small time intervals, $R_E$ decreases as the time interval $\tau$ increases. A corresponding behavior is found in $\varepsilon$. The area under the $R_E(\tau)$ curve is of special significance and is given by:

$$T_E = \int_0^\infty R_E(\tau)d\tau. \tag{4}$$

$T_E$ is the Eulerian integral time scale, a typical "persistence" time of concentrations subjected to turbulent diffusion. It is, in other words, a measure of the time over which the observed concentration is correlated with itself.

The quantity $\varepsilon$ can be computed from Eq. (3) for all averaging times T only if the functional form for $R_E$ is known. The actual shape of the autocorrelation function for homogeneous and stationary turbulence has not so far been predicted theoretically in any satisfactory way. The only argument which appears to provide modest success, at least in a laboratory setting, is that of a Markov process (of the exponential decay type), where $T_E$ has been chosen as the characteristic time scale. In atmospheric applications more complex circumstances prevail which may require substantial modifications of the theoretical model. Fortunately, the asymptotic behavior of Eq. (3) can be deduced without having to specify the actual form for $R_E$. Thus, when $T \longrightarrow 0$, $R_E \longrightarrow 1$ and Eq. (3) reduces to:

$$\varepsilon = \pm \frac{\sqrt{\overline{c^2}}}{\overline{C}} \qquad T/T_E \ll 1 \tag{5}$$

which is the maximum possible value of $\varepsilon$. In other words, the largest error between predicted and observed concentration values occurs when the averaging time is very short, which might have been expected. On the other hand, when $T \longrightarrow \infty$, then $\tau/T \longrightarrow 0$ and Eq. (3) becomes:

$$\varepsilon = \pm \sqrt{\frac{2\overline{c^2}}{\overline{C}^2}} \sqrt{\frac{T_E}{T}} \qquad T/T_E \gg 1 \tag{6}$$

by virtue of Eq. (4). It is evident, therefore, that $\varepsilon$ can be made as small as desired, provided that $T_E$ is always finite. It must be stressed again that $\varepsilon$ is the result of the fundamental difference between ensemble mean values and their time average counterparts. Therefore, values of $\varepsilon$ computed from Eq. (6) (of special interest to us) do not represent the total possible error, because additional sources of error have not been considered. Such errors are instead treated as part of the normal evaluation of air quality models.

Table 1 shows the expected error $\varepsilon$ computed from Eq. (6) for four different averaging times and for $\overline{c^2}/\overline{C}^2 = 1.0$, believed to apply at those distances from the source where the maximum ground level concentration occurs.

Table 1. Expected Concentration Error Due to Finite Averaging Time.

| | T = 1/2 | T = 1 | T = 3 | T = 24 (hr.) |
|---|---|---|---|---|
| $\|\varepsilon\|$% | 41 | 29 | 17 | 6 |

The value of $T_E$ = 152s was adopted from Draxler's (1976) scheme and pertains to the horizontal component of dispersion. This scheme is based on data from several older but carefully conducted dispersion experiments which apply to elevated releases.

Table 1 suggests that from the model user's point of view, a 24-hr. averaging period would be ideal, because measurements would then be a good estimate of the ensemble mean concentration (which is what the model predicts). At the same time one would like to ensure that meteorological conditions do not change appreciably (remain stationary) so to this end a 3-hr. averaging period must reasonably be regarded as an upper limit to short term events. It is also clear that a sufficiently stable estimate of the concentration mean cannot be generated from either a 1/2-hr. or a 1-hr. record (indicated by the large values of $\varepsilon$), so with reference to the dispersion model an air quality standard based on these periods is of little value.

## THE PROBABILITY DISTRIBUTION OF OBSERVED CONCENTRATIONS

For a given averaging time, Eq. (6) provides only the expected *average* error. This implies of course that a whole range of concentrations may be expected albeit with different probabilities. An important question must therefore, also be, what, for example, is the probability of observing a value twice as large as the predicted value? To answer this the probability distribution of observed concentrations must be studied. Investigations of concentration probability distributions have revealed that such distributions are approximately log-normal, i.e.,

$$P(N) = \frac{1}{2}\left[1 + \operatorname{erf}\left(\frac{\ln N/C_o}{\sqrt{2}\sigma}\right)\right] \tag{7}$$

where P(N) is the probability that the observed concentration is less than or equal to N. Equation (7) is applicable to the concentration field of a continuous plume at ground level, assuming that the intermittency factor (the fraction of non-zero concentrations) is near unity. This (assumption) must be very nearly true below the plume axis at the location for the maximum concentration, which is of particular interest to us. The log-normal distribution has two parameters, the median concentration $C_o$ and the logarithmic standard deviation $\sigma$, both of which may be related to the local mean and variance of the observed concentrations. The magnitude of the observed variance must depend on averaging time and can in fact be shown to be directly proportional to the rms error $\varepsilon$ (Eq. 6). We obtain:

$$\begin{aligned} C_o/\overline{C} &= (1 + \varepsilon^2)^{-\frac{1}{2}} \\ \sigma &= \sqrt{\ln\,(1 + \varepsilon^2)} \end{aligned} \tag{8}$$

where $\overline{C}_T = \overline{C}$, the ensemble mean concentration.

Table 2 shows the fraction (in %) of observed concentrations which fall within specified limits of the predicted concentration, for four different averaging times.

Table 2. Probability Distribution of Observed Concentrations as a Function of Averaging Time.

| Range / T | ±0.1 | ±0.25 | ±0.5 |
|---|---|---|---|
| ½ | 20 | 48 | 83 |
| 1 | 27 | 63 | 93 |
| 3 | 45 | 87 | 99 |
| 24 | 91 | 100 | 100 |

Thus, for example, in the case of T = 1/2 hr. we find that 83% of all observed concentrations fall within ±50% of the predicted value, while only 20% fall within ±10% of the same. By comparison, when T = 3-hr., 99% fall within ±50% and almost half of the observed values fall within ±10% of the predicted value. Table 2 supports the conclusion drawn earlier, that for the purpose of model predictions a 3-hr. average concentration is preferable to either 1/2 or 1-hr. average concentrations. Again it must be remembered that in the foregoing we dealt with minimum errors which of necessity must be kept small in order that model predictions be at all credible.

## AIR QUALITY STANDARD EQUIVALENCE

From a regulatory point of view, the adoption of a 3-hr. air quality standard for model purposes must be accomplished without loss of regulatory stringency. The task becomes one of developing a 3-hr. "modeling standard", which is equivalent in stringency to e.g. the 1-hr. standard applied to observed concentrations (the 1-hr. standard is apparently the Alberta government's base standard). Absolute equivalence can be obtained only via well-behaved mathematical relationships such as the probability distribution, Eq. (7). By a reverse application of this equation, one can find the mean concentration value $\overline{C}_T$, which would cause exceedance of the critical value $C_L^T$ (the standard) with only a small probability of 1 - P. We obtain:

$$\overline{C}_T / C_L^T = \exp\left[ - \sqrt{2}\sigma \ \mathrm{erf}^{-1} (2P - 1) + \sigma^2/2 \right] \qquad (9)$$

where $C_L^T$ is the air quality standard associated with averaging time T. Note that the ensemble mean value of a concentration time series is independent of the averaging time used to obtain a single point in the series. As a result, it must then be true that e.g. $\overline{C}_1 = \overline{C}_3$. We shall now define two air quality standards to be equivalent if:

- the existing standard and the equivalent standard are both exceeded with the same frequency 1 - P.

It is important to realize that although the existing standard and the equivalent standard are both exceeded with the same frequency, this does not imply that they are exceeded on the same occasion. In addition, the frequency 1 - P is not to be confused with the frequency with which the ambient standard is actually exceeded at a given location during a given time period. Rather it must be interpreted as the value which defines the mean value of the local concentration, consistent with exceeding the ambient standard with the probability in question. As an example of the use of Eq. (9), the 3-hr. "modeling standard" equivalent to the Alberta 1-hr. base standard, applied to sulfur dioxide, is derived for 1 - P = 0.1%. We have:

$$C_L^3 = KC_L^1 = \frac{0.43}{0.61} \times 0.17 = 0.12 \text{ (ppm)} \qquad (10)$$

Thus, a 1-hr. ensemble mean value of 0.17 ppm is exceeded just as often as a 3-hr. ensemble mean value of 0.12 ppm. In Table 3 is shown equivalent standards corresponding to all existing short term air quality standards, calculated for 1 - P = 0.1% (sulfur dioxide).

Table 3. Computed Equivalent Air Quality Standards Corresponding to Existing Standards, for 1 - P = 0.1%.

| | Existing Standard | | |
|---|---|---|---|
| Equivalent Standard (hr.) | 1/2 | 1 | 24 (hr.) |
| 24 | 0.08 | 0.09 | 0.06 |
| 3 | 0.10 | 0.12 | 0.08 |
| 1 | 0.15 | 0.17 | 0.12 |
| ½ | 0.20 | 0.23 | 0.16 |

It is interesting to observe that in the case of the existing 1-hr. standard, the equivalent 1/2 and 24-hr. values are greater than those permitted by regulations (0.2 and 0.06 ppm, respectively). Furthermore, we find that the 24-hr. existing standard is the most stringent of the short term standards, in that it leads to equivalent 1/2 and 1-hr. values which are lower than the present legislated ones. In Table 4 is shown equivalent standards corresponding to different probabilities of exceedance, calculated for the existing 1-hr. standard (sulfur dioxide).

Table 4. Computed Equivalent Air Quality Standards Corresponding to Different Probabilities of Exceedance and for the Existing 1-hr. Standard

| | Probability of Exceedance | | |
|---|---|---|---|
| Equivalent Standard (hr.) | 0.05 | 0.01 | 0.001 |
| 24 | 0.12 | 0.10 | 0.09 |
| 3 | 0.14 | 0.13 | 0.12 |
| 1 | 0.17 | 0.17 | 0.17 |
| ½ | 0.20 | 0.21 | 0.23 |

Thus, as the existing 1-hr. standard is allowed to be exceeded more frequently, the values of the equivalent standards predictably increase, with one notable exception, the 1/2-hr. standard.

## SUMMARY

The important points of the paper can be summarized as follows:

- Both government and industry are committed to the use of atmospheric dispersion models.
- Models are able to predict average concentrations only for time periods greater than those given by the present short term (1/2-hr. and 1-hr.) air quality standards.
- An air quality standard consistent with model ability must be adopted for the purpose of model predictions.
- The shortest compatible "modeling standard" appears to be a 3-hr. standard.
- The adoption of such a standard must be accomplished without loss of regulatory stringency.
- A 3-hr. value of 0.12 ppm for sulfur dioxide is equivalent to a 1-hr. value of 0.17 ppm.

## Reference

Draxler, R. R. 1976: Determination of Atmospheric Diffusion Parameters, Atm. Environ. Vol. 10, pp 99-105.

# TRAITEMENT AMELIORE DE LA PRECIPITATION DANS UN MODELE DE POLLUTION DE L'AIR PAR L'UTILISATION D'UNE DOUBLE CHAINE DE MARKOV

par

Claude Lelièvre
Service de la Météorologie,
194 St-Sacrement,
Québec G1N 4J5

Résumé: Une méthode statistique, basée sur le calcul de la somme de deux chaînes de Markov, a été développée dans le but d'améliorer le traitement de la précipitation dans un modèle statistique de transport à grande distance des polluants atmosphériques. Nous obtenons 4 cycles de périodes sèches et humides à partir des données horaires de précipitation. Les cycles courts représentent les averses et la pluie intermittente, tandis que les cycles longs représentent le temps synoptique entre les systèmes météorologiques. Cette méthode peut être appliquée à toutes données sur lesquelles deux processus agissent sur des échelles de temps différentes.

## INTRODUCTION

Une chaîne de Markov implique qu'un état donné ne dépend que de l'état précédent (modèle autorégressif d'ordre 1). Plusieurs phénomènes météorologiques ont été décrits par une simple chaîne de Markov à deux états. Par exemple, des résultats satisfaisants ont été obtenus sur la précipitation journalière (Leduc, 1977; Gabriel et Neumann, 1961; Weiss, 1964). Toutefois, on observe fréquemment qu'à la fois les courtes et les longues séquences sont sous-estimées par le modèle Markovien. On peut généralement améliorer le modèle Markovien en supposant que l'on observe la somme de deux chaînes de Markov qui agissent sur des périodes différentes. Une méthode mathématique a été développée afin de reconstituer ces deux chaînes.

Environnement-Québec développe présentement un modèle statistique du transport à grande distance des polluants atmosphériques qui sera similaire à celui de Fisher (1978). Nous vérifierons bientôt les conséquences du traitement amélioré des périodes sèches et humides.

## 1- MODELE D'UNE DOUBLE CHAINE DE MARKOV: DEVELOPPEMENT MATHEMATIQUE

Soit $N_{1s}$ (k) le nombre de séquences d'exactement k heures consécutives de pluie et qui provient de la somme des deux chaînes de Markov: $N_{1\alpha}$ (k) et $N_{1\beta}$ (k) (voir Figure 1). Définissons les termes suivants:

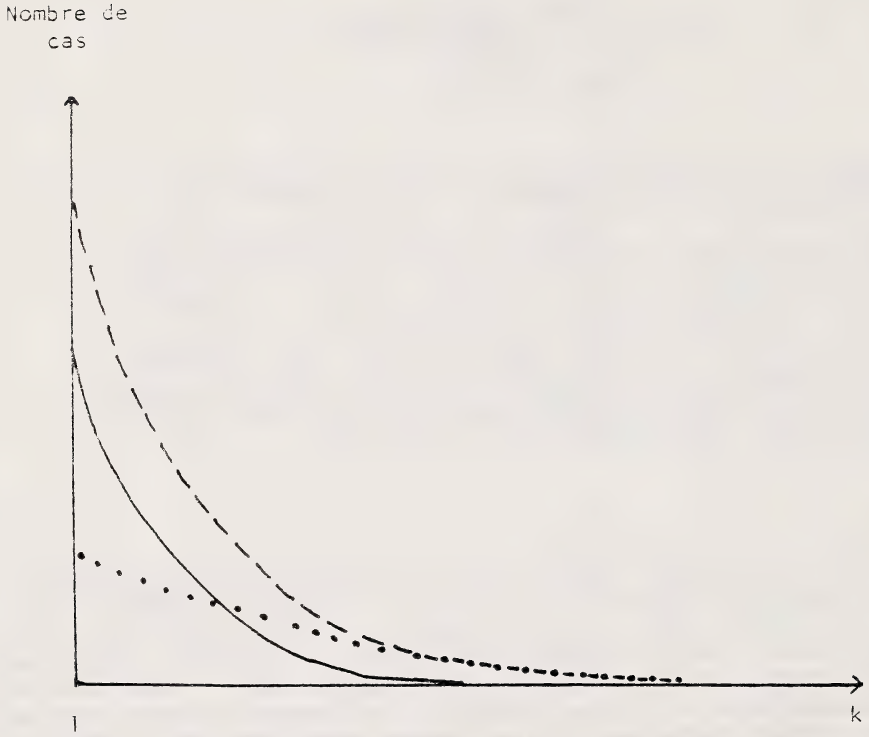

Figure 1. Courbes du nombre de séquences d'exactement k périodes consécutives à l'état 1.

———— $N_{1\alpha}(k)$: plus important aux basses valeurs de k

........ $N_{1\beta}(k)$: plus important aux valeurs élevées de k

------- $N_{1s}(k) = N_{1\alpha}(k) + N_{1\beta}(k)$ qui est la courbe observée

$\alpha$ = probabilité de transition de l'état 1 (pluie) à l'état 2 (sécheresse) pour la courbe $N_{1\alpha}$
$\beta$ = probabilité de transition de l'état 1 à l'état 2 pour la courbe $N_{1\beta}$
$N_1 = \sum_{k=1}^{\infty} N_{1s}(k)$ = nombre total de séquences
$A$ = contribution relative de $N_{1\alpha}$ à $N_1$
$B$ = contribution relative de $N_{1\beta}$ à $N_1$

Les équations de base sont alors

$$N_{1s}(k) = N_1 \left[ A\alpha\,(1-\alpha)^{k-1} + B\beta\,(1-\beta)^{k-1} \right] \qquad (1)$$

$$A + B = 1 \qquad (2)$$

L'équation 1 représente la somme de deux chaînes de Markov dont la somme de leurs coefficients A et B est normalisée à l'unité. Nous désirons trouver les valeurs de $\alpha$, $\beta$, A et B à partir des variables suivantes

$m_{r1}$ = longueur de la séquence qui sépare les données en deux groupes.
$\overline{m}_1$ = longueur moyenne des séquences entre $k = 1$ et $k = m_{r1}$
$\overline{M}_1$ = longueur moyenne des séquences entre $k = m_{r1} + 1$ et $k = \infty$
$N_{r1}$ = nombre de séquences entre $k = m_{r1} + 1$ et $k = \infty$

Cette façon de procéder nous permet de conserver exactement la longueur moyenne des séquences ainsi que le nombre de séquences dans les deux parties de la courbe autour du point $m_{r1}$. A partir de la théorie des séries géométriques et des équations (1) et (2) nous obtenons

$$\begin{aligned}\overline{m}_1 = {} & \Big(\Big((1-\beta)^{m_{r1}} - \frac{N_{r1}}{N_1}\Big) \Big(\frac{1}{\alpha} - (m_{r1} + \frac{1}{\alpha})\,(1-\alpha)^{m_{r1}}\Big) \\ & + \Big(\frac{N_{r1}}{N_1} - (1-\alpha)^{m_{r1}}\Big)\Big(\frac{1}{\beta} - (m_{r1} + \frac{1}{\beta})\,(1-\beta)^{m_{r1}}\Big)\Big) \\ & \div \Big(\Big((1-\beta)^{m_{r1}} - (1-\alpha)^{m_{r1}}\Big)\Big(1 - \frac{N_{r1}}{N_1}\Big)\Big)\end{aligned} \qquad (3)$$

$$\begin{aligned}\overline{M}_1 = {} & \Big(\Big((1-\beta)^{m_{r1}} - \frac{N_{r1}}{N_1}\Big)(1-\alpha)^{m_{r1}}\Big(\frac{1}{\alpha} + m_{r1}\Big) \\ & + \Big(\frac{N_{r1}}{N_1} - (1-\alpha)^{m_{r1}}\Big)\,(1-\beta)^{m_{r1}}\Big(\frac{1}{\beta} + m_{r1}\Big) \\ & \div \Big(\frac{N_{r1}}{N_1}\,\big((1-\beta)^{m_{r1}} - (1-\alpha)^{m_{r1}}\big)\Big)\end{aligned} \qquad (4)$$

Les équations (3) et (4) forment un système de deux équations transcendentales à deux inconnues. Une méthode itérative basée sur le développement en séries de Taylor à deux variables autour d'un point a été élaborée. Cette méthode converge généralement en moins de 4 itérations si on choisit judicieusement le point de départ. Dans l'annexe A nous décrivons en détail cette méthode ainsi que les équations obtenues. La valeur de $m_{r1}$ est obtenue par essais successifs en choisissant celle qui procure le meilleur ajustement. Notons qu'en utilisant $m_{r1} = 2$, on force un ajustement parfait aux deux premiers points, tout comme dans le cas d'un modèle autorégressif du troisième ordre. La méthode ne garantie pas que $\alpha$, $\beta$, A et B soient normalisés entre 0 et 1. En effet la courbe totale peut provenir de la soustraction de deux chaîne de Markov. La méthode peut devenir instable dans le cas où il n'y a qu'une seule distribution présente ainsi que dans le cas où une simple chaîne de Markov surestime les basses fréquences.

## 2- DETERMINATION D'UN CYCLE MOYEN SEC-HUMIDE

Soient

$\gamma$ = probabilité de transition de l'état 2 (sécheresse) à l'état 1 (pluie) pour la courbe $N_2$

$\delta$ = probabilité de transition de l'état 2 à l'état 1 pour la courbe $N_2$

$N_2 = \sum_{k=1}^{\infty} N_{2s}(k)$ = nombre total de séquences observées

C = contribution relative de $N_{2\gamma}$ à $N_2$

D = contribution relative de $N_{2\delta}$ à $N_2$

$m_{r2}$ = longueur de séquence de référence

$\overline{m_2}$ = longueur moyenne des séquences entre $k = 1$ et $k = m_{r2}$

$\overline{M}_2$ = longueur moyenne des séquences entre $k = m_{r2} + 1$ et $k = \infty$

$N_{r2}$ = nombre de séquences entre $k = m_{r2} + 1$ et $k = \infty$

On calcule C, D, $\gamma$ et $\delta$ selon la méthode exposée dans la section 1. On trouve qu'il y a 4 combinaisons des cycles secs-humides qui existent:

$$(\alpha,\gamma),\ (\alpha,\delta),\ (\beta,\gamma) \text{ et } (\beta,\delta)$$

Les cycles courts sont représentés par $\alpha$ et $\gamma$ tandis que les longs sont représenté par $\beta$ et $\delta$. Lorsqu'on traite la précipitation horaire, on trouve qu'au Québec:

$\alpha$ = durée moyenne des averses ou de la pluie intermittente

$\beta$ = durée moyenne de la pluie continue

$\gamma$ = temps sec moyen entre deux averses

$\delta$ = temps sec moyen entre le passage de deux systèmes synoptiques

## 3- EXEMPLE: VILLE DE QUEBEC

La méthode décrite plus haut a été appliquée aux données horaires du pluviographe de l'aéroport de Québec pour les mois de mai à septembre 1968 à 1977. Au tableau 1, on retrouve la valeur des paramètres calculés pour un seuil de précipitation égal à 0,3mm de pluie par heure. La somme du carré des erreurs de l'estimé a généralement été réduite par un facteur de 5 à 10 par rapport à une chaîne de Markov simple.

La méthode utilisée diverge surtout quand un seul processus agit sur les données. Par exemple, au mois de juin la valeur de A atteint 99%; dans ce cas-là, il vaut mieux de ne pas mettre trop de poids sur l'interprétation d'un cycle humide de 21h, car celui-ci est probablement fictif.

Tableau 1. Valeur des paramètres de la double chaîne de Markov pour les données horaires de précipitation à Québec (1968-1977), pour un seuil de précipitation égal à 0.3mm $h^{-1}$.

| Paramètre \ mois | | 5 | 6 | 7 | 8 | 9 |
|---|---|---|---|---|---|---|
| symbole | unités | | | | | |
| $\alpha$ | $h^{-1}$ | 0.6603 | 0.4281 | 0.9638 | 0.5508 | 0.6134 |
| $\beta$ | $h^{-1}$ | 0.1958 | 0.0463 | 0.3536 | 0.2381 | 0.1691 |
| $\gamma$ | $h^{-1}$ | 0.4444 | 0.4469 | 0.3328 | 0.3818 | 0.5252 |
| $\delta$ | $h^{-1}$ | 0.0200 | 0.0245 | 0.0237 | 0.0204 | 0.0250 |
| A | | 0.4295 | 0.9901 | 0.2861 | 0.6579 | 0.7057 |
| B | | 0.5705 | 0.0099 | 0.7139 | 0.3421 | 0.2943 |
| C | | 0.4878 | 0.4191 | 0.4092 | 0.4135 | 0.3764 |
| D | | 0.5122 | 0.5809 | 0.5908 | 0.5865 | 0.6236 |
| $\frac{1}{\alpha}$ | h | 1.5 | 2.3 | 1.0 | 1.8 | 1.6 |
| $\frac{1}{\beta}$ | h | 5.1 | 21.6 | 2.8 | 4.2 | 5.9 |
| $\frac{1}{\gamma}$ | h | 2.3 | 2.2 | 3.0 | 2.6 | 1.9 |
| $\frac{1}{\delta}$ | h | 50.0 | 40.8 | 42.2 | 49.0 | 40.0 |

On observe que la longueur des épisodes humides courts varie entre 1 et 2 heures; ceci implique qu'il faudrait avoir une résolution temporelle accrue afin de bien isoler la vraie durée moyenne des averses. L'intervalle de temps sec entre deux averses ou deux périodes de pluie intermittente est un peu plus long: 2 à 3 heures.

La durée des épisodes longs de pluie varie entre 3 et 6 heures avec une diminution de cette durée en été. Il serait intéressant d'étendre cette étude aux autres mois de l'année afin de vérifier la variation annuelle.

L'intervalle moyen entre deux systèmes synoptiques est d'environ deux jours au Québec, tandis qu'il est de trois jours en Europe (Rodhe et Grandell, 1972).

## CONCLUSION

Une nouvelle méthode a été élaborée afin de déterminer des cycles Markoviens sur un ensemble de données. Son emploi s'avère très utile dans les cas où il y a évidence que deux processus agissent sur des durées différentes. Les données horaires de précipitation au Québec indiquent la présence de processus qui produisent des durées de pluie d'environ 1,5h (pluie intermittente) et 5h (pluie continue) et des périodes sèches de 2,5h (temps entre les averses) et 45h (temps entre les systèmes synoptiques). L'utilisation de ces 4 cycles secs-humides trouvés au lieu d'un cycle moyen d'environ 25 à 30h devrait améliorer la performance du modèle statistique qu'Environnement-Québec utilisera en 1981.

## Références

Fisher, B.E.A. 1978: Long term sulphur deposition in Europe, Atmos. Env., 12, 489-502

Gabriel, K.R. et Neumann J. 1962: A Markov chain model for daily rainfall occurences at Tel Aviv. Quart. J. Roy, Meteor. Soc. 88, 90-95.

Leduc, R. 1977: The evolution of Montreal's precipitation: climate. Thèse de maîtrise, Université McGill.

Rodhe, H. et Grandell, J. 1972: On the removal time of aerosol particles from atmosphere by precipitation scavenging. Tellus, 24, 442-454.

Weiss, L.L. 1964: Sequences of wet or dry days described by a Markov chain probability model. Monthly Weather Rev., 92, 169-176.

## Annexe A. Solution d'un système des deux équations transcendentales à deux inconnues.

La série de Taylor à deux variables autour du point $(\alpha_0,\beta_0)$ nous fournit, en ne gardant que les termes du premier ordre.

$$f(\alpha,\beta) = f(\alpha_0,\beta_0) + (\alpha-\alpha_0) \left.\frac{\partial f}{\partial \alpha}\right|_{\substack{\alpha=\alpha_0\\ \beta=\beta_0}} + (\beta-\beta_0) \left.\frac{\partial f}{\partial \beta}\right|_{\substack{\alpha=\alpha_0\\ \beta=\beta_0}} \tag{A.1}$$

Nous avons deux équations pour lesquelles on désire connaître les valeurs ($\alpha$ et $\beta$) telles que l'on ait simultanément.

$$f_1\ (\alpha,\beta) = 0 \tag{A.2}$$

$$f_2\ (\alpha,\beta) = 0 \tag{A.3}$$

On fait l'expansion de Taylor de ces deux équations autour de $(\alpha_0,\beta_0)$.

$$0 = f_1\ (\alpha_0,\beta_0) + (\alpha-\alpha_0) \left.\frac{\partial f_1}{\partial \alpha}\right|_{\substack{\alpha=\alpha_0\\ \beta=\beta_0}} + (\beta-\beta_0) \left.\frac{\partial f_1}{\partial \beta}\right|_{\substack{\alpha=\alpha_0\\ \beta=\beta_0}} \tag{A.4}$$

$$0 = f_2\ (\alpha_0,\beta_0) + (\alpha-\alpha_0) \left.\frac{\partial f_2}{\partial \alpha}\right|_{\substack{\alpha\ \alpha_0\\ \beta\ \beta_0}} + (\beta-\beta_0) \left.\frac{\partial f_2}{\partial \beta}\right|_{\substack{\alpha=\alpha_0\\ \beta=\beta_0}} \tag{A.5}$$

Finalement,

$$\beta = \beta_0 + \frac{f_1 \frac{\partial f_2}{\partial \alpha} - f_2 \frac{f_1}{\partial \alpha}}{- \frac{\partial f_1}{\partial \beta} \frac{\partial f_2}{\partial \alpha} + \frac{\partial f_2}{\partial \beta} \frac{\partial f_1}{\partial \alpha}} \tag{A.6}$$

$$\alpha = \alpha_0 - \frac{(f_1 + (\beta-\beta_0) \frac{\partial f_1}{\partial \beta})}{\frac{\partial f_1}{\partial \alpha}} \tag{A.7}$$

Si on connaît $f_1$, $f_2$ et leurs dérivées à $(\alpha_0,\beta_0)$ on peut alors estimer $\alpha$ et $\beta$. Utilisant (3) et (4) et posant

$$\begin{aligned} f_1 = {} & (((1-\beta)^{m_{r1}} - \frac{N_{r1}}{N_1}) (\frac{1}{\alpha} - (m_{r1} + \frac{1}{\alpha}) (1-\alpha)^{m_{r1}}) \\ & + (\frac{N_{r1}}{N_1} - (1-\alpha)^{m_{r1}}) (\frac{1}{\beta} - (m_{r1} + \frac{1}{\beta}) (1-\beta)^{m_{r1}})) \\ & \div (((1-\beta)^{m_{r1}} - (1-\alpha)^{m_{r1}}) (1 - \frac{N_{r1}}{N})) - \bar{m}_1 \end{aligned} \tag{A.8}$$

$$f_2 = (((1-\beta)^{m_{r1}} - \frac{N_{r1}}{N_1}) \ (1-\alpha)^{m_{r1}} \ ( \frac{1}{\alpha} + m_{r1})$$

$$+ (\frac{N_{r1}}{N_1} - (1-\alpha)^{m_{r1}}) \ (1-\beta)^{m_{r1}} \ ( \frac{1}{\beta} + m_{r1}))$$

$$\div (\frac{N_{r1}}{N_1} \ ((1-\beta)^{m_{r1}} - (1-\alpha)^{m_{r1}})) - \overline{M}_1 \qquad \text{(A.9)}$$

$$\frac{\partial f_1}{\partial \alpha} = (((1-\beta)^{m_{r1}} - \frac{N_{r1}}{N_1}) \ ( \frac{1}{\alpha 2} \ (-1 + (1-\alpha)^{m_{r1}}) + m_{r1} \ (m_{r1} + \frac{1}{\alpha}) \ (1-\alpha)^{m_{r1}-1}) +$$

$$m_{r1} \ (1-\alpha)^{m_{r1}-1} \ ( \frac{1}{\beta} - (m_{r1} + \frac{1}{\beta} ) \times (1-\beta)^{m_{r1}})) \div (((1-\beta)^{m_{r1}} - (1-\alpha)^{m_{r1}})$$

$$(1 - \frac{N_{r1}}{N_1}))$$

$$- \frac{(f_1 + \overline{m}_1) m_{r1} \ (1-\alpha)^{m_{r1}-1}}{(1-\beta)^{m_{r1}} - (1-\alpha)^{m_{r1}}} \qquad \text{(A.10)}$$

$$\frac{\partial f_1}{\partial \beta} = ((\frac{N_{r1}}{N_1} - (1-\alpha)^{m_{r1}}) \ ( \frac{1}{\beta 2} \ (-1 + (1-\beta)^{m_{r1}}) + m_{r1} \ (m_{r1} + \frac{1}{\beta})$$

$$\times \ (1-\beta)^{m_{r1}-1}) - m_{r1} \ (1-\beta)^{m_{r1}-1} \ (\frac{1}{\alpha} - (m_{r1} + \frac{1}{\alpha}) \ (1-\alpha)^{m_{r1}}))$$

$$\div (((1-\beta)^{m_{r1}} - (1-\alpha)^{m_{r1}}) \ (1 - \frac{N_{r1}}{N}))$$

$$- \frac{(f_1 + \overline{M}_1) \ m_{r1} \ (1-\beta)^{m_{r1}}}{((1-\beta)^{m_{r1}} - (1-\alpha)^{m_{r1}})} \qquad \text{(A.11)}$$

$$\frac{\partial f_2}{\partial \alpha} = (((1-\beta)^{m_{r1}} - \frac{N_{r1}}{N}) \ (- m_{r1}(1-\alpha)^{m_{r1}-1} \ (\frac{1}{\alpha} + m_{r1})$$

$$- \frac{1}{\alpha 2} \ (1-\alpha)^{m_{r1}}) + m_{r1} \ (1-\alpha)^{m_{r1}-1} \ (1-\beta)^{m_{r1}} \ ( \frac{1}{\beta} + m_{r1}))$$

$$\div (\frac{N_{r1}}{N_1} \ ((1-\beta)^{m_{r1}} - (1-\alpha)^{m_{r1}}))$$

$$- \frac{(f_2 + \overline{M}_1) \ m_{r1} \ (1-\alpha)^{m_{r1}-1}}{((1-\beta)^{m_{r1}} - (1-\alpha)^{m_{r1}})} \qquad \text{(A.12)}$$

$$\begin{aligned}\frac{\partial f_2}{\partial \beta} = & - ((m_{r1}\ (1-\beta)^{m_{r1}-1}\ (1-\alpha)^{m_{r1}}\ (\ \frac{1}{\alpha} + m_{r1}) \\ & - (\frac{N_{r1}}{N_1} - (1-\alpha)^{m_{r1}})\ (m_{r1}\ (1-\beta)^{m_{r1}-1}\ (\ \frac{1}{\beta} + m_{r1}) \\ & + \frac{1}{\beta^2}\ (1-\beta)^{m_{r1}}))\ \div\ (\ \frac{N_{r1}}{N}\ ((1-\beta)^{m_{r1}} - (1-\alpha)^{m_{r1}}))) \\ & - \frac{(f_2+\overline{M}_1)\ m_{r1}\ (1-\beta)^{m_{r1}-1}}{(1-\beta)^{m_{r1}} - (1-\alpha)^{m_{r1}}} \qquad \text{(A.13)}\end{aligned}$$

On débute avec une valeur initiale pour $\alpha_0$ et $\beta_0$. On évalue ensuite $f_1$, $f_2$ et leurs dérivées à ce point à partir des équation (A.8) à (A.13). On calcule ensuite les nouvelles valeurs de $\alpha$ et $\beta$ à partir de (A.6) et (A.7). On peut continuer ce processus jusqu'à ce que l'on ait atteint la précision désirée.

# A MODEL FOR ESTIMATING STATIC STABILITY IN THE SURFACE AND PLANETARY BOUNDARY LAYERS FROM STANDARD HOURLY TEMPERATURE DATA

by

R.Verreault
and
L.Pérelman
Université du Québec à Chicoutimi
Chicoutimi, Quebec, G7H 2B1

Abstract: By taking advantage of the height dependence of the atmospheric thermal diffusivity, we present the theoretical basis and the experimental evidence for a simple and reliable method of obtaining the statistics of temperature gradients over a given site. The only needed data is the hourly screen-height temperature time series or, at worst, the climatological dayly maximum and minimum temperatures. The model can then be applied to establish both the annual and the diurnal stability regimes in the form usually needed for environmental impact studies about air polluting industries.

## INTRODUCTION

In implementing impact studies about air polluting installations, one usually needs statistical data on the atmospheric stability over the site of interest. When this information is not available, the use of indirect methods such as the Pasquill-Turner scheme (Pasquill, 1961; Turner, 1964) can be of some help. However, according to comparative studies by Luna and Church (1972), Portelli (1976) and Fulle (1976), one should not be too optimistic about the capabilities of the Pasquill-Turner method. Fulle suggests that the temperature gradient or the Richardson number should be more reliable for establishing stability classes. This paper develops a model for estimating temperature gradients in both the surface and planetary boundary layers from a minimum of surface meteorological information, namely the amplitude of the diurnal temperature wave. At worst, the climatological measurements of maximum and minimum temperatures may be sufficient.

## THEORETICAL BASIS

The heart of the present model rests on the height dependence of the turbulent and radiative diffusivities in the heat-transfer equation for the atmosphere

$$\frac{\partial\theta(z,t)}{\partial t} = \frac{\partial\bar{\theta}}{\partial t} + \frac{\partial\theta'}{\partial t} = \frac{\partial}{\partial z}\left[K(z,t)\frac{\partial\theta}{\partial z} + \frac{S\cos\zeta}{\rho c_p}\right] - a^2(\theta-\theta_N) \qquad (1)$$

where $\theta$ is the potential temperature; $\bar{\theta}$ is the daily mean of $\theta$, varying slowly from day to day due to advection and daily radiative unbalance; $K$ $(=K_t + K_r)$ is the sum of eddy diffusivity and radiative diffusivity for short range strongly absorbed infrared radiation; $S\cos\zeta$ is the solar radiation intensity at the height $z$ with the sun at zenith angle $\zeta$; $\theta_N$ is a reference potential temperature for long range exchange of weakly absorbed infrared radiation in the form $\sigma\bar{T}^3(T - T_N)$.

Kuo (1968) has solved the wave part of Eq. (1) for various diffusivity profiles in the air and in the ground. He also found some interesting features by considering the interaction between the diurnal wave of diffusivity

$$K(z,t) = \bar{K}(z) + \sum_{n=1}^{\infty} K_n(z)\cos nqt \qquad (2)$$

and the temperature wave, namely a net upward energy transfer with zero mean potential-temperature gradient. On rewriting Eq. (1) explicitely for $\partial\theta/\partial z$ and inserting the boundary conditions, all the variables can be expressed as products between their surface values $(\theta_o, S_o, \theta_{no})$ and various functions of height, namely

$$\frac{\partial\theta}{\partial z} = \frac{1}{\partial K/\partial z}\left\{\varphi_o(z)\left[\left(u\frac{\partial\bar{\theta}_o}{\partial x} + v\frac{\partial\bar{\theta}_o}{\partial y}\right) + h(\bar{\theta}_o - T_N) - S_o b_o\right]\right. \qquad (3a)$$

$$- \varphi_c(z)\sum_{n=1}^{\infty} K_{no}\frac{\partial\theta_{no}}{\partial z} \qquad (3b)$$

$$+ \sum_{n=1}^{\infty}\left\{\varphi_n(z)\,\theta_{no}\left[\sin(nqt - \alpha_n(z)) - \varphi_n'(z)\cos(nqt - \alpha_n(z))\right]\right. \qquad (3c)$$

$$\left.\left. + \sum_{\substack{m=1\\ m\neq n}}^{\infty} \varphi_{cm}(z)\,K_{no}\frac{\partial\theta_{mo}}{\partial z}\,\psi_{nm}(t)\right\}\right\} , \qquad (3d)$$

with all $\varphi_i > 0$ for $\dfrac{\partial K}{\partial z} > 0$ , and where $$\theta_{no} = \frac{S_o\, b_n \cos e_n}{(\lambda_n + \lambda_{en} + h)} \quad ; \qquad (4)$$

$b_n$, $e_n$ are the Fourier coefficient and phase of the $n^{th}$ harmonic of the surface solar radiation wave and the surface temperature wave, respectively;
$\lambda_n$, $\lambda_{en}$, h are the so-called "effective heat capacities" (Kuo, 1968) of the media energetically connected with the surface, respectively the boundary layer, the underground and the upper air.

In Eq. (3), the first part of Term (3a) represents the gradient contribution due to advection, especially important when $\theta_{no} = 0$ (heavy overcast). At mid-latitudes, it is generally stronger in winter than in summer, partly because of a lower $\partial K/\partial z$ in winter. Part 2 and 3 in Term (3a) form the net daily radiative balance. Both parts are in first approximation linearly dependent on $\theta_{no}$, the first one through Eq. (4) and the second one due to the fact that, with low $\theta_{no}$ (overcast), $T_N$ increases from 240 K to approximately the cloud-base temperature. Those two terms form together a non-periodic linear term in $\theta_{no}$.

Term (3b), due to the periodic part of K, brings a positive non-periodic contribution to $\partial\theta/\partial z$, since both factors are negatively correlated. Moreover, Kuo (1968) states that the periodic part of K is associated with the presence of an intense thermal boundary layer (hot summer days at O'Neill) while it is not needed to quantitatively explain the winter data at Leafield, England. On the other hand, our own experimental evidence at Mont Valin, near Chicoutimi, Que., also suggests the presence of a periodic part in K in winter by the strong night inversions of the Canadian cA air mass. In first approximation, one has then

$$K_n \propto \theta_{no} \quad . \qquad (5)$$

Applying perturbation theory to the wave part of Eq. (3) without variable K, one also finds

$$\frac{\partial\theta_{no}}{\partial z} \propto \theta_{no} \quad . \qquad (6)$$

Hence, Term (3b) brings a positive non-periodic quadratic contribution to $\partial\theta/\partial z$.

In Term (3c), the main influence comes from the negative cosinusoidal part. At O'Neill, for $z = 70$ m, $\varphi_1'(70) = 2{,}8$. The phase $\alpha_n$ being of the order $20^o$, this shifts the strongest negative temperature gradients into the afternoon hours.

Finally, Term (3d) is mainly quadratic in $\theta_{no}$ since the higher harmonics generally have large amplitudes at the same time as the first one. The Fourier terms

$$K_1 \frac{\partial\theta_2}{\partial z} \quad \text{and} \quad K_2 \frac{\partial\theta_1}{\partial z}$$

have periodic parts of the form

$$\cos(qt)\cos(2qt)$$

which retain a strong first-harmonic character.

By limiting the approximations to the first harmonic and to the second power in $\theta_{1o}$ , one should therefore be able to represent the potential-temperature gradient in the boundary layer by the statistical relation

$$\frac{\partial\theta}{\partial z} = F(\theta_{1o},t) + s(\sigma) \quad , \tag{7}$$

with

$$F(\theta_{1o},t) = a + (b + c\cos(qt - \alpha))\,\theta_{1o} + (d + e\cos(qt - \alpha))\,\theta_{1o}^2 \tag{8}$$

and $s(\sigma)$ being a gaussian statistical variable with standard deviation $\sigma$.

This model is not expected to hold in the very first few meters from the surface, since rapid transients (e.g. the passing of a fair-weather cumulus) produce an important high-harmonic content in the surface wave. Fortunately, however, the damping functions $\varphi_n(z)$ constitute a "low-pass filter" which, for a typical K-profile of the form

$$K(z) = K_o\,(z + z_o)^{4/3} \quad , \tag{9}$$

include the factors

$$\frac{n^{1/2}\; e^{-3\, n^{\frac{1}{2}}\,(z + z_o)^{1/3}}}{(z + z_o)} \quad .$$

According to the results of the next section, the model appears to be reasonably reliable above $z = 10$ m.

## RESULTS

### The Wangara experiment

The hourly screen-height temperature time series of the Wangara experiment has been analysed in relation to the routine three-hourly soundings in the surface layer between 50 and 100 m. Although heavy overcast conditions were practically absent from the observation period, linear regressions through the experimental data for the eight daily soundings all lead to negative gradients for $\theta_{1o} = 0$ . Fig. 1 and 2 show the two extreme cases at 1500 hr and 0300 hr, local time. They effectively correspond to different values of both the linear and the quadratic terms. The best fit of a single expression through the eight 3-hourly scatter diagrams available gives the following expression for the gradients in K/100m (cf. Fig. 3)

$$\begin{aligned} F(A,t) = 0{,}2 &- (0{,}138 + 0{,}090\cos(15t - 20^\circ))\,A \\ &+ (0{,}070 - 0{,}057\cos(15t - 20^\circ))\,A^2 \quad , \end{aligned} \tag{10}$$

where $t$ is measured in hours from local noon, and $A$ is an estimate of $\theta_{1o}$ obtained by computing at three-hour intervals the difference between the upper and lower envelopes of the screen-height temperature time series. In practice , the consecutive daily afternoon maxima were joined by straight lines, and so were the consecutive daily morning minima. Here, due to a lack of low-amplitude data in the Wangara experiment, we have arbitrarily assumed a zero - amplitude potential-temperature gradient of 0,2 K/100m . Our own measurements at Mont Valin give 0,2 K/100m in summer and 0,6 K/100m in winter.

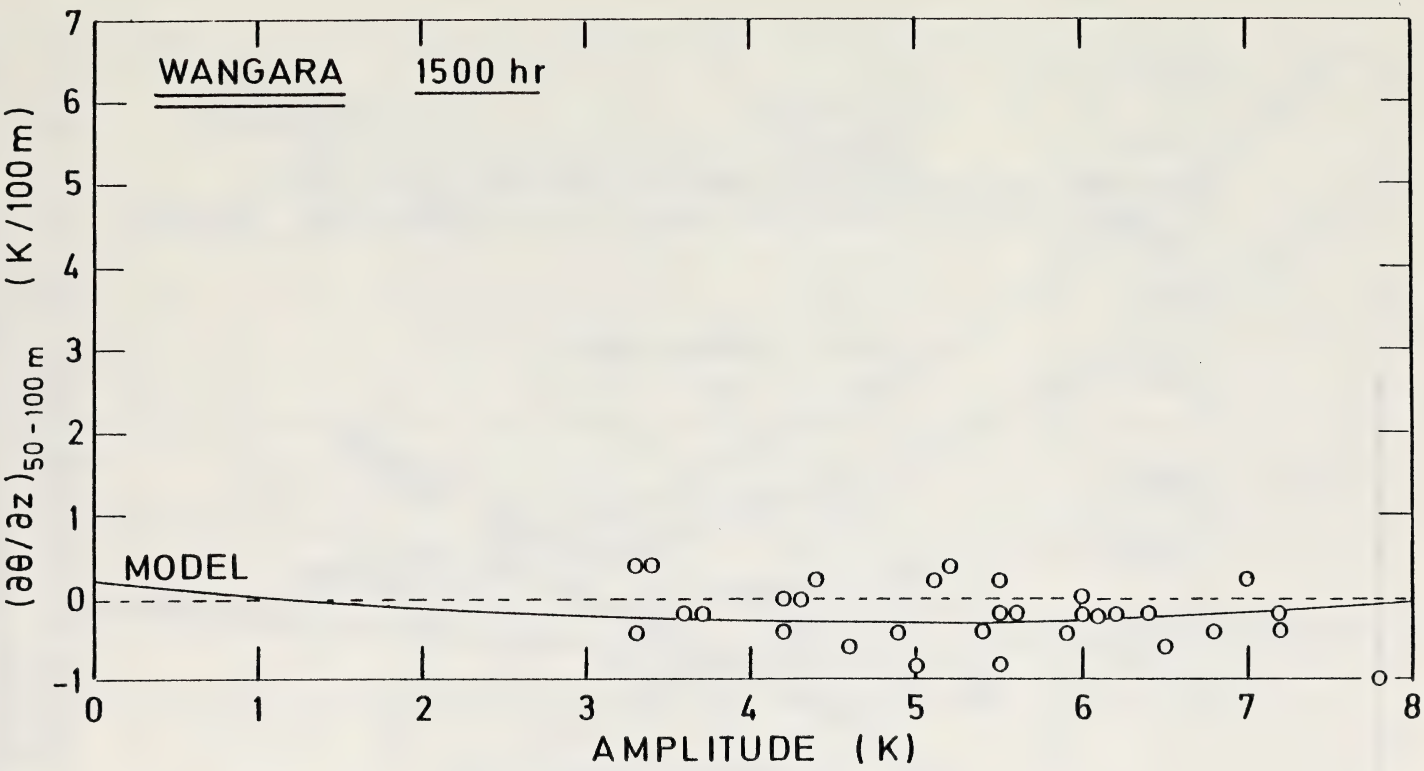

Fig. 1. Scatter diagram of the potential-temperature gradient at 1500 hr local time for the Wangara experiment, as a function of the amplitude of the diurnal temperature wave at screen height.

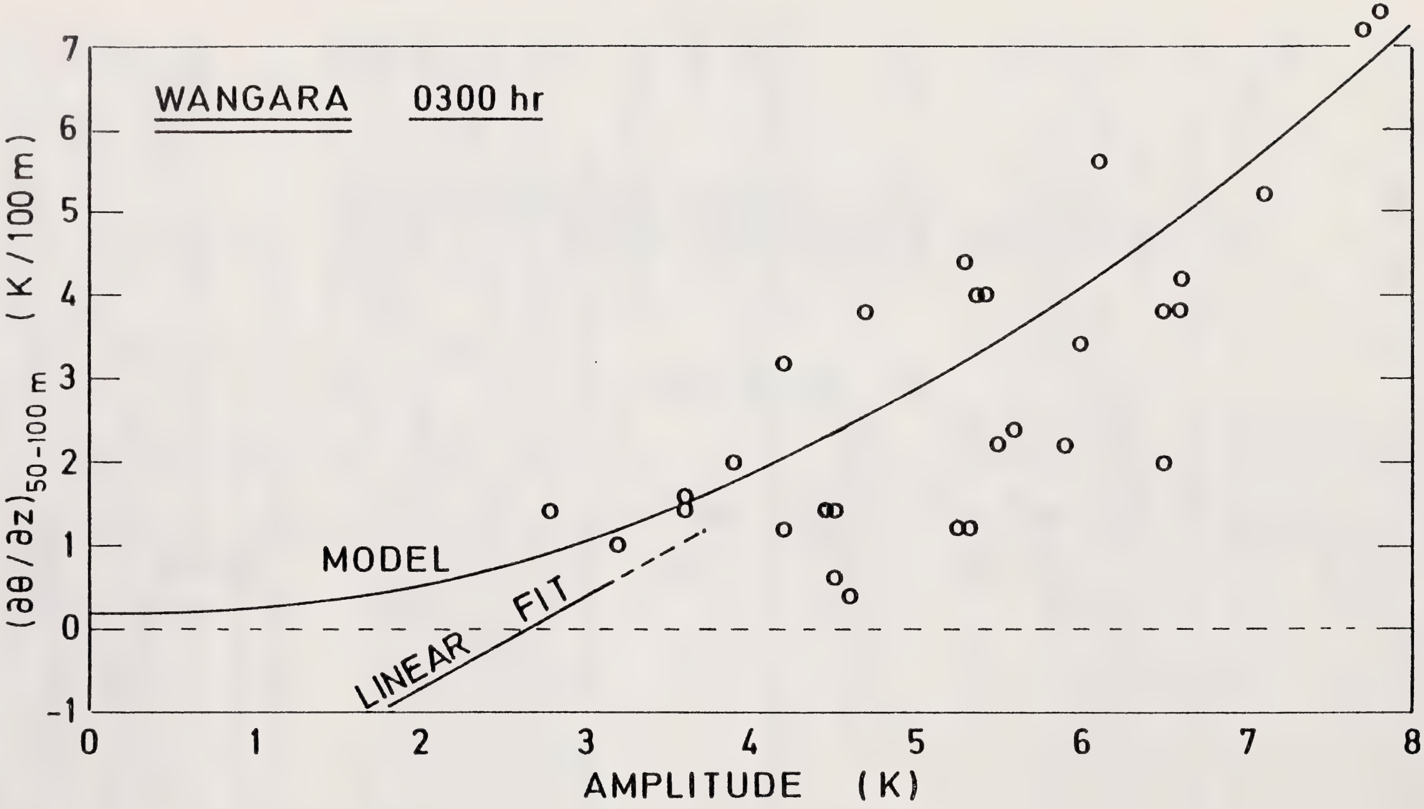

Fig. 2. Scatter diagram of the potential-temperature gradient at 0300 hr local time for the Wangara experiment, as a function of the amplitude of the diurnal temperature wave at screen height.

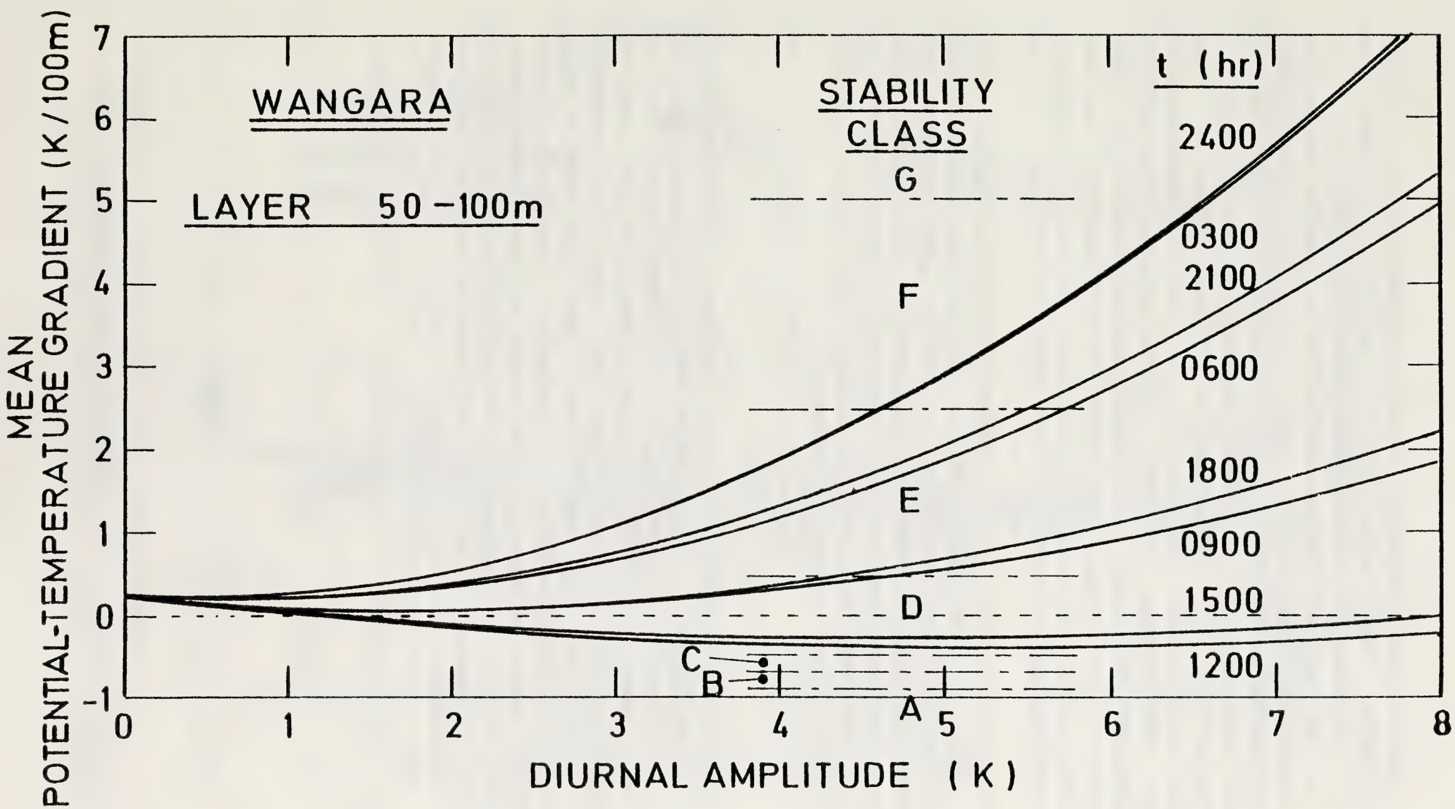

Fig. 3. Behaviour of the function $F(\theta_{1o},t)$ calibrated for the 50-100m layer with the data of the Wangara experiment, as given by Eq. (10).

## The Mont Valin data

Fig. 4 and 5 show the day and night scatter diagrams for the 10-700 m layer in August at Mont Valin. They include all the available hourly data from 0900 to 1700 EST incl. in daytime, and those from 2100 to 0500 EST incl. at night. The amplitude is the computed first-harmonic Fourier coefficient of the actual screen-height temperature time series. Again, there is a strong experimental evidence for the quadratic term in Eq. (8). Moreover, we found that the complete three-year time series can be reproduced by adding an annual periodic variation to the constants of Eq. (8). Regarding the diurnal variation, instead of using the simple cosinusoidal time function, we have analysed these data by dividing the day into four periods with mobile limits adjusted from month to month on the times of sunrise and sunset. The short morning and evening transition periods, 3 hours each in duration, show about 50% more scatter than those reported in Fig. 4 and 5, but they have little wheight in the whole gradient statistics. They can nevertheless be treated as the other two periods.

In accordance with the above theory suggesting that the higher levels of the boundary layer should be more closely related to the first harmonic $\theta_{1o}$ only, we found that the Mont Valin diagrams for the 10-700m layer show much less scatter than the corresponding ones for the 50-100m layer of the Wangara experiment. The average standard deviation from both regression curves amounts to 0,3 K/100m at Mont Valin, as compared to values ranging from 0,5 K/100m in daytime to 2 K/100m at night in the Wangara experiment.

## USE OF THE MODEL

In order to establish the annual and daily regimes of atmospheric stability, one first calibrates the model by analysing available sounding data, in an area close or similar to the one of interest, for two times during the day and for two groups of days showing different mean amplitudes. One then runs the model through the actual temperature time series of the closest hourly-reporting meteorological station to find the hourly variations of the first Fourier amplitude. The distribution of the computed potential-temperature gradients through the appropriate stability classes is done by first computing the standard deviation $\sigma$ of Eq. (7) from the scatter diagrams of the calibrating soundings, and then filling the stability classes, in the domain of potential-temperature gradients, with weighted "fractional" events according to the portion of the area under the bell-shaped curve of the statistical variable which falls within the limits $a_i$ and $b_i$ of a given stability class. Hence, the wheight of an event in the $i^{th}$ stability class is

$$W_i = (2\pi)^{-\frac{1}{2}} \int_{a_i}^{b_i} e^{-\frac{1}{2}\left(x(\theta_{1o},t)\right)^2} dx \quad , \tag{11}$$

where

$$x(\theta_{1o},t) = \sigma^{-1}\left(\frac{\partial\theta}{\partial z} - F(\theta_{1o},t)\right) \quad . \tag{12}$$

The final output is then the frequency of occurrence of each stability class at a given time (or time period) of the day and for a given month of the year.

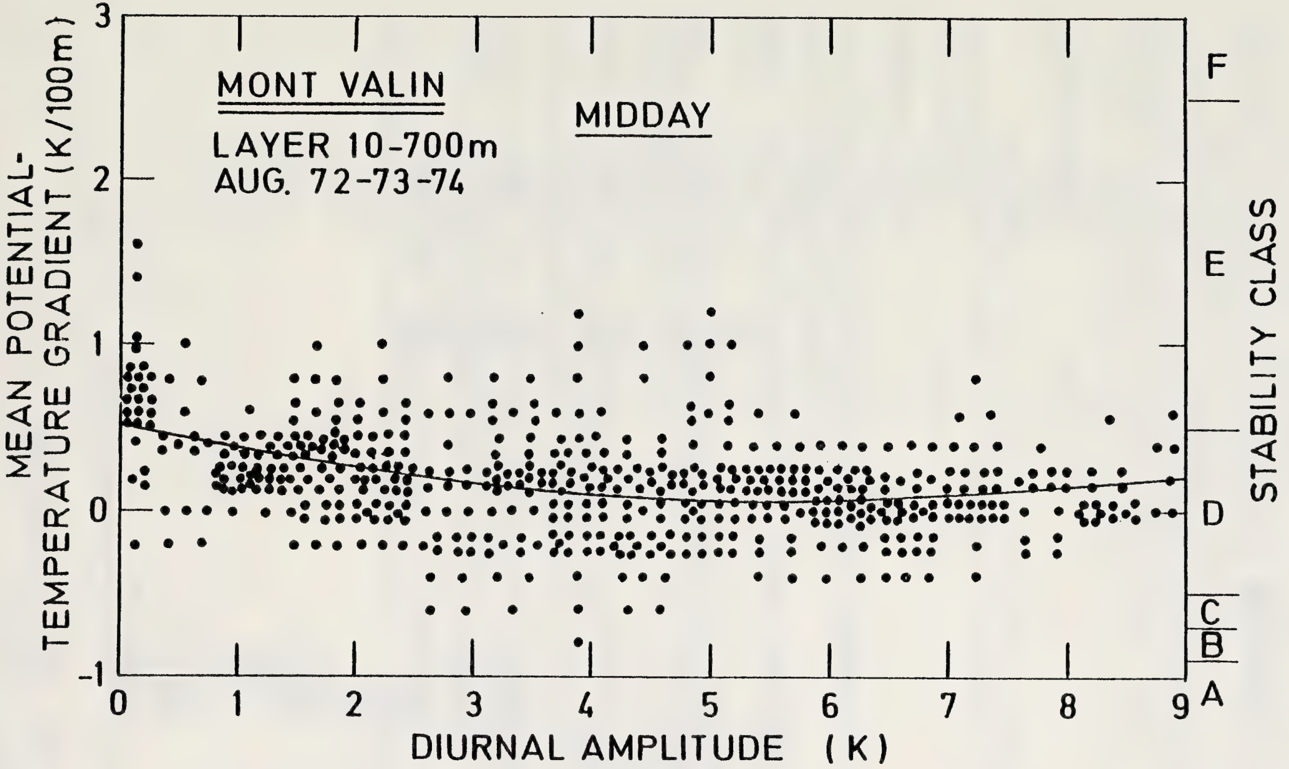

Fig. 4. Scatter diagram of the Mont Valin August data for the 10-700m layer and the time period running from 0900 to 1700 EST inclusively. The mean value of $\sigma$ about the regression curve is 0,32 K/100m.

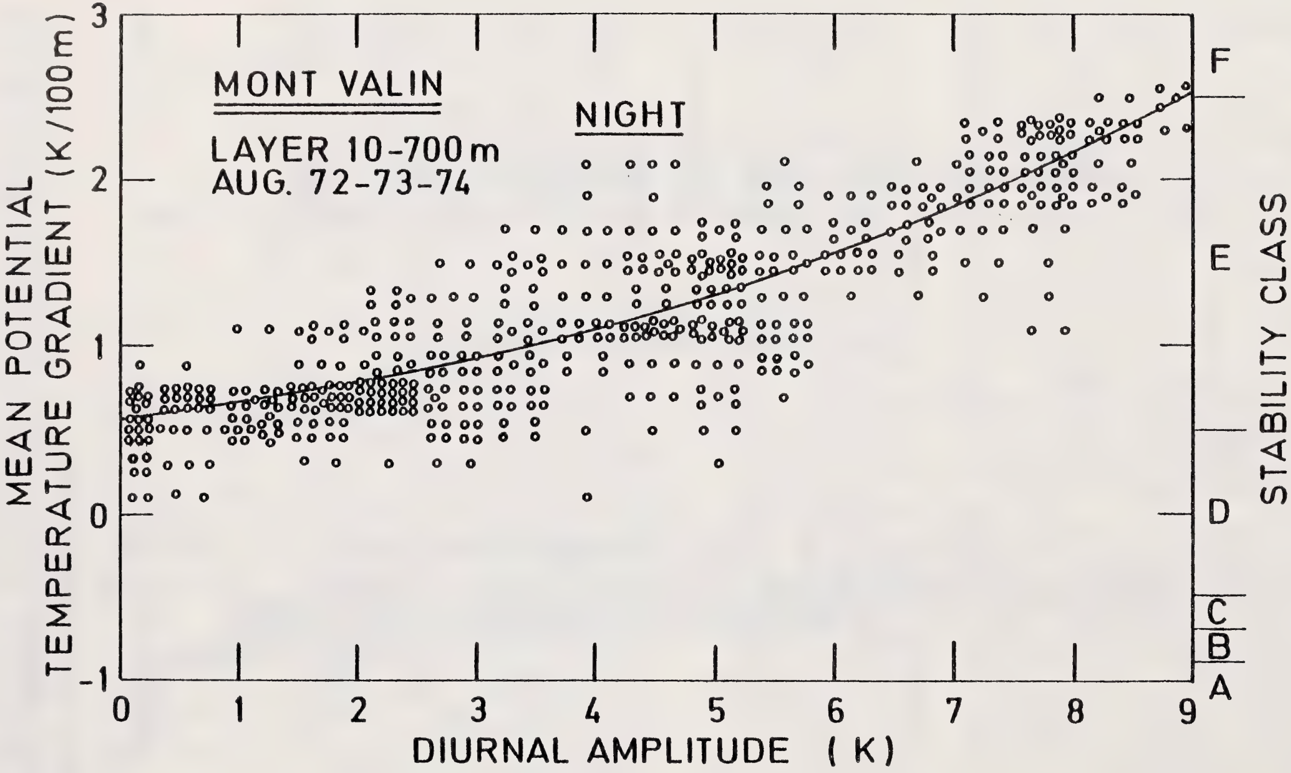

Fig. 5. Scatter diagram of the Mont Valin August data for the 10-700m layer for the time period running from 2100 to 0500 EST inclusively. The mean value of $\sigma$ about the regression curve is 0,31 K/100m.

## CONCLUSION

By taking advantage of the height dependence of the atmospheric thermal diffusivity, we have presented in this paper the theoretical basis and the experimental evidence for a simple and reliable method of obtaining the statistics of temperature gradients over a given site. The model can then be applied to the determination of both the annual and the diurnal stability regimes in the form usually required for environmental impact studies about air polluting installations. The accuracy of these results should allow us to proceed one step further and estimate the corresponding mixing height regimes.

## ACKNOWLEDGEMENTS

The authors are grateful to the Société de Chimie et d'Electrolyse ALCAN Ltée and to the Fondation de l'Université du Québec à Chicoutimi for financial support.

## REFERENCES

Pasquill, F., 1961: "The estimation of the dispersion of windborne material". Meteor. Mag. 90, pp 33-49.

Turner, D.B., 1964: "A diffusion model for an urban area". J. Appl. Meteor. 3, pp 83-91.

Luna, R.E. and Church, H.W., 1972: "A comparison of the turbulence intensity and stability ratio measurements to Pasquill stability classes". J. Appl. Meteor. 11, pp 663-669.

Portelli, R.V., 1976: "A comparative study of experimentally measured atmospheric stability and "Star Program" predictions". Proc. 3rd Symposium on Atmospheric Turbulence, Diffusion and Air Quality, Oct. 76, Raleigh, N.Car., USA, pp 124-129.

Fulle, D., 1976: "A comparison of three stability classification systems using surface and radiosonde data for four cities in the Western United States". Proc. 3rd on Atmospheric Turbulence, Diffusion and Air Quality, Oct.76, Raleigh, N.Car., USA, pp 141-148.

Kuo, H.L., 1968: "The thermal interaction between the atmosphere and the earth and propagation of diurnal temperature waves". J. Atmos. Sci. 25, pp 687-706.

# A LONG-RANGE CLIMATOLOGICAL DISPERSION MODEL (LRCDM)

by

C.S. MATTHIAS
A.K. LO
Atmospheric Environment Service,
Downsview, Ontario, M3H 5T4

Abstract: The long-range and long-term transport of pollutants from a localized source to a receptor can be described as a diffusion problem in which the diffusion elements or eddies consist of the large scale synoptic weather systems. If we assume that the pollutants (1) are uniformly distributed in the vertical direction, (2) drift with the vector mean wind, and (3) undergo dispersion, deposition, and chemical change in a uniform mean annual meteorological field, the problem can be solved analytically.

By applying this model to several sources and by superimposing the contributions to the receptors, the pollutant distribution of air and ground (deposition) patterns over North America are examined for the transport of $SO_2$ and $SO_4$.

## INTRODUCTION

The LRCDM is a Long Range Climatological Diffusion Model and is a modified version of the model described by Fay and Rosenzweig (1980). We will examine the LRCDM and its ability to model the long-term $SO_2$ and $SO_4$ concentrations fields and deposition patterns resulting from a distribution of pollutant sources spread across North America. The source distribution has been prepared by the Long Range Transport group at the Atmospheric Environment Service (AES) and is described in a report by Voldner and Shah (1979). The sources are given in terms of tonnes per year of $SO_2$, $NO_2$, and total suspended particulates (TSP) for each square of the LRTAP grid system. The grid is fitted over a polar stereographic projection of North America and is described in more detail in a report by Matthias and Lo (1981). The grid length is 127 km.

The equation which describes the long-term or climatological concentration field of the primary pollutant emanating from a point source is an analytical solution of a two-dimensional diffusion equation. The source is assumed to be at the center of a grid square, with the pollutant becoming immediately uniformly mixed in the vertical direction. The pollutant undergoes chemical transformation and deposition as it advects and diffuses. Chemical transformation occurs by a simple first order process with a constant rate coefficient.

A second analytical solution describes the evolution of the secondary pollutant. Both primary and secondary pollutants are depleted by wet and dry deposition characterized by constant rate coefficients.

The multiple source model consists of the superposition of solutions of dispersion from many sources. All $SO_2$ sources within each 127 km grid square are considered as emanating from the center of the square. Receptors are located at the corners of each square. A typical run has 3025 receptors and requires about 180 seconds of CPU time on a Cyber 7600 computer.

Within this report, we examine:

1) the equations describing the advection, dispersion, transformation, and deposition of a pollutant on a continental scale.

2) a comparison of LRCDM annual concentrations and deposition estimates with measured values for $SO_2$ and $SO_4$.

3) a comparison of LRCDM model results with those of other long-term models.

## THE FAY AND ROSENZWEIG MODEL

A variety of models exists for the purpose of estimating pollutant concentrations and deposition patterns in long range transport studies. For the purpose of calculating climatological or long-term means (seasonal and annual), the analytical model of Fay and Rosenzweig (1980) offers an agreeable combination of simplicity, economy, and accuracy. It represents the net effect of a plume carried by the wind in all directions during a season as a diffusive process described by a horizontal diffusivity D, and transported by a vector mean wind having a speed U and a direction $\alpha$. Ideally, D, U, and $\alpha$ are independent of position within the region of application. Similarily, other meteorological parameters appearing in the formulae should be time - as well as space-independent. These are the mixing height h, the primary pollutant decay time $\tau_p$, and the secondary pollutant decay time $\tau_s$. Decay of both pollutants occurs by dry and wet deposition, and by chemical change for the primary pollutant.

The equations describing the primary pollutant $C_p$ and the secondary pollutant $C_s$ emanating from a point source having an emission rate Q are:

$$C_p = \frac{Q}{2\pi h D} \exp\left(\frac{Us}{2D}\right) K_o\,(\gamma r) \tag{1}$$

$$C_s = \frac{\beta Q}{2\pi h D^2 \bar{\tau}_c} \exp\left(\frac{Us}{2D}\right) \frac{K_o(\gamma r) - K_o(\alpha r)}{\alpha^2 - \gamma^2} \tag{2}$$

where

$$\alpha^2 = \left(\frac{1}{\bar{\tau}_s D} + \frac{U^2}{4D^2}\right) \tag{3}$$

$$\gamma^2 = \left(\frac{1}{\bar{\tau}_p D} + \frac{U^2}{4\,D^2}\right) \tag{4}$$

$$\bar{\tau}_p^{-1} = \bar{\tau}_{pd}^{-1} + \bar{\tau}_{pw}^{-1} + \bar{\tau}_c^{-1} \tag{5}$$

$$\bar{\tau}_s^{-1} = \bar{\tau}_{sd}^{-1} + \bar{\tau}_{sw}^{-1} \tag{6}$$

$$r^2 = s^2 + t^2$$

In these equations, $\beta$ is the mass ratio of the molecular weights of secondary to primary pollutants, $\bar{\tau}_{id}$ and $\bar{\tau}_{iw}$ are the decay times for dry and wet deposition respectively for species i, and $\bar{\tau}_c$ is the decay time for chemical change from primary species to secondary species. The decay times are constants and describe first order processes. The parameters s, t, and r are the streamwise distance, the crosswind distance, and the rectilinear distance from source to receptor.

Equations (1) and (2) describe concentrations of pollutants as they evolve within a mean meteorological field. It is a field in which dry and wet deposition and chemical reactions occur continuously at constant rates for the entire time period of interest. These mean rates $\bar{\tau}^{-1}$ can be estimated from a knowledge of $T_D$ and $T_W$, the total time in seconds of dry and wet periods respectively. We can then write, using $T = T_D + T_W$,

$$\bar{\tau}_{iw}^{-1} = \frac{T_W}{T} \tau_{iw}^{-1} \qquad (7)$$

$$\bar{\tau}_{c}^{-1} = \frac{T_W \tau_{cW}^{-1} + T_D \tau_{cD}^{-1}}{T} \qquad (8)$$

Here $\tau_{iw}^{-1}$ is the mean wet removal rate during a precipitation event, and $\bar{\tau}_{cW}^{-1}$ and $\tau_{cD}^{-1}$ are the mean reaction rates during wet and dry periods respectively. If $\tau_{iw}^{-1}$ is expressible in terms of rainfall rate J, then a mean rainfall rate for the year will give a mean value of $\bar{\tau}_{iw}^{-1}$ for the year. Since dry deposition rates are assumed to be unaffected by rainfall, we have:

$$\bar{\tau}_{id} = \tau_{id} \qquad (9)$$

The ground concentration $G_i$ is the amount of pollutant i deposited on a square meter of surface by dry and wet processes in a time period T (number of seconds in a season or a year). Considering the dry depostion of the primary pollutant, the removal rate per unit volume is $\bar{\tau}_{pd}^{-1} C_p$. Multiplying by h, we have the removal rate per square meter from the mixed layer. Multiplying by T gives the ground concentrations $G_{pd}$ in a period T. In general we can write:

$$G_{pd} = \bar{\tau}_{pd}^{-1} C_p hT \qquad (10)$$

$$G_{pw} = \bar{\tau}_{pw}^{-1} C_p hT \qquad (11)$$

$$G_{sd} = \bar{\tau}_{sd}^{-1} C_s hT \qquad (12)$$

$$G_{sw} = \bar{\tau}_{sw}^{-1} C_s hT \qquad (13)$$

where $G_{id}$ and $G_{iw}$ are the mass per square meter of species i deposited on the ground by dry and wet processes, respectively, in a time T.

The philosophy so far has been to first define a mean atmospheric state and then to calculate the concentrations for that state using Eqs. (1) and (2). The mean atmospheric state in this case was decided by a combination of two processes: rain, and no rain.

## MODIFIED FAY AND ROSENZWEIG MODEL

A more meaningful way of arriving at a climatological average concentration is to calculate the concentration for each meteorological state and then to determine the mean of the concentrations. For the two atmospheric states, wet and dry, we have:

$$\bar{C}_p = \frac{T_W C_{pW} + T_D C_{pD}}{T} \tag{14}$$

$$\bar{C}_s = \frac{T_W C_{sW} + T_D C_{sD}}{T} \tag{15}$$

where $C_{iD}$ amd $C_{iW}$ are the mean concentrations for species i during dry and wet conditions. Using Eqs. (1) and (2) with the appropriate dry and wet decay times, we have:

$$C_{pD} = \frac{Q}{2\pi h D} \exp\left(\frac{Us}{2D}\right) K_o(\gamma_D r) \tag{16}$$

$$C_{pW} = \frac{Q}{2\pi h D} \exp\left(\frac{Us}{2D}\right) K_o(\gamma_W r) \tag{17}$$

$$C_{sD} = \frac{\beta Q}{2\pi h D^2 \tau_{cD}} \exp\left(\frac{Us}{2D}\right) \frac{K_o(\gamma_D r) - K_o(\alpha_D r)}{\alpha_D^2 - \gamma_D^2} \tag{18}$$

$$C_{sW} = \frac{\beta Q}{2\pi h D^2 \tau_{cW}} \exp\left(\frac{Us}{2D}\right) \frac{K_o(\gamma_W r) - K_o(\alpha_W r)}{\alpha_W^2 - \gamma_W^2} \tag{19}$$

where

$$\alpha_D^2 = \left(\frac{1}{\bar{\tau}_{sD} D} + \frac{U^2}{4D^2}\right), \qquad \alpha_W^2 = \left(\frac{1}{\bar{\tau}_{sW} D} + \frac{U^2}{4D^2}\right) \tag{20}$$

$$\gamma_D^2 = \left(\frac{1}{\bar{\tau}_{pD} D} + \frac{U^2}{4D^2}\right), \qquad \gamma_W^2 = \left(\frac{1}{\bar{\tau}_{pW} D} + \frac{U^2}{4D^2}\right) \tag{21}$$

$$\bar{\tau}_{pD}^{-1} = \tau_{pd}^{-1} + \tau_{cD}^{-1}, \qquad \bar{\tau}_{pW}^{-1} = \tau_{pd}^{-1} + \tau_{pw}^{-1} + \tau_{cW}^{-1} \tag{22}$$

$$\bar{\tau}_{sD}^{-1} = \tau_{sd}^{-1}, \qquad \bar{\tau}_{sW}^{-1} = \tau_{sd}^{-1} + \tau_{sw}^{-1} \tag{23}$$

In order to calculate the ground concentration within a time period T, we have:

$$G_{pd} = \tau_{pd}^{-1} \; C_{pD} \; h \; T_D + \tau_{pd}^{-1} \; C_{pW} \; h \; T_W \tag{24}$$

$$G_{pw} = \tau_{pw}^{-1} \; C_{pw} \; h \; T_W \tag{25}$$

$$G_{sd} = \tau_{sd}^{-1} \; C_{sD} \; h \; T_D + \tau_{sd}^{-1} \; C_{sW} \; h \; T_W \tag{26}$$

$$G_{sw} = \tau_{sw}^{-1} \; C_{sW} \; h \; T_W \tag{27}$$

where $G_{id}$ and $G_{iw}$ are surface concentrations of species i deposited by dry and wet processes, respectively, during a time T.

## A COMPARISON OF THE TWO MODELS

Let us name the Fay and Rosenzweig model as FR, and the modified version as LRCDM. The basic differences are that in FR, the meteorological parameters are averaged and then entered into the concentration equations. In LRCDM, concentrations are found for each meteorological condition (dry and wet) and are then averaged. Since the latter approach is more correct, let us examine the deviation of FR from LRCDM. We can simplify the task by considering Gaussian models, which are an asymptotic form of Eqs (1) and (14) and which should give qualitatively similar results. Retaining only an exponential decay term explicitly, we have, for the primary pollutant,

$$C_p(1) = C_{po} \exp\left(-\bar{\lambda}\, x/U\right) \qquad \text{(FR)} \tag{28}$$

$$\bar{C}_p\,(2) = \frac{T_W \, C_{po} \exp\left(-\bar{\lambda}_W x/U\right) + T_D \, C_{po} \exp\left(-\bar{\lambda}_D x/U\right)}{T} \qquad \text{(LRCDM)} \tag{29}$$

In these equations, $C_{po}$ comprises terms common to both equations, and

$$\bar{\lambda} = \bar{\tau}_p^{-1}, \quad \bar{\lambda}_W = \bar{\tau}_{pW}^{-1}, \quad \bar{\lambda}_d = \bar{\tau}_{pD}^{-1} \tag{30}$$

If we choose $T_W$ = 19 days, $T_D$ =346 days, U = 2.5 $ms^{-1}$, $\tau_{pw} = 10^4$ sec, and $\tau_{cW} = \tau_{cD} = \infty$, we find

$$\frac{\overline{C_p}\ (2)}{C_p\ (1)} \simeq \exp\left(\frac{T_W\ x}{T\ \tau_{pw}\ U}\right) \simeq \exp\left(\frac{x}{500 \times 10^3}\right)$$

It is evident that $C_p$ (1) is significantly smaller than $\overline{C_p}$ (2) for x larger than 500 km. Similarily for ground concentrations due to deposition, we find;

$$\frac{G_{pd}\ (2)}{G_{pd}\ (1)} \simeq \exp\left(\frac{T_W\ x}{T\ \tau_{pw}\ U}\right) \simeq \exp\left(\frac{x}{500 \times 10^3}\right)$$

$$\frac{G_{pw}\ (2)}{G_{pw}\ (1)} \simeq \exp\left(\frac{-x}{\tau_{pw}U}\right) \simeq \exp\left(\frac{-x}{25 \times 10^3}\right)$$

These ratios show that FR greatly underestimates dry deposition beyond 500 km and greatly overestimates wet deposition beyond 25 km.

These results apply to a single source. As the distance x from the source diminishes, the two model results approach each other. If the models are applied to a region with a high density of sources, the receptor may never be far from a source which dominates the pollutant input to the receptor. In this case, the differences between FR and LRCDM will be small. The differences should become more apparent for receptors located in large source - free areas, especially for wet deposition.

## PROPOSED APPLICATION OF LRCDM TO NORTH AMERICA

Using the modified Fay and Rosenzweig model, a multiple source version is being developed and is suitable for application to any continental-sized region. Ideally, the model requires that the vector mean wind speed and direction, the mixing height, and transformation and deposition parameters remain constant over the domain of application of the model. In reality, all these parameters vary across the continent. However, because the model concentrations are a maximum near the source and drop off rapidly with distance, source-oriented meteorological parameters are most suitable within this region of maximum impact. Far from the source in a region where the meteorology is different, the concentrations, although in error, will be small.

Let us examine the length scales of interest. Firstly, we are limited in how close to the source we can utilize the concentration equation because of the assumption that the pollutant is uniformly mixed within a height h. The distance from the source at which uniform vertical mixing occurs can be estimated from the Workbook of Atmospheric Dispersion Estimates (Turner, 1970). If the mean atmospheric stability is a Pasquill D category, then a 100 km travel distance may be required to achieve a uniform vertical distribution in 1 km mixed layer.On the other hand, the wet deposition expressions $G_{pw}$ and $G_{sw}$ are valid at any distance since the amount of material washed out of the plume is proportional to the vertically - integrated concentration, regardless of the distribution.

Since all regional sources are assumed to be emitting from the center of a 127 km square grid, the uncertainty in source location is of the order of 60 km. These considerations indicate that nearest receptors need be no closer than the corners of the grid square which contains the source. These modelling approximations limit the spatial resolution of any concentration estimate to the order of one grid length. Model estimates should therefore be compared with measurements that have been averaged over the same area, i.e., over a 100 km square.

The distances beyond which the concentrations become relatively small can be estimated from Eqs. (16) to (19). These characteristic lengths are given by $\gamma_D^{-1}$, $\gamma_W^{-1}$, $\alpha_D^{-1}$, and $\alpha_W^{-1}$. Choosing typical $SO_2$ and $SO_4$ decay times $\tau_{ij}$ from Venkatram (1981), we have $\tau_{pd} = 2 \times 10^5$, $\tau_{sd} = 2 \times 10^6$, $\tau_{pw} = 3 \times 10^4$, $\tau_{sw} = 10^4$, and $\tau_{cD} = \tau_{cW} = 3.6 \times 10^5$. Using $D = 6 \times 10^5$ and $U = 3.5$ from Fay and Rosenzweig (mks units), we find;

$$\gamma_D^{-1} = 220 \text{ km}$$

$$\gamma_W^{-1} = 110 \text{ km}$$

$$\alpha_D^{-1} = 330 \text{ km}$$

$$\alpha_W^{-1} = 75 \text{ km}$$

Hence the characteristic lengths for the overall decay of $SO_2$ during dry and wet conditions are 220 km and 110 km respectively. For $SO_4$, the decay of C with distance as given by Eqs. (18) and (19) depends on the relative sizes of $\gamma$ and $\alpha$ but is of the same order as for $SO_2$.

These length scales are characteristic decay distances due to combined processes of diffusion, deposition, and transformation. For a long-lived particle which undergoes only diffusion, the charcteristic decay scale is

$$\gamma^{-1} = \frac{2D}{U} = 340 \text{ km}$$

These order-of-magnitude arguments imply that the model requires the meteorological parameters to remain constant over a distance of 300-400 km at least. The minimum distance over which we need to define these parameters is then about 3 grid lengths or 381 km. The major part of North America can be covered by 15 x 15 of these meteorological grids. Two dimensional arrays can be prepared for U, $\alpha$, h, D, $T_W$, $T_D$ and the rainfall rate J. The latter array is required since the washout times $\tau_{pw}$ and $\tau_{sw}$ are in general rainfall-rate dependent. Meteorological arrays can be prepared for each season as well as for the annual case.

Intuitively, the amount of material $G_{iw}$ washed into a receptor is proportional to the local rainfall rate J and to the local annual duration of rainfall $T_W$. Although not entirely consistent with the theory which requires a constant $T_W$ over the domain of interest, it may be useful to use receptor values of $T_W$ and $T_D$ rather than source values for only the depostion equations (24) to (27) (Machta, 1979).

## MODEL RESULTS

### Application of FR to Eastern North America

The goals for LRCDM remain for future development. Initial runs have so far been applied to only eastern North America using the FR model with constant meteorological parameters over the entire domain. Fortunately the parameters describing the mean meteorology are more uniform over this region than over central or western North America. Furthermore, this region contains the largest number of sources and monitors. By applying the model using a simple meteorological field and by evaluating its accuracy using measured data, we can repeat the analysis using more complex meteorological fields and determine whether or not the quality of the output improves in proportion to the complexity of the input.

The run reported here uses meteorological parameters direct from the literature. The parameters are those used by Venkatram (1981) and by Fay and Rosenzweig (1980). Annual averages for air and ground concentrations are compared to other model results and to measured data. No attempt was made to modify the input parameters so as to improve the correlation of modelled and measured data.

The basic input parameters are:

$h = 1000\ m$
$U = 3.2\ m\ s^{-1}$
$D = 6.4 \times 10^5\ m^2\ 5^1$
$\omega = 270°$
$T_D = 2.7 \times 10^7\ s$
$T_W = 4.2 \times 10^6\ s$

$\tau_{cD} = 3.6 \times 10^5\ s$
$\tau_{pw} = 3.3 \times 10^4\ s$
$\tau_{pd} = 2.0 \times 10^5\ s$
$\tau_{sw} = 1.0 \times 10^4\ s$
$\tau_{sd} = 2.0 \times 10^6\ s$
$\tau_{cW} = 3.6 \times 10^5\ s$

from which the FR parameters are found to be;

$\bar{\tau}_{pd} = 2.0 \times 10^5\ s$
$\bar{\tau}_{pw} = 2.5 \times 10^5\ s$
$\bar{\tau}_{sd} = 20. \times 10^5\ s$
$\bar{\tau}_{sw} = .77 \times 10^5\ s$

$\bar{\tau}_c = 3.6 \times 10^5\ s$
$\bar{\tau}_p = .85 \times 10^5\ s$
$\bar{\tau}_s = .74 \times 10^5\ s$

A single run was made using these input parameters and the North American source inventory. The output consists of grid-point calculations of annual average concentrations of $SO_2$ and $SO_4$ and the ground deposition concentration of sulphur due to dry processes, and due to wet processes.

Figure 1a shows isopleths of $SO_2$ in $\mu g\ m^{-3}$, ranging from a high value in the mid 40's in southern Ohio to a value of 5 over Lake Superior, Nova Scotia, and Florida. Most of the $SO_2$ data which has been gathered is from cities and over-estimates the mean concentration within a grid square. Using the two data isopleths presented in Fay and Rosenzweig (1980), we find that the 30 $\mu g\ m^{-3}$ data contour coincides approximately with our 10 to 20 $\mu g\ m^{-3}$ model contours. Dimples in the model contours are produced by large sources in otherwise weak source areas, such as in Florida and in Northern Ontario.

Figure 1b shows isopleths of sulphate air concentration in $\mu g\ m^{-3}$, ranging from a high of 9 or 10 in West Virginia to a value of 1 over Lake Superior, Cape Breton Island and southern Florida. Note that the sulphate contours are much smoother than the $SO_2$ contours. The irregularities in the $SO_2$ contours reflect the irregularities in the source distribution. The sulphate reaction product, on the other hand, tends to grow in absolute number with distance from the source but decreases in concentration due to dispersion. The net effect is to maintain sulphate concentrations more uniform than $SO_2$ concentrations. Some sulphate measurements are presented in a Memorandum of Intent (1981). They are far more irregular than the modelled output but range from a high of 8.8 in southern Ohio to values of 3 in Michigan and Maine which agrees very well with the model results.

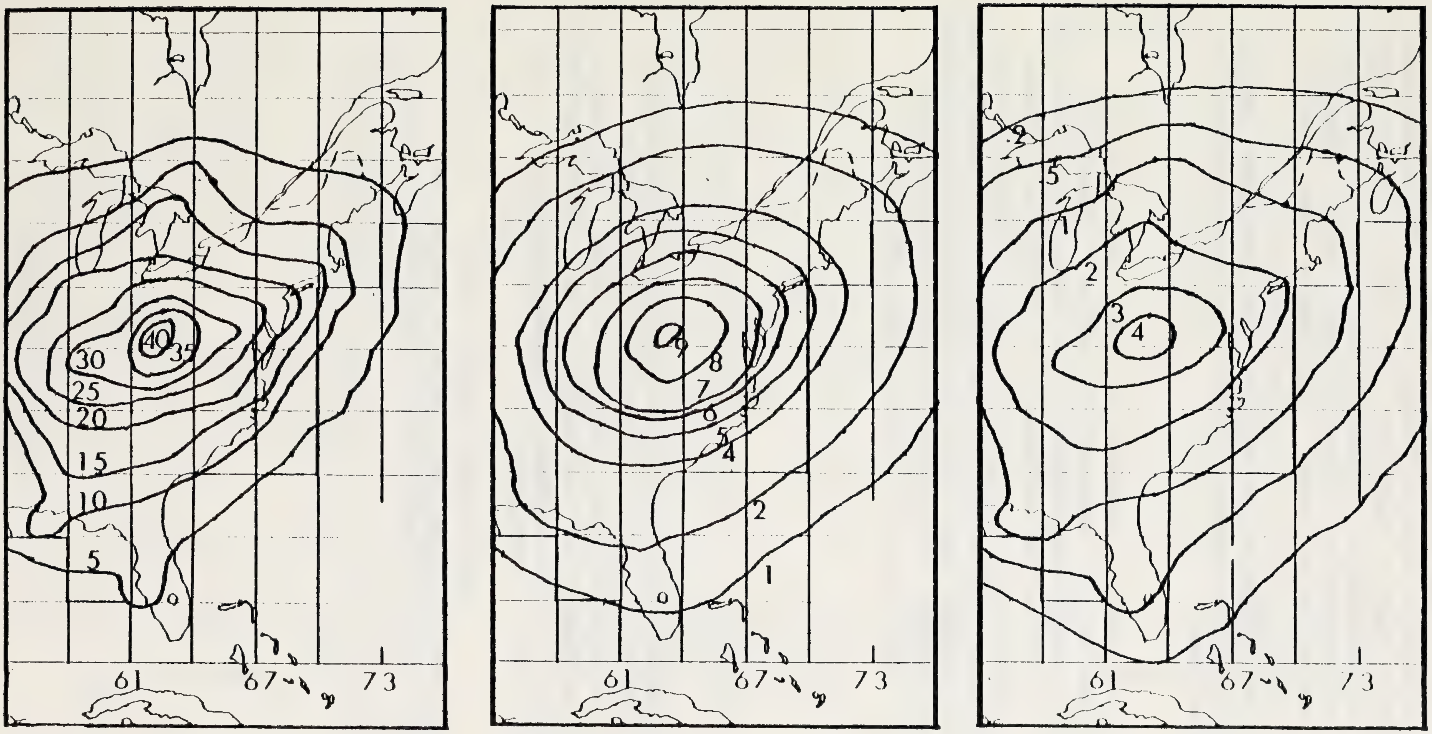

1a SO$_2$ Isopleths ($\mu g\ m^{-3}$)

1b SO$_4$ Isopleths ($\mu g\ m^{-3}$)

1c Sulphur Deposition by Wet Removal ($g\ m^{-2} yr^{-1}$)

Figure 1. Annual average air and ground concentration isopleths resulting from the FR model applied to eastern North America

The modelled values of annual surface concentration of total sulphur removed to the earth's surface by wet deposition are shown in Figure 1c. These contour shapes are similar to those of Figure 1a since $SO_2$ contributes more to the sulphur deposition than do sulphates. Although the washout rate for sulphates is larger, the sulphate air concentrations are smaller and the fraction of sulphur in each particle is smaller. A sample of wet sulphur deposition data from the Memorandum of Intent (1981) shows a very irregular distribution with highs of 7.6 g $m^{-2}$ $yr^{-1}$ in northern Indiana, 5.9 in Massachusetts, and 4.0 in West Virginia. Along the eastern seaboard, values are of order 1. The high values are probably reported by monitors which are relatively close to a large source.

Figure 2 gives a qualitative assessment of model performance by comparing the results of 3 models with measured $SO_4$ data at 7 receptor points. All the models are roughly comparable in their ability to cluster the computed values near the line of perfect agreement. The FR results (Figure 2a) slightly underpredict the data. The MOE model results (Figure 2b) seem slightly better in that although the scatter is comparable, the points lie on both sides of the perfect agreement line. The A.E.S. trajectory model results are similar but tend to overpredict the data values (Figure 2c). A more comprehensive assessment of the FR model will await a more extensive comparison with data.

## CONCLUSIONS

The analytical model developed by Fay and Rosenzweig seems to be a very simple, economical, and useful tool for estimating annual average concentration and deposition patterns over a continental area. The results compare favourably with other models and with measured data. No attempt has yet been made to tune the model so as to improve agreement with data. Only the simplest meteorological input is required.

The model is being modified with the hope of improving the correlation with data and to utilize a more detailed meteorological input in order to calculate the pollutant distribution over a larger fraction of North America. This modified version, referred to as LRCDM in this paper, was not developed in time to produce results for the CMOS conference.

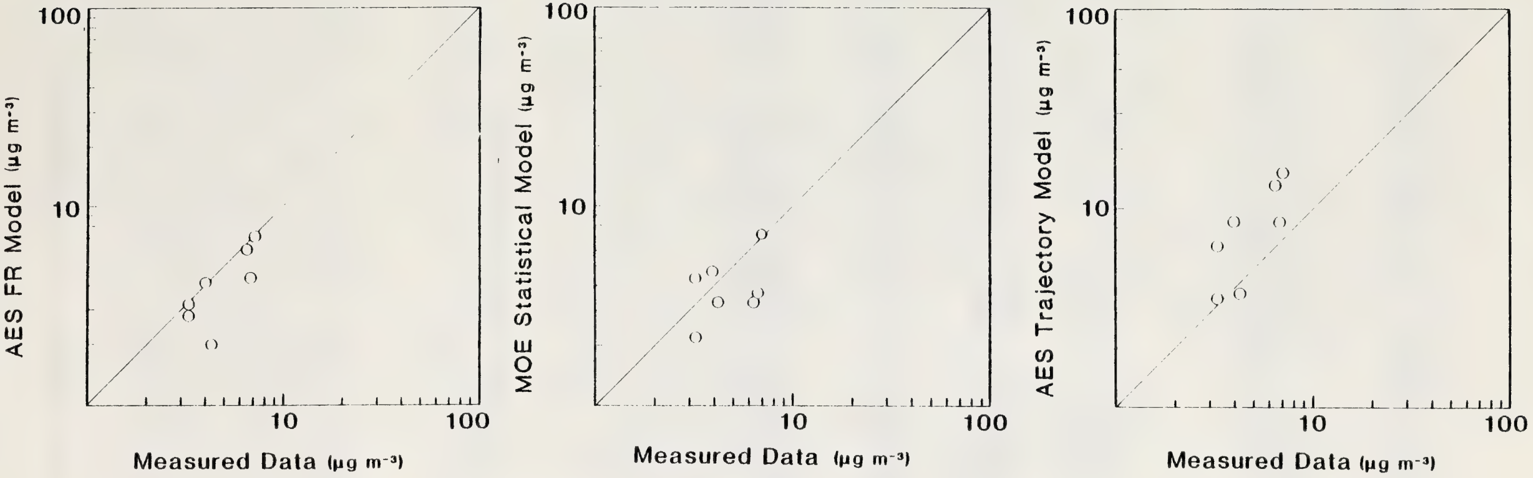

Figure 2. A comparison of measured data with results from three long-range transport models for annual average sulphate concentrations

REFERENCES

Fay, J.A., and J.J. Rosenzweig, 1980: "An analytical diffusion model for long distance transport of air pollutants", Atmos. Environ., 14, 355-365.

Machta, L., 1979: "A handbook to estimate climatological concentration, deposition, and horizontal fluxes of pollutants on a regional scale", Monitoring and Assessment Research Centre, Chelsea College, University of London.

Matthias, C.S., and A.K. Lo, 1981: "A long-range climatological dispersion model. Part 1: Initial implementation of model", Report-81-022-N, Atmospheric Environment Service, Downsview, Ontario, Canada.

"Memorandum of Intent on Transboundary Air Pollution - Atmospheric Modelling - 1981", U.S. Dept. of Commerce, NOAA, Environmental Research Laboratories.

Venkatram, A., 1981: "Ontario Ministry of Environment Statistical Model", Ministry of the Environment, 880 Bay Street, Toronto, Canada, M5S 1Z8.

Voldner, E.C., and Y. Shah, 1979: "Preliminary North American emissions inventories for sulphur and nitrogen oxides and total suspended particulates - a summary", Report LRTAP 70-4, Atmospheric Environment Service, Downsview, Ontario, Canada.

# RESULTS OF THE NANTICOKE SHORELINE DIFFUSION EXPERIMENT: JUNE, 1978

by

R. V. Portelli*

Concord Scientific Corporation
2 Tippett Road
Downsview, Ontario
M3H 2V2

Abstract: This paper provides a summary of the experimental program of an intensive shoreline diffusion experiment [6-10] and discusses some of the results of this and a few associated studies. The experiment was carried out in June 1978 and focused on observations of the development of the coastal internal boundary layer during onshore flows and observations of fumigation (primarily $SO_2$) of the plume from the two 200 m stacks of the 4000 MW Nanticoke Generating Station, located on the north shore of Lake Erie near Nanticoke, Ontario.

Eight days of observed onshore flows and coastal fumigation indicated that fumigation commences about 1100 - 1300 h and can persist through to 1700 - 1900 h with the fumigation zones typically beginning at 7 to 20 km or more inland from the plant. A noteworthy temporal distribution of b.l. growth during a lake breeze dominated flow was observed, in which the peak b.l. height was attained hours prior to maximum surface heating. The fumigation zone on this day rotated clockwise about the plant revealing the influence of the Coriolis force.

The experiment has provided a good data set for model evaluation. Misra's fumigation model [22] performed reasonably well against this data.

## INTRODUCTION

In a shoreline environment, onshore flows frequently result in the formation of an internal boundary layer (IBL) over land. These coastal boundary layers are caused by differences in surface temperatures (thermal b.l.) and by differences in surface roughness (roughness b.l.). During the warm season in temperate zones when the air over land is often 10°C or more warmer than over the water, these boundary layers are often referred to as thermal internal boundary layers (TIBL) due to the dominant influence of the thermal (connective) turbulence in the development of the boundary layer. With typically cool stable onshore flow, the TIBL, which grows with distance inland, is capped by a stable layer aloft. Elevated plumes from coastal industrial stacks therefore travel inland with little dispersion in the stable flow until they intersect the internal boundary layer several kilometers inland where the underlying connective turbulence rapidly mixes the pollutants to ground-level, in potentially high concentrations. This phenomenon of "coastal fumigation" of industrial plumes is an important air quality consideration in view of the fact that shoreline environments are favoured locations for industrial development as well as population centers. Previous studies [1-5] in coastal zones provide some valuable insights into the problem.

---

*Previously with the Atmospheric Environment Service, Downsview, Ontario

One of the difficulties of researchers in developing an understanding and models representative of the physical processes in coastal b.l. development and the resulting pollutant diffusion mechanisms has been the sparseness of observational data. In this paper, some results of a recent intensive field investigation of internal boundary layer growth and coastal fumigation will be presented.

The study was conducted in the spring of 1978 at Nanticoke, Ontario on the north shore of Lake Erie - the site of a large new industrial complex, which includes the 4000 MW coal-fired Nanticoke Generating Station, an oil refinery and a steel mill. The Nanticoke experiments were mounted by the Atmospheric Environment Service (AES) in cooperation with the Ontario Ministry of the Environment and Ontario Hydro to obtain detailed measurements of the vertical structure of onshore flows and internal boundary layer development and surface and airborne pollutant measurements to study diffusion conditions resulting in fumigation of the coastal power plant plume.

In a previous paper, Portelli [6] presented a preliminary description of the experimental program and some of the results. In a recent series of four papers by Portelli,[7] Kerman et al,[8] Hoff et al,[9] and Anlauf et al,[10] which are currently in press, a detailed description of the experiments and results is given. After a brief review of some relevant studies on coastal internal boundary layers and fumigation modelling, this paper will provide a summary of some of the results of the Nanticoke '78 shoreline diffusion experiments and a few associated studies.

## COASTAL INTERNAL BOUNDARY LAYERS AND FUMIGATION MODELLING

Two early reviews on coastal boundary layers and data available at the time were given by Prophet[11] and Van der Hoven[3]. Prophet covered the basic concepts of coastal meteorology, discussing onshore and offshore trajectories and the modification of air flowing from one surface to another. Van der Hoven also dealt with the transition from overwater to overland transport.

In a study[12] on a Texas beach during four days in June, the growth of the IBL to a distance of 90 m inland was found to have an average slope of 1:13. Elliott[13] and Panofsky and Townsend[14] found the slope to be about 1:10. In Brookhaven National Lab's (BNL) study [15] observations indicated the average slope of the IBL is steep (∿1:4) within the first few hundred meters from the shoreline and shallow (∿1:100) at greater distances (beyond 20 - 30 km). Raynor et al[16] proposed a scheme for predicting the height h, of the IBL as a function of land-water buoyancy contrast which DiVecchio et al [17] tested against observations and found a correlation coefficient of 0.90. Venkatram [18] derived from basic principles a similar yet improved formulation compared to Raynor et al's [16] - he incorporated momentum flux considerations. Raynor et al [15] recommend use of Venkatram's model for h given below:

$$h = \frac{U_\star}{Um} \left[ \frac{2\,(\Theta\ell - \Theta\omega)\,X}{\gamma(1 - 2F)} \right]^{\frac{1}{2}} \qquad (1)$$

where: $U_\star$ = friction velocity ($M\ S^{-1}$)
Um = average wind speed in b.l. ($M\ S^{-1}$)
$\Theta\ell$ = land temperature (k)
$\Theta\omega$ = water temperature (k)
X = fetch, or distance (m)
$\gamma$ = upwind vertical potential temperature gradient ($K\ m^{-1}$)
F = a fraction which depends on the temperature difference across the top of the internal b.l.)

For steady state flows over a homogeneous land surface, h varies parabolically with inland distance. Where data to satisfy equation (1) is not available, an often used approximation is given by:

$$h = a\ x^{\frac{1}{2}} \qquad (2)$$

where all the physics of the b.l. development is contained in the coefficient a (typical value of $a \cong 4\ m^{\frac{1}{2}}$). In the absence of free convection or a lake/sea breeze return flow, an equilibrium height (he) is usually reached at some point inland. Jensen[19] looked at the IBL in terms of changes in surface roughness and the resulting modifications to the wind profile and found from his data that at 20 km inland, there remained of the order of 20% excess surface stress compared with equilibrium conditions. This lead to the conclusion that more than 20 km of downstream flow is required to affect adjustment (to the new surface) leading to an equilibrium b.l. height: at this point the IBL has possibly grown to contain the whole PBL (planetary b.l.).

Several models have been proposed for the prediction/estimation of ground level concentrations in coastal fumigation situations. In the Lyons and Cole model[5], it is assumed that a Gaussian plume becomes uniformly distributed in the vertical inside the TIBL. Meroney et al[20] use a similar method. van Dop et al[21] solve the diffusion equation within the TIBL assuming a uniform vertical destribution of concentration field. Misra [22] recently extended the model of van Dop et al. His model assumes that the dispersion of pollutants in the stable layer and within the TIBL proceed independently (the turbulence characteristics of the two layers are different). The model disperses pollutants in the TIBL from an elevated area source along the upper edge of the TIBL. The source strength is determined by the concentration field within the stable layer and the rate of growth of the TIBL, which is taken to be parabolic with distance inland, as discussed earlier.

Both van Dop et al's and Misra's model formulations require numerical solution of integral equations. In the particular case of a Gaussian distribution in the stable layer and a Gaussian crosswind and uniform distribution in the TIBL, the solutions of the two are similar[22]. The difference lies in that Misra's model is not constrained to a constant horizontal eddy diffusivity, as is that of van Dop et al, thus placing it on a stronger physical basis; in addition, it is simpler to use. Generally good agreement has been found between Misra's model and observations.[23]

## NANTICOKE 1978 EXPERIMENT

The study was conducted from May 29 through June 16, 1978 at Nanticoke, Ontario which is located on the north shore of Lake Erie. Only a brief description will be given here of the experiment as the details are contained in other papers.[6-10]

The Nanticoke coal-fired power plant, with a design capacity of 4000 MW has two 198 m stacks at the shoreline, 273 m apart. The plumes from these stacks merge into a single plume within about 1 km of the plant. The plant uses coal containing approximately 2.3% sulphur and would emit about 16 kg $S^{-1}$ of $SO_2$ at full load. During the study, the plant was operating at roughly 1/3 full load and $SO_2$ emissions were of the order of 5 kg $S^{-1}$.

Figure 1 depicts the experimental design employed to a) observe the structure of onshore flows and the growth of the IBL and b) obtain plume/air quality measurements from surface-based and airborne units during fumigation events. The height and structure of the IBL was measured at six inland locations by tethersonde (TS), minisonde (MS), and acoustic sounder (AS) systems. A tower system also provided 3 level wind and temperature data to 85 m. A sonic anemometer provided data for surface heat flux determinations and observations of $SO_2$ fluxes were also made at this site. Particulate plume rise and dispersion were remotely sensed by

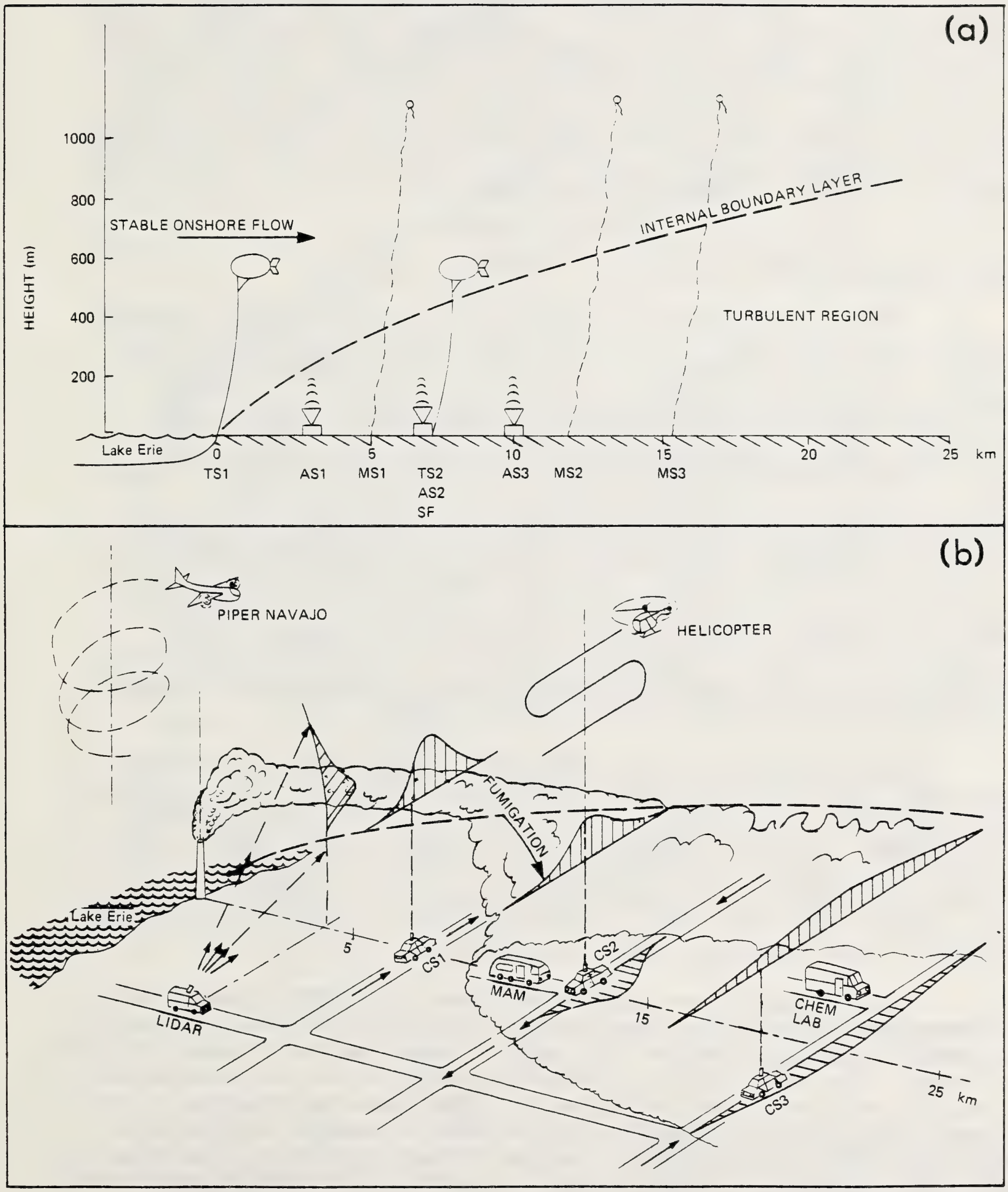

FIGURE 1
EXPERIMENTAL DESIGN (Ref. 6):

a) Meteorological observations of b.l. development.
b) Surface and airborne measurements of air quality upwind, within and downwind of fumigation zone

(TS = tethersonde; MS = minisonde; AS = acoustic sounder; SF = Surface fluxes; CS = COSPEC/SIGN-X) a LIDAR system. Three mobile COSPEC (CS) units monitored $SO_2$ burden aloft - the two downwind units also measured ground-level $SO_2$ concentrations with sign-X monitors. Two mobile chemistry laboratories (MAM and CHEM LAB) monitored various gaseous ($SO_2$, $NO_X$, $O_3$, hydrocarbons) and particulate (sulphates, nitrates, metals, light scattering) pollutants. In addition, continuous $SO_2$ monitoring data was available from Ontario Hydro's fixed 16 station network. Airborne $SO_2$ plume observations were made by helicopter and a fixed winged aircraft monitored $SO_2$, $O_3$, light scattering particles, sulphates, temperature, and relative humidity in the upwind (background) air as well as downwind of the plant.

## RESULTS AND DISCUSSION

During the study period, there were 8 days of onshore gradient or lake breeze flows which transported the Nanticoke power plant plume inland. Fumigation of the plume was observed on each of these days. In general, it was found that the onset of fumigation occurred at 1100 - 1300 h (when the TIBL had built up to plume height - typically about 400 m above the ground) and persisted through to 1700 - 1900 h (when decay of the TIBL led to decoupling of the plume from the surface layer). The location of the ground level fumigation zone shifted toward or away from the plant during the day corresponding to TIBL build up or decay. The near-shore edge of the fumigation zones were observed at distances of 7 to 20 km from the plant. The areas where fumigations were found to occur most consistently were to the NE of the plant - the predominant winds in the region are from the SW. An additional general finding was the observation of a clockwise rotation of the fumigation zone about the plant during light gradient conditions which evidenced the influence of the Coriolis force acting on lake breeze flows[6].

In the analysis of the data from the 8 days of fumigation observations, two stood out as most interesting. On June 1, light gradient flow allowed for a lake breeze which veered with time of day resulting in a systematic clockwise rotation of the fumigation zone and on June 6, moderate south-westerly gradient flow with little variation in wind direction throughout the day maintained fumigation to a relatively fixed zone. Results for these days, in particular June 1, are discussed below followed by some fumigation modelling predictions and data comparisons.

The boundary layer profiles for June 1 for 0900 through 1700 h[6] are presented in Figure 2. The growth of the TIBL with inland distance is generally parabolic and the TIBL depths compare well with those of Knox and Lyons[4]. The normalized b.l. heights at the 5 sites are presented as a function of time of day in Figure 3[6]. From these two figures, it can be seen that a relatively shallow b.l. at 0900 h deepened rapidly to a maximum at 1000 - 1100 h and then decayed through to 1700 h. One might expect the maximum b.l. depth to occur at maximum solar heating which would be about 1300 - 1400 h. This is probably the case during gradient onshore flows, however, as was explained,[6,7] light winds to 1000 h coupled with increasing surface heating produced a connective b.l. which quickly deepened. With the onset of the lake breeze, a sharp increase in wind

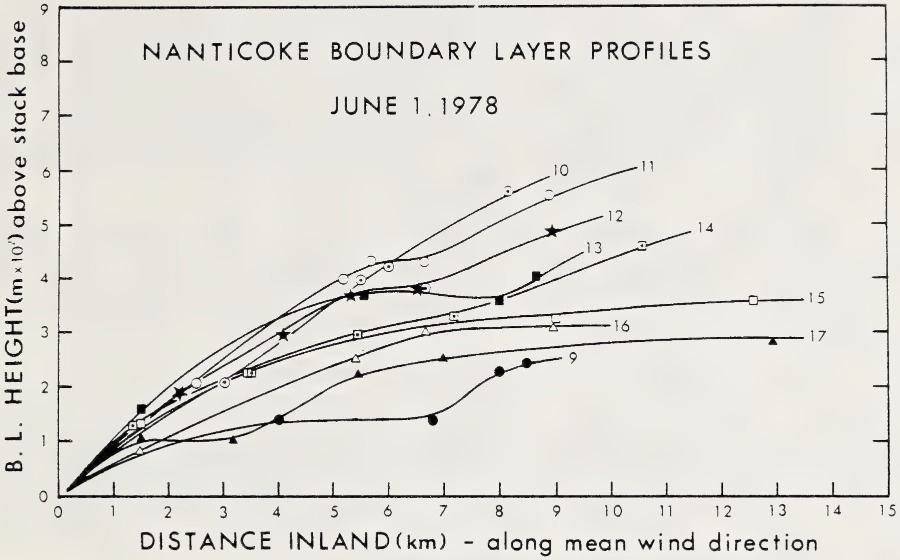

FIG. 2 Boundary Layer Profiles at 0900 through 1700 h on June 1, 1978[6] (Data points for each hour denoted by various symbols)

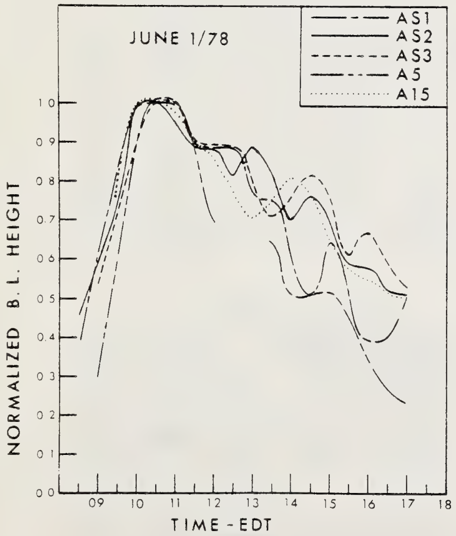

FIG. 3 Time variation of normalized b.l. heights at 5 sites on June 1/78. (A5 & A15: sites for MS1 and MS2)[6]

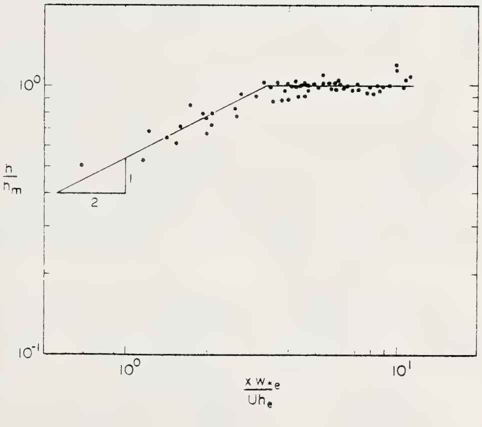

FIG. 4 Boundary Layer growth (h) normalized by the equilibrium height $(h_e)$ then renormalized (by $h_m$) for unity in the equilibrium region. Advected time inland $(XU^{-1})$ has been normalized by the turbulent time scale $(h_e W_{*e}^{-1})$.[8]

speed occurred between 1000 and 1100 h accounting for the levelling off of the b.l. height at this time. Although the surface heat flux continued to increase monotonically to a maximum at 1330 h, further increases in wind speed and subsequent reductions in solar heating led to a continued fall in b.l. height. Since these wind and surface heating conditions (see ref. 6 & 7) are somewhat typical for lake breeze situations, it would therefore appear that the temporal distribution of b.l. height in Figure 3 is a representative one for the lake breeze case.

In Figure 4 (Kerman et al[8]) normalized b.l. heights ($\hat{h} = h/h_m$) for June 1 and 6 as a function of normalized advection time (or distance) inland ($\hat{X} = X\, W_{*e} / Uh_e$) are presented. The observed b.l. heights, h, were first normalized by the equilibrium height, $h_e$ (h grows parabolically inland approaching $h_e$ asymptotically [18]). A plot of $h/h_e$ indicates a parabolic growth inland reaching asymptotically a height identified as $h_m$. The b.l. heights were then renormalized by $h_m$ for unity in the equilibrium region (this accounts for the time variations or diurnal effects on $h_e$). Time or inland distance is normalized by the rate of connective turnover or the characteristic time for turbulent exchange throughout the evolving b.l. given by $h_e\, W_{*e}^{-1}$ (where $W_{*e}$ = depth averaged turbulent velocity). Figure 4 indicates that there is an initial b.l. growth resembling a 1/2 form which equilibrates near $\hat{X} = 3.5$.

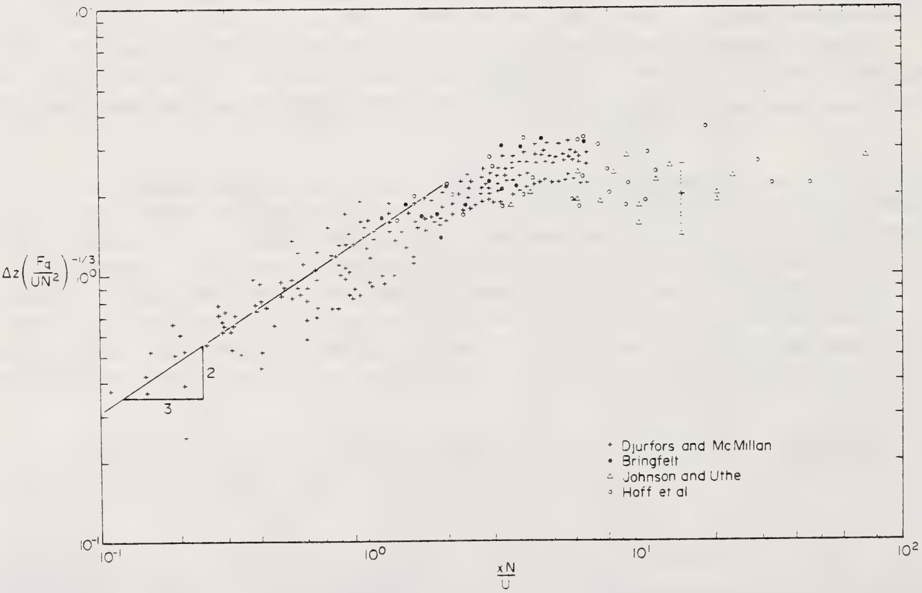

FIG. 5 Plume rise ($\Delta z$) normalized by its ultimate equilibrium height $(F_q/UN^2)1/3$ as a function of the advected time inland $(XU^{-1})$ normalized by the characteristic time scale ($\sim N^{-1}$) in the onshore stably stealified flow (where Fq = buoyancy flux)[24]

The Nanticoke plume rise data of Hoff et al[9] are displayed in Figure 5 (Kerman[24]) along with similar data from other published experiments: previous Nanticoke data obtained by plume photography and LIDAR reported by Djurfors and McMillan[25]; Bringfelt's[26] plume photography data from Swedish power plants; and Johnson and Uthe's[27]LIDAR data from the Keystone, Pennsylvania power plant. The vertical bar indicates the 1975 Nanticoke [25] equilibrated data, arbitrairly placed at XN/U = 15. As shown here and by Hoff et al[9], the Nanticoke plume rise follows a $t^{2/3}$ growth to about XN/U or tN ≈ 5 (approx. 300 - 500 S) and is consistent with other observations. Hoff et al demonstrated their data to be in general agreement with Briggs[28] plume rise relationships which are also supported by the other data of Figure 5[24].

The observed ranges of plume rise of the Nanticoke plume in the stable prefumigation region for June 1 and 6, 1978 were 150 to 280 m (average ∿197 m) and 130 to 250 m (average ∿188 m), respectively[9]. This means the actual plume height was at about 400 m above ground on both days and on referring back to Figure 2, it is obvious that a plume of this height would intercept the TIBL and fumigate for several hours on June 1.

The observed ground-level $SO_2$ concentrations resulting from the fumigation of the Nanticoke plume on June 1 are shown in Figure 6[9], in a sequence of two 1-hour averaged breakdowns and six ½-hour breakdowns from 0900 to 1700 h. Prior to 0900 h, the plume was observed heading offshore in the light NE gradient flow. By 0900 h, the lake breeze front had started inland and the plume bearing change to NNW. Fumigation began in the 1000 - 1100 h period, as would be expected from the b.l. profiles in Figures 2 and 3 and plume rise observations discussed earlier. From about 1000 to 1200 h the fumigation zone remained to the NNW of the plant. After 1200 h the lake breeze flow began to turn clockwise from the initial SSE flow eventually to a SW flow. This resulted in the observed swing of the fumigation zone through about a 50° rotation relative to the plant, between 1200 and 1700 h. After 1700 h, the plume decoupled from the surface layer as the b.l. fell to below 300 m. Hoff et al[9] present the results for June 6 in a similar format. With the nearly stationary conditions of gradient SSW flows, the location of the fumigation zone remained relatively fixed throughout the period of fumigation.

Figure 6 clearly illustrates the importance of the slope of the b.l. to the fumigation problem. The most intense fumigation occurred when the b.l. slope was at its steepest. From Figure 2 around noon, the slope was about 1:10 within the first 2 km and about 1:20 from 2 to 10 km. During this fumigation period, a mobile chemistry laboratory (MAM) was positioned in the fumigation zone at site M1 and sampled continuously from 1135 to 1415 h (site M1 is identified in Figure 6). The observed levels of $SO_2$ and $NO_X$ at this site are shown in Figure 7, where the curves represent ½-hour running averages of the continuous observations. Initially, the MAM unit was in the area of peak concentration recording 0.41 ppm $SO_2$ as its first ½-hour average. The subsequent drop-off in the curves represent the distribution of $SO_2/NO_X$ in the trailing half of the fumigation zone as it swings eastward.

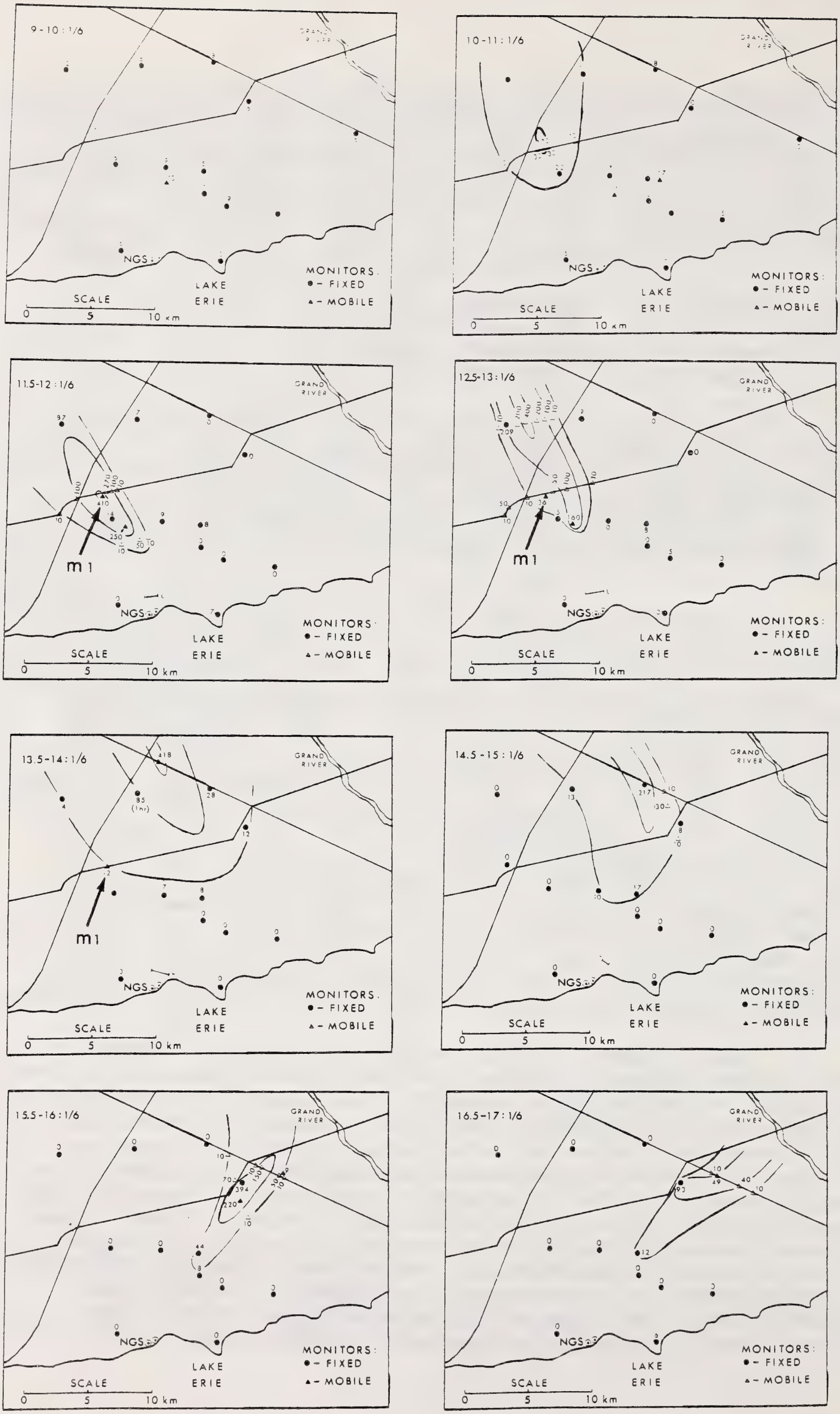

FIG. 6 Sequence of contours of ground-level $SO_2$ observations (ppb) from 0900 to 1700 h on June 1, 1978 exhibiting fumigation of the Nanticoke Generating Station (NGS) plume (LIDAR observations of plume lateral spread marked "L").[6]

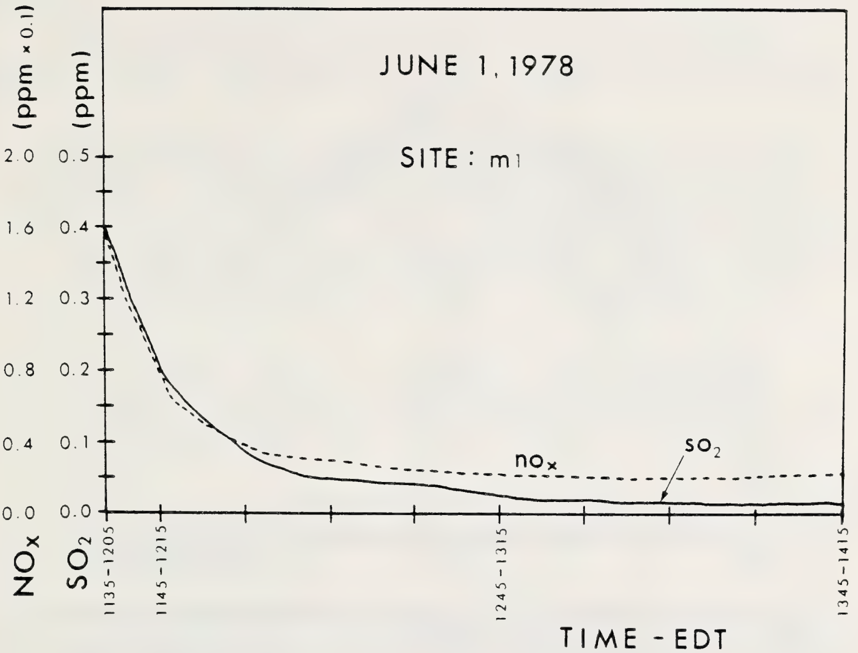

FIG. 7 Observed $SO_2$ and $NO_X$ concentrations at site M1 during fumigation of the Nanticoke Power Plant plume on June 1, 1978 (curves represent 1/2-hour running averages).[6]

The fumigation model of Misra[22], has been tested against the observations of the Nanticoke study discussed above by Misra and Onlock[29]. Figure 8 exhibits their profiles of the downwind variation of the relative centerline ground-level concentration (glc) predicted by the model for 1100 through 1500 h on June 1. The location of the peak glc was predicted to shift farther downwind and decrease in magnitude as the day progressed. Recalling from Figure 2 that the TIBL continued to drop after 1100 h, this is the expected general trend which the observations of Figure 6 support. The results of a comparison of the computed versus observed $SO_2$ concentrations for June 1 and 6 are shown in the scatter diagram of Figure 9. The model predictions are reasonably well verified by the observed data with an $r^2$ for these data points of 0.67[29].

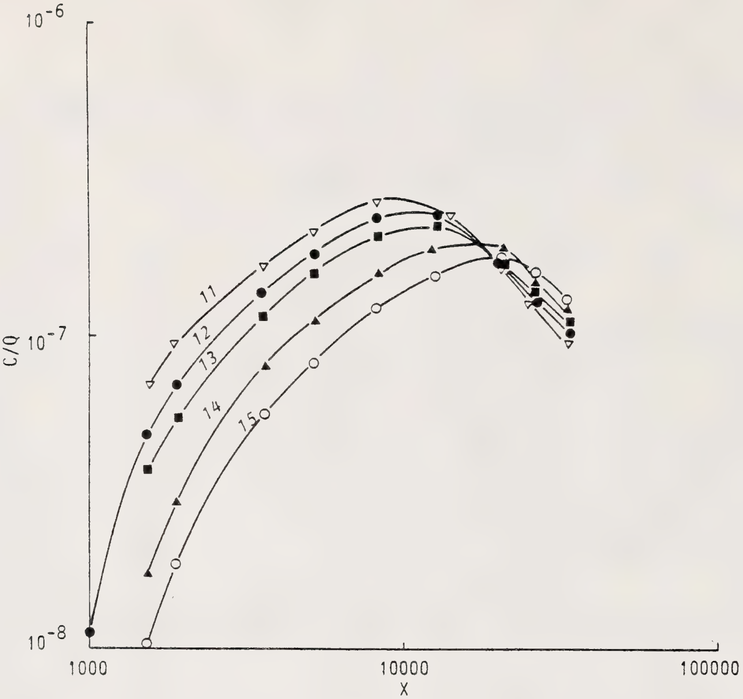

FIG. 8 Predicted relative concentration C/Q vs downwind distance for 1100 - 1500 h on June 1, 1978[29]

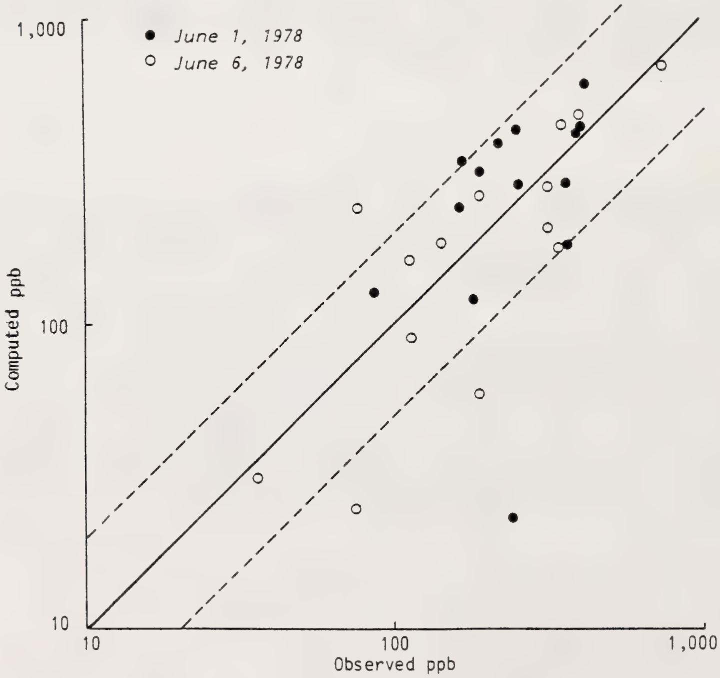

FIG. 9 Observed vs predicted GLC for June 1 and 6, 1978[29]

## CONCLUSIONS

Some conclusions which can be drawn from the Nanticoke '78 shoreline diffusion experiments and the associated studies discussed above are:

1) When conditions allow for a lake breeze to develop, the height of the internal b.l. will rise rapidly and peak prior to the time of maximum surface heating and just after the passage of the lake breeze front which in the case presented in this paper was 1000 - 1100 h. The temporal distribution of Figure 3 is considered to be representative;

2) The growth of the b.l. is parabolic with increasing distance inland and it reaches an equilibrium height at $\hat{X}$ (= $XW_{*e}/Uh_e$) = 3.5 which supports Venkatram's[18] argument;

3) The plume rise observations follow a $t^{2/3}$ growth and compare well with data of other experiments and Briggs'[28] relationships;

4) Fumigation of the Nanticoke plume can occur continuously from about 1100 - 1300 h through to 1700 - 1900 h with the fumigation zones typically beginning at 7 to 20 km or more from the plant;

5) Coastal fumigation during lake breeze dominated flows has the significant characteristic that the fumigation zone rotates clockwise about the plant as a result of the Coriolis force turning the lake breeze as the day progresses. During gradient onshore flows, much more stationary fumigation conditions exist;

6) The fumigation model of Misra performs reasonably well against the Nanticoke data of June 1 and 6, 1978.

The observations of the Nanticoke shoreline diffusion experiment of June 1978 afforded a rather comprehensive data set on the development of internal boundary layers and the problem of coastal fumigation. In depth analysis of two of the eight days of observational data has led to valuable insights and provided a good data set for the purposes of model development and evaluation.

## ACKNOWLDEDGEMENTS

The author would like to thank the many participants from the Atmospheric Environment Service, the Ontario Ministry of the Environment and Ontario Hydro, who cooperated on the 1978 Nanticoke shoreline diffusion experiment. Also, the support of the Atmospheric Environment Service on this presentation is gratefully acknowledged.

## REFERENCES

1. Bierly, E. W., and Hewson, E. W., 1963: "Atmospheric Diffusion Studies Near a Lakeshore," J. of Applied Meteor. 1, 390-396.

2. Hewson, E. W. and Olsson, L. E., 1967: "Lake Effects on Air Pollution Dispersion," J. of APCA, Vol. 17, No. 11, 757-761.

3. Van der Hoven, I., 1967: "Atmospheric Transport and Diffusion at Coastal Sites," Nuclear Safety, 7(5), 490-499.

4. Knox, N. E., and Lyons, W., 1975: "The Thermal Internal Boundary Layer in a Shoreline Environment During Summer Fumigation Episodes," presented at 1st Conference on Regional and Mesoscale Analysis and Prediction, AMS, LasVegas, Nevada.

5. Lyons, W., and Cole, H., 1973: "Fumigation and Plume Trapping on the Shores of Lake Michigan During Stable Onshore Flow," J. of Applied Meteor., 2, 494-510.

6. Portelli, R. V., 1979, "The Nanticoke Study: Experimental Investigation of Diffusion From Tall Stacks in a Shoreline Environment". Proceedings of 10th NATO/CCMS Int'l. Tech. Mtg. on Air Pollution Modeling and Its Application, Rome, Italy, October.

7. Portelli, R. V., 1981: "The Nanticoke Shoreline Diffusion Experiment, June 1978: Part I. Experimental Design and Program Overview", In press, Atmospheric Environment.

8. Kerman, B. R., Mickle, R. E., Portelli, R. V., Trivett, N.B.A., and Misra, P. K., 1981: "The Nanticoke Shoreline Diffusion Experiment, June 1978: Part II. Internal Boundary Layer Structure", In press, Atmospheric Environment.

9. Hoff, R. M., Trivett, N. B. A., Millan, M. M., Fellin, P., Anlauf, K. G., Wiebe, H. A., and Bell, R., 1981: "The Nanticoke Shoreline Diffusion Experiment, June 1978: Part III Ground-based Air Quality Measurements", In press, Atmospheric Environment.

10. Anlauf, K. G., Fellin, P., Wiebe, H. A., and Melo, O. T., 1981: "The Nanticoke Shoreline Diffusion Experiment, June 1978: Part IV. A. Oxidation of Sulphur Dioxide in a Power Plant Plume. B. Ambient Concentration and Transport of Sulphur Dioxide, Particulates and Ozone," In press, Atmospheric Environment.

11. Prophet, D. T., 1961: "Survey of available information pertaining to the transport and diffusion of airborne material over ocean and shoreline complexes." Tech. Report 89, Aerosol Lab., Stanford University, 53 pp.

12. Echols, W. T. and Wagner, N. K., 1972: "Surface Roughness and Internal Boundary Layer near a Coastline," J. Appl. Meteorol, 11:658-662.

13. Elliot, W. P., 1958: "The Growth of the Atmospheric Internal Boundary Layer," Trans. Am. Geophys. Union, 39(6); 1048-1054.

14. Panofsky, H. A., and Townsend, A. A., 1974: "Change of Terrain Roughness and the Wind Profile," Q. J. R. Meteorol. Soc. 90(384): 147-155.

15. Raynor, G.S., Sethuraman, S. and Brown, R. M., 1979: "Formation and characteristics of coastal internal boundary layers during onshore flows," Boundary Layer Met., 16, 487-514.

16. Raynor, G. S. et al, 1975: "Studies of Atmospheric Diffusion from a Nearshore Oceanic Site", J. Appl. Meteor., 14: 1080-1094.

17. DiVecchio, R. A., Smith, D. B., and Martin, G., 1976: "Performance of a recent formulation for rate of growth of boundary layers near shorelines". Presented at Conf. Coastal Meteorology, Sept. 21-23, Virginia Beach, Va., Amer. Met. Soc.

18. Venkatram, A., 1977: "A model of internal boundary layer development". Boundary-Layer Met., 11, 419-437.

19. Jensen, N. O., 1978: "Simultaneous Measurements of Turbulence Over Land and Water," Boundray Layer Meteorology 15:95-108.

20. Meroney, R. W., Cermak, J. E., and Yang, B. T., 1975: "Modelling of atmospheric transport and fumigation at shoreline sites". Boundary-Layer Met., 9, 69-90.

21. van Dop, H., Steenkist, R., and Nieuwstadt, 1979: "Revised Estimates for Continuous Shoreline Fumigation", J. Appl. Meteor., 18:133-137.

22. Misra, P. K., 1980: "Dispersion from Tall Stacks Into a Shoreline Environment", Atmos. Environ., 14, 397-400.

23. Misra, P. K., 1980: "Verification of a Shoreline Dispersion Model for Continuous Fumigation", Boundary-Layer Meteorology, 19,4.

24. Kerman, B. R., 1981: "A Similarity Model of Shoreline Fumigation", Submitted to Atmospheric Environment.

25. Djuifors, S. and McMillan, A. C., 1976; "Nanticoke Diffusion Study", Ontario Hydro Research Division Report 76-245-K.

26. Bringfelt, B., 1969: "A Study of Buoyant Chimney Plumes in Neutral and Stable Atmospheres". Atmos. Environ., 3, 609-623.

27. Johnson, W. B. and Uthe, E. E., 1971: "LIDAR Study of the Keystone Stack Plume," Atmos. Environ., 5, 703-724.

28. Briggs, G. A., 1975; "Plume Rise Predictions", A.M.S. Workshop on Meteorology and Environmental Assessment, Boston, Mass.

29. Misra, P. K., and Onlock, S., 1981: "Modelling Continuous Fumigation of Nanticoke Generating Station Plume", In press, Atmospheric Environment.

# THE MOVEMENT OF ST. HELEN'S ASH CLOUD
# OVER WESTERN CANADA

G. Barrie Atkinson
Scientific Services Meteorologist
Central Region
266 Graham Avenue, Room 1000
Winnipeg, Manitoba.
R3C 3V4.

Abstract In the first hours after the Mount St. Helen's eruption of May 18, 1980, the ash cloud moved considerably faster than the wind field. This implies that the eruption produced its own circulation rather like a large thunderstorm. After about 18 hours the movement of the ash cloud conforms well with the indicated wind field.

The eruption of Mount St. Helen's volcano on Sunday, May 18, 1980 shortly after 8:30 a.m. spread an ash cloud across much of North America. This cloud subsequently covered an area which ranged from James Bay to just North of the Gulf of Mexico and extended eastward over the Atlantic Ocean. I have not encountered any reports of the ash cloud reaching Europe in amounts noticeable to the public but it was detectable by scientific means.

The initial eruption was significantly larger than any of the subsequent events. It forced a plume of ash from 17 to 20 kilometres and continued for a few hours. The tropopause in the vicinity of Mt. St. Helen's at the time was 11 to 12 kilometres so a significant portion of this ash entered the stratosphere. The ash cloud initially moved eastward at all levels so that the heavier fraction of the ash was deposited up to 800 kilometres east of the volcano, reaching this distance downwind in approximately eight hours.

Subsequently, over North America the cloud appeared to have two distinct parts (see Attachment I). That portion above the tropopause, in the stratosphere, moved southeast, then east and finally northeast over new England and the Maritimes. This portion of the cloud took 60 to 72 hours to reach the Atlantic coast. No fallout of ash from this portion of the cloud has been reported. It must be assumed that some of it did eventually reach the surface of the earth along this track, but so widely dispersed as to be unnoticeable. The greatest effect of this portion of the cloud was to enhance the brillance of sunsets and sunrises.

That portion of the ash cloud within the troposphere moved east-north-eastward, with a centre line running approximately from Harve, Montana through Broadview, Saskatchewan, Hecla Island, Manitoba, Lansdowne House, Ontario to Moosonee, Ontario. This cloud first entered southwest Saskatchewan about 16 hours after the initial eruption; reached western Manitoba after about 36 hours; and crossed Manitoba somewhat more rapidly to reach northwest Ontario about 45 hours after the initial eruption.

Accumulations of ash on the ground in Canada were measurable only in southern Alberta and southeastern British Columbia where up to 0.5 cm was reported. Elsewhere amounts were unmeasurable, and ranged from a 'complete thin covering of everything' in southwest Saskatchewan (Regina Leader Post 30/5/20) to a 'noticeable film on smooth surfaces' in western Manitoba (Eric Stanzeleit - pers. comm.), to spots left where raindrops had fallen in northwestern Ontario.

Visibilities were restricted by the ash cloud, but were not reduced to such low values as to be bothersome to the travelling public in Canada, as they were in many locations in the northwestern United States. For example, no, (to my knowledge) airline flights in Canada were cancelled because of the ash. Visibilities as low as one-half mile were reported from southern Alberta and southwest Saskatchewan. In Manitoba, 3 miles at Brandon was the lowest reported, while in northwest Ontario, 6 miles was the lowest reported. By the time the ash cloud reached Quebec, visibilities were not being restricted, but the atmosphere appeared hazy.

Size of the particles comprising the ash cloud in Canada ranged from one to ten micrometres (Regina Leader Post 80/6/10) with the larger particles constituting a higher percentage in southwest Saskatchewan. The particle size range was greater in southern Alberta and in Montana. For example, at Butte, Montana particle size ranged up to more than 15 micrometres.

Concentration of the ash approached 1000 micrograms per cubic meter Tuesday and Wednesday in southern Alberta, and decreased eastward. Normal dust concentrations are about 50-60 micrograms per cubic meter.

Another eruption on July 22, 1980 spread another tropospheric cloud northeastward into southeast British Columbia, southern Alberta and ultimately southern Saskatchewan. Visibilities were reduced somewhat, but the effects of this cloud were less than the initial eruption.

The stratospheric portion of the ash cloud appears reasonably easy to forecast, but its effects are not so significant to the public. This portion of the cloud was visible on satellite photographs, despite some interference by cloud, and hence its position was forecast by advection with a good deal of success in the short (24 hour) range (see Attachment I).

Also, the fallout forecasts prepared by NORAD at Colorado Springs, Colorado, as evaluated in the Prairie Weather Centre, appear to have handled the movement of this portion of the cloud reasonably well.

The stratospheric portion of the cloud also appears to have followed the flow pattern of 250 mb rather well (see Attachment II). The speed at which the leading edge of the cloud moved also agrees well with the speeds reported on the 250 mb chart, advecting in two days with about 105% of the reported speed (see Table I).

Table I 250 mb

| Time E+ | Distance Cloud Moved | Average Wind Speed | Wind Speed x Time |
|---|---|---|---|
| 6 | 300 | 45 | 270 |
| 20 | 1050 | 50 | 1000 |
| 20 to 44 | 1025 | 45 | 1080 |
| 44 | 2075 | 45 | 1980 |

For this portion of the cloud then, the problem seems to reduce to how well the 250 mb flow is forecast.

The tropospheric portion of the ash cloud is of much more consequence to the public. It also appears to be more difficult to forecast at the present time.

At first the lower portion of the cloud is hidden by the upper portion. Thus, for some period of time it is not possible to use satellite photographs to detect the motion of the lower cloud. Also, if any amount of cirrus cloud is present in the area, it probably would not be possible to use satellite photos to determine the motion of the tropospheric cloud. However, the cloud that moved across Saskatchewan, Manitoba and Northwest Ontario did so under clear skies and was easy to follow on these pictures.

The forecasts received from NORAD did not perform as well in the troposphere, according to the Prairie Weather Center. It forecast the ash cloud to reach only about three-quarters of the way across South Dakota by 210000Z, when actually the cloud was almost to Lansdowne House, Ontario by that time.

Tables II, III and IV compare winds at 850, 700 and the 500 mb levels with the motion of the ash cloud. It is readily apparent that the tropospheric cloud moved with a speed much closer to that reported at the 500 mb level than that reported at the other two levels.

Table II 850 mb

| Time E+ | Distance Cloud Moved | Average Wind Speed | Wind Speed x Time |
|---|---|---|---|
| 6 | 240 | 10 | 60 |
| 20 | 600 | 15 | 300 |
| 20 to 44 | 600 | 25 | 600 |
| 44 | 1200 | 20 | 880 |

Table III 700 mb

| | | | |
|---|---|---|---|
| 6 | 240 | 12 | 70 |
| 20 | 600 | 17 | 340 |
| 20 to 44 | 600 | 25 | 600 |
| 44 | 1200 | 22 | 960 |

Table IV 500 mb

| | | | |
|---|---|---|---|
| 6 | 240 | 15 | 90 |
| 20 | 600 | 25 | 500 |
| 20 to 44 | 600 | 25 | 600 |
| 44 | 1200 | 25 | 1100 |

Attachments III, IV and V are the charts from which the tables were taken.

In the period up to about 18 hours after the eruption, and particularly just after the eruption, the ash cloud appears to have moved considerably faster than the wind fields at all three levels would indicate. This may have been the result of a local circulation set up by the eruption itself. I visualize this to be much like the circulation of a large thunderstorm.

After about 18 hours, (20-44 hours) the movement of the ash cloud conforms very well with the flow indicated at all three levels.

Thus it appears that the long term motion in the troposphere of any future ash clouds can best be forecast by the weather office using 100% of the 500 mb wind flow.

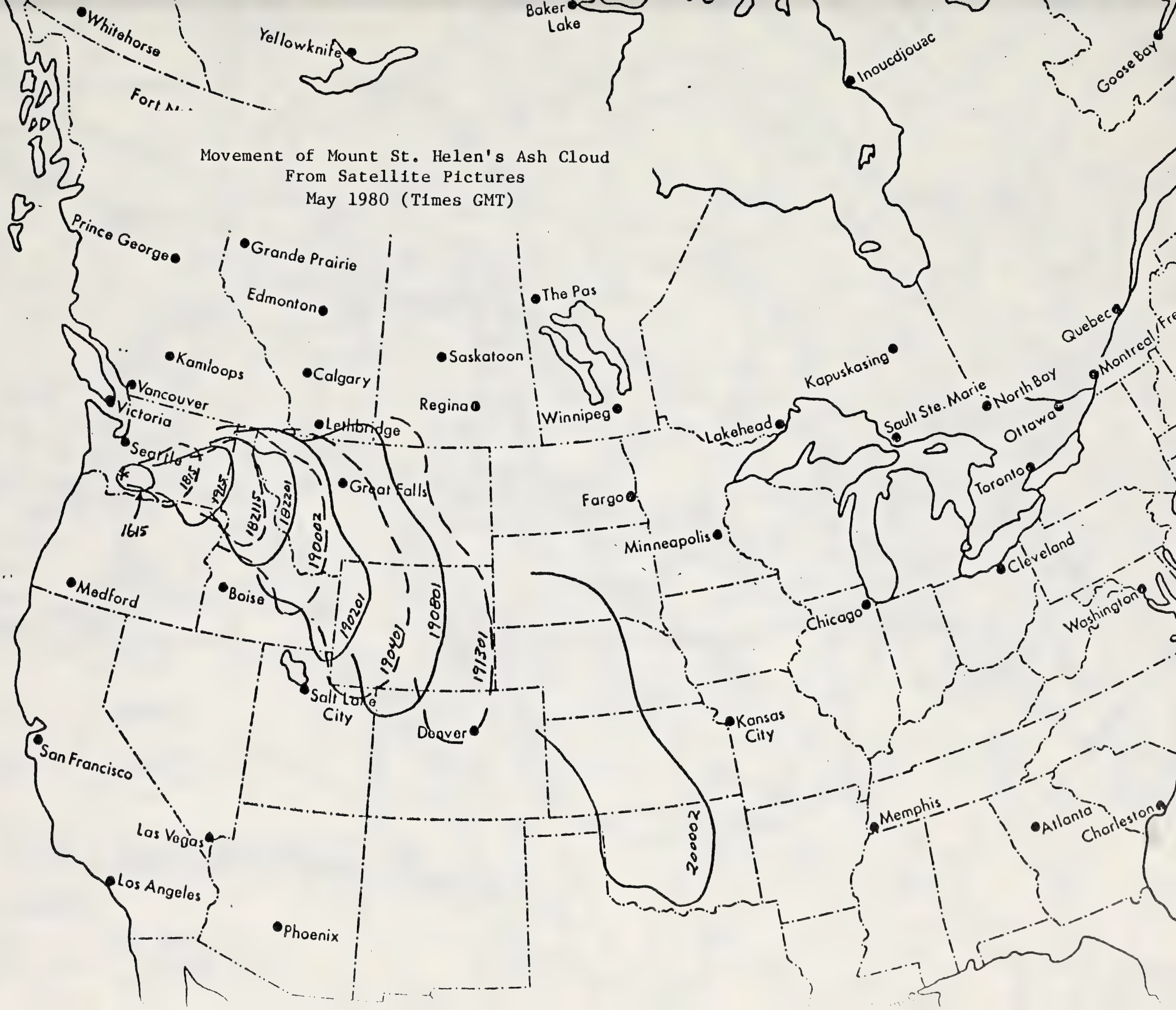

Movement of Mount St. Helen's Ash Cloud
From Satellite Pictures
May 1980 (Times GMT)

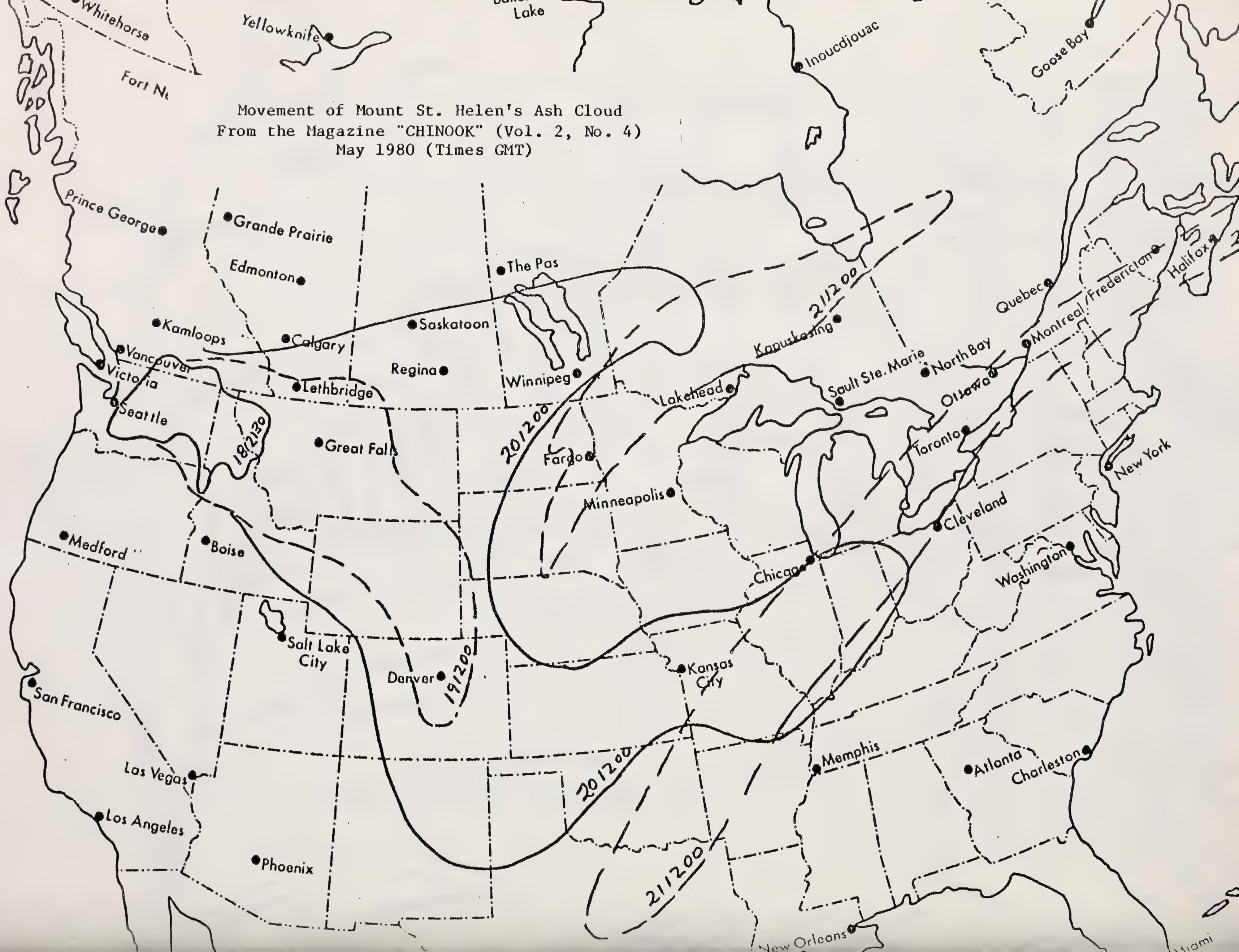

Movement of Mount St. Helen's Ash Cloud
From the Magazine "CHINOOK" (Vol. 2, No. 4)
May 1980 (Times GMT)

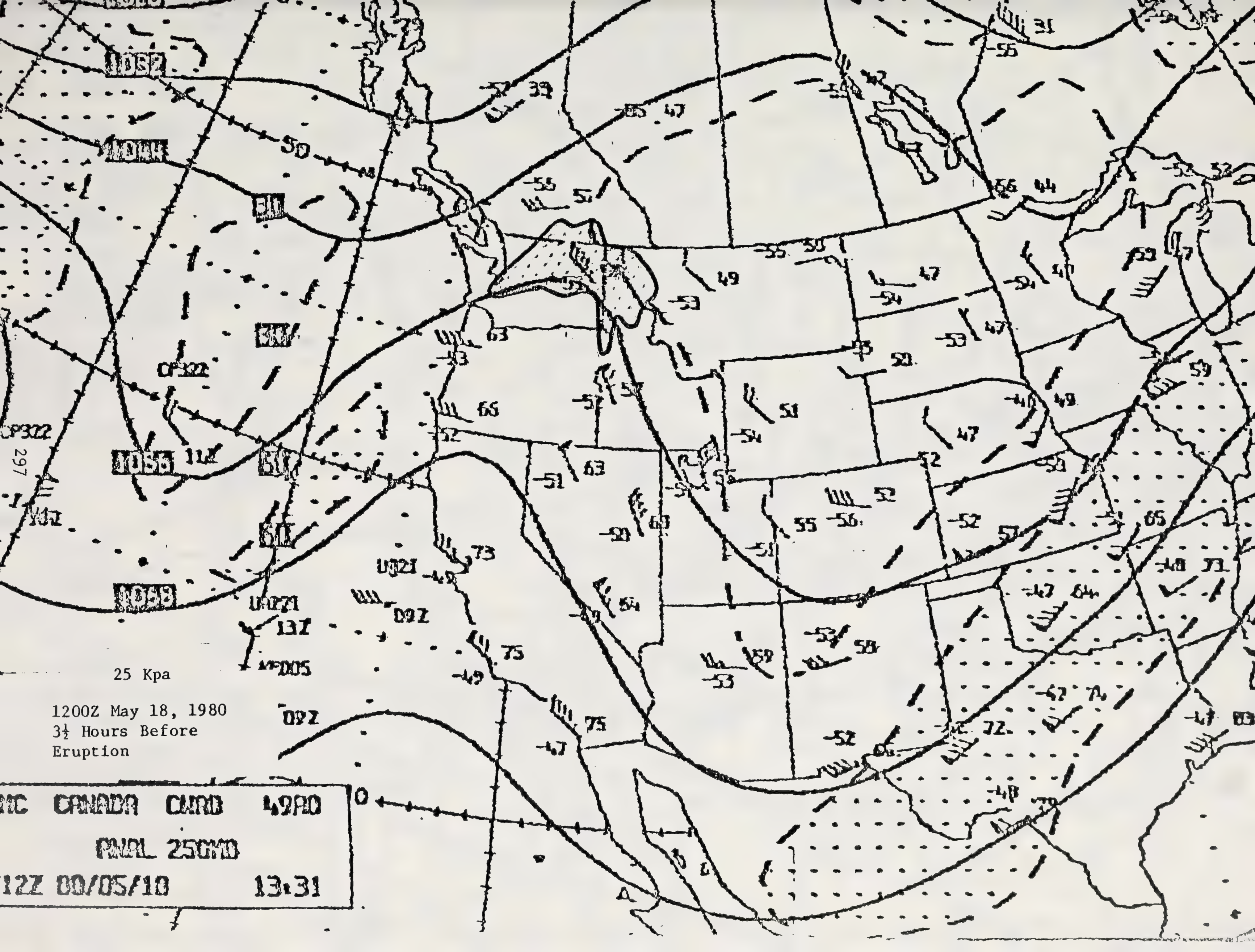

25 Kpa

1200Z May 18, 1980
3½ Hours Before
Eruption

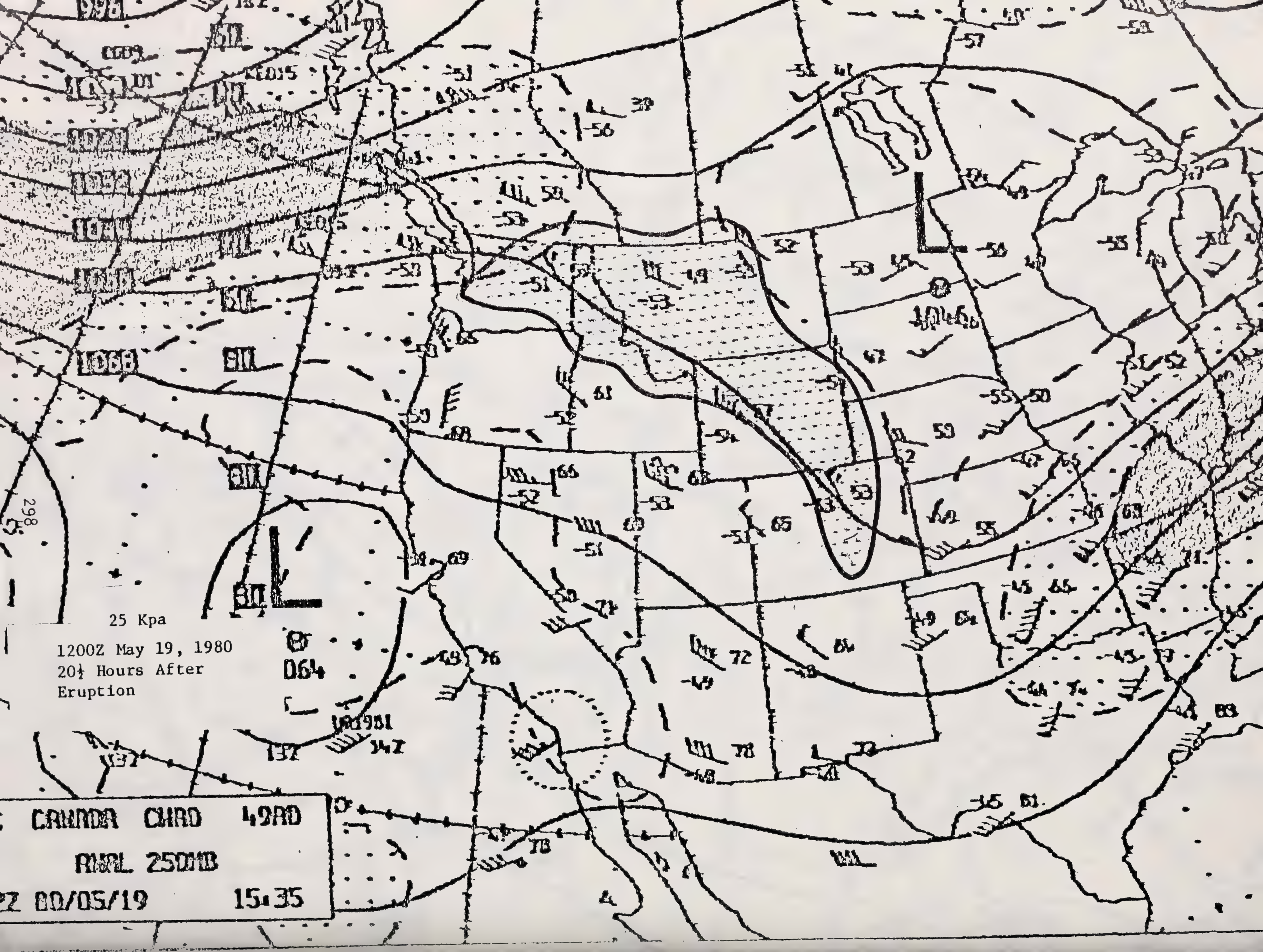

25 Kpa

1200Z May 19, 1980
20¼ Hours After
Eruption

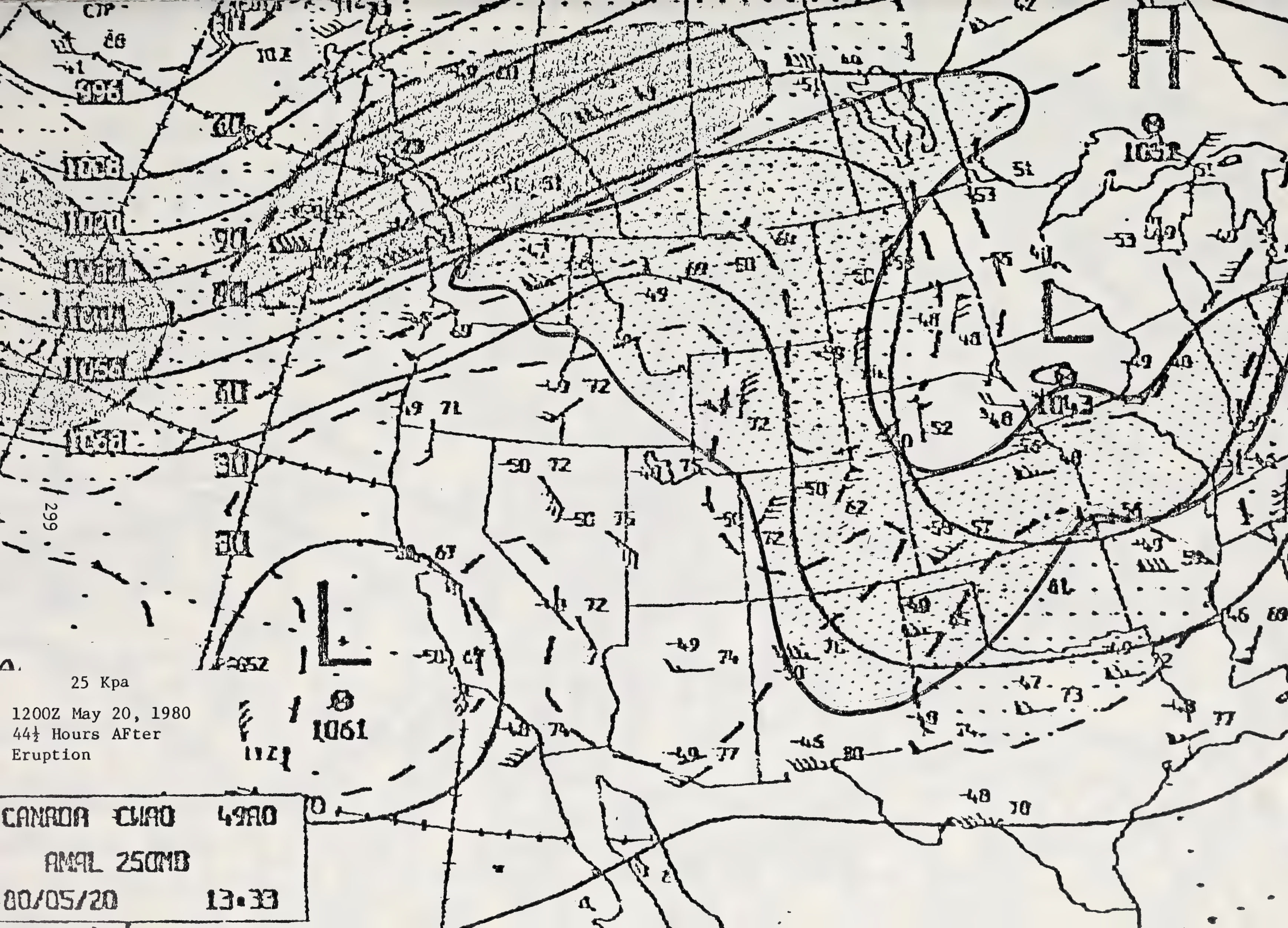

A.

25 Kpa

1200Z May 20, 1980
44½ Hours AFter
Eruption

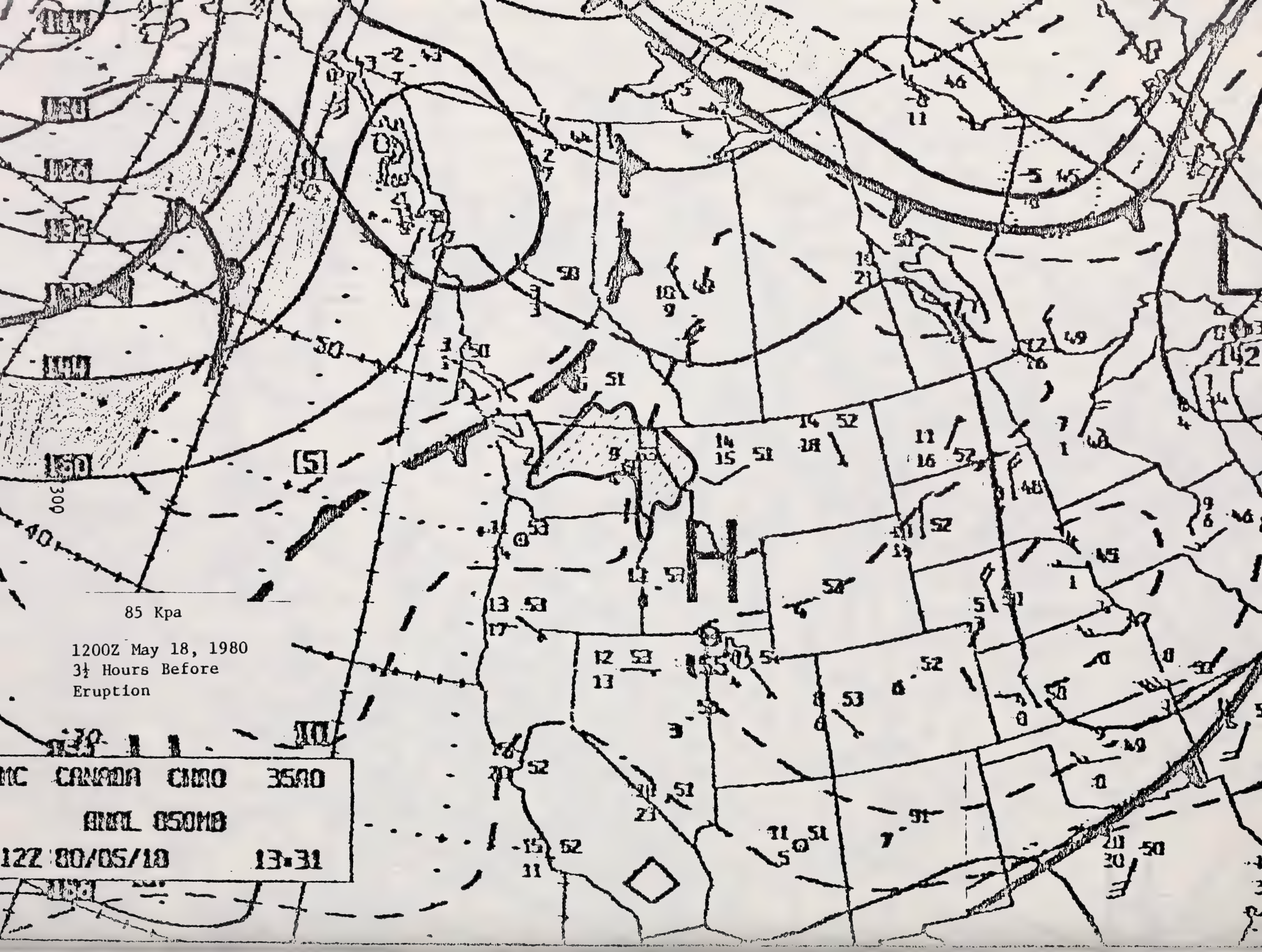

85 Kpa

1200Z May 18, 1980
3½ Hours Before
Eruption

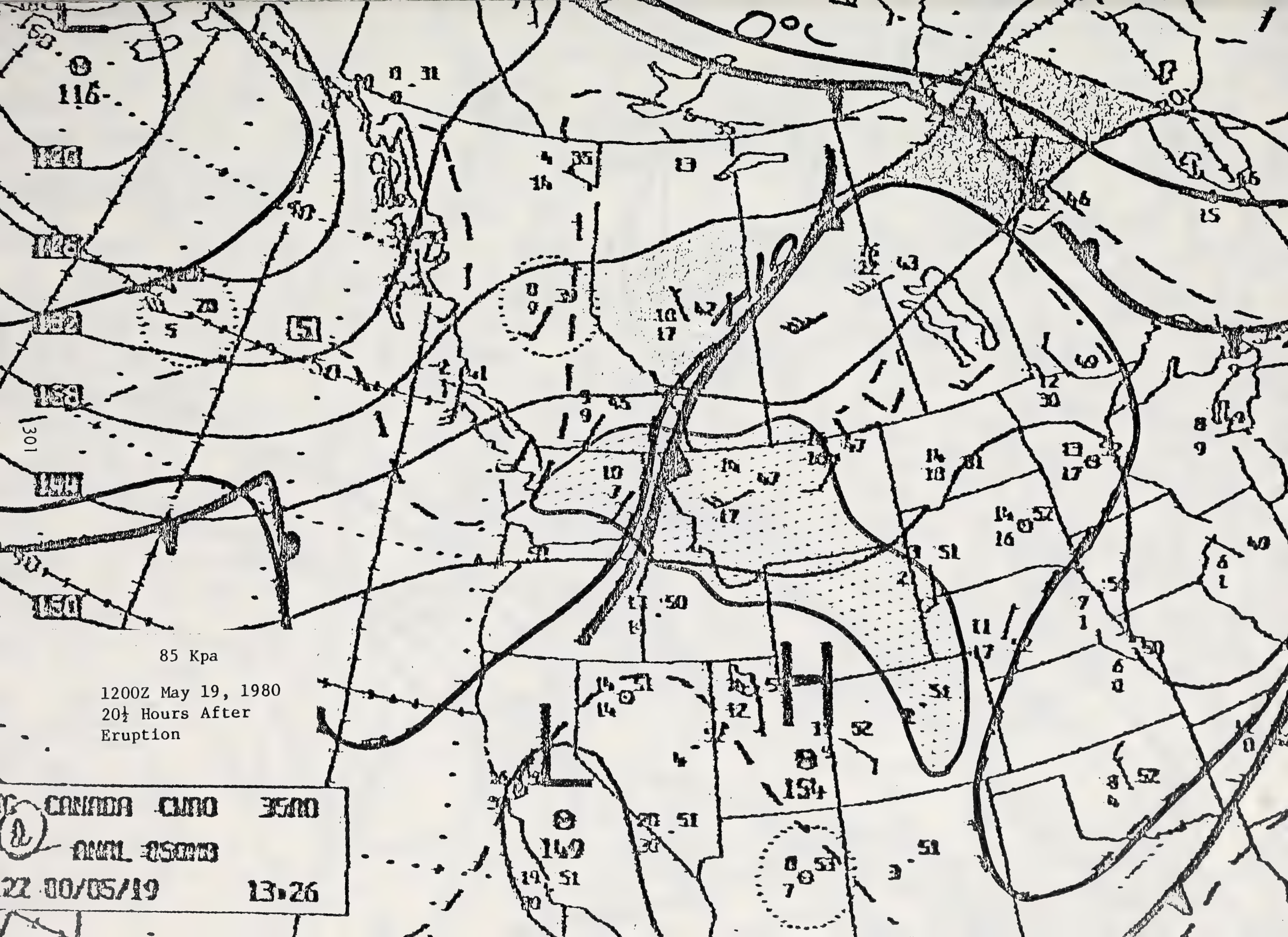

85 Kpa

1200Z May 19, 1980
20½ Hours After
Eruption

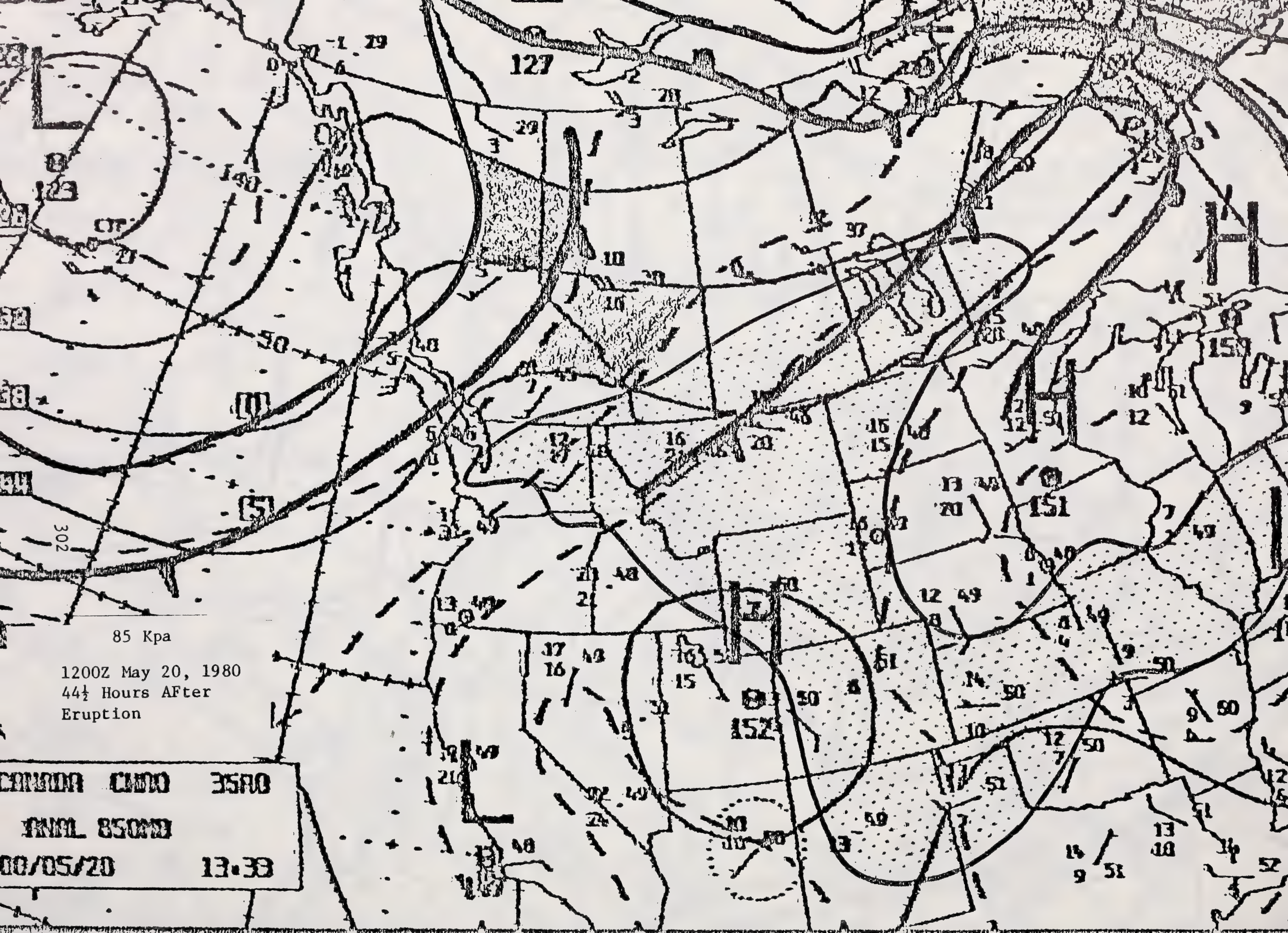

85 Kpa

1200Z May 20, 1980
44½ Hours AFter
Eruption

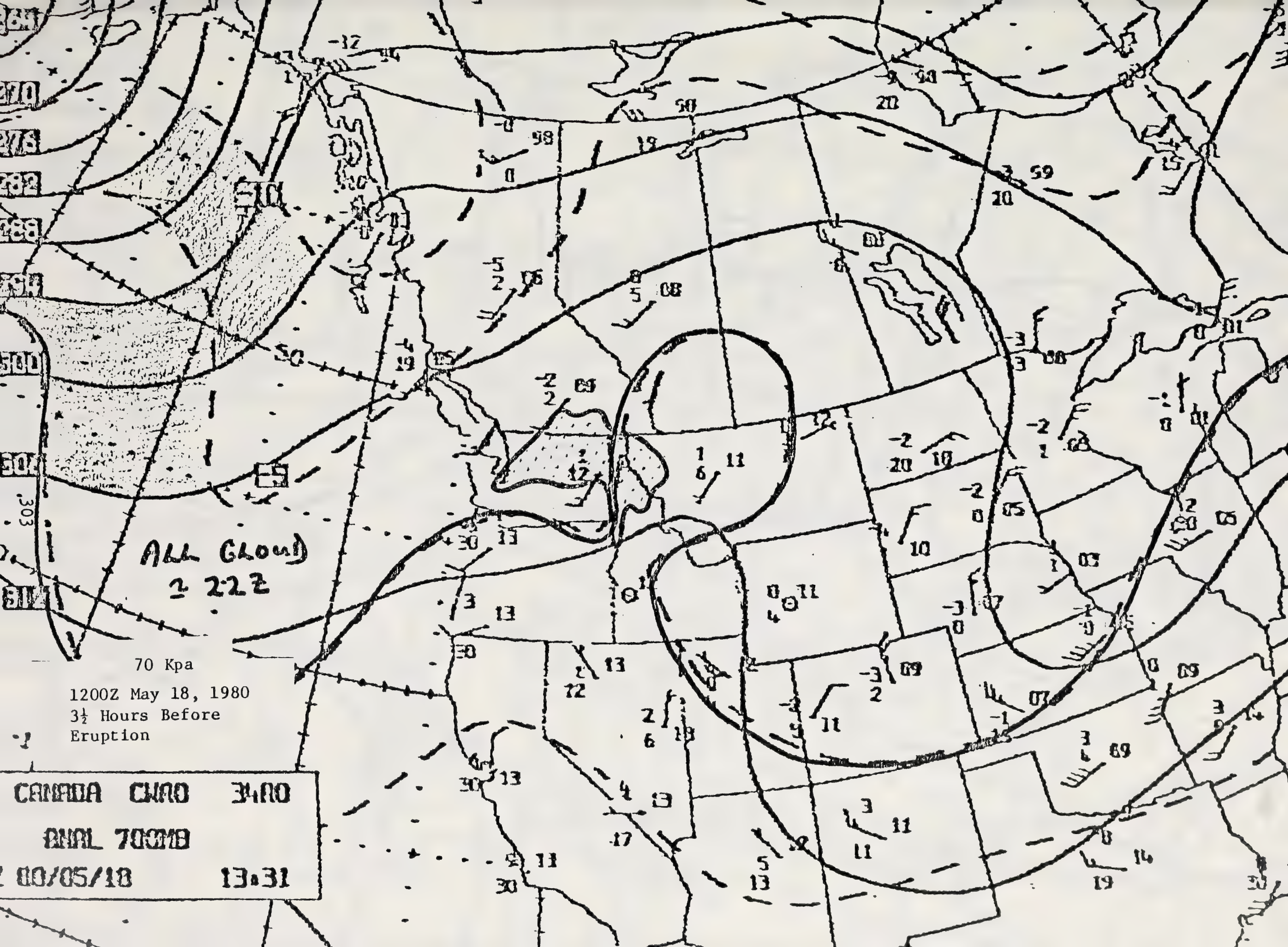

70 Kpa

1200Z May 18, 1980
3½ Hours Before
Eruption

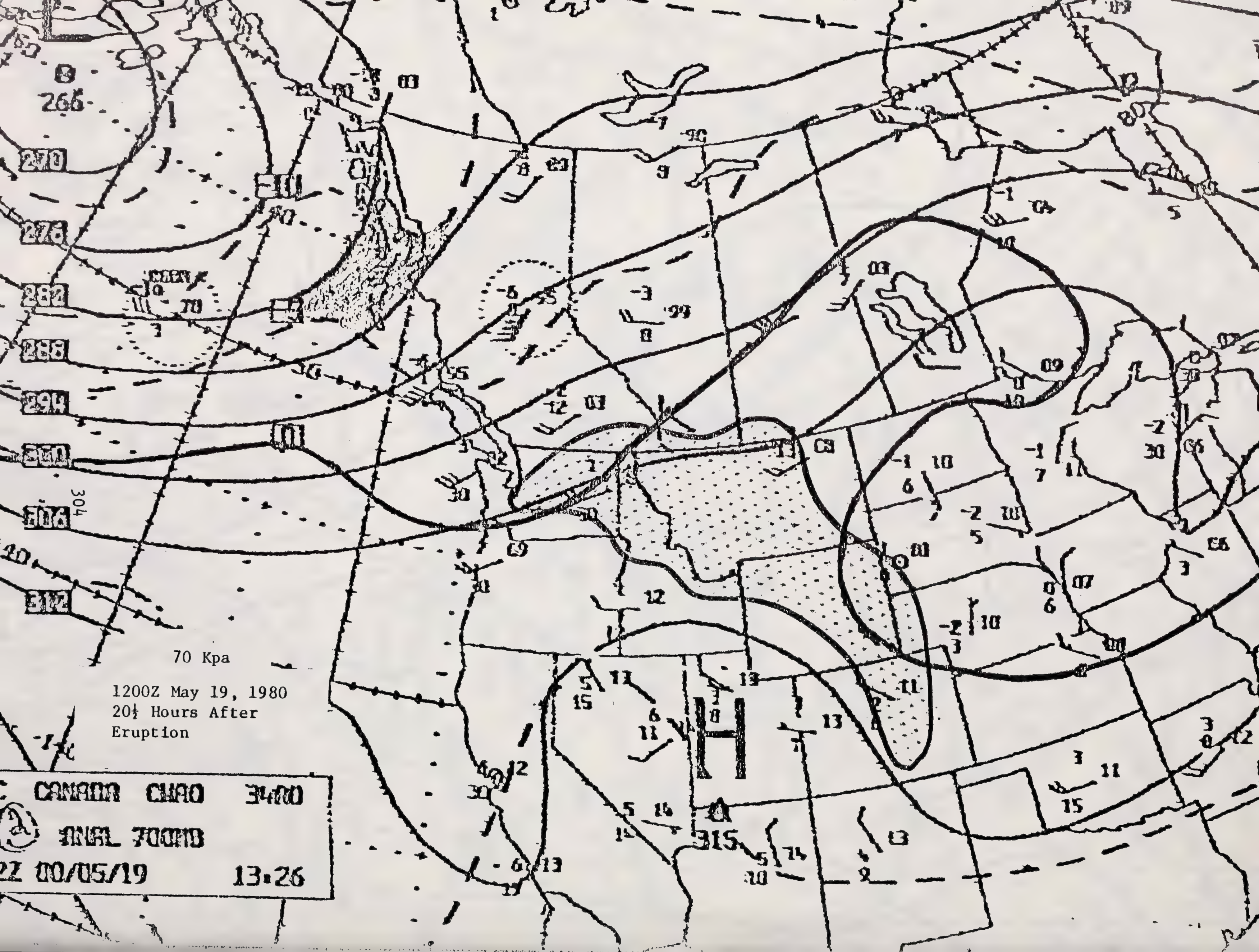

70 Kpa

1200Z May 19, 1980
20½ Hours After
Eruption

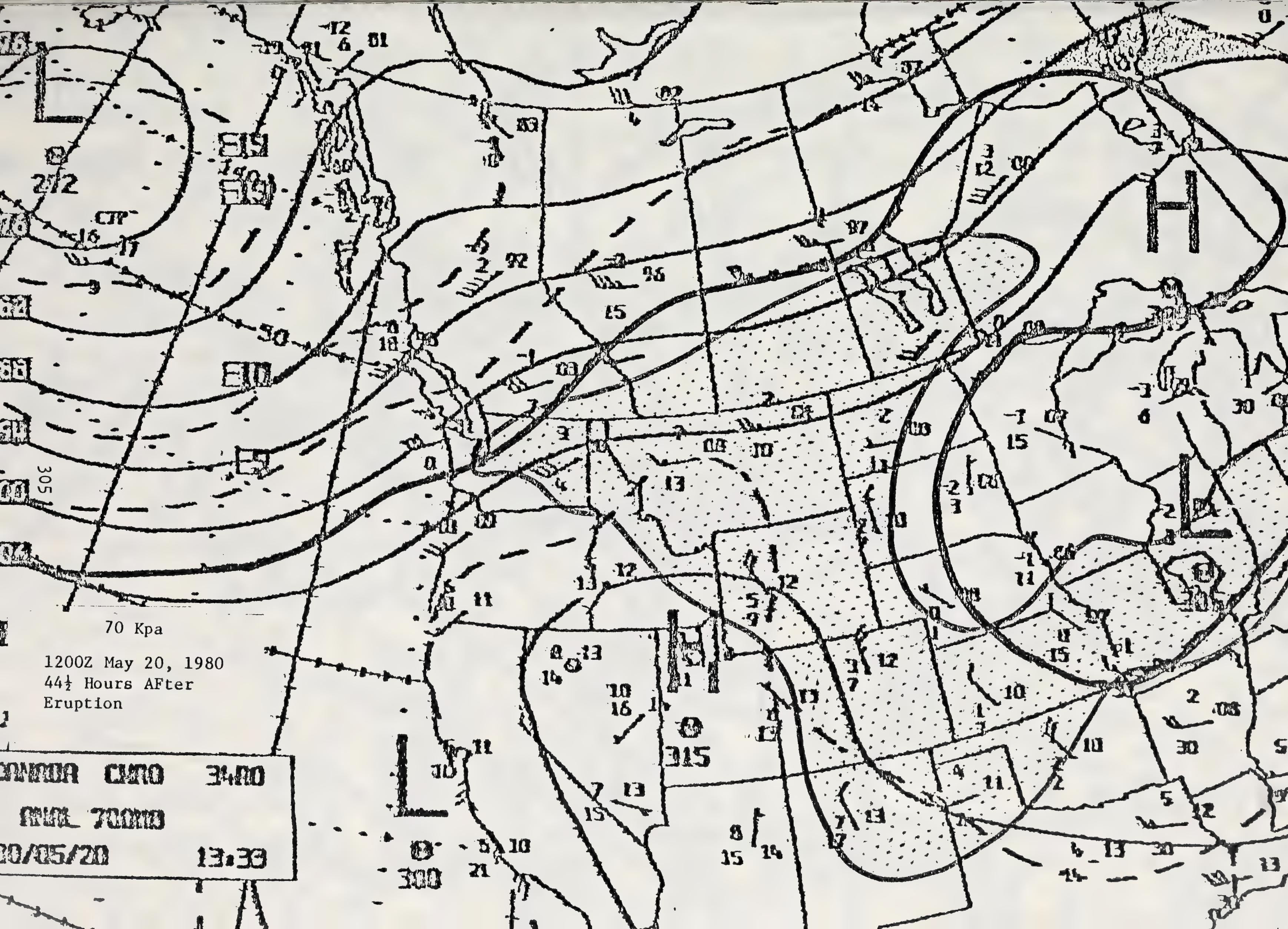

70 Kpa

1200Z May 20, 1980
44½ Hours AFter
Eruption

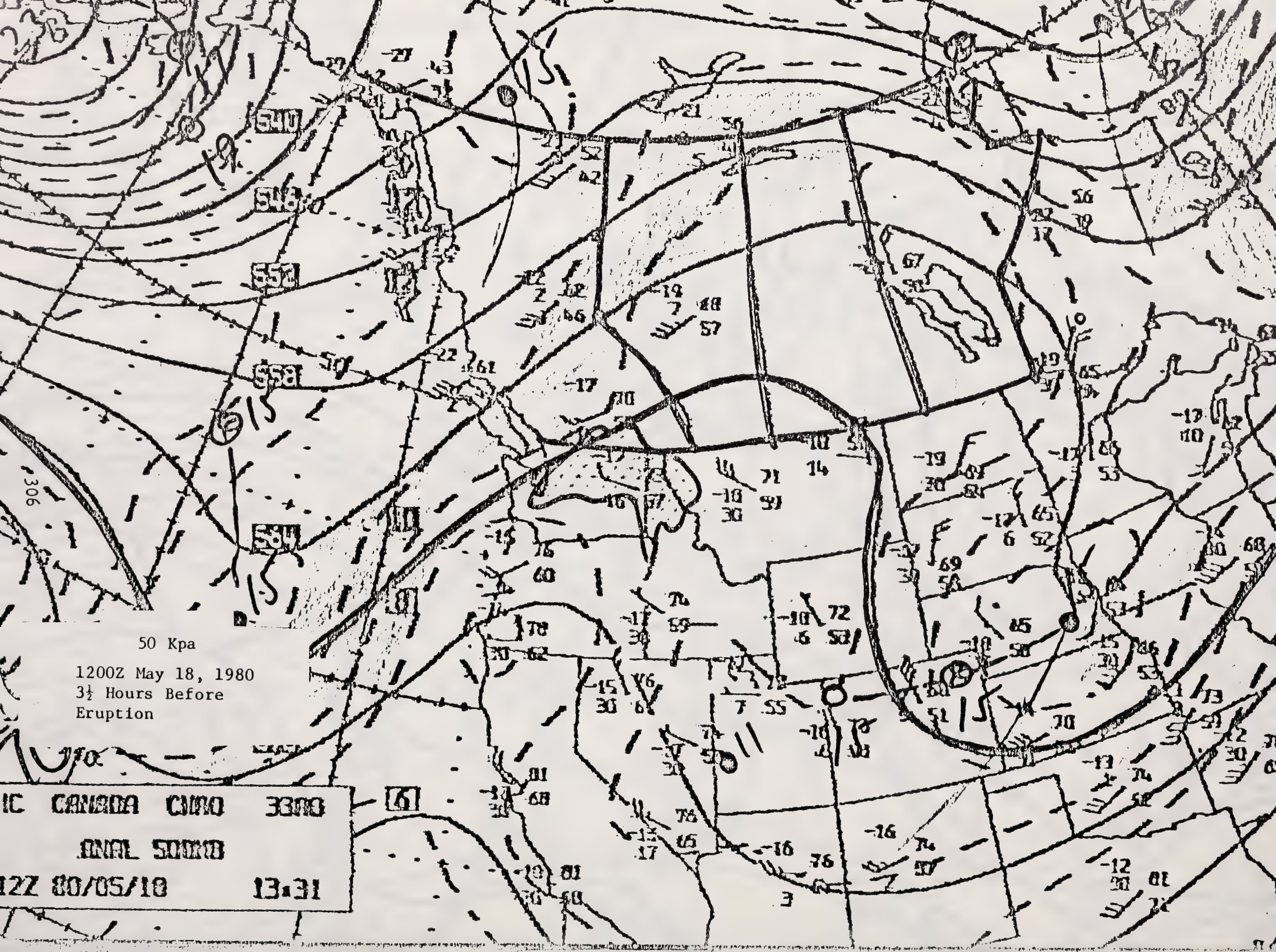

50 Kpa

1200Z May 18, 1980
3½ Hours Before
Eruption

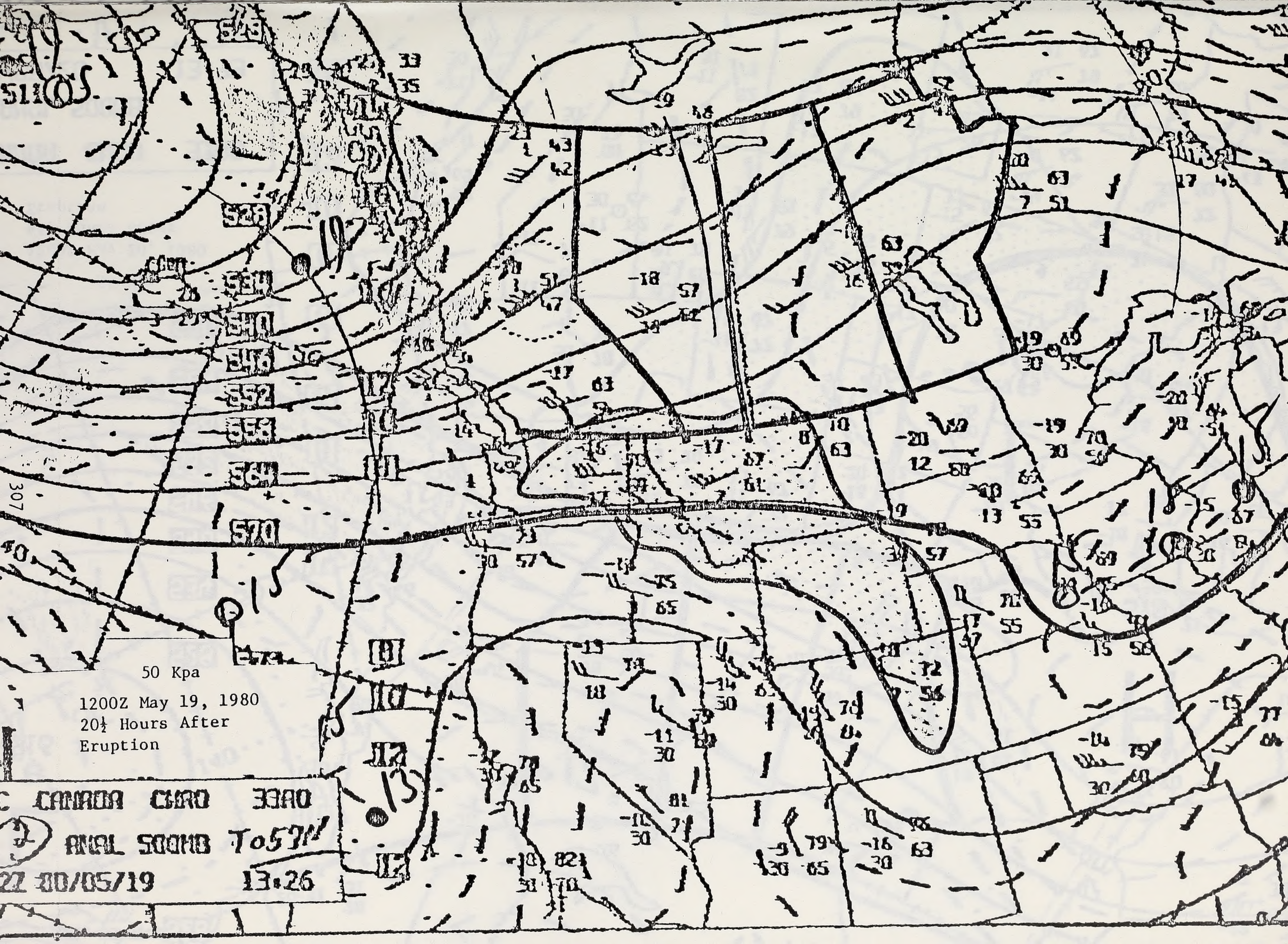

50 Kpa

1200Z May 19, 1980
20½ Hours After
Eruption

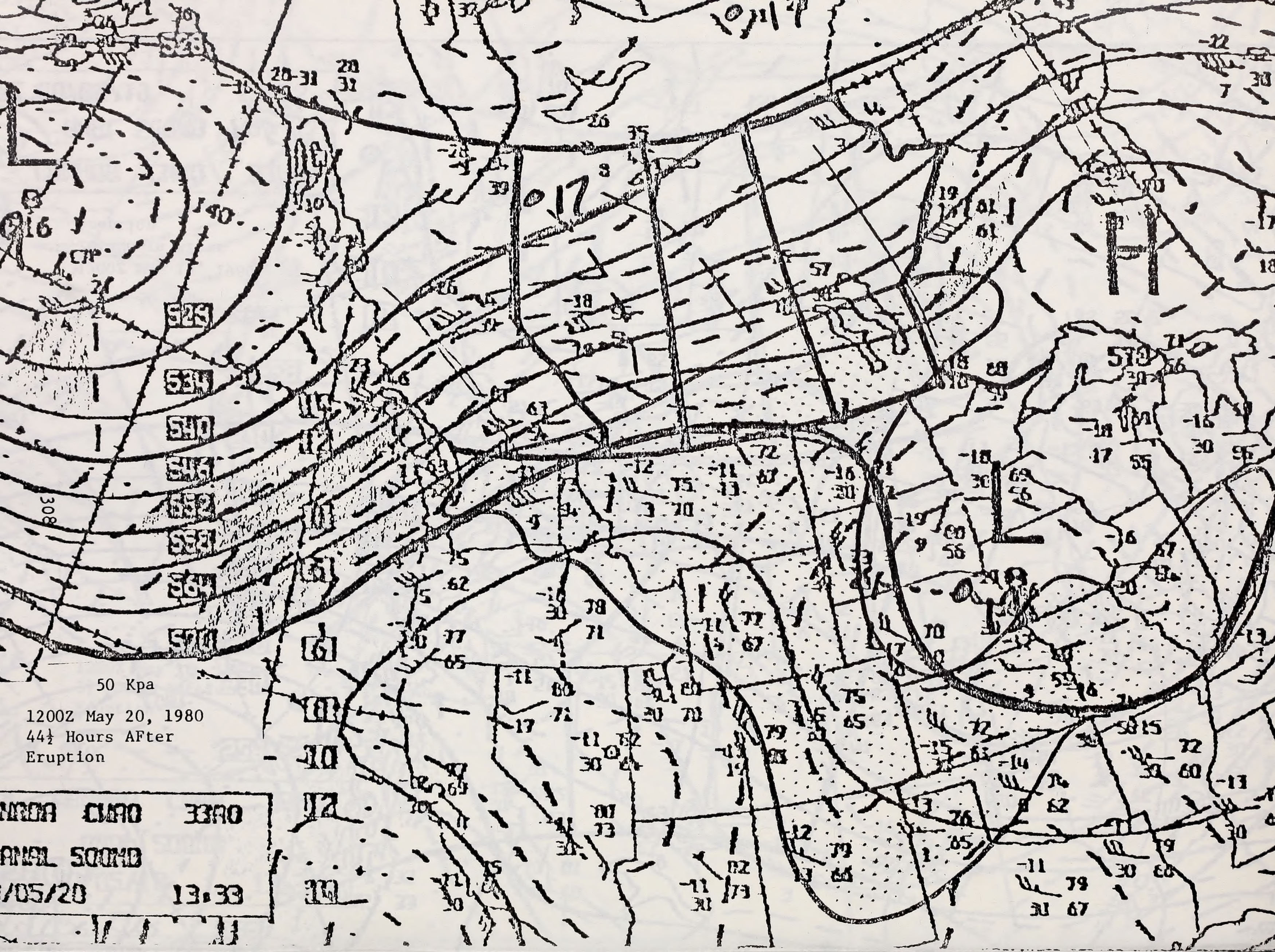

50 Kpa

1200Z May 20, 1980
44½ Hours AFter
Eruption

N.L.C. - B.N.C.
3 3286 06389290 1